Mechanisms of Neuronal Death in a Transgenic Mouse Model for Amyotrophic Lateral Sclerosis

Angela Vlug

Mechanisms of Neuronal Death in a Transgenic Mouse Model for Amyotrophic Lateral Sclerosis

Mechanismen voor Neuronale Celdood in een Transgeen Muismodel voor Amyotrofische Lateraal Sclerose

Proefschrift

ter verkrijging van de graad van doctor aan de

Erasmus Universiteit Rotterdam

op gezag van de rector magnificus

Prof.dr. S.W.J. Lamberts

en volgens besluit van het College voor Promoties.

De openbare verdediging zal plaatsvinden op

woensdag 27 april 2005 om 15.45 uur

door

Angela Vlug

geboren te Hilversum

Contents   **Pages**

Voor Opa

omdat niemand zo trots op me is als hij

Chapter 1

GENERAL INTRODUCTION

1   Introduction

Neurons are large post-mitotic cells with a highly complex morphology, characterized by a dendritic tree that consists of a network of processes with a length up to 100 fold the diameter of the cell body, and an axon that can have a length of up to 10^4 times the diameter of the cell body (i.e. 1 m and 100 µm respectively). Therefore, the maintenance of the functional and structural integrity of neurons throughout life is a complex task that requires sophisticated transport, damage control and repair machineries. Hence, it is not surprising that aging is associated with structural and functional deterioration of the central nervous system and that neurodegenerative diseases (diseases that cause the premature loss of neurons) are among the dominant disorders associated with aging. Identifying the mechanisms underlying the aging and degeneration of neurons is an important task in clinical neuroscience. Genetic studies in the past decades have considerably increased our understanding of proteins that play a role in familial forms of neurodegenerative diseases [153]. However, our knowledge about how these protein abnormalities lead to neuronal degeneration is still very incomplete, and, more importantly, there has been little advance in the development of effective treatments for neurodegenerative disorders.

In general, neurodegenerative disease are characterized by the degeneration of specific groups of neurons, e.g. cortical neurons in Alzheimer's disease, dopaminergic neurons of the substantia nigra in Parkinson's disease, and medium-size spiny neurons of the striatum in Huntington's disease. The subject of this thesis is amyotrophic lateral sclerosis (ALS), a neurodegenerative disorder of motoneurons. A major breakthrough in ALS research came with the identification of mutations in the superoxide dismutase 1 (SOD1) gene in 1993 [128]. This has enabled the production of transgenic mutant SOD1 expressing mice that develop an ALS-like motoneuron disease. The ALS-mutant SOD1 mice provided the first realistic animal model for ALS [60]. In the studies presented in this thesis we use this mouse model to unravel factors that contribute to the pathogenesis of ALS focusing on two potential pathogenic factors: oxidative stress and proteolytic stress.

This chapter provides an introduction on ALS and experimental ALS models.

1.1 Amyotrophic lateral sclerosis

1.1.1   Upper and lower motoneurons

The term motoneurons is used for those neurons in the spinal cord and the brain stem that innervate skeletal muscle fibers. These neurons are also referred to as α-motoneurons. A single α-motoneuron innervates multiple muscle fibers. An α-motoneuron and its muscle fibers are called a motor unit, which is the smallest contractile unit of a muscle. The number of muscle fibers innervated by a motoneuron, i.e. the size of a motor unit, varies, in most muscles, from 100 up to 2000 depending on the type and function of the muscle. α-Motoneurons are usually
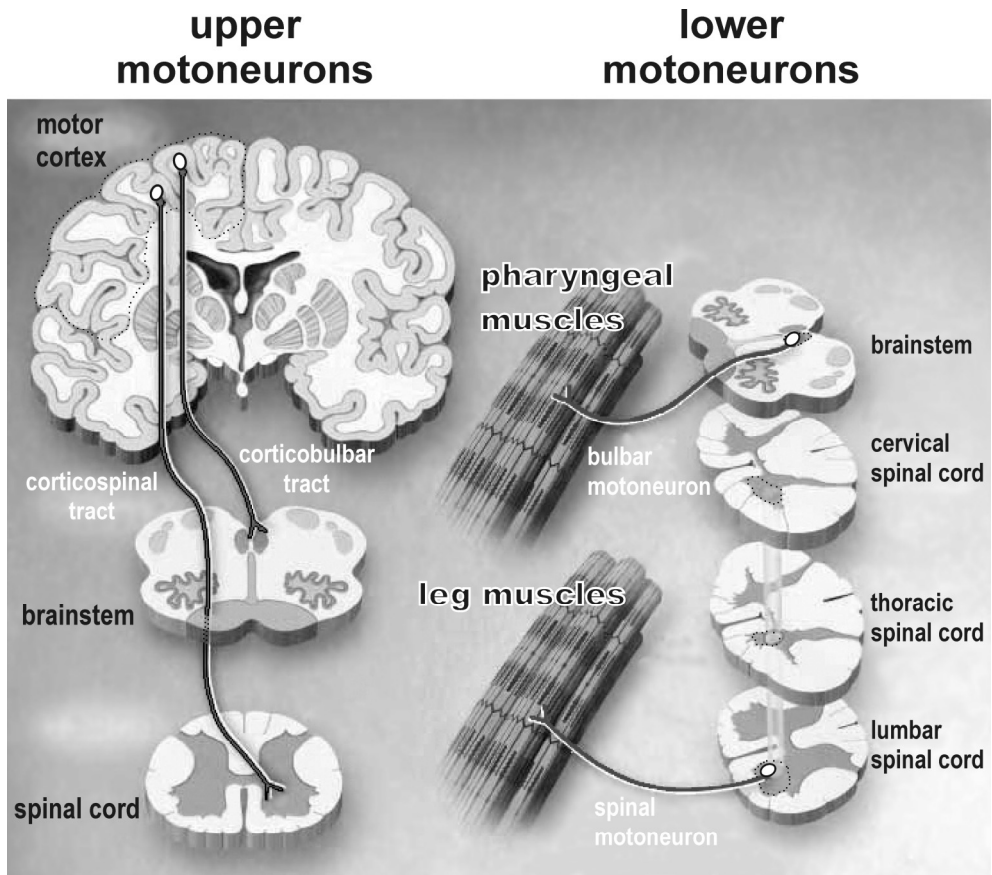
Figure 1: Upper motoneurons (white circles, upper left) are situated in the motor cortex (dotted line, upper left) and connect via the corticospinal or corticobular tract to respectively the spinal cord or brainstem. Lower motoneurons (white circles in right part) are situated in the brainstem or ventral horn (dotted line) of the spinal cord. Lower motoneurons connect directly with the muscles in all parts of the body. (from Rowland et al., 2001)

grouped into three classes depending on their the size and firing properties and the properties of their muscle fibers: small tonically active α-motoneurons innervate muscle fibers that contract relatively slowly and generate small forces, but are fatigue resistant. These slow motor units are involved in 'background' muscle activity such as those required for the control of posture. Large α-motoneurons innervate muscle fibers that are rapidly fatigued but are fast and produce large forces as required for running or jumping. A third class of α-motoneurons is intermediate in size and innervates muscle fibers with intermediate properties. The small α-motoneurons are relatively unaffected in ALS [112]. Also α-motoneurons innervating the extra-ocular muscles and the bladder are relatively spared [22]. In addition, γ-motoneurons, a class of small motoneurons that innervate muscle fibers within a muscle spindle (a specialized structure in the muscle that senses its length and tension), are mostly unaffected in ALS.

Table 1: Motor neuron diseases and the mutations that cause them.
Motoneuron diseases are categorized according to upper and or lower motoneuron involvement, sensory involvement, and sometimes specific clinical characteristics. Sporadic forms of the diseases are not specified.

Disease	Mutation	Normal function of mutated protein	Pathology	Symptoms	Age of onset	Non-motor involvement	Ref.
Motor axonopathies							
Charcot Marie Tooth 2 (HMSN2)	*Kif1B* (AD)	Antero– and retrogr microtubule transport		slow progressive weakness & muscle atrophy in distal legs	<20 yrs	rarely sensory	[173]
	Mitofusin 2 (AD)	Mitochondrial GTPase / mitochondrial fusion		slow progressive weakness & muscle atrophy in distal legs. Sometimes tremors	3–50 yrs	mild sensory	[175]
	Rab7	Intracellular membrane transport		slow progressive weakness & muscle atrophy in distal legs, sometimes also in hands	10–25 yrs	sensory foot ulcerations	[163]
	GARS	tRNA synthetase		slow progressive weakness & muscle atrophy more in arms than legs	10–30 yrs	sensory	[8]
	NF–L	Intermediate filament subunit		slow progressive weakness & muscle atrophy in distal legs	10–30 yrs	sensory	[110]
	HSP27	Molecular chaperone	Peripheral axonopathy without demyelinization	slow progressive weakness & muscle atrophy in distal limbs	15–25 yrs	sensory	[43]
	HSP22 (AD)	Molecular chaperone		slow progressive weakness & muscle atrophy in distal limbs	15–25 yrs	none	[75]
	MPZ (P0) (AD)	Myelin protein		slow progressive weakness & muscle atrophy in distal limbs	>35 yrs	sensory	[105]
	Connexin 32 (X-linked)	Gap junction protein		slow progressive weakness & muscle atrophy in distal limbs	10–40 yrs	often sensory	[154] [16]
	Lamin A/C a) (AD) b) (AR)	Nuclear envelope protein (intermediate filament)		a) slow progressive weakness & muscle atrophy in distal legs b) slow progressive weakness & muscle atrophy in legs and dist arms	a)<20 yrs b) 5–25 yrs	-sensory cardiac -often sensory	-[53] -[36]
	GDAP1 (AR)	unknown		slow progressive weakness & muscle atrophy in distal limbs, sometimes vocal cords	<10 yrs	sensory	[35]
HSP	*Alsin* (AR)	GTPase regulator	demyelinization & axonopathy of pyramidal & gracile tract	slow progressive weakness & spasticity starting in the legs progressing to paralysis of whole body	<3 yrs	mild sensory	[44]
	Paraplegin (AR)	Mitochondrial ATPase (chaperon-like)	demyelinization & axonopathy of pyramidal & gracile tract. Sometimes cerebellar atrophy	slow progressive weakness & spasticity in the legs. sometimes mild vision deficits	All ages	mild sensory	[26]
	Spartin (AR)	Endosomal trafficking	demyelinization & axonopathy of pyramidal & gracile tract	slow progressive weakness & spasticity in the legs. dist mus wasting	All ages	mild sensory	[121]
	Spastin (AD)	Microtubule interacting ATPase	demyelinization & axonopathy of pyramidal & gracile tract	slow progressive weakness & spasticity in the legs	All ages	mild sensory rarely cognitive	[46]

	Gene	Function	Cell type affected	Age of onset	Symptoms	Other features	Ref
	HSP60 (AD)	Mitochondrial protein folding chaperone	demyelinization & axonopathy of pyramidal & gracile tract	All ages	Slow progressive weakness & spasticity in the legs	mild sensory	[64]
	Kinesin heavy chain (AD)	Antero- and retrogr transport along microtubules	demyelinization & axonopathy of pyramidal & gracile tract	<40 yrs	slow progressive weakness & spasticity starting in the legs progressing to paralysis of whole body	mild sensory	[126]
	Atlastin (AD)	Dynamin-like ? GTPase	demyelinization & axonopathy of pyramidal & gracile tract	<10 yrs	slow progressive weakness & spasticity in the legs	mild sensory	[174]
	NIPA1 (AD)	unknown	demyelinization & axonopathy of pyramidal & gracile tract	15-25 yrs	slow progressive weakness & spasticity in the legs	mild sensory	[124]
	L1CAM (X-linked)	Cell-cell adhesion	demyelinization & axonopathy of pyramidal & gracile tract. Hydrocephalus	At birth	slow progressive weakness & spasticity in the legs	mental retardation	[83]
	PLP (X-linked)	Myelin protein	demyelinization & axonopathy of pyramidal & gracile tract. Sometimes cortical white matter lesions or peripheral axonpathy	<0.5 yrs	slow progressive weakness & spasticity in the legs. Nystagmus	mental retardation	[94]

Motor neuronopathies

	Gene	Function	Cell type affected	Age of onset	Symptoms	Other features	Ref
ALS & juvenile ALS	see table 2		upper and lower MNs	>20 yrs	weakness and muscle atrophy spreading to whole body paralysis except eye movement and sphincter control	none	
PLS	non-hereditary		upper MNs and pyramidal tract	>30 yrs	stiffness and spasticity of legs slowly progressing to paralysis of whole body	none	[93]
Juvenile PLS	Alsin (AR)	GTPase regulator	upper MNs and pyramidal tract	<2 yrs	stiffness and spasticity of legs slowly progressing to paralysis of whole body	none	[170]
SMA	SMN1 (AR)	Pre-mRNA transport and splicing	spinal MNs	<30 yrs	weakness and muscle atrophy in whole body except face and diaphragm	none	[118]
	IGHMBP2 (AR or AD)	RNA/DNA helicase	spinal MNs	<4 mths	weakness and muscle atrophy in distal limbs and diaphragm	none	[56]
	VAPB	Vesicle trafficking	lower MNs	35-55 yrs	weakness and muscle atrophy in whole body except face and diaphragm	none	[119]
Kennedy disease	androgen receptor (X-linked)	Hormone-dependent transcription factor	lower MNs, DRG sensory neurons	10-40 yrs	fasciculations. weakness and muscle atrophy spreading from 1 part to whole body	breast formation mild sensory	[47]

In the clinic, α-motoneurons are referred to as 'lower motoneurons' (figure 1). 'Upper motoneurons' are neurons primarily localized in the motor cortex that control movement by directly or indirectly controlling the activity of α-motoneurons. Symptoms due to loss of upper motoneurons are distinct from lower motoneuron symptoms. Lower motoneuron symptoms include paresis (weakness), atrophy of muscles, loss of reflexes, loss of muscle tone, and fasciculations (spontaneous twitches of denervated muscle fibers). Upper motoneuron symptoms are spasticity due to increase in muscle tone, and increased reflexes, which may lead to pathological reflexes like the Babinski sign.

There is a continuum of disorders affecting lower and/or upper motoneurons. These various diseases are usually distinguished can be further distinguished on the basis of criteria like the part of the motoneurons that are primarily affected (axon versus cell body), the extent of non-motor system pathology, age of onset, and rate of disease progression. Diseases of the axon of lower motoneurons include the various forms of Charcot Marie Tooth type 2 (CMT2), which are peripheral axonopathies without demyelinisation, usually characterized by both sensory and motor defects. Similarly, disorders of the axons of upper motoneurons usually show both sensory and motor deficits. Disorders that selectively affect lower motoneurons include spinal muscular atrophy (SMA) and Kennedy disease. SMA is one of the most common autosomal recessive disorders in childhood, with an incidence of 1 in 6,000–10,000 births. Pure upper motoneuron disorders, i.e. primary lateral sclerosis (PLS), are rare. The identification of the genetic defects underlying many of these disorders has revealed valuable information about the molecular pathways that are important for the structural and functional integrity of motoneurons (Table 1).

1.1.2   Clinical and pathological features of ALS

Amyotrophic lateral sclerosis (ALS) is defined as an adult onset progressive disease that (eventually) involves both lower and upper motoneurons. It is the most common adult onset motoneuron disease, and often the term motor neuron disease is used instead of ALS. Other names are Charcot disease after the French neurologist who first described the disease, or, in the USA, Lou Gehrig's disease after the New York Yankees baseball player who died of the disorder in 1936. The distinction between ALS and late onset pure upper or pure lower motoneuron diseases, (i.e. late onset PLS, late onset spinal muscular atrophy (SMA) and progressive bulbar palsy (PBP)) is not always clear [93,162]. It is a matter of debate whether it is useful to differentiate between late onset upper or lower motoneuron diseases and ALS, since genetic forms of motoneuron disease do not seem to obey such a classification (see below). On the other hand a more refined classification of ALS based on upper or lower motoneuron onset, disease progression and the presence of other symptoms is useful in clinic.

The incidence of ALS in most European countries is between 2 and 3 per 100.000 persons, which means that approximately 300-450 people per year are diagnosed with ALS in the Netherlands. In total there are 750-1200 ALS patients in the Netherlands. ALS-patients die on average 3 years after disease onset, although

20% of the patients survive for more than 5 year [159]. The first symptoms are usually fatigue, muscle cramps, and weakness in the muscles of one of the limbs, progressing to paralysis and spreading to other parts of the body. These symptoms are accompanied by fasciculation (muscular twitching) and atrophy (decrease in size) of the muscles involved, and by hypertonia and hyperreflexia due to involvement of upper motoneurons. In some cases symptoms start with difficulties in swallowing or slurred speech (bulbar ALS) [131]. In clinically 'unaffected' muscles, electromyography may reveal denervation activity. In a subset of ALS, in particular in familiar forms, atypical features such as sensory deficits or dementia occur.

Neuropathologically ALS is characterized by degeneration of the corticospinal tracts, loss of motoneurons, astrogliosis in the ventral horn of the spinal cord and the motor cortex and atrophy of the ventral roots. Different types of subcellular abnormalities have been identified in surviving motoneurons, including an abnormal Golgi apparatus and the appearance of various abnormal intracellular structures. A constant and characteristic pathological feature in ALS motoneurons is the presence of ubiquitinated structures, consisting of irregular loosely arranged bundles ('skeins') of filamentous-appearing material and/or spherical inclusions [95]. These ubiquitin-immunoreactive inclusions are more prevalent than Bunina bodies that are small (2-3 µm) granular inclusions found in the majority of sALS and some fALS patients but not in other neurodegenerative diseases. Bunina bodies contain tubules and vesicular structures, but except for cystatin C the composition of these inclusions is still unclear. Another pathological feature is the accumulation of phosphorylated neurofilament in the proximal axon [68].

1.1.3   Familial ALS

The pathogenesis of ALS is still poorly understood [22,132]. In the majority of the patients (90%) the disease is sporadic, i.e. without a clear inheritance pattern, whereas in 10% of the cases ALS is familial, usually with autosomal dominant inheritance. This distribution of familial and sporadic disease is similar to other adult-onset neurodegenerative diseases, such as Parkinson disease and Alzheimer disease. In general, familial ALS is clinically and pathologically similar to sporadic ALS. The genetic causes underlying familial ALS are now beginning to be unraveled [89].

At the moment of writing this chapter, 5 ALS genes and 6 additional disease loci were identified [89] (see table 3). A major breakthrough came in 1993 with the identification of SOD1 mutations in familial ALS [128]. which more than a decade later, are still the main known cause of ALS. Recently, mutations in other genes have been uncovered, but these genes, so far, are associated with small numbers of patients and relatively atypical forms of ALS (see table 2).

Superoxide dismutase 1 (SOD1)-gene: Mutations in *SOD1* were the first causes of familial ALS that were identified and SOD1-mutations represent 20% of familial ALS [6]. SOD1 is small dimeric copper and zinc-containing enzyme constitutively expressed in all eukaryotic cells. Its dominant function is believed to be the detoxification of super oxide radicals in most compartments of the cell with exception of the mitochondrial matrix where super oxide radicals are detoxified by

Table 2: Genes involved in different types of familial ALS.
In typical fALS not all genes corresponding to know loci have been discovered yet. Some loci of atypical ALS have not been listed in this table.

Disease	Mutation (locus, pattern)	Normal function of mutated protein	Pathology	Age of onset (average)	Symptoms	Non-motor involvement	Ref
Familial ALS	SOD1 missense (AD or AR)	Superoxide scavenging	upper and lower MNs astrogliosis. lewy body-like inclusions, sometimes Bunina or Hirano bodies.	>20 yrs	weakness, fasciculation, and muscle atrophy		[128]
	Unknown (18q21 AD)			>20 yrs (45)	weakness, fasciculation, and muscle atrophy		[63]
	Unknown (16q12 AD)			>20 yrs (44)	weakness, fasciculation, and muscle atrophy	none	[133]
	Unknown (20p13 AD)			>20 yrs (56)	weakness, fasciculation, and muscle atrophy		[134]
	VAPB (AD)	Vesicle trafficking		25-55 yrs (39)	weakness, fasciculation, muscle atrophy, often tremors		[119]
	Unknown (X-linked)			NP	weakness, fasciculation and muscle atrophy		[142]
ALS-FTD	Unknown (9q21 AD)		upper and lower MNs frontal cortex	40-65 (54)	weakness, fasciculation and muscle atrophy Sometimes personality changes and/or dementia	none	[71]
ALS-FTDP	MAPT intronic (AD)	Tau	upper and lower MNs frontal cortex, substantia nigra, amygdale. astrogliosis	NP (49)	weakness, fasciculation and muscle atrophy. sometimes with parkinsonism, personality changes and/or dementia	none	[74]
Juvenile ALS	Alsin truncation (AR)	GTPase regulator		<20 yrs	weakness, spasticity and muscle atrophy	none	[170]
	SETX (AD)	DNA repair, RNA processing ?	upper and lower MNs	<35 yrs (15)	weakness, spasticity and muscle atrophy mainly in limbs. some families: normal life expectancy	rarely	[30]
	unknown (15q AR)			8-18 yrs	weakness, spasticity and muscle atrophy	none	[67]

AD, autosomal dominant; AR, autosimal recessive; FTD, frontotemporal dementia; FTDP, frontotemporal dementia with parkinsonism; MNs, motoneurons; NP, not published

SOD2. Although SOD1 is a highly abundant protein that comprises as much as 1% of total cytosolic protein, studies with SOD1 knockout mice have shown that its complete absence has no effect on viability and life span [48]. In contrast mice with targeted deletion of SOD2 die shortly after birth because of oxidative stress mediated damage to mitochondria that can be attenuated by SOD mimetics [109]. Studies with transgenic mice and rats overexpressing SOD1 have suggested that SOD1 may be important in conditions of ischemia, hypoxic stress, and after oxidative insults like paraquat intoxication [29]. However, extra SOD1 does not influence life span [73], and may be deleterious [77]. Thus the precise advantage of expressing very high levels of SOD1 in mammals remains to be determined. In this context it should be noted that in yeast and invertebrates cytosolic SOD is a relevant protein for survival and aging. Significantly, studies in Drosophila have shown that transgenic expression of different ALS-related mutant SOD1 in motoneurons increases life span [42].

How SOD1 mutations cause ALS is not yet understood. Currently, more than 110 mutations (mostly missense point mutations) spanning all five exons have been identified. Mutant SOD1s show a great variability of biochemical and biophysical properties, varying from highly unstable mutants to mutants with virtual identical properties as wild-type SOD1 [6]. The commonality among mutants may be their conformational instability and increased tendency to aggregate in a monomeric or metal-free configuration or after disulfide reduction [157]. Structure analysis has confirmed that mutant SOD1s can form stable aggregates [157].

Significant advance in identifying the disease mechanism has come from a recent study with spinal cord tissue from ALS patients and transgenic mice expressing SOD1 with the G127insTGGG mutation, which shows that minute quantities of mutant SOD1 (below 0.5% of control SOD1 levels) are sufficient to cause motoneuron degeneration [81]. This offers an explanation why wild-type-like and unstable mutants cause a similar disease, since these mutants may generate different levels of total SOD1, but the same levels of SOD1 in a toxic configuration [81]. Another recent finding indicate that the toxic effect of mutant SOD1 may not be caused by a direct effect on motoneurons, but rather indirectly via an effect on neighboring cells [32].

Since mild genetic modifications in almost any of its amino acid residues can cause ALS, mechanisms can be envisioned in which wild-type SOD1 may also become toxic. For instance, various post-translational modifications that may afflict its stability or degradation have been identified in wild-type SOD1 [157]. In addition, transgenic expression of a high level of wild-type SOD1 causes mitochondrial pathology and axonal degeneration in aged mice, and dramatically accelerates the disease phenotype in transgenic mice expressing ALS-mutant SOD1 [77]. Wild-type SOD1 transgenic mice like ALS-mutant SOD1 mice also develop insoluble aggregated SOD1 species while aging (Jaarsma, unpublished observation).

In sum, data so far suggest a mechanism where a small fraction of misfolded, possibly oligomerised or aggregated mutant SOD1 causes the disease [157]. There are many ways for misfolded and aggregated proteins to disturb cell function [140], but which organelles or cell biological processes are affected by mutant SOD1 and why it selectively afflicts motoneurons is still unknown (see below).

However, neuropathological and biochemical studies in ALS-mutant SOD1 mice indicate that the mitochondrial outer membrane and intermembrane space are sites of early mutant SOD1 accumulation [79][Liu, 2004] resulting in malfunction of mitochondria.

ALS2/alsin gene: Mutations in the *Alsin* gene (also known as ALS2) have been identified as the second cause of ALS. Two different mutations in alsin have been linked to a rare autosomal recessive juvenile form of familial ALS but they can also lead to juvenile hereditary spastic paraplegia [44,61,170]. Alsin is a 184-kDa protein with a yet unknown function. It has three putative guanine-nucleotide-exchange factor (GEF) domains, and it can act as a guanine nucleotide exchange factor for Rac1, and alsin can also influence endosomal dynamics [88,155]. Like SOD1, alsin is not selectively expressed in motoneurons, but in most, if not all, cells of the body. ALS-related mutant alsin is highly unstable, which together with its recessive inheritance suggests a loss of function mechanism of disease. Alsin-knockout mice do not develop a motor neuron disease-like phenotype (reviewed in [89]).

Senataxin gene: 3 different missense mutations in the *Senataxin* gene have been linked to ALS4; an autosomal dominant form of juvenile ALS with an unusual slow disease progression [30]. Senataxin is a large protein with a superfamily I DNA/RNA helicase domain. However, the majority of the protein has no domain conservation or homology to other proteins. The exact function of senataxin is not known, but DNA/RNA helicases are generally involved in DNA repair, replication, recombination, transcription, RNA processing, transcript stability, and the initiation of translation. The nature of the mutations and pattern of inheritance suggest a toxic gain-of-function mechanism of disease. Interestingly, recessive loss-of-function mutations in senataxin are associated with another neurodegenerative disorder: ataxia-oculomotor apraxia type 2, a heterogeneous disorder characterized by cerebellar ataxia/atrophy, oculomotor apraxia, loss of reflexes, late peripheral neuropathy, and immunodeficiency [113].

VAPB gene: Recently, a missense mutation in the *vesicle-associated membrane protein B* (VAPB) gene has been linked to ALS in a number of Brazilian families probably derived from a single Caucasian founder [119]. Interestingly, the clinical presentation of disease was variable among families, varying from typical ALS to a mild slowly progressing adult onset spino-muscular atrophy. Members of the vesicle-associated proteins are intracellular membrane proteins that can associate with microtubules and have a function in membrane transport [149]. Preliminary transfection studies in HEK 293 cells and hippocampal neurons show that mutant VAPB is mislocalized and may aggregate [119]. Like SOD1, alsin and senataxin, VAPB is ubiquitously distributed throughout the body, again raising the question about the selective vulnerability of motoneurons.

p150 dynactin (DCTN1): A heterozygous missense mutation (G59S) in the p150 dynactin subunit was first reported in a patient with a slowly progressing autosomal dominant form of lower motoneuron disease [123]. More recently, a genetic screen with 250 ALS patients and 150 controls has revealed 3 new heterozygous missense mutations in conserved portions of p150 dynactin [116]. The mutations were found in both sporadic and familial ALS patients, and one of the mutations was also found in unaffected relatives. Dynactin is an essential protein in dynein-

dependent trafficking linking the cargo to the dynein motor complex (see below). Recent studies with mutant mouse models have shown that abnormalities in dynein trafficking cause motoneuron disorders in these mice. Together these data indicate that dynein trafficking is important for the health of motoneurons, and that abnormalities afflicting this trafficking machinery may be one of the risk factors of ALS [70].

1.1.4   Susceptibility factors in ALS

Aging is a dominant risk factor for ALS. In addition, there is slight male to-female predominance. Multiple studies have been devoted at identifying other risk or modifying factors (e.g. heavy metal intoxication, physical activity), but no consistent data have emerged. Table 3 summarizes a number of potential genetic susceptibility factors linked to ALS, but again the data are still inconclusive [22,132]. For instance, the apoE4 allele which is a risk factor in Alzheimer's disease, has been associated with earlier onset and faster disease progression in ALS [40,96,115], but no association was found in other studies [143,147].

Other potential susceptibility factors are the survival of motor neuron protein (SMN) genes. SMN is a ubiquitous 38 kDa protein that is important for cellular survival. SMN is involved in mRNA processing but in neurons also may be important in

Table 3: Potential genetic susceptibility factors in ALS

Gene	Normal function	Variant	Effect of variation	Effect on fenotype	ALS-type	Ref
NF-H	Neurofilament subunit	Repeat shortening	accumulation	High probability	sALS (fALS?)	[4]
VEGF	Growth factor	Homozygous promoter mutation → decreased expression	decreased protein levels	High probability	sALS	[91]
CNTF	Growth factor	Homozygous truncation	inactive	Early onset	fALS (SOD1)	[51]
SMN1	Pre-mRNA transport and splicing	Heterozygous deletion or extra gene copy	unknown	High probability	sALS	[33]
SMN2	Pre-mRNA transport and splicing	Heterozygous deletion	unknown	Short survival	sALS	[161]
ApoE	Lipid transport and metabolism	allele 4	Unknown	Earlier onset, short survival, high probability	sALS	[40]
		allele 2	Unknown	Delays onset, longer survival	sALS fALS	[96]
mtDNA	Mitochondrial DNA	haplogroup I	Unknown	Decreased probability	sALS	[103]
EAAT2	Glutamate transporter	Decreased expression, different splicing	Decreased activity	High probability?	sALS, fALS	[19]
GluR2	AMPA receptor subunit	Altered RNA-editing	Ca^{2+}-permeable AMPA-R	High probability?	sALS	[152]

controlling mRNA transport of specific proteins. SMN is encoded by two highly homologous genes on chromosome 5, SMN1 and SMN2, but full-length transcripts are derived almost exclusively from the SMN1 gene because of a nucleotide replacement in exon 7 of SMN2 [49]. Homozygous deletions or loss-of-function mutations of SMN1 cause spinal muscular atrophy (SMA). In contrast, SMN2 is dispensable since it is homozygously deleted in 5-10% of the population. However, the presence of SMN2 attenuates disease in SMA patients [49]. A recent study indicates that homozygous SMN2 deletions are over-represented in patients with sporadic ALS and hence may form a risk factor for this disease [161]. However, others failed to reproduce these findings and instead found heterozygous SMN1 deletions to correlate with ALS [89].

Another approach aimed at identifying susceptibility and pathogenic factors of ALS (and other neurodegenerative diseases) is the analysis of the proteomes and transcriptomes of ALS patients. Usually this is done with postmortem spinal cord and brain tissue, but as an alternative blood cells of living patients may be considered. One of the rationales underlying these approaches is the hope that the disease-inducing factors may leave a molecular signature in the tissue of ALS patients. Unfortunately, no consistent data providing new insights in the disease mechanisms have been reported so far (reviewed in [102]). The main problem associated with the analysis of postmortem spinal cord and brain tissue from ALS patients is that only tissue from end-stage disease can be analyzed, when there is complete tissue reorganization due to loss of neurons and proliferation of glial cells. This causes a complete reshuffling of the proteome and transcriptome. Accordingly, analysis of protein and mRNA expression in the spinal cord of SOD1-ALS mice shows that at end stage disease many neuron and glia-specific proteins show a differential expression, whereas prior to disease onset no changes in gene expression have occurred (Jaarsma, non-published observations; [102]). One way to resolve this problem is to selectively isolate mRNA from surviving motoneurons using the laser capture technique [98].

1.2   Disease mechanisms in sporadic and familial ALS

Many pathological mechanisms have been suggested to play a role in the etiology of sporadic ALS, including virus intoxication, autoimmunity, heavy metal intoxication, accumulation of oxidative stress mediated damage, accumulation of misfolded and aggregated proteins (proteolytic stress), excessive excitation of motoneurons (excitotoxicity), abnormalities in intracellular transport, abnormal activation of cell death pathways, lack of trophic support, and insufficient mitochondrial function [22,132]. It has been repeatedly proposed that several of these pathogenetic factors may operate together or sequentially and that therapeutic approaches should be designed to target all these different factors [22,132]. Below we will discuss the hypotheses that have been most influential in the past decade.

1.2.1 Impaired retrograde trafficking

The genetic defects identified so far in ALS and other diseases of upper and lower motoneurons (tables 1 and 2) can be grossly linked to a number of related cell biological processes, i.e. intracellular transport (p150 dynactin, KIF1B, kinesin heavy chain (KIF5A), alsin, spartin, spastin, atlastin, VAPB, seipin; mitofusin, rab7, SMN, NIPA1); RNA-processing and transport (SETX, SMN, GARS) cytoskeleton maintenance (neurofilament L, neurofilament H, lamin, L1-CAM, Hsp27); and mitochondrial maintenance and transport (Hsp60, mitofusin1, paraplegin, SOD1). The many mutations involved in intracellular transport are consistent with the notion that transport may represent the Achilles heel of long-axon neurons like motoneurons [69,70].

The long distance transport machinery of neurons (and other cells) consists of multiple anterograde motor proteins, the kinesin superfamily proteins (KIFs), which transport their cargo from the cell body to the periphery, and one retrograde motor complex, the dynein-dynactin complex [69,70]. The specificity, direction and dynamics of the transport of different types of cargo depend on cargo-specific adaptors and a network of regulatory factors. Knowledge about the control of motors-cargo interactions is still preliminary [69,70]. It is important to note that abnormalities in anterograde transport do not lead to motoneuron death but cause diseases of the axon and usually affect both sensory and motor neurons (table 1). In contrast, several lines of evidence have linked impaired dynein-dynactin dependent (i.e. retrograde) trafficking to ALS. 1) mutations in the p150 dynactin subunit have been identified in ALS and late onset SMA patients [116,123]. 2) Mutations in dynein causing impaired retrograde axonal transport cause motor neuron disease in two lines of induced mouse mutants [62]. 3) Overexpression of the p50 dynactin subunit (dynamitin), which impairs dynactin trafficking, causes motoneuron disease in mice [92]. 4) Dynein-dynactin plays an important role in proteolytic waste product management by transporting misfolded and aggregated proteins to the cell body [85]. This links misfolded protein stress (see below) to impaired retrograde trafficking. 5) Abnormalities in dynein-dynactin trafficking can be induced by expressing mutant SOD1 *in vitro* and has also been observed in mutant SOD1 mice [22,80]. 6) Finally, aberrant neurofilament aggregation, a common pathological hallmark in ALS motoneurons, has been linked to abnormal dynein trafficking [22]. Why impairment of dynein trafficking selectively afflicts motoneurons is not understood. A possible explanation is that motoneurons more than other cells depend on retrograde trophic signaling [69,70].

1.2.2 Misfolded protein stress

Improperly folded and unfolded proteins are an inevitable byproduct of protein synthesis and degradation. Misfolded proteins also arise through oxidation, isomerization, or glycation and by transcriptional or translational errors [148,166]. Unfolded proteins are potentially dangerous since they can engage in non-native interactions and aggregate to form oligomeric complexes that are insoluble and metabolically stable, ultimately harm the cell [148,166]. To prevent damage from unfolded and aggregated protein the cell has a quality control machinery that consists of 1) molecular chaperones that chaperone nascent and unfolded proteins

Box 1: The ubiquitin-proteasome (UPS) proteolytic system

The degradation of proteins plays an important role in many cellular processes like cell division and differentiation, stress responses, transcription regulation and biogenesis of organelles. Proteins can be degraded by two different systems. The lysosomal system is mainly involved in degradation of extracellular proteins, while intracellular and cell surface proteins are mostly degraded by the ubiquitin-proteasome system (UPS). The UPS works in two main steps: polyubiquitination of proteins and subsequent degradation of ubiquitinated proteins by the proteasome.

Ubiquitination is a multi-step process in which ubiquitin is coupled to a substrate protein that is coupled to a protein from the E3 enzyme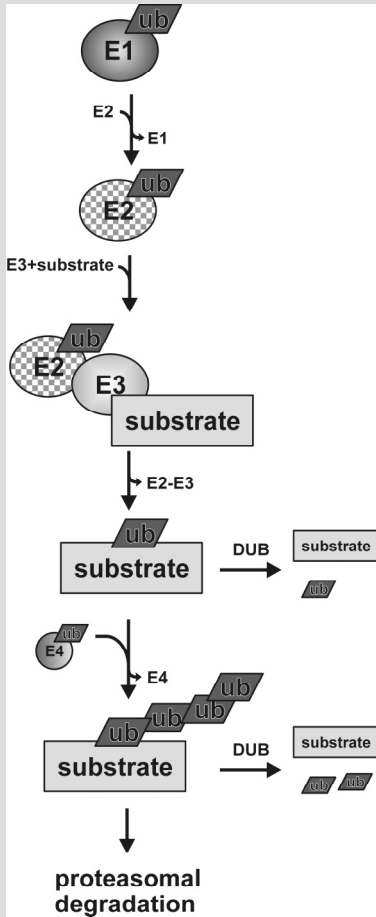 family (see figure a). The E3 enzymes, sometimes with the help of other proteins, recognize which proteins are candidates for degradation. Substrate proteins are recognized for example because they are phosphorylated or oxidized, their NH_2-terminal is modified, or because they are already bound to an intermediary protein (e.g. a molecular chaperone). How mutated and misfolded proteins are recognized is still unknown, but it has been hypothesized that the exposure of hydrophobic domains is a factor. Once one ubiquitin protein is attached to a protein more ubiquitin is attached to that complex by ubiquitin chain assembly factors (E4s), forming a poly-ubiquitin chain. Ubiquitination can be reversed: de-ubiquitinating enzymes (DUBs) can specifically cleave ubiquitin from substrates, thereby preventing degradation of specific proteins. [45,52,111].

Figure a: E1, E2, E3, and E4 enzymes work together to connect ubiquitin (ub) to substrate proteins. De-ubiquitinizing proteins can remove ub from substrates, preventing their degradation.

Once the substrate-protein is ubiquitinated, the actual degradation is performed by the proteasome. The proteasome cleaves proteins into peptides varying between 3 and 23 amino acids long. The proteasome consists of multiple proteins; the 20S proteasome, which is the catalytic part of the proteasome, and a regulatory protein complex. The *20S proteasome* consists of a stack of four rings, making it barrel-shaped (see figure b). The proteasome has 3 different types of proteolytic active sites (each with a preference for different cleavage sites) that face the core of the barrel. Without regulatory proteins the channel through the proteasome is internally blocked, but even if the channel is forced in an open conformation the 20S proteasome alone can only degrade small peptides and some unfolded proteins. [10,52,65].
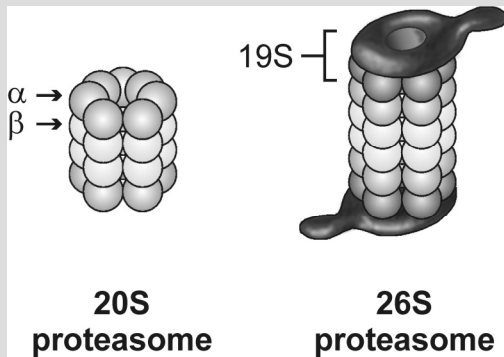
Figure b: The main catalytic part of the proteasome, the 20S proteasome, is a barrel-shaped protein consisting of 2 x 7 α subunits and 2x 7 β subunits. The 20S proteasome can together with the 19S regulatory complex form the 26S proteasome, which has full proteolytic functionality.

The *19S regulatory complex* (PA700) is involved in recognition of poly-ubiquitinated proteins, unfolding the substrate protein and feeding the protein into the 20S proteasome. The 19S regulatory complex may also be involved in closing of the opening of the barrel, in that way inhibiting proteolysis. The 20S and 19S together form a complex that is also known as the 26S proteasome. Mammalian cells also contain another regulatory complex that associates with the 20S proteasome: the *11S regulator* (PA28). Unlike the 19S complex, 11S does not catalyze the degradation of large proteins. Evidence indicates a role for the 11S complex in promoting the production of antigenic peptides or perhaps in facilitating the delivery of peptides to the lumen of the endoplasmic reticulum. In some cases the proteasome consists of 19S-20S-11S complexes forming a hybrid proteasome [1,10,38].

and assist in their folding or refolding; 2) the ubiquitin proteasome proteolytic pathway that recognizes and degrades misfolded proteins (see box 1); and 3) the aggresome-autophagosome pathway that degrades aggregated proteins [86,108,140,171]. The rate of misfolded protein production can increase markedly upon exposure of cells to oxidative or thermal stress, or increase as a result of mutations, and in these conditions the amount of misfolded protein production may exceed the capacity of the protein quality control machinery, disturb cell function and induce cell death [140].

Several disorders including most neurodegenerative disorders (Alzheimer's disease, Parkinson's disease, Huntington's disease, several cerebellar ataxias, and ALS) are characterized by the presence of insoluble aggregates of proteins that are deposited in intracellular inclusions or extracellular plaques, which generally are characteristic for the diseases. This and other findings have led to the notion that most neurodegenerative diseases are misfolded protein disorders (also termed conformational disorders), where accumulation of misfolded aggregate-prone proteins is the central pathogenic event. Mechanisms by which misfolded and aggregated proteins may afflict cell function include trapping of essential proteins, inhibition of the proteolytic and quality control machinery, induction of apoptotic pathways, or hindrance of transport processes. It should be noted that although the presence of inclusions containing aggregated proteins are a sign of misfolded protein stress, these inclusions themselves do not necessarily harm the cell, but may also reflect a protective response of the cell to detoxify aggregated proteins [86,140]. For instance Lewy bodies as identified in Parkinson's disease may

represent aggresomes, an organelle that 'stores' aggregated proteins prior to degradation by the autophagosome pathway [86,108,171].

A number of data indicate that misfolded protein stress may contribute to the pathogenesis of ALS: 1) Ubiquitinated structures, consisting of irregular loosely arranged bundles ('skeins') or spherical inclusions, are a constant and pathognomic feature in ALS [95]. Ultrastructurally, these ubiquitinated structures consist of various types of filamentous or amorphous material consistent with protein aggregation. In SOD1-linked ALS patients inclusions contain mutant SOD1 [141], but in sporadic ALS patients SOD1 usually is not present in ubiquitinated structures. 2) In the case of SOD1 mutations conformational instability and an increased propensity to aggregate is the only property shared by the more than 110 mutant forms of SOD1 that are linked to ALS [157]. 3) Ubiquitinated and non-ubiquitinated aggregates of SOD1 are a constant feature prior to the death and disappearance of motoneurons in transgenic mutant SOD1 mice (see chapters 4 and 5). However, the presence of ubiquitinated structures in mutant SOD1 mice should be interpreted with care since studies in chimeric mutant SOD1 mice (see below) have shown that also motoneurons that do not express mutant SOD1 may become strongly immunoreactive for ubiquitin ([32]; see also discussion of chapter 5). 4) Because of their size and high metabolic activity motoneurons may be relatively vulnerable to misfolded protein stress. In addition, there is evidence suggesting that motoneurons are relatively deficient in protein-quality control management, since they show a high threshold for induction of heat shock protein 70 (Hsp70), a stress inducible factor that can detoxify misfolded proteins including mutant SOD1 [11]. However, this does not explain the selective vulnerability of motoneurons towards mutant SOD1, since Hsp70 is not induced in any cell in mutant SOD1 mice with the exception of very sick motoneurons (see chapter 5), whereas motoneurons are among the few cells in the brain that express high levels of another heat shock protein, the small heat shock protein Hsp27, that can 'detoxify' mutant SOD1 (see chapter 4).

1.2.3 Oxidative stress

Oxidative stress is implicated in the pathogenesis of both normal aging and neurodegenerative diseases. Oxidative stress is a condition where the concentration of oxidants in the cell is higher than normal. Most oxidants are free radicals which are molecules containing at least one unpaired electron. Free radicals have an intrinsic 'need' to gain or lose an electron and in that process they can damage almost everything in the cell, including proteins, membranes, and DNA. Because of cellular metabolism most biological free radicals contain oxygen. Other oxygen-containing molecules like hydrogen peroxide (H_2O_2) and peroxynitrite ($ONOO^-$) can easily form oxygen free radicals and are therefore together with oxygen free radicals called reactive oxygen species (ROS). ROS are formed as a by-product of normal mitochondrial metabolism and are sometimes even produced specifically for physiological functions. An example of this is the production of $NO^{\bullet}$ by nitric oxide synthases, which has a function in neurotransmission, vascular relaxation and in inflammatory processes [12]. Free radical scavenging proteins like SOD1, mitochondrial manganese SOD (SOD2), catalase, and cytochrome c can neutralize free radicals but this cannot prevent cellular damage by ROS. It has

been shown that during normal aging the amount of damage caused by oxidative stress increases [120,146]. The rate of oxidation of proteins increases dramatically in the last decades of life, such that an average of 1 in 3 proteins is affected [12]. Some of the processes involved in normal aging are thought to be caused by this oxidative damage. Since ROS seem to be selective in inactivating particular proteins preferentially [9,101], it is possible that oxidative stress is involved in degenerative processes in neurodegenerative diseases like Alzheimer's disease, Parkinson's disease, and ALS. Levels of damaged proteins are higher in these diseases than in age-matched controls [2,66,138] indicating that oxidative stress is taking place.

One toxic effect of oxidative stress is the oxidation of amino acids, e.g. the carbonylation of lysine, proline, arginine, and threonine, the glycoxidation of lysine, and the nitration of tyrosine [156]. Products of these processes have been found in both familial ALS and sporadic ALS patients, and much attention has been paid especially to tyrosine nitration (see chapter 2). Because 3-nitrotyrosine is bulkier and more hydrophilic than tyrosine, nitration of protein-linked tyrosine residues can impair the function of proteins [14,55,136]. Nitration of tyrosine is caused by a sub-group of the ROS that is called the reactive nitrogen species (RNS). $ONOO^-$ is the reactive nitrogen species thought to be responsible for the formation of most 3-nitrotyrosine under physiological conditions. RNS mediated toxic actions have been considered as a dominant pathogenic factor in SOD1-linked ALS [14,55,136]. However, several lines of evidence including data presented in this thesis (see chapter 2) favor against their involvement in SOD1-ALS pathogenesis.

1.2.4   Mitochondrial dysfunction

There are now several observations which suggest that energy metabolism, and more specifically mitochondria, are involved in ALS. Abnormalities in mitochondrial function have been found in familial ALS- and some sporadic ALS patients [17,18,20]. In ALS-mutant SOD1 mice swelling and vacuolization of mitochondria are the first signs of pathology [76]. Oxidative stress and mitochondrial dysfunction are strongly interlaced, since oxidative stress can cause mitochondrial dysfunction [27,172] and vice versa free radical production can directly and indirectly be caused by mitochondrial (dys)function [41,107].

1.2.5   Glutamate excitotoxicity

This hypothesis poses that excessive synaptic glutamate has a toxic effect on motoneurons. Elevated glutamate levels have been found in at least a subset of ALS patients [129,137]. This could be explained by a selective loss of the astroglial glutamate transporter EAAT-2 in spinal cord and motor cortex of ALS patients [130]. This means that less glutamate is removed from the synaptic cleft after neurotransmission, which can lead to over-activation of the post-synaptic glutamate receptors. The specific vulnerability of motoneurons in comparison with other glutamatergic neurons can be explained by a difference in the combination of subunits that form the AMPA-type glutamate receptor. The AMPA-receptor in human motoneurons lacks the GluR2 subunit [139,167], which normally makes the ion channel from this receptor Ca^{2+}-impermeable. This means that activation of the

AMPA receptor by excessive amounts of glutamate cause a high rise in $[Ca^{2+}]_i$, which does not happen in other types of neurons.

Several therapies to either reduce the amount of glutamate or inhibit the AMPA-type glutamate receptor have had moderate effects on the survival of mutant SOD1-ALS mice [25,50,59,145,158]. Only 2 of those have been tested in clinical trial with ALS-patients. Riluzole inhibits pre-synaptic glutamate release, but has also been shown to inhibit NMDA-type and AMPA-type glutamate receptors [3,39]. Clinical trials showed that riluzole can slow the progression of ALS, and improve survival by several months [15,90]. However, topiramate, another anti-exitotoxic drug that has the ability to diminish pre-synaptic glutamate release and antagonizes the activation of the AMPA-type glutamate receptor by kainate [144], had no effect on the survival of SOD1-ALS mice [104]. Furthermore, it had a negative effect in ALS patients [34].

1.3   Experimental models in ALS research

Prior to the discovery of SOD1-mutations and the generation of SOD1-transgenic mice as a dominant ALS research model there was no good animal model for ALS. Several spontaneous mutant mouse lines (wobbler, pmn, wasted, mnd) were used in ALS research, but their phenotype was more consistent with early onset SMA or axonopathy and effects of drugs poorly predicted the effect in ALS patients (table 4). Recently, new mouse models have appeared based on abnormalities in dynein trafficking (table 4). Their value as disease models for ALS remains to be determined.The main characteristics of mutant SOD1-ALS mice are summarized below. Since a number of experiments have also been performed with motoneurons in culture, also different systems with cultured motoneurons are reviewed

1.3.1   SOD1-transgenic mice

After the discovery of SOD1-mutations in ALS, transgenic mice expressing mutant SOD1 were created [21,60,127,168]. The transgene constructs used for these mice consisted of 12 to 15-kb genomic fragments of the human [21,60,168] or mouse [127] SOD1 gene containing the glycine-93-to-alanine (G93A) [60], glycine-37-to-arginine (G37R) [168], or the arginine-85-to-alanine (G85R) [21] mutations, and in case of the murine SOD1 construct the arginine-86-to-alanine mutation (G86R, which corresponds to the G85R substitution in human SOD1) [127]. All these mice showed high-level expression of mutant SOD1 in all cells of the body, and they all developed an adult onset motoneuron disease [21,60,127,168]. The mice developed normally and non-motor systems were usually unaffected until a very late phase of disease [21,60,127,168].

In 1995 the G93A mice generated by Gurney et al. [60] were made commercially available by Jackson Laboratories and subsequently have become a tool in many ALS labs. All G93A mice reported in the literature are derived from the G1 line [60]. However, due to intra-locus recombination events, changes in the transgene copy

Table 4: Spontaneous and transgenic non-SOD1 mouse models for motoneuron diseases.

Mouse	Gene	Motor symptoms	Motoneurons	Inclusions	Remarks	Ref
dynein	dynein heavy chain 1	Homozygotes: letal <24 h postnatally. Heterozygotes: progressive motor weakness	>40% loss	-Homozygotes: Lewy body-like -Ubiquitin/neurofilament inclusions	Decreased fast retrograde axonal transport	[62]
Dynamitin (p50)	dynamitin	progressive motor weakness starting at 5-9 months	Swollen axons, loss of axons, moderate loss of cell bodies	-spheroid-like inclusions in axons	Delay of retrograde axonal transport	[92]
wasted	Eef1a2	Fast progressive motor weakness starting at 14-18 days. Death at 28-31 days	Vacuolization in cell bodies and axons. Loss of axons	-axonal neurofilament H aggregates	Eef1a2 codes for a translation elongation factor	[99] [28]
pmn	Tbce	Fast progressive motor weakness starting at 2 weeks. Death around 40 days	Distal axonopathy: vacuolization and loss of axons. Minimal secondary cell body loss.	none	Normal myelination. Tbce: involved in the maintenance of microtubules in axons. Used as model for SMA	[135] [106]
Mnd	CLN8	Slow progressive motor weakness starting at 7-13 months. Death at 14-25 months	Minimal loss of cell bodies	-ubiquitin/neurofilament inclusions in cell body -lipofuscin accumulation	Also sensory symptoms. Function of CLN8 unknown. Used as a model for progressive epilepsy with mental retardation, and Batten's disease	[125]
wobbler	unknown	Slow progressive motor weakness starting at 3 weeks. Death at 4-11 months.	Vacuolization and cell body loss mainly in cervical spinal cord and brainstem. Axonopathy	none	Used as model for SMA	

number have generated different subtypes of G1-G93A mice (reviewed in [57]): The original G1-G93A mice have 25 transgene copies, develop motor symptoms at 90 days of age, and die at 135 days of age. These mice are often referred to as the G1H mice and are used in most studies with G93A mice. Another subline of G1-G93A mice used in many laboratories, including ours, has 8 transgene copies, develops muscle weakness at 6-8 months and dies 6-8 weeks after symptom onset [79,87]. This line is referred to as the G1del or the low-copy G1 line, and is sometimes confused with the G1L line, which is a second 'low-copy' line with about 18 transgene copies that has been used in a highly cited paper on the effects of Riluzole, gabapentin and vitamin E on survival of G93A mice [58]. Our G1del colony bred at the Erasmus MC in a FVB background has shown a stable phenotype for over 40 generations. Nevertheless, in view of the possibility of recombination events, it is important to keep track of survival of the mice used for breeding [57]. The low and high-copy G1 sublines each have their specific advantages: The high copy line is suited for rapid screening of potential drugs because of their short survival. However, the high copy mice develop atypical neuropathological features that do not occur in other lines of SOD1-ALS mice and in human ALS patients. Hence for studies aimed at identifying disease mechanisms low copy mice are more suitable.

In addition to early lines of transgenic ALS-mutant SOD1 mice, more recently other lines of transgenic ALS mice have been reported (see table 5), and transgenic SOD1-ALS rats were generated [72,117]. The transgenic rat models show the same clinical and pathological features as transgenic SOD-ALS mice, but may be more suited to test interventional approaches requiring surgery, like for instance chronic intraventricular infusions.

Several important data have been obtained so far with ALS-SOD1 mice:

1) Within a single line there is a linear correlation between the level of transgene expression and the severity of motoneuron disease. This has been established by generating 'homozygote' transgenics [77] and by comparing distinct sublines of G1-G93A mice (see above; [5]). This linear relationship between the level of transgene expression and disease phenotype has some important implications: First, low expressing ALS-SOD1 lines may not develop disease within their normal life span. Second, any pharmacological or genetic intervention that influences transgene expression in motoneurons will affect survival of the mice. This may explain, for instance, why crossing mutant SOD1 mice with mutant mice with compromised motoneurons because of neurofilament abnormalities has a dramatic and surprisingly beneficial effect on survival [22].

2) Comparison between ALS-SOD1 transgenic expressing wild-type like mutant (G93A, G37R, D90A) and unstable mutants (G85R, G127X), respectively, show that the severity of disease does not correlate with the absolute levels of mutant SOD1 protein, since these mice show similar life spans in spite of more than a tenfold difference in the amount of mutant SOD1 protein. In fact, only minute quantities of mutant SOD1 protein are needed to express a phenotype as in G127X-SOD1-ALS mice [81].

Table 5:. Lines of mutant SOD1 ALS mice.

Mutation	Ratio mutant SOD1 / mouse SOD1	Motoneuron loss	Mitochondrial vacuolization	Ubiquitin pathology	Astrogliosis	Ref
Wild-type like						
G93A	3-6	yes	yes	yes	yes	[31,60]
G37R	5-12	yes	yes	yes	yes	[168]
D90A	10	yes	yes	yes	yes	[82]
Unstabe mutants						
G85R	0.8-1	yes	no	yes	yes	[21,114]
G127X	0.45-1	yes	no	yes	yes	[81]
Cu-binding site						
H46R + H48Q	3-5	yes	no	yes	yes	[165]
Quad His	3-5	yes	no	yes	yes	[164]
G93A + CCS knockout	3-6	yes	yes	yes	yes	[151]
Cell type specific						
Thy1.2-G93A	3-5 ?	no	no	none	no	[97]
Thy1.2-G85R	<1	no	no	none	no	[97]
NFL-G37R	3-4?	no	no	none	no	[122]
GFAP-G85R	?	no	no	none	yes	[54]

3)   Studies with chimeric SOD1-ALS mice, generated by injecting non-transgenic embryonic stem cells in blastocysts from G85R or G93A mice or by fusion of non-transgenic and transgenic morulae, have shown that motoneuron degeneration in SOD1-ALS mice strongly depends on mutant SOD1 expression in surrounding glial cells. Furthermore, data from some chimeric mice indicate that also motoneurons that do not express mutant SOD1 may die, because of mutant SOD1 expression in surrounding cells [32]. These data indicate that toxicity to motoneurons requires damage from mutant SOD1 acting within non-neuronal cells. The same conclusions have been drawn from studies with transgenic mice in which mutant SOD1 expression is driven by cell specific promoters. These studies showed neuron-specific [97,122] nor glia-specific [54] expression of mutant SOD1 was sufficient to cause motor neuron disease. These studies, however, were not conclusive since the level of mutant SOD1 expression in these cell-specific transgenic mice may have been too low to induce disease.

4)   A series of studies including experiments in yeast and a study with mice deficient in copper chaperone for SOD1 (CCS) have shown that CCS is a critical protein for the delivery of the catalytic copper in SOD1 [169]. CCS has two

domains. The N-terminal domain is very similar to the metallochaperone protein Atx1 and likely plays a role in copper delivery and/or uptake. The second domain is homologous to SOD1 and is involved in the recognition of SOD1. CCS knockout mice possess normal levels of SOD1 protein, but have marked reductions in SOD1 activity [169]. Importantly, crossing mutant SOD1 transgenes into CCS knockout mice does not influence disease progression and survival [151]. These findings challenge hypotheses suggesting that mutant-SOD1 toxicity is linked to abnormal catalytic copper-mediated activities of mutant SOD1, although alternative sources of copper have been proposed for SOD1 [13].

Mutations in the copper-binding site (H46R and H48Q) have been found in ALS-patients. Transgenic mice expressing mutant SOD1 containing both these mutations [165], or SOD1 in which all histidine residues in the copper-binding site have been mutated (Quad His-SOD1) [164] also develop motoneuron disease. Together the data indicate the toxicity of mutant SOD1 is not linked to the presence of the catalytic copper.

5)   A constant feature among distinct lines of SOD1-ALS mice is the age-related accumulation of oligomeric and aggregated SOD1 species, and the appearance of ubiquitinated structures prior to the onset of motoneuron degeneration [22]. The subcellular localization of oligomeric and aggregated SOD1 species is still poorly understood. However, abnormal SOD1 in part is associated with mitochondria [79]. Hence, mitochondria may be the primary target of mutant-SOD1 toxicity. Another part of abnormal SOD1 is associated with ubiquitinated structures that appear prior to the onset of motoneuron degeneration. The precise identity of these ubiquitinated structures and their role in motoneuron degeneration is still poorly understood (see chapters 4 and 5).

6)   All transgenic ALS-SOD1 mice, like many familial SOD1-ALS patients, develop a 'lower-motoneuron-first disease'. Thus in an early 'preclinical' phase of disease prior to the onset of motor symptoms, neurodegenerative changes are predominantly associated with α-motoneurons. In a late phase of disease neurodegenerative changes also spread to specific subsets of 'pre-motoneurons' and glia [77-79,100].

1.3.2   Motoneurons in culture

In addition to *in vivo* models, a number of techniques to study motoneurons in culture have been used in ALS research. These *in vitro* systems offer an ease of manipulation by the possibility of direct pharmacological administration or simple gene transfections that cannot be attained in live animals.

Neuroblastoma cell lines are derived from tumors composed of cells derived from precursors of the autonomic nervous system, and are capable of unlimited proliferation *in vitro*. These cell lines have the ability to differentiate into neuronal cell types after treatment with various agents. The advantage of using neuroblastoma cell lines is that they proliferate and can be used for a long time. The disadvantage is that, although it is possible to differentiate the cells to specific neuron types, it is not sure that those cells will may ever get the same characteristics as differentiated neurons since they originate from tumor cells.

Primary cultures of motoneurons are usually derived from embryonic mouse or rat spinal cord, although newborn animals can also be used [7,24]. The isolation of motoneurons is based on differences between the buoyant density of motoneurons and other cells. Large motoneurons stay afloat on a cushion of dense material while being centrifuged whereas smaller neurons sink into the cushion [24,84]. This method results in cultures that consist of ~95% neurons with ~80% motoneurons. Sometimes this selection is combined with a cell selection method using antibodies to the p75 growth factor receptor only present on motoneurons, which enriches the cultures to ~95% motoneurons [24]. Although working with motoneuron *monocultures* makes it easy to experiment with motoneurons without the influence of glia, a very big disadvantage is that motoneurons in these cultures survive only for ~4 days. The survival can be extended for 3 more days by adding neurotrophic factors (usually in the form of horse blood serum or embryonic chicken muscle extract) to the cultures [84]. If the conditions in which the motoneurons are cultured are closer to the natural conditions the survival increases. This can be achieved by combining the motoneuron cultures with glial cultures, which is usually done by growing the motoneurons on a layer of glia (direct glial-neuronal contact). Neurons in these *co-cultures* seem healthier because they develop larger cell bodies, extensively branched dendrites and an axon-like process, which are all less developed in monocultures [160]. Survival in these cultures is ~2 weeks. These cultures are very useful in acute studies but if more chronic effects, which might be of importance in slow degenerative processes, have to be studied than the survival is too short. Furthermore the relationship between neurons and glia is still non-natural in these co-cultures.

Organotypic spinal cord cultures consist of 350 µm thick slices of spinal cord from 5-9-day-old mice or rats. The first method that was developed was the organotypic *roller tube culture* [37]. The slices are attached on a glass coverslip using a combination of chicken plasma and thrombin. The coverslip with the slice is then placed inside a culture tube that is incubated in a roller drum. Because the tube is rotated at an angle the culture media that is placed in the tube flows over the slice with every rotation while the rest of the time the slice is exposed to the air in the tube. The other technique is the organotypic *interface technique*, which was developed by Stoppini et al. [150]. In these cultures the slices of spinal cord grow on a membrane; on the interface of CO_2-enriched air and fluid, providing the tissue with sufficient access to both culture medium and oxygen (see fig 2). If the roller tube and interface technique are compared there is less glial proliferation in interface cultures than in roller tube cultures. When using this method tissues retain an adequate three-dimensional organization [23].
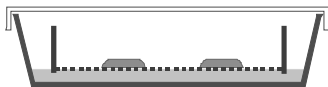

Figure 2: Side-view of a culture dish. Spinal cord slices are cultured on a microporous membrane (dotted line), which is placed in a dish containing culture medium

1.4 Outline of this thesis

As explained in this introduction multiple factors have been implicated in SOD1-linked and sporadic ALS. The overall aim of the studies in this thesis to unravel factors that contribute to the pathogenesis in SOD1-ALS mice, focusing on two potential pathogenic factors: oxidative stress and misfolded protein stress. The study in *chapter 2* was intended to further clarify the role of reactive nitrogen species in ALS. Reactive nitrogen species have been frequently implicated in the pathogenesis of SOD1-linked and sporadic ALS. Evidence favoring this hypothesis predominantly consists of the demonstration of nitrosylated tyrosine residues in post-mortem tissue. However, increased tyrosine nitrosylation in SOD1-ALS mice predominantly affects free nitrotyrosine residues. We show that these free 3-nitrotyrosine residues, even at high doses, are harmless to the cell. In the studies presented in this thesis we use this mouse model

The studies in *chapters 3 to 5* were aimed to clarify the role of proteolytic stress in SOD1-ALS mice. The proteolytic stress hypothesis is partly triggered by the presence of ubiquitinated structures in motoneurons of ALS patients suggestive of abnormalities in the ubiquitin-proteasome proteolytic pathway. In *chapter 3* we have studied the effect of prolonged mild proteasome inhibition in spinal cord organotypic cultures of normal and SOD1-ALS mice. In *chapter 4* we show that simultaneously with the appearance of ubiquitinated pathology in SOD1-ALS mice there is a reduction in expression of the heat shock protein Hsp27, a multifunctional protein that may protect cells against misfolded and aggregated proteins. In *chapter 5* using immunohistological techniques we have correlated the appearance of ubiquitinated structures with the expression of injury transcription factors in motoneurons. As discussed in *chapter 6*, together the data indicate that reactive nitrogen species do not play a significant role in motoneuron degeneration in SOD1-ALS mice, whereas abnormalities in protein quality control machinery occur relatively early in the degeneration process.

References

[1]   J. Adams, The proteasome: a suitable antineoplastic target, Nat Rev Cancer 4 (2004) 349-360.
[2]   Z.I. Alam, S.E. Daniel, A.J. Lees, D.C. Marsden, P. Jenner, B. Halliwell, A generalised increase in protein carbonyls in the brain in Parkinson's but not incidental Lewy body disease, J Neurochem 69 (1997) 1326-1329.
[3]   F. Albo, M. Pieri, C. Zona, Modulation of AMPA receptors in spinal motor neurons by the neuroprotective agent riluzole, J Neurosci Res 78 (2004) 200-207.
[4]   A. Al-Chalabi, P.M. Andersen, P. Nilsson, B. Chioza, J.L. Andersson, C. Russ, C.E. Shaw, J.F. Powell, P.N. Leigh, Deletions of the heavy neurofilament subunit tail in amyotrophic lateral sclerosis, Hum Mol Genet 8 (1999) 157-164.
[5]   G.M. Alexander, K.L. Erwin, N. Byers, J.S. Deitch, B.J. Augelli, E.P. Blankenhorn, T.D. Heiman-Patterson, Effect of transgene copy number on survival in the G93A SOD1 transgenic mouse model of ALS, Brain Res Mol Brain Res 130 (2004) 7-15.
[6]   P.M. Andersen, K.B. Sims, W.W. Xin, R. Kiely, G. O'Neill, J. Ravits, E. Pioro, Y. Harati, R.D. Brower, J.S. Levine, H.U. Heinicke, W. Seltzer, M. Boss, R.H. Brown, Jr., Sixteen novel mutations in the Cu/Zn superoxide dismutase gene in amyotrophic lateral sclerosis: a decade of discoveries, defects and disputes, Amyotroph Lateral Scler Other Motor Neuron Disord 4 (2003) 62-73.
[7]   K.N. Anderson, A.C. Potter, L.G. Piccenna, A.K. Quah, K.E. Davies, S.S. Cheema, Isolation and culture of motor neurons from the newborn mouse spinal cord, Brain Res Brain Res Protoc 12 (2004) 132-136.
[8]   A. Antonellis, R.E. Ellsworth, N. Sambuughin, I. Puls, A. Abel, S.Q. Lee-Lin, A. Jordanova, I. Kremensky, K. Christodoulou, L.T. Middleton, K. Sivakumar, V. Ionasescu, B. Funalot, J.M. Vance, L.G. Goldfarb, K.H. Fischbeck, E.D. Green, Glycyl tRNA synthetase mutations in Charcot-Marie-Tooth disease type 2D and distal spinal muscular atrophy type V, Am J Hum Genet 72 (2003) 1293-1299.
[9]   K.S. Aulak, M. Miyagi, L. Yan, K.A. West, D. Massillon, J.W. Crabb, D.J. Stuehr, Proteomic method identifies proteins nitrated in vivo during inflammatory challenge, Proc Natl Acad Sci U S A 98 (2001) 12056-12061.
[10]   M. Bajorek, M.H. Glickman, Keepers at the final gates: regulatory complexes and gating of the proteasome channel, Cell Mol Life Sci 61 (2004) 1579-1588.
[11]   Z. Batulan, G.A. Shinder, S. Minotti, B.P. He, M.M. Doroudchi, J. Nalbantoglu, M.J. Strong, H.D. Durham, High threshold for induction of the stress response in motor neurons is associated with failure to activate HSF1, J Neurosci 23 (2003) 5789-5798.
[12]   M.F. Beal, Oxidatively modified proteins in aging and disease, Free Radic Biol Med 32 (2002) 797-803.
[13]   J.S. Beckman, A.G. Esetvez, L. Barbeito, J.P. Crow, CCS knockout mice establish an alternative source of copper for SOD in ALS, Free Radic Biol Med 33 (2002) 1433-1435.
[14]   J.S. Beckman, W.H. Koppenol, Nitric oxide, superoxide, and peroxynitrite: the good, the bad, and ugly, Am J Physiol 271 (1996) C1424-1437.
[15]   G. Bensimon, L. Lacomblez, V. Meininger, A controlled trial of riluzole in amyotrophic lateral sclerosis., N Engl J Med 330 (1994) 585-591.
[16]   C.F. Boerkoel, H. Takashima, C.A. Garcia, R.K. Olney, J. Johnson, K. Berry, P. Russo, S. Kennedy, A.S. Teebi, M. Scavina, L.L. Williams, P. Mancias, I.J. Butler, K. Krajewski, M. Shy, J.R. Lupski, Charcot-Marie-Tooth disease and related neuropathies: mutation distribution and genotype-phenotype correlation, Ann Neurol 51 (2002) 190-201.
[17]   G.M. Borthwick, M.A. Johnson, P.G. Ince, P.J. Shaw, D.M. Turnbull, Mitochondrial enzyme activity in amyotrophic lateral sclerosis: implications for the role of mitochondria in neuronal cell death, Ann Neurol 46 (1999) 787-790.
[18]   A.C. Bowling, J.B. Schulz, R.H. Brown, Jr., M.F. Beal, Superoxide dismutase activity, oxidative damage, and mitochondrial energy metabolism in familial and sporadic amyotrophic lateral sclerosis, J Neurochem 61 (1993) 2322-2325.
[19]   L.A. Bristol, J.D. Rothstein, Glutamate transporter gene expression in amyotrophic lateral sclerosis motor cortex, Ann Neurol 39 (1996) 676-679.
[20]   S.E. Browne, A.C. Bowling, M.J. Baik, M. Gurney, R.H. Brown, Jr., M.F. Beal, Metabolic dysfunction in familial, but not sporadic, amyotrophic lateral sclerosis, J Neurochem 71 (1998) 281-287.
[21]   L.I. Bruijn, M.W. Becher, M.K. Lee, K.L. Anderson, N.A. Jenkins, N.G. Copeland, S.S. Sisodia, J.D. Rothstein, D.R. Borchelt, D.L. Price, D.W. Cleveland, ALS-linked SOD1 mutant G85R mediates

damage to astrocytes and promotes rapidly progressive disease with SOD1-containing inclusions, Neuron 18 (1997) 327-338.

[22]   L.I. Bruijn, T.M. Miller, D.W. Cleveland, Unraveling the Mechanisms Involved in Motor Neuron Degeneration in ALS, Annu Rev Neurosci 27 (2004) 723-749.

[23]   P.A. Buchs, L. Stoppini, D. Muller, Structural modifications associated with synaptic development in area CA1 of rat hippocampal organotypic cultures, Brain Res Dev Brain Res 71 (1993) 81-91.

[24]   W. Camu, C.E. Henderson, Purification of embryonic rat motoneurons by panning on a monoclonal antibody to the low-affinity NGF receptor, J Neurosci Methods 44 (1992) 59-70.

[25]   T. Canton, G.A. Bohme, A. Boireau, F. Bordier, S. Mignani, P. Jimonet, G. Jahn, M. Alavijeh, J. Stygall, S. Roberts, C. Brealey, M. Vuilhorgne, M.W. Debono, S. Le Guern, M. Laville, D. Briet, M. Roux, J.M. Stutzmann, J. Pratt, RPR 119990, a novel alpha-amino-3-hydroxy-5-methyl-4-isoxazolepropionic acid antagonist: synthesis, pharmacological properties, and activity in an animal model of amyotrophic lateral sclerosis, J Pharmacol Exp Ther 299 (2001) 314-322.

[26]   G. Casari, M. De Fusco, S. Ciarmatori, M. Zeviani, M. Mora, P. Fernandez, G. De Michele, A. Filla, S. Cocozza, R. Marconi, A. Durr, B. Fontaine, A. Ballabio, Spastic paraplegia and OXPHOS impairment caused by mutations in paraplegin, a nuclear-encoded mitochondrial metalloprotease, Cell 93 (1998) 973-983.

[27]   A. Cassina, R. Radi, Differential inhibitory action of nitric oxide and peroxynitrite on mitochondrial electron transport, Arch Biochem Biophys 328 (1996) 309-316.

[28]   D.M. Chambers, J. Peters, C.M. Abbott, The lethal mutation of the mouse wasted (wst) is a deletion that abolishes expression of a tissue-specific isoform of translation elongation factor 1alpha, encoded by the Eef1a2 gene, Proc Natl Acad Sci U S A 95 (1998) 4463-4468.

[29]   P.H. Chan, M. Kawase, K. Murakami, S.F. Chen, Y. Li, B. Calagui, L. Reola, E. Carlson, C.J. Epstein, Overexpression of SOD1 in transgenic rats protects vulnerable neurons against ischemic damage after global cerebral ischemia and reperfusion, J Neurosci 18 (1998) 8292-8299.

[30]   Y.Z. Chen, C.L. Bennett, H.M. Huynh, I.P. Blair, I. Puls, J. Irobi, I. Dierick, A. Abel, M.L. Kennerson, B.A. Rabin, G.A. Nicholson, M. Auer-Grumbach, K. Wagner, P. De Jonghe, J.W. Griffin, K.H. Fischbeck, V. Timmerman, D.R. Cornblath, P.F. Chance, DNA/RNA helicase gene mutations in a form of juvenile amyotrophic lateral sclerosis (ALS4), Am J Hum Genet 74 (2004) 1128-1135.

[31]   A.Y. Chiu, P. Zhai, M.C. Dal Canto, T.M. Peters, Y.W. Kwon, S.M. Prattis, M.E. Gurney, Age-dependent penetrance of disease in a transgenic mouse model of familial amyotrophic lateral sclerosis, Mol Cell Neurosci 6 (1995) 349-362.

[32]   A.M. Clement, M.D. Nguyen, E.A. Roberts, M.L. Garcia, S. Boillee, M. Rule, A.P. McMahon, W. Doucette, D. Siwek, R.J. Ferrante, R.H. Brown, Jr., J.P. Julien, L.S. Goldstein, D.W. Cleveland, Wild-type nonneuronal cells extend survival of SOD1 mutant motor neurons in ALS mice, Science 302 (2003) 113-117.

[33]   P. Corcia, V. Mayeux-Portas, J. Khoris, B. de Toffol, A. Autret, J.P. Muh, W. Camu, C. Andres, Abnormal SMN1 gene copy number is a susceptibility factor for amyotrophic lateral sclerosis, Ann Neurol 51 (2002) 243-246.

[34]   M.E. Cudkowicz, J.M. Shefner, D.A. Schoenfeld, R.H. Brown Jr, Jr., H. Johnson, M. Qureshi, M. Jacobs, J.D. Rothstein, S.H. Appel, R.M. Pascuzzi, T.D. Heiman-Patterson, P.D. Donofrio, W.S. David, J.A. Russell, R. Tandan, E.P. Pioro, K.J. Felice, J. Rosenfeld, R.N. Mandler, G.M. Sachs, W.G. Bradley, E.M. Raynor, G.D. Baquis, J.M. Belsh, S. Novella, J. Goldstein, J. Hulihan, A randomized, placebo-controlled trial of topiramate in amyotrophic lateral sclerosis, Neurology 61 (2003) 456-464.

[35]   A. Cuesta, L. Pedrola, T. Sevilla, J. Garcia-Planells, M.J. Chumillas, F. Mayordomo, E. LeGuern, I. Marin, J.J. Vilchez, F. Palau, The gene encoding ganglioside-induced differentiation-associated protein 1 is mutated in axonal Charcot-Marie-Tooth type 4A disease, Nat Genet 30 (2002) 22-25.

[36]   A. De Sandre-Giovannoli, M. Chaouch, S. Kozlov, J.M. Vallat, M. Tazir, N. Kassouri, P. Szepetowski, T. Hammadouche, A. Vandenberghe, C.L. Stewart, D. Grid, N. Levy, Homozygous defects in LMNA, encoding lamin A/C nuclear-envelope proteins, cause autosomal recessive axonal neuropathy in human (Charcot-Marie-Tooth disorder type 2) and mouse, Am J Hum Genet 70 (2002) 726-736.

[37]   J. Delfs, J. Friend, S. Ishimoto, D. Saroff, Ventral and dorsal horn acetylcholinesterase neurons are maintained in organotypic cultures of postnatal rat spinal cord explants, Brain Res 488 (1989) 31-42.

[38]   Q. Ding, J.N. Keller, Proteasomes and proteasome inhibition in the central nervous system, Free Radic Biol Med 31 (2001) 574-584.

[39]   A. Doble, The pharmacology and mechanism of action of riluzole, Neurology 47 (1996) S233-241.

[40]   V.E. Drory, M. Birnbaum, A.D. Korczyn, J. Chapman, Association of APOE epsilon4 allele with survival in amyotrophic lateral sclerosis, J Neurol Sci 190 (2001) 17-20.

[41]   J.A. Dykens, Isolated cerebral and cerebellar mitochondria produce free radicals when exposed to elevated CA2+ and Na+: implications for neurodegeneration, J Neurochem 63 (1994) 584-591.

[42]   A.J. Elia, T.L. Parkes, K. Kirby, P. St George-Hyslop, G.L. Boulianne, J.P. Phillips, A.J. Hilliker, Expression of human FALS SOD in motorneurons of Drosophila, Free Radic Biol Med 26 (1999) 1332-1338.

[43]   O.V. Evgrafov, I. Mersiyanova, J. Irobi, L. Van Den Bosch, I. Dierick, C.L. Leung, O. Schagina, N. Verpoorten, K. Van Impe, E. Fedotov, E. Dadali, M. Auer-Grumbach, C. Windpassinger, K. Wagner, Z. Mitrovic, D. Hilton-Jones, K. Talbot, J.J. Martin, N. Vasserman, S. Tverskaya, A. Polyakov, R.K. Liem, J. Gettemans, W. Robberecht, P. De Jonghe, V. Timmerman, Mutant small heat-shock protein 27 causes axonal Charcot-Marie-Tooth disease and distal hereditary motor neuropathy, Nat Genet 36 (2004) 602-606.

[44]   E. Eymard-Pierre, G. Lesca, S. Dollet, F.M. Santorelli, M. di Capua, E. Bertini, O. Boespflug-Tanguy, Infantile-onset ascending hereditary spastic paralysis is associated with mutations in the alsin gene, Am J Hum Genet 71 (2002) 518-527.

[45]   S. Fang, A.M. Weissman, A field guide to ubiquitylation, Cell Mol Life Sci 61 (2004) 1546-1561.

[46]   J.K. Fink, S. Rainier, Hereditary spastic paraplegia: spastin phenotype and function, Arch Neurol 61 (2004) 830-833.

[47]   K.H. Fischbeck, Kennedy disease, J Inherit Metab Dis 20 (1997) 152-158.

[48]   D.G. Flood, A.G. Reaume, J.A. Gruner, E.K. Hoffman, J.D. Hirsch, Y.G. Lin, K.S. Dorfman, R.W. Scott, Hindlimb motor neurons require Cu/Zn superoxide dismutase for maintenance of neuromuscular junctions, Am J Pathol 155 (1999) 663-672.

[49]   T. Frugier, S. Nicole, C. Cifuentes-Diaz, J. Melki, The molecular bases of spinal muscular atrophy, Curr Opin Genet Dev 12 (2002) 294-298.

[50]   G.D. Ghadge, B.S. Slusher, A. Bodner, M.D. Canto, K. Wozniak, A.G. Thomas, C. Rojas, T. Tsukamoto, P. Majer, R.J. Miller, A.L. Monti, R.P. Roos, Glutamate carboxypeptidase II inhibition protects motor neurons from death in familial amyotrophic lateral sclerosis models, Proc Natl Acad Sci U S A (2003).

[51]   R. Giess, B. Holtmann, M. Braga, T. Grimm, B. Muller-Myhsok, K.V. Toyka, M. Sendtner, Early onset of severe familial amyotrophic lateral sclerosis with a SOD-1 mutation: potential impact of CNTF as a candidate modifier gene, Am J Hum Genet 70 (2002) 1277-1286.

[52]   M.H. Glickman, A. Ciechanover, The ubiquitin-proteasome proteolytic pathway: destruction for the sake of construction, Physiol Rev 82 (2002) 373-428.

[53]   C. Goizet, R.B. Yaou, L. Demay, P. Richard, S. Bouillot, M. Rouanet, E. Hermosilla, G. Le Masson, A. Lagueny, G. Bonne, X. Ferrer, A new mutation of the lamin A/C gene leading to autosomal dominant axonal neuropathy, muscular dystrophy, cardiac disease, and leuconychia, J Med Genet 41 (2004) e29.

[54]   Y.H. Gong, A.S. Parsadanian, A. Andreeva, W.D. Snider, J.L. Elliott, Restricted expression of G86R Cu/Zn superoxide dismutase in astrocytes results in astrocytosis but does not cause motoneuron degeneration, J Neurosci 20 (2000) 660-665.

[55]   S.A. Greenacre, H. Ischiropoulos, Tyrosine nitration: localisation, quantification, consequences for protein function and signal transduction, Free Radic Res 34 (2001) 541-581.

[56]   K. Grohmann, M. Schuelke, A. Diers, K. Hoffmann, B. Lucke, C. Adams, E. Bertini, H. Leonhardt-Horti, F. Muntoni, R. Ouvrier, A. Pfeufer, R. Rossi, L. Van Maldergem, J.M. Wilmshurst, T.F. Wienker, M. Sendtner, S. Rudnik-Schoneborn, K. Zerres, C. Hubner, Mutations in the gene encoding immunoglobulin mu-binding protein 2 cause spinal muscular atrophy with respiratory distress type 1, Nat Genet 29 (2001) 75-77.

[57]   M.E. Gurney, Transgenic animal models of familial amyotrophic lateral sclerosis, J Neurol 244 (1997) S15-S20.

[58]   M.E. Gurney, F.B. Cuttings, P. Zhai, A. Doble, C.P. Taylor, P.K. Andrus, E.D. Hall, Benefit of Vitamine E, Riluzole, and gabapentin in a transgenic model of familial amyotrophic lateral sclerosis, Ann. Neurol. 39 (1996) 147-157.

[59]   M.E. Gurney, T.J. Fleck, C.S. Himes, E.D. Hall, Riluzole preserves motor function in a transgenic model of familial amyotrophic lateral sclerosis, Neurology 50 (1998) 62-66.

[60]   M.E. Gurney, H. Pu, A.Y. Chiu, M.C. Dal Canto, C.Y. Polchow, D.D. Alexander, J. Caliendo, A. Hentati, Y.W. Kwon, H.X. Deng, et al., Motor neuron degeneration in mice that express a human Cu,Zn superoxide dismutase mutation, Science 264 (1994) 1772-1775.

[61]   S. Hadano, C.K. Hand, H. Osuga, Y. Yanagisawa, A. Otomo, R.S. Devon, N. Miyamoto, J. Showguchi-Miyata, Y. Okada, R. Singaraja, D.A. Figlewicz, T. Kwiatkowski, B.A. Hosler, T. Sagie, J. Skaug, J. Nasir, R.H. Brown, Jr., S.W. Scherer, G.A. Rouleau, M.R. Hayden, J.E. Ikeda, A gene

encoding a putative GTPase regulator is mutated in familial amyotrophic lateral sclerosis 2, Nat Genet 29 (2001) 166-173.

[62]   M. Hafezparast, R. Klocke, C. Ruhrberg, A. Marquardt, A. Ahmad-Annuar, S. Bowen, G. Lalli, A.S. Witherden, H. Hummerich, S. Nicholson, P.J. Morgan, R. Oozageer, J.V. Priestley, S. Averill, V.R. King, S. Ball, J. Peters, T. Toda, A. Yamamoto, Y. Hiraoka, M. Augustin, D. Korthaus, S. Wattler, P. Wabnitz, C. Dickneite, S. Lampel, F. Boehme, G. Peraus, A. Popp, M. Rudelius, J. Schlegel, H. Fuchs, M.H. de Angelis, G. Schiavo, D.T. Shima, A.P. Russ, G. Stumm, J.E. Martin, E.M. Fisher, Mutations in dynein link motor neuron degeneration to defects in retrograde transport, Science 300 (2003) 808-812.

[63]   C.K. Hand, J. Khoris, F. Salachas, F. Gros-Louis, A.A. Lopes, V. Mayeux-Portas, C.G. Brewer, R.H. Brown, Jr., V. Meininger, W. Camu, G.A. Rouleau, A novel locus for familial amyotrophic lateral sclerosis, on chromosome 18q, Am J Hum Genet 70 (2002) 251-256.

[64]   J.J. Hansen, A. Durr, I. Cournu-Rebeix, C. Georgopoulos, D. Ang, M.N. Nielsen, C.S. Davoine, A. Brice, B. Fontaine, N. Gregersen, P. Bross, Hereditary spastic paraplegia SPG13 is associated with a mutation in the gene encoding the mitochondrial chaperonin Hsp60, Am J Hum Genet 70 (2002) 1328-1332.

[65]   W. Heinemeyer, P.C. Ramos, R.J. Dohmen, The ultimate nanoscale mincer: assembly, structure and active sites of the 20S proteasome core, Cell Mol Life Sci 61 (2004) 1562-1578.

[66]   K. Hensley, M.L. Maidt, Z. Yu, H. Sang, W.R. Markesbery, R.A. Floyd, Electrochemical analysis of protein nitrotyrosine and dityrosine in the Alzheimer brain indicates region-specific accumulation, J Neurosci 18 (1998) 8126-8132.

[67]   A. Hentati, K. Ouahchi, M.A. Pericak-Vance, D. Nijhawan, A. Ahmad, Y. Yang, J. Rimmler, W. Hung, B. Schlotter, A. Ahmed, M. Ben Hamida, F. Hentati, T. Siddique, Linkage of a commoner form of recessive amyotrophic lateral sclerosis to chromosome 15q15-q22 markers, Neurogenetics 2 (1998) 55-60.

[68]   A. Hirano, Neuropathology of ALS: an overview, Neurology 47 (1996) S63-66 Bij reviews; achter Advances in ALS (Gutmann).

[69]   N. Hirokawa, R. Takemura, Molecular motors in neuronal development, intracellular transport and diseases, Curr Opin Neurobiol 14 (2004) 564-573.

[70]   E.L. Holzbaur, Motor neurons rely on motor proteins, Trends Cell Biol 14 (2004) 233-240.

[71]   B.A. Hosler, T. Siddique, P.C. Sapp, W. Sailor, M.C. Huang, A. Hossain, J.R. Daube, M. Nance, C. Fan, J. Kaplan, W.Y. Hung, D. McKenna-Yasek, J.L. Haines, M.A. Pericak-Vance, H.R. Horvitz, R.H. Brown, Jr., Linkage of familial amyotrophic lateral sclerosis with frontotemporal dementia to chromosome 9q21-q22, Jama 284 (2000) 1664-1669.

[72]   D.S. Howland, J. Liu, Y. She, B. Goad, N.J. Maragakis, B. Kim, J. Erickson, J. Kulik, L. DeVito, G. Psaltis, L.J. DeGennaro, D.W. Cleveland, J.D. Rothstein, Focal loss of the glutamate transporter EAAT2 in a transgenic rat model of SOD1 mutant-mediated amyotrophic lateral sclerosis (ALS), Proc Natl Acad Sci U S A 99 (2002) 1604-1609.

[73]   T.T. Huang, E.J. Carlson, A.M. Gillespie, Y. Shi, C.J. Epstein, Ubiquitous overexpression of CuZn superoxide dismutase does not extend life span in mice, J Gerontol A Biol Sci Med Sci 55 (2000) B5-9.

[74]   M. Hutton, C.L. Lendon, P. Rizzu, M. Baker, S. Froelich, H. Houlden, S. Pickering-Brown, S. Chakraverty, A. Isaacs, A. Grover, J. Hackett, J. Adamson, S. Lincoln, D. Dickson, P. Davies, R.C. Petersen, M. Stevens, E. de Graaff, E. Wauters, J. van Baren, M. Hillebrand, M. Joosse, J.M. Kwon, P. Nowotny, P. Heutink, Association of missense and 5'-splice-site mutations in tau with the inherited dementia FTDP-17, Nature 393 (1998) 702-705.

[75]   J. Irobi, K. Van Impe, P. Seeman, A. Jordanova, I. Dierick, N. Verpoorten, A. Michalik, E. De Vriendt, A. Jacobs, V. Van Gerwen, K. Vennekens, R. Mazanec, I. Tournev, D. Hilton-Jones, K. Talbot, I. Kremensky, L. Van Den Bosch, W. Robberecht, J. Van Vandekerckhove, C. Broeckhoven, J. Gettemans, P. De Jonghe, V. Timmerman, Hot-spot residue in small heat-shock protein 22 causes distal motor neuropathy, Nat Genet 36 (2004) 597-601.

[76]   D. Jaarsma, E.D. Haasdijk, Mutant SOD1 protein accumulates in vacuolated mitochondria, in cytosolic filamentous aggregates, and in periaxonal glia in ALS-SOD1 mouse spinal cord, Soc. Neurosci. abstr 27 (2001) 984.982.

[77]   D. Jaarsma, E.D. Haasdijk, J.A. Grashorn, R. Hawkins, H.W. van Duijn, H.W. Verspaget, J. London, J.C. Holstege, Human Cu/Zn superoxide dismutase (SOD1) overexpression in mice causes mitochondrial vacuolization, axonal degeneration, and premature motoneuron death and accelerates motoneuron disease in mice expressing a familial amyotrophic lateral sclerosis mutant SOD1, Neurobiol Dis 7 (2000) 623-643.

[78]   D. Jaarsma, J.C. Holstege, D. Troost, M. Davis, J. Kennis, E.D. Haasdijk, V.J. de Jong, Induction of c-Jun immunoreactivity in spinal cord and brainstem neurons in a transgenic mouse model for amyotrophic lateral sclerosis, Neurosci Lett 219 (1996) 179-182.

[79]   D. Jaarsma, F. Rognoni, W. van Duijn, H.W. Verspaget, E.D. Haasdijk, J.C. Holstege, CuZn superoxide dismutase (SOD1) accumulates in vacuolated mitochondria in transgenic mice expressing amyotrophic lateral sclerosis-linked SOD1 mutations, Acta Neuropathol (Berl) 102 (2001) 293-305.

[80]   J.A. Johnston, M.J. Dalton, M.E. Gurney, R.R. Kopito, Formation of high molecular weight complexes of mutant Cu,Zn-superoxide dismutase in a mouse model for familial amyotrophic lateral sclerosis, Proc Natl Acad Sci U S A 97 (2000) 12571-12576.

[81]   P.A. Jonsson, K. Ernhill, P.M. Andersen, D. Bergemalm, T. Brannstrom, O. Gredal, P. Nilsson, S.L. Marklund, Minute quantities of misfolded mutant superoxide dismutase-1 cause amyotrophic lateral sclerosis, Brain 127 (2004) 73-88.

[82]   P.A. Jonsson, K. Ernhill, T. Brannstrom, P.M. Andersen, L. Forsgren, S.L. Marklund, Comparison of SOD1 enzymic and physical properties in mice transgenically overexpressing wild type and ALS-linked mutant enzyme, Soc. Neurosci. abstr (2000) 182.187.

[83]   M. Jouet, A. Rosenthal, G. Armstrong, J. MacFarlane, R. Stevenson, J. Paterson, A. Metzenberg, V. Ionasescu, K. Temple, S. Kenwrick, X-linked spastic paraplegia (SPG1), MASA syndrome and X-linked hydrocephalus result from mutations in the L1 gene, Nat Genet 7 (1994) 402-407.

[84]   E.C.A. Kaal, E.A.J. Joosten, P.R. Bar, Prevention of apoptotic motoneuron death in vitro by neurotrophins and muscle extract, Neurochemistry International 31 (1997) 193-201.

[85]   Y. Kawaguchi, J.J. Kovacs, A. McLaurin, J.M. Vance, A. Ito, T.P. Yao, The deacetylase HDAC6 regulates aggresome formation and cell viability in response to misfolded protein stress, Cell 115 (2003) 727-738.

[86]   R.R. Kopito, Aggresomes, inclusion bodies and protein aggregation, Trends Cell Biol 10 (2000) 524-530.

[87]   V. Kostic, V. Jacksonlewis, F. Debilbao, M. Duboisdauphin, S. Przedborski, Bcl-2: prolonging life in a transgenic mouse model of familial amyotrophic lateral sclerosis, Science 277 (1997) 559-562.

[88]   R. Kunita, A. Otomo, H. Mizumura, K. Suzuki, J. Showguchi-Miyata, Y. Yanagisawa, S. Hadano, J.E. Ikeda, Homo-oligomerization of ALS2 through its unique carboxy-terminal regions is essential for the ALS2-associated Rab5 guanine nucleotide exchange activity and its regulatory function on endosome trafficking, J Biol Chem 279: (2004) 38626 - 38635.

[89]   C.B. Kunst, Complex Genetics of Amyotrophic Lateral Sclerosis, Am J Hum Genet 75 (2004).

[90]   L. Lacomblez, G. Bensimon, P.N. Leigh, P. Guillet, L. Powe, S. Durrleman, J.C. Delumeau, V. Meininger, A confirmatory dose-ranging study of riluzole in ALS. ALS/Riluzole Study Group-II, Neurology 47 (1996) S242-250.

[91]   D. Lambrechts, E. Storkebaum, M. Morimoto, J. Del-Favero, F. Desmet, S.L. Marklund, S. Wyns, V. Thijs, J. Andersson, I. van Marion, A. Al-Chalabi, S. Bornes, R. Musson, V. Hansen, L. Beckman, R. Adolfsson, H.S. Pall, H. Prats, S. Vermeire, P. Rutgeerts, S. Katayama, T. Awata, N. Leigh, L. Lang-Lazdunski, M. Dewerchin, C. Shaw, L. Moons, R. Vlietinck, K.E. Morrison, W. Robberecht, C. Van Broeckhoven, D. Collen, P.M. Andersen, P. Carmeliet, VEGF is a modifier of amyotrophic lateral sclerosis in mice and humans and protects motoneurons against ischemic death, Nat Genet 34 (2003) 383-394.

[92]   B.H. LaMonte, K.E. Wallace, B.A. Holloway, S.S. Shelly, J. Ascano, M. Tokito, T. Van Winkle, D.S. Howland, E.L. Holzbaur, Disruption of dynein/dynactin inhibits axonal transport in motor neurons causing late-onset progressive degeneration, Neuron 34 (2002) 715-727.

[93]   N. Le Forestier, T. Maisonobe, A. Piquard, S. Rivaud, L. Crevier-Buchman, F. Salachas, P.F. Pradat, L. Lacomblez, V. Meininger, Does primary lateral sclerosis exist? A study of 20 patients and a review of the literature, Brain 124 (2001) 1989-1999.

[94]   E.S. Lee, H.K. Moon, Y.H. Park, J. Garbern, G.M. Hobson, A case of complicated spastic paraplegia 2 due to a point mutation in the proteolipid protein 1 gene, J Neurol Sci 224 (2004) 83-87.

[95]   P.N. Leigh, H. Whitwell, O. Garofalo, J. Buller, M. Swash, J.E. Martin, J.M. Gallo, R.O. Weller, B.H. Anderton, Ubiquitin-immunoreactive intraneuronal inclusions in amyotrophic lateral sclerosis. Morphology, distribution, and specificity, Brain 114 (1991) 775-788.

[96]   Y.J. Li, M.A. Pericak-Vance, J.L. Haines, N. Siddique, D. McKenna-Yasek, W.-Y. Hung, P. Sapp, C.I. Allen, W. Chen, B. Hosler, A.M. Saunders, L.M. Dellafave, R.H. Brown Jr, Jr., T. Siddique, Apolipoprotein E is associated with age at onset of amyotrophic lateral sclerosis, Neurogenetics Epub ahead of print (2004).

[97]   M.M. Lino, C. Schneider, P. Caroni, Accumulation of SOD1 mutants in postnatal motoneurons does not cause motoneuron pathology or motoneuron disease, J Neurosci 22 (2002) 4825-4832.

[98]   L. Luo, R.C. Salunga, H. Guo, A. Bittner, K.C. Joy, J.E. Galindo, H. Xiao, K.E. Rogers, J.S. Wan, M.R. Jackson, M.G. Erlander, Gene expression profiles of laser-captured adjacent neuronal subtypes [published erratum appears in Nat Med 1999 Mar;5(3):355], Nat Med 5 (1999) 117-122.

[99] H.L. Lutsep, M. Rodriguez, Ultrastructural, morphometric, and immunocytochemical study of anterior horn cells in mice with "wasted" mutation, J Neuropathol Exp Neurol 48 (1989) 519-533.

[100] A. Maatkamp, A. Vlug, E. Haasdijk, D. Troost, P.J. French, D. Jaarsma, Decrease of HSP25 protein expression precede degeneration of motoneurons in ALS-SOD1 mice, Eur J Neurosci 20 (2004) 14-28.

[101] L.A. MacMillan-Crow, J.P. Crow, J.D. Kerby, J.S. Beckman, J.A. Thompson, Nitration and inactivation of manganese superoxide dismutase in chronic rejection of human renal allografts, Proc Natl Acad Sci U S A 93 (1996) 11853-11858.

[102] A. Malaspina, J. de Belleroche, Spinal cord molecular profiling provides a better understanding of amyotrophic lateral sclerosis pathogenesis, Brain Res Brain Res Rev 45 (2004) 213-229.

[103] M. Mancuso, F.L. Conforti, A. Rocchi, A. Tessitore, M. Muglia, G. Tedeschi, D. Panza, M. Monsurro, P. Sola, J. Mandrioli, A. Choub, A. Delcorona, M.L. Manca, R. Mazzei, T. Sprovieri, M. Filosto, A. Salviati, P. Valentino, F. Bono, M. Caracciolo, I.L. Simone, V. La Bella, G. Majorana, G. Siciliano, L. Murri, A. Quattrone, Could mitochondrial haplogroups play a role in sporadic amyotrophic lateral sclerosis?, Neurosci Lett 371 (2004) 158-162.

[104] N.J. Maragakis, M. Jackson, R. Ganel, J.D. Rothstein, Topiramate protects against motor neuron degeneration in organotypic spinal cord cultures but not in G93A SOD1 transgenic mice, Neurosci Lett 338 (2003) 107-110.

[105] M.G. Marrosu, S. Vaccargiu, G. Marrosu, A. Vannelli, C. Cianchetti, F. Muntoni, Charcot-Marie-Tooth disease type 2 associated with mutation of the myelin protein zero gene, Neurology 50 (1998) 1397-1401.

[106] N. Martin, J. Jaubert, P. Gounon, E. Salido, G. Haase, M. Szatanik, J.L. Guenet, A missense mutation in Tbce causes progressive motor neuronopathy in mice, Nat Genet 32 (2002) 443-447.

[107] B.A. McLaughlin, D. Nelson, I.A. Silver, M. Erecinska, M.F. Chesselet, Methylmalonate toxicity in primary neuronal cultures, Neuroscience 86 (1998) 279-290.

[108] A.J. Meijer, P. Codogno, Regulation and role of autophagy in mammalian cells, Int J Biochem Cell Biol 36 (2004) 2445-2462.

[109] S. Melov, P. Coskun, M. Patel, R. Tuinstra, B. Cottrell, A.S. Jun, T.H. Zastawny, M. Dizdaroglu, S.I. Goodman, T.T. Huang, H. Miziorko, C.J. Epstein, D.C. Wallace, Mitochondrial disease in superoxide dismutase 2 mutant mice, Proc Natl Acad Sci U S A 96 (1999) 846-851.

[110] I.V. Mersiyanova, A.V. Perepelov, A.V. Polyakov, V.F. Sitnikov, E.L. Dadali, R.B. Oparin, A.N. Petrin, O.V. Evgrafov, A new variant of Charcot-Marie-Tooth disease type 2 is probably the result of a mutation in the neurofilament-light gene, Am J Hum Genet 67 (2000) 37-46.

[111] R.J. Miller, S.M. Wilson, Neurological disease: UPS stops delivering!, Trends Pharmacol Sci 24 (2003) 18-23.

[112] M.H. Mohajeri, D.A. Figlewicz, M.C. Bohn, Selective Loss of alpha Motoneurons Innervating the Medial Gastrocnemius Muscle in a Mouse Model of Amyotrophic Lateral Sclerosis, Exp Neurol 150 (1998) 329-336.

[113] M.C. Moreira, S. Klur, M. Watanabe, A.H. Nemeth, I. Le Ber, J.C. Moniz, C. Tranchant, P. Aubourg, M. Tazir, L. Schols, M. Pandolfo, J.B. Schulz, J. Pouget, P. Calvas, M. Shizuka-Ikeda, M. Shoji, M. Tanaka, L. Izatt, C.E. Shaw, A. M'Zahem, E. Dunne, P. Bomont, T. Benhassine, N. Bouslam, G. Stevanin, A. Brice, J. Guimaraes, P. Mendonca, C. Barbot, P. Coutinho, J. Sequeiros, A. Durr, J.M. Warter, M. Koenig, Senataxin, the ortholog of a yeast RNA helicase, is mutant in ataxia-ocular apraxia 2, Nat Genet 36 (2004) 225-227.

[114] B.M. Morrison, W.G. Janssen, J.W. Gordon, J.H. Morrison, Time course of neuropathology in the spinal cord of G86R superoxide dismutase transgenic mice, J Comp Neurol 391 (1998) 64-77.

[115] B. Moulard, A. Sefiani, A. Laamri, A. Malafosse, W. Camu, Apolipoprotein E genotyping in sporadic amyotrophic lateral sclerosis: evidence for a major influence on the clinical presentation and prognosis, J Neurol Sci 139 Suppl (1996) 34-37.

[116] C. Munch, R. Sedlmeier, T. Meyer, V. Homberg, A.D. Sperfeld, A. Kurt, J. Prudlo, G. Peraus, C.O. Hanemann, G. Stumm, A.C. Ludolph, Point mutations of the p150 subunit of dynactin (DCTN1) gene in ALS, Neurology 63 (2004) 724-726.

[117] M. Nagai, M. Aoki, I. Miyoshi, M. Kato, P. Pasinelli, N. Kasai, R.H. Brown, Jr., Y. Itoyama, Rats expressing human cytosolic copper-zinc superoxide dismutase transgenes with amyotrophic lateral sclerosis: associated mutations develop motor neuron disease, J Neurosci 21 (2001) 9246-9254.

[118] S. Nicole, C.C. Diaz, T. Frugier, J. Melki, Spinal muscular atrophy: recent advances and future prospects, Muscle Nerve 26 (2002) 4-13.

[119] A.L. Nishimura, M. Mitne-Neto, H.C. Silva, A. Richieri-Costa, S. Middleton, D. Cascio, F. Kok, J.R. Oliveira, T. Gillingwater, J. Webb, P. Skehel, M. Zatz, A Mutation in the Vesicle-Trafficking Protein

VAPB Causes Late-Onset Spinal Muscular Atrophy and Amyotrophic Lateral Sclerosis, Am J Hum Genet 75 (2004) 822-831.

[120] O. Pansarasa, L. Bertorelli, J. Vecchiet, G. Felzani, F. Marzatico, Age-dependent changes of antioxidant activities and markers of free radical damage in human skeletal muscle, Free Radic Biol Med 27 (1999) 617-622.

[121] H. Patel, H. Cross, C. Proukakis, R. Hershberger, P. Bork, F.D. Ciccarelli, M.A. Patton, V.A. McKusick, A.H. Crosby, SPG20 is mutated in Troyer syndrome, an hereditary spastic paraplegia, Nat Genet 31 (2002) 347-348.

[122] A. Pramatarova, J. Laganiere, J. Roussel, K. Brisebois, G.A. Rouleau, Neuron-specific expression of mutant superoxide dismutase 1 in transgenic mice does not lead to motor impairment, J Neurosci 21 (2001) 3369-3374.

[123] I. Puls, C. Jonnakuty, B.H. LaMonte, E.L. Holzbaur, M. Tokito, E. Mann, M.K. Floeter, K. Bidus, D. Drayna, S.J. Oh, R.H. Brown, Jr., C.L. Ludlow, K.H. Fischbeck, Mutant dynactin in motor neuron disease, Nat Genet 33 (2003) 455-456.

[124] S. Rainier, J.H. Chai, D. Tokarz, R.D. Nicholls, J.K. Fink, NIPA1 gene mutations cause autosomal dominant hereditary spastic paraplegia (SPG6), Am J Hum Genet 73 (2003) 967-971.

[125] S. Ranta, Y. Zhang, B. Ross, L. Lonka, E. Takkunen, A. Messer, J. Sharp, R. Wheeler, K. Kusumi, S. Mole, W. Liu, M.B. Soares, M.F. Bonaldo, A. Hirvasniemi, A. de la Chapelle, T.C. Gilliam, A.E. Lehesjoki, The neuronal ceroid lipofuscinoses in human EPMR and mnd mutant mice are associated with mutations in CLN8, Nat Genet 23 (1999) 233-236.

[126] E. Reid, A.M. Dearlove, M. Rhodes, D.C. Rubinsztein, A new locus for autosomal dominant "pure" hereditary spastic paraplegia mapping to chromosome 12q13, and evidence for further genetic heterogeneity, Am J Hum Genet 65 (1999) 757-763.

[127] M.E. Ripps, G.W. Huntley, P.R. Hof, J.H. Morrison, J.W. Gordon, Transgenic mice expressing an altered murine superoxide dismutase gene provide an animal model of amyotrophic lateral sclerosis, Proc Natl Acad Sci U S A 92 (1995) 689-693.

[128] D.R. Rosen, T. Siddique, D. Patterson, D.A. Figlewicz, P. Sapp, A. Hentati, D. Donaldson, J. Goto, Mutations in Cu/Zn superoxide dismutase gene are associated with familial amyotrophic lateral sclerosis, Nature 362 (1993) 59-62.

[129] J.D. Rothstein, G. Tsai, R.W. Kuncl, L. Clawson, D.R. Cornblath, D.B. Drachman, A. Pestronk, B.L. Stauch, J.T. Coyle, Abnormal excitatory amino acid metabolism in amyotrophic lateral sclerosis, Ann Neurol 28 (1990) 18-25.

[130] J.D. Rothstein, M. Van Kammen, A.I. Levey, L.J. Martin, R.W. Kuncl, Selective loss of glial glutamate transporter GLT-1 in amyotrophic lateral sclerosis, Ann Neurol 38 (1995) 73-84.

[131] L.P. Rowland, Diagnosis of amyotrophic lateral sclerosis, J Neurol Sci 160 Suppl 1 (1998) S6-24.

[132] L.P. Rowland, N.A. Shneider, Amyotrophic lateral sclerosis, N Engl J Med 344 (2001) 1688-1700.

[133] D.M. Ruddy, M.J. Parton, A. Al-Chalabi, C.M. Lewis, C. Vance, B.N. Smith, P.N. Leigh, J.F. Powell, T. Siddique, E.P. Meyjes, F. Baas, V. de Jong, C.E. Shaw, Two families with familial amyotrophic lateral sclerosis are linked to a novel locus on chromosome 16q, Am J Hum Genet 73 (2003) 390-396.

[134] P.C. Sapp, B.A. Hosler, D. McKenna-Yasek, W. Chin, A. Gann, H. Genise, J. Gorenstein, M. Huang, W. Sailer, M. Scheffler, M. Valesky, J.L. Haines, M. Pericak-Vance, T. Siddique, H.R. Horvitz, R.H. Brown, Jr., Identification of two novel loci for dominantly inherited familial amyotrophic lateral sclerosis, Am J Hum Genet 73 (2003) 397-403.

[135] H. Schmalbruch, H.J. Jensen, M. Bjaerg, Z. Kamieniecka, L. Kurland, A new mouse mutant with progressive motor neuronopathy, J Neuropathol Exp Neurol 50 (1991) 192-204.

[136] F.J. Schopfer, P.R. Baker, B.A. Freeman, NO-dependent protein nitration: a cell signaling event or an oxidative inflammatory response?, Trends Biochem Sci 28 (2003) 646-654.

[137] P.J. Shaw, V. Forrest, P.G. Ince, J.P. Richardson, H.J. Wastell, CSF and plasma amino acid levels in motor neuron disease: elevation of CSF glutamate in a subset of patients, Neurodegeneration 4 (1995) 209-216.

[138] P.J. Shaw, P.G. Ince, G. Falkous, D. Mantle, Oxidative damage to protein in sporadic motor neuron disease spinal cord, Ann Neurol 38 (1995) 691-695.

[139] P.J. Shaw, T.L. Williams, J.Y. Slade, C.J. Eggett, P.G. Ince, Low expression of GluR2 AMPA receptor subunit protein by human motor neurons, Neuroreport 10 (1999) 261-265.

[140] M.Y. Sherman, A.L. Goldberg, Cellular defenses against unfolded proteins: a cell biologist thinks about neurodegenerative diseases, Neuron 29 (2001) 15-32.

[141] N. Shibata, A. Hirano, M. Kobayashi, S. Sasaki, T. Kato, S. Matsumoto, Z. Shiozawa, T. Komori, A. Ikemoto, T. Umahara, et al., Cu/Zn superoxide dismutase-like immunoreactivity in Lewy body-like inclusions of sporadic amyotrophic lateral sclerosis, Neurosci Lett 179 (1994) 149-152.

[142] T. Siddique, S.-T. Hong, B.R. Brooks, W.Y. Hung, N.A. Siddique, J. Rimmler, J. Kaplan, J.L. Haines, R.H. Brown Jr, Jr., M. Pericak-Vance, X-linked dominant locus for late-onset familial amyotrophic lateral sclerosis, Am J Hum Genet 63 (1998) A308.

[143] T. Siddique, M.A. Pericak-Vance, J. Caliendo, S.T. Hong, W.Y. Hung, J. Kaplan, D. McKenna-Yasek, J.B. Rimmler, P. Sapp, A.M. Saunders, W.K. Scott, N. Siddique, J.L. Haines, R.H. Brown, Lack of association between apolipoprotein E genotype and sporadic amyotrophic lateral sclerosis, Neurogenetics 1 (1998) 213-216.

[144] S. Skradski, H.S. White, Topiramate blocks kainate-evoked cobalt influx into cultured neurons, Epilepsia 41 Suppl 1 (2000) S45-47.

[145] B.S. Slusher, K.M. Wozniak, T. Hartman, P. Jada, M. Chadran, M. DalCanto, NAALADase inhibition increases survival and delays clinical symptoms in SOD transgenic model of ALS, Soc. Neurosci. Abstr. 26 (2000) 43.10.

[146] C.D. Smith, J.M. Carney, P.E. Starke-Reed, C.N. Oliver, E.R. Stadtman, R.A. Floyd, W.R. Markesbery, Excess brain protein oxidation and enzyme dysfunction in normal aging and in Alzheimer disease, Proc Natl Acad Sci U S A 88 (1991) 10540-10543.

[147] R.G. Smith, L.J. Haverkamp, S. Case, V. Appel, S.H. Appel, Apolipoprotein E epsilon 4 in bulbar-onset motor neuron disease, Lancet 348 (1996) 334-335.

[148] C. Soto, Unfolding the role of protein misfolding in neurodegenerative diseases, Nat Rev Neurosci 4 (2003) 49-60.

[149] L. Soussan, D. Burakov, M.P. Daniels, M. Toister-Achituv, A. Porat, Y. Yarden, Z. Elazar, ERG30, a VAP-33-related protein, functions in protein transport mediated by COPI vesicles, J Cell Biol 146 (1999) 301-311.

[150] L. Stoppini, P.A. Buchs, D. Muller, A simple method for organotypic cultures of nervous tissue, J Neurosci Methods 37 (1991) 173-182.

[151] J.R. Subramaniam, W.E. Lyons, J. Liu, T.B. Bartnikas, J. Rothstein, D.L. Price, D.W. Cleveland, J.D. Gitlin, P.C. Wong, Mutant SOD1 causes motor neuron disease independent of copper chaperone-mediated copper loading, Nat Neurosci 5 (2002) 301-307.

[152] H. Takuma, S. Kwak, T. Yoshizawa, I. Kanazawa, Reduction of GluR2 RNA editing, a molecular change that increases calcium influx through AMPA receptors, selective in the spinal ventral gray of patients with amyotrophic lateral sclerosis, Ann Neurol 46 (1999) 806-815.

[153] J.P. Taylor, J. Hardy, K.H. Fischbeck, Toxic proteins in neurodegenerative disease, Science 296 (2002) 1991-1995.

[154] V. Timmerman, P. De Jonghe, P. Spoelders, S. Simokovic, A. Lofgren, E. Nelis, J. Vance, J.J. Martin, C. Van Broeckhoven, Linkage and mutation analysis of Charcot-Marie-Tooth neuropathy type 2 families with chromosomes 1p35-p36 and Xq13, Neurology 46 (1996) 1311-1318.

[155] J.D. Topp, N.W. Gray, R.D. Gerard, B.F. Horazdovsky, Alsin is a Rab5 and Rac1 guanine nucleotide exchange factor, J Biol Chem 279 (2004) 24612-24623.

[156] J.S. Valentine, Do oxidatively modified proteins cause ALS?, Free Radic Biol Med 33 (2002) 1314-1320.

[157] J.S. Valentine, P.J. Hart, Misfolded CuZnSOD and amyotrophic lateral sclerosis, Proc Natl Acad Sci U S A 100 (2003) 3617-3622.

[158] P. Van Damme, M. Leyssen, G. Callewaert, W. Robberecht, L. Van Den Bosch, The AMPA receptor antagonist NBQX prolongs survival in a transgenic mouse model of amyotrophic lateral sclerosis, Neurosci Lett 343 (2003) 81-84.

[159] L.H. van den Berg, J.P. van den Berg, F.G.I. Jennekens, Amyotrofe Lateraal Sclerose: Begeleiding en behandeling, Elsevier Gezondheidszorg, Maarssen, the Netherlands, 2002, 110 pp.

[160] W. Vandenberghe, L. Van Den Bosch, W. Robberecht, Glial cells potentiate kainate-induced neuronal death in a motoneuron- enriched spinal coculture system, Brain Res 807 (1998) 1-10.

[161] J.H. Veldink, L.H. van den Berg, J.M. Cobben, R.P. Stulp, J.M. De Jong, O.J. Vogels, F. Baas, J.H. Wokke, H. Scheffer, Homozygous deletion of the survival motor neuron 2 gene is a prognostic factor in sporadic ALS, Neurology 56 (2001) 749-752.

[162] J.H. Veldink, L.H. Van Den Berg, J.H. Wokke, The future of motor neuron disease: The challenge is in the genes, J Neurol 251 (2004) 491-500.

[163] K. Verhoeven, P. De Jonghe, K. Coen, N. Verpoorten, M. Auer-Grumbach, J.M. Kwon, D. FitzPatrick, E. Schmedding, E. De Vriendt, A. Jacobs, V. Van Gerwen, K. Wagner, H.P. Hartung, V. Timmerman, Mutations in the small GTP-ase late endosomal protein RAB7 cause Charcot-Marie-Tooth type 2B neuropathy, Am J Hum Genet 72 (2003) 722-727.

[164] J. Wang, H. Slunt, V. Gonzales, D. Fromholt, M. Coonfield, N.G. Copeland, N.A. Jenkins, D.R. Borchelt, Copper-binding-site-null SOD1 causes ALS in transgenic mice: aggregates of non-native SOD1 delineate a common feature, Hum Mol Genet 12 (2003) 2753-2764.

[165] J. Wang, G. Xu, V. Gonzales, M. Coonfield, D. Fromholt, N.G. Copeland, N.A. Jenkins, D.R. Borchelt, Fibrillar inclusions and motor neuron degeneration in transgenic mice expressing superoxide dismutase 1 with a disrupted copper-binding site, Neurobiol Dis 10 (2002) 128-138.

[166] R. Wetzel, Mutations and off-pathway aggregation of proteins, Trends Biotechnol 12 (1994) 193-198.

[167] T.L. Williams, N.C. Day, P.G. Ince, R.K. Kamboj, P.J. Shaw, Calcium-permeable alpha-amino-3-hydroxy-5-methyl-4-isoxazole propionic acid receptors: a molecular determinant of selective vulnerability in amyotrophic lateral sclerosis, Ann Neurol 42 (1997) 200-207.

[168] P.C. Wong, C.A. Pardo, D.R. Borchelt, M.K. Lee, N.G. Copeland, N.A. Jenkins, S.S. Sisodia, D.W. Cleveland, D.L. Price, An adverse property of a familial ALS-linked SOD1 mutation causes motor neuron disease characterized by vacuolar degeneration of mitochondria, Neuron 14 (1995) 1105-1116.

[169] P.C. Wong, D. Waggoner, J.R. Subramaniam, L. Tessarollo, T.B. Bartnikas, V.C. Culotta, D.L. Price, J. Rothstein, J.D. Gitlin, Copper chaperone for superoxide dismutase is essential to activate mammalian Cu/Zn superoxide dismutase, Proc Natl Acad Sci U S A 97 (2000) 2886-2891.

[170] Y. Yang, A. Hentati, H.X. Deng, O. Dabbagh, T. Sasaki, M. Hirano, W.Y. Hung, K. Ouahchi, J. Yan, A.C. Azim, N. Cole, G. Gascon, A. Yagmour, M. Ben-Hamida, M. Pericak-Vance, F. Hentati, T. Siddique, The gene encoding alsin, a protein with three guanine-nucleotide exchange factor domains, is mutated in a form of recessive amyotrophic lateral sclerosis, Nat Genet 29 (2001) 160-165.

[171] T. Yoshimori, Autophagy: a regulated bulk degradation process inside cells, Biochem Biophys Res Commun 313 (2004) 453-458.

[172] Y. Zhang, O. Marcillat, C. Giulivi, L. Ernster, K.J. Davies, The oxidative inactivation of mitochondrial electron transport chain components and ATPase, J Biol Chem 265 (1990) 16330-16336.

[173] C. Zhao, J. Takita, Y. Tanaka, M. Setou, T. Nakagawa, S. Takeda, H.W. Yang, S. Terada, T. Nakata, Y. Takei, M. Saito, S. Tsuji, Y. Hayashi, N. Hirokawa, Charcot-Marie-Tooth disease type 2A caused by mutation in a microtubule motor KIF1Bbeta, Cell 105 (2001) 587-597.

[174] X. Zhao, D. Alvarado, S. Rainier, R. Lemons, P. Hedera, C.H. Weber, T. Tukel, M. Apak, T. Heiman-Patterson, L. Ming, M. Bui, J.K. Fink, Mutations in a newly identified GTPase gene cause autosomal dominant hereditary spastic paraplegia, Nat Genet 29 (2001) 326-331.

[175] S. Zuchner, I.V. Mersiyanova, M. Muglia, N. Bissar-Tadmouri, J. Rochelle, E.L. Dadali, M. Zappia, E. Nelis, A. Patitucci, J. Senderek, Y. Parman, O. Evgrafov, P.D. Jonghe, Y. Takahashi, S. Tsuji, M.A. Pericak-Vance, A. Quattrone, E. Battaloglu, A.V. Polyakov, V. Timmerman, J.M. Schroder, J.M. Vance, E. Battologlu, Mutations in the mitochondrial GTPase mitofusin 2 cause Charcot-Marie-Tooth neuropathy type 2A, Nat Genet 36 (2004) 449-451.

Chapter 2

INCREASED 3-NITROTYROSINE DOES NOT CAUSE NEURONAL DEGENERATION

Angela S. Vlug, Elize D. Haasdijk, Johannes Gerritsen, Hans van den Burg and
Dick Jaarsma

Department of Neuroscience, Erasmus MC, Rotterdam, The Netherlands

2.1 Abstract

3-Nitrotyrosine is a modified amino acid that is formed by a reaction between nitric oxide-derived reactive species and tyrosine. Because of a number of studies indicating that 3-nitrotyrosine may be neurotoxic to particular populations of neurons, we have examined the effect of acute and prolonged application of 3-nitrotyrosine in the brain of mice and in murine organotypic spinal cord cultures. Using an antibody that labels 3-nitrotyrosine injected into the brain, we showed that after a single microinjection into the cortex, striatum or hippocampus, 3-nitrotyrosine is predominantly distributed in neurons, but subsequently disappears within 60 min. Neither single microinjections nor prolonged intra-striatal delivery of 3-nitrotyrosine via osmotic minipumps resulted in any evidence for neuronal degeneration. Also prolonged exposure of organotypic spinal cord cultures to high doses of 3-nitrotyrosine did not influence neuronal viability. We conclude that increased levels of free 3-nitrotyrosine as reported for various neurodegenerative diseases, are unlikely to contribute to neuronal degeneration.

2.2 Introduction

3-Nitrotyrosine is a modified amino acid that is formed by a reaction between nitric oxide-derived reactive species and tyrosine [3,11]. Because of its relative stability, 3-nitrotyrosine has been widely used as a marker for damage left by nitric oxide-derived species *in vivo* [7,11]. Increased levels of both free and protein-linked 3-nitrotyrosine have been reported for a wide array of disorders, including neurodegenerative diseases like Alzheimer's disease, Parkinson's disease and amyotrophic lateral sclerosis (ALS) [11,14]. A number of studies have indicated that 3-nitrotyrosine, in addition of being a marker of reactive nitrogen species formation, also may be noxious by itself and contribute to cell death. Because 3-nitrotyrosine is bulkier and more hydrophilic than tyrosine, nitration of protein-linked tyrosine residues can impair the function of proteins [3,11,25]. Furthermore, nitration may play a role in oligomerization of specific proteins, such as synuclein in synucleopathies and tau in tauopathies, and hence contribute to the formation of intracellular inclusions [10,12]. Nitration also may involve free tyrosine residues, and increased levels of free 3-nitrotyrosyne have been reported in neurodegenerative diseases [2,11]. A number of data suggest that free 3-nitrotyrosine may affect cell function and contribute the pathogenesis of these diseases [11,25]. One putative deleterious action of 3-nitrotyrosine is caused by its post-translational incorporation into α-tubulin, which affects microtubule dynamics and cell function [1,8,30]. However, it also has been reported that nitrotyrosination of tubulin has no effect on many cell lines at doses up to 500 µM [4]. Alternatively, a deleterious action independent from α-tubulin incorporation was suggested by a recent study with cultured motoneurons, which showed that 3-nitrotyrosine induced apoptotic death in these cells, without incorporation of 3-nitrotyrosine into α-tubulin [23]. A neurotoxic action of 3-nitrotyrosine also has been found *in vivo* after a striatal 3-nitrotyrosine injection which resulted in degeneration of nigral dopaminergic neurons [22]. The mechanism underlying this toxicity was not investigated, although on the basis of immunocytochemical data the authors concluded that micro-injected 3-nitrotyrosine was not incorporated into proteins [22]. In the present study we have further investigated potential neurotoxic action of 3-nitrotyrosine *in vivo* and in organotypic spinal cord culture. Our data indicate that 3-nitrotyrosine microinjected into the brain is predominantly distributed in neurons, but rapidly disappears. However, prolonged exposure to elevated levels of 3-nitrotyrosine did not cause neuronal degeneration *in vivo* and in cultures.

2.2 Materials and Methods

2.2.1   Animals and surgery

Experiments were performed with Fvb/N mice that were housed at a 12-12 h dark-light cycle, and were fed ad libitum with a standard diet. Animal procedures were performed in accordance with the 'NIH Guide for the Care and Use of Laboratory Animals' and were approved by the local ethical committee of the Erasmus MC (protocol # 115-02-05 and 115-03-01). For acute 3-nitrotyrosine injections mice

were anesthetized with a mixture of O_2, N_2O and 2% halothane, and a small hole was drilled in the skull. 1-10 nmol of 3-nitro-L-tyrosine (10 -100 mM diluted in 100 nl saline; Sigma) was injected stereotactically during 2 min in hippocampus (n=6) or in the striatum (n=18) using a glass micropipette (tip diameter 20-25 µm). Following injection animals were perfused transcardially with 4% paraformaldehyde in 0.1 M phosphate buffer (pH 7.3) immediately (n=6), or 15 min (n=3), 30 min (n=3), 1 h (n=2), 2 h (n=2), 1 day (n=2) and 2 days (n=6) after injection.

For the chronic intra-striatal 3-nitrotyrosine injection mice were anesthetized and a stainless steel cannula (30 G) was implanted in the striatum through a small hole in the cranium, fixed with dental cement, and connected via a polyvinylchloride catheter to an Alzet micro-osmotic pump (1007 D; Alza, Mountainview, CA), which had been filled with 3-nitro-L-tyrosine (100 mM in saline) or L-tyrosine (100 mM in saline; Sigma) and implanted under the skin on the back as described before [5]. After 7 days the mice were perfused transcardially with 4% paraformaldehyde, the brain was carefully dissected out and further processed for immunocytochemistry.

2.2.2   Immunocytochemistry

Brains were cryoprotected overnight in 30% sucrose, and cut into 40 µm coronal sections on a freezing microtome. Every tenth section was collected in 4% paraformaldehyde, and processed with a Nadler-Gallyas silver staining procedure that selectively labels degenerating neurons and their processes [15]. An additional series of sections was processed for acetylcholine esterase histochemistry. Other sections were collected in Tris-buffered saline (TBS), pH 7.6, and processed free-floating, employing standard avidin-biotin-immunoperoxidase-diaminobenzidine or immunofluorescence methods [16]. The following primary antibodies diluted in TBS containing 2% normal horse serum and 0.4% Triton X-100 were used: rabbit anti-ATF3 (Santa Cruz, 1:1000), rabbit anti-GFAP (DAKO, 1:10000), mouse anti-MAP2 (Sigma, 1:2000), mouse anti-nitrotyrosine (clone 1A6, Upstate Biotechnology, 1: 100 - 1: 400), rabbit anti-nitrotyrosine (cat# 06-284, Upstate Biotechnology, 1: 500 - 1: 2.000), mouse anti-SMI32 (Sternberger Monoclonals, 1:7.000), and sheep anti-tyrosine hydroxylase (Novus Biologicals, 1: 2.000). For avidin-biotin-peroxidase immunocytochemistry biotinylated secondary antibodies from Vector Laboratories diluted 1:200 were used. For immunofluorescence FITC and Cy3-conjugated secondary antibodies raised in donkey (Jackson Immunoresearch, USA) were used. In control experiments for 3-nitrotyrosine-staining sections were pretreated with sodium dithionite (100 mM in 100 mM sodium borate) [28]. Alternatively, 3-nitro-tyrosine (1 µM - 100 mM) or L-tyrosine (100 mM) were included during the primary antibody incubations step.

2.2.3   Organotypic spinal cord culture

350 µm thick slices from spinal cord of 7-day-old mice were cultured on 0.4 µm Millicell-CM culture plate inserts (Millipore, UK) as described before [29]. After two weeks cultures were treated with 3-nitrotyrosine (50, 100 or 150 µM) for one week. 3-Nitrotyrosine was dissolved in physiological salt solution in a concentration of 10 mM and 5, 10 or 15 µl of this solution or 15 µl physiological salt solution for controls was added to 1 ml of culture medium. After treatment cultures were rinsed with
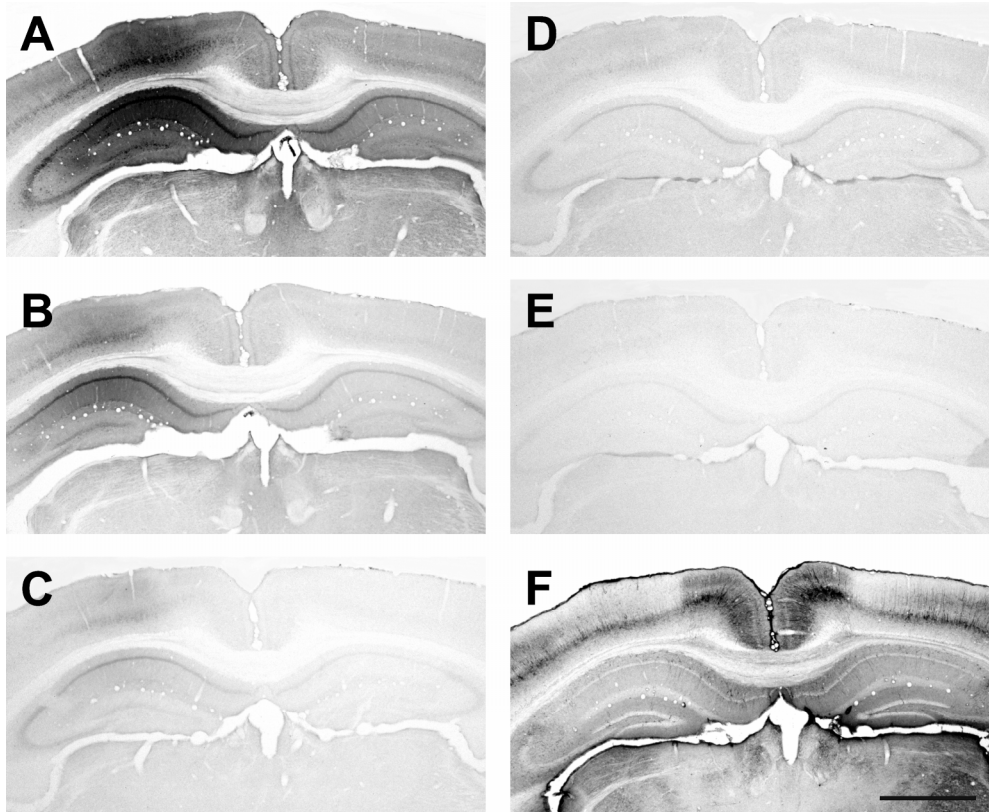
Figure 1:   Polyclonal rabbit anti-nitrotyrosine antibody immunoreacts with different affinities to endogenous 3-nitrotyrosine epitopes and micro-injected 3-nitrotyrosine.
Immunostaining of 3-nitrotyrosine in the hippocampus and overlying neocortex after microinjection of 1 nmol 3-nitrotyrosine (solved in 100 nl saline, pH 7.4) using different concentrations of the rabbit-nitrotyrosine antibody (A, 1:1.000, B 1:3.000, C 1:10.000) or the antibody diluted 1:1000 and pre-incubated with 10 µM (D) or 10 mM (E) 3-nitrotyrosine. Note that 10 µM of free 3-nitrotyrosine blocks the staining of the micro-injected 3-nitrotyrosine, but not endogenous 3-nitrotyrosine-immunoreactivity (D), whereas 10 mM of free 3-nitrotyrosine inhibits both. (F) Section stained with an antibody against non-phosphorylated neurofilament (SMI32) to evaluate whether the injection procedure causes tissue damage. Scale bar = 1 mm

PBS, fixed for 1 h in 3.5% paraformaldehyde in 0.1 M phosphate buffer. The slices were immunostained with SMI32 antibody (Sternberger Monoclonals, USA 1:3.000), ChAT polyclonal antibody (Chemicon, USA, 1:800) 3-nitrotyrosine rabbit polyclonal antibody (cat# 06-284, Upstate Biotechnology, USA 1:10.000) and/or 3-nitrotyrosine monoclonal antibody (clone 1A6 cat # 05-233, Upstate Biotechnology, USA 1:750), using avidin-biotin-immunoperoxidase-diaminobenzidine or immunofluorescence methods (see above). Motoneurons were counted in ChAT or SMI32-labeled slices as described before [29]. They were defined as ChAT-immunoreactive neurons in the ventrolateral parts of the slices or as large SMI32-positive cell bodies in this region. In SMI32-labeled cultures also SMI32-immunoreactive neurons in the dorsal horn or intermediate zone, representing a subset of spinal interneurons were counted [21]. In each experiment the numbers

of motoneurons and interneurons, were calibrated against the number of motoneurons and interneurons, respecively against control cultures. Results are presented as means ± SEM.

2.3 Results

2.3.1   Micro-injected 3-nitrotyrosine can be detected immunocytochemically in paraformaldehyde-fixed brain sections

To be able to localize 3-nitrotyrosine after microinjection in the brain we have examined whether it could be labeled immunocytochemically using commercially available antibodies raised against nitrated-keyhole limpet hemocyanin (KLH) [28]. These antibodies have been shown to preferentially bind to 3-nitrotyrosine in peptides and proteins, but their immunoreactivity towards free 3-nitrotyrosine was not explored [28]. As shown in figures 1 and 2 intense immunostaining was obtained with a polyclonal antibody (Ab06-284, Upstate) in paraformaldehyde-fixed brain sections after microinjection of 3-nitrotyrosine (1 or 10 nmol diluted in 100 nl saline) in the striatum (Fig. 2a) or dorsal hippocampus and cortex (Fig. 1a). In contrast a monoclonal antibody (Mab1A6, Upstate) did not immunoreact with microinjected 3-nitrotyrosine (not shown). The staining obtained with Ab06-284 was specific for a 3-nitrotyrosine epitope, since it was inhibited by pre-adsorbing the antibody with 3-nitrotyrosine (Fig. 1d and e), or after treatment of the sections with sodium dithionite, which reduces 3-nitrotyrosine to amino-tyrosine (not shown). Importantly labeling of micro-injected 3-nitrotyrosine by Ab06-284 showed different properties as compared to 3-nitrotyrosine staining in non-injected brain. First, staining of micro-injected 3-nitrotyrosine could be obtained with relatively high antibody dilutions as compared to the concentration required to obtain immunolabeling in non-injected brain (1:10.000 vs. 1:1.000; Fig. 1a-c). Second, immunostaining of microinjected 3-nitrotyrosine was inhibited by preabsorption with relatively low concentrations of 3-nitrotyrosine (100 µm; Fig.1d) while the staining of 3-nitrotyrosine in non-injected hemisphere could only be blocked by preadsorption with high concentration of 3-nitrotyrosine (10 mM; Fig. 1e). Together the data indicate that Ab06-284 recognizes free 3-nitrotyrosine in aldehyde-fixed brain sections.

2.3.2   Micro-injected 3-nitrotyrosine is predominantly distributed in neurons and rapidly disappears

Figures 1a and 2a show free 3-nitrotyrosine labeling in mice perfused with paraformaldehyde immediately after the micro-injection, i.e. within 3 min after the onset of microinjecton. Typically fixative reached the brain tissue within 60 s after onset of perfusion, i.e. within 4 min after the beginning of the injection. The volume of the region stained for microinjected 3-nitrotyrosine was 6.5 ± 1.7 (mean ± SD) mm^3, indicating that within 4 min after the beginning of the injection 3-nitrotyrosine reached a relatively large area. Analysis of the cellular distribution of microinjected 3-nitrotyrosine indicated a predominant neuronal distribution (Fig. 3). Analysis of brains perfused at different time points after injection, showed that the amount of 3-
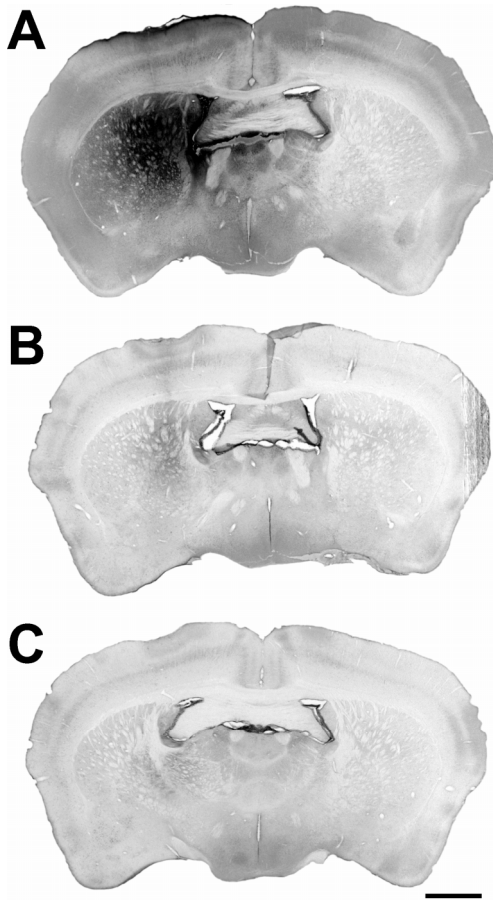
Figure 2: Micro-injected 3-nitrotyrosine disappears within 60 min. after injection.
Brains were perfused at 4 min (A), 30 min (B) or 60 min (C) after injection. Staining with the rabbit anti-nitrotyrosine antibody in a brain after unilateral intra-striatal micro-injection of 10 nmol 3-nitrotyrosine (in 100 nl saline, pH 7.4) showed that the amount of 3-nitrotyrosine labeling was high minutes after injection (A), low 30 min after injection (B), and absent at 60 min after injection (C). Scale bar = 1 mm

nitrotyrosine labeling was substantially reduced 15 min after injection, very low 30 min after injection (Fig 2b), and absent at later time points (Fig. 2c). At all post-injections times there was also no change in labeling with Mab1A6, which reacts with protein-bound 3-nitrotyrosine epitopes, but not with microinjected 3-nitrotyrosine (see above).

2.3.3 Chronic exposure to elevated levels of 3-nitrotyrosine does not cause neuronal degeneration in vivo in the striatum

To examine whether 3-nitrotyrosine induced neuronal degeneration we have examined brain sections for neurodegenerative changes 1 and 2 days after injection using a silver staining procedure that selectively labels degenerating neurons and their processes [15] as well as a number of immunocytochemical markers that usually show altered expression after neuronal degeneration, i.e. glial acidic fibrillary protein (GFAP, a marker for reactive astrogliosis), MAP2 (a dendritic marker) and ATF3 (a marker for injured neurons) [15,21]. However, these methods
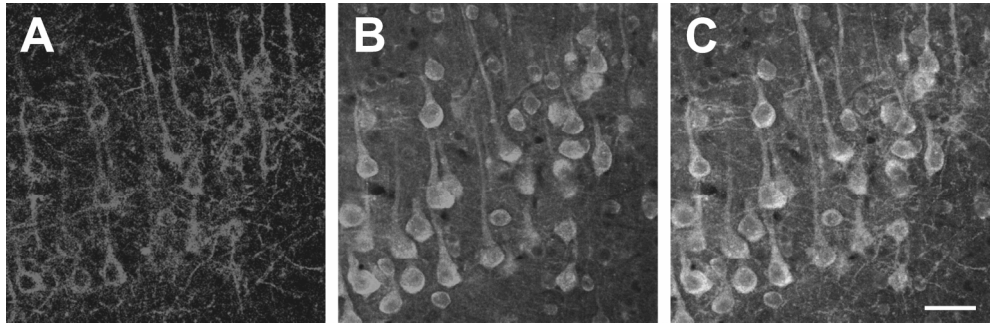
Figure 3:   Microinjected 3-nitrotyrosine shows a predominant neuronal distribution.
Confocal immunofluorescence of lamina V of the cortex in a section adjacent to the section shown in Fig. 2a double-labeled for phosphorylated neurofilament (SMI32, A) and micro-injected 3-nitrotyrosine (B). Note the co-localization of SMI32 and 3-nitrotyrosine labeling. Scale bar = 50 µm
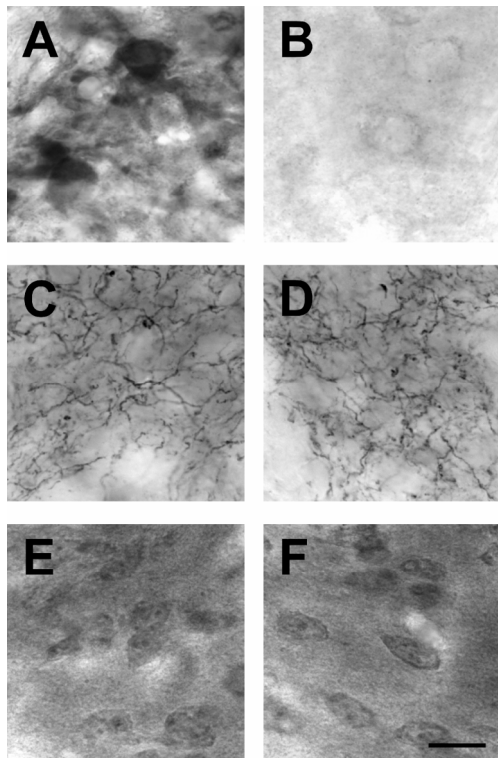

Figure 4:   Chronic intra-striatal delivery of 3-nitrotyrosine does not cause neuronal degeneration.
Polyclonal 3-nitrotyrosine (A, B) and tyrosine hydroxylase (C, D) immunoreactivity and acetylcholine esterase activity in the striatum after chronic (1 week) intrastriatal delivery of 3-nitrotyrosine (A, C, E) or L-tyrosine (B, D, F) via an osmotic pump (Alzet 1007D) coupled to a 30 G canula. Note that 3-nitrotyrosine treatment resulted in very high intraneuronal polyclonal 3-nitrotyrosine labeling, but does not alter tyrosine hydroxylase and acetylcholine esterase staining. Scale bar = 25 µm

did not demonstrate any sign of neuronal degeneration after striatal or hippocampal 3-nitrotyrosine injections (not shown).

In view of the rapid disappearance of microinjected 3-nitrotyrosine we examined the effect of prolonged delivery of 3-nitrotyrosine using Alzet osmotic minipumps coupled to intrastriatal cannulae. However, no signs of neuronal degeneration were

observed after 7 days of 3-nitrotyrosine infusion, although Ab06-284 staining confirmed the presence of high levels of 3-nitrotyrosine in the striatum (Fig. 4a and b). Furthermore we found no changes in other markers for the viability of nigral and striatal neurons, i.e. tyrosine hydroxylase immunoreactivity (Fig. 4c and d) and acetylcholine esterase histochemistry (Fig 4e and f).

2.3.4 Chronic exposure to elevated levels of 3-nitrotyrosine does not cause neuronal degeneration in organotypic spinal cord cultures

To further examine whether 3-nitrotyrosine may be neurotoxic, we have studied the effect of 3-nitrotyrosine on neuronal viability in organotypic spinal cord culture, which is a well established system to screen for factors that influence the viability of motoneurons and other spinal cord neurons [9,17,21,24]. Treatment of spinal cord cultures for 1 week with 50 or 100 µM 3-nitrotyrosine did not result in a change in the number of motoneurons as identified by non-phosphorylated neurofilament (SMI32) staining (Fig. 5i). Also the number of another population of spinal neurons, i.e. interneurons that were SMI-32 positive, was unchanged (Fig. 5i). Also in a second experiment increasing the 3-nitrotyrosine concentration up to 150 µM of 3-nitrotyrosine and using another marker to label motoneurons (ChAT) there was no effect on the number of surviving motoneurons and their morphological appearance (Fig. 5j). Immunohistochemistry with Ab06-284 confirmed the presence of high-levels of 3-nitrotyrosine immunoreactivity in motoneurons from 3-nitrotyrosine treated slices. Interestingly, 3-nitrotyrosine-treated slices also showed increased staining with Mab1A6, which does not immunoreact with free 3-nitrotyrosine (see above), but specifically recognizes protein-bound 3-nitrotyrosine epitopes, indicating that 3-nitrotyrosine is incorporated into proteins.

2.4   Discussion

Because of a number of studies indicating that 3-nitrotyrosine may be neurotoxic we have examined the effect of acute and prolonged application of 3-nitrotyrosine in the brain and in organotypic spinal cord culture. Our data show that 3-nitrotyrosine microinjected into cortical areas or striatum is predominantly localized in neurons. However, neither a single microinjection nor prolonged intrastriatal delivery of 3-nitrotyrosine by osmotic minipumps, nor prolonged treatment of organotypic cultures with 3-nitrotyrosine resulted in any evidence of neuronal degeneration.

To localize microinjected 3-nitrotyrosine we used immunocytochemistry with a commercially available antibody raised against nitrated keyhole limpet hemocyanin [28]. Microinjection of 3-nitrotyrosine (1 or 10 nmol) in cortical areas resulted in very intense and a predominantly neuronal staining. Although the antibody has been shown to preferentially immunoreact with protein bound 3-nitrotyrosine [28], we hypothesize that the staining after microinjection represents free rather than protein bound 3-nitrotyrosine. First, immunostaining of microinjected 3-nitrotyrosine was inhibited after preadsorption of the antibody with relatively low concentrations
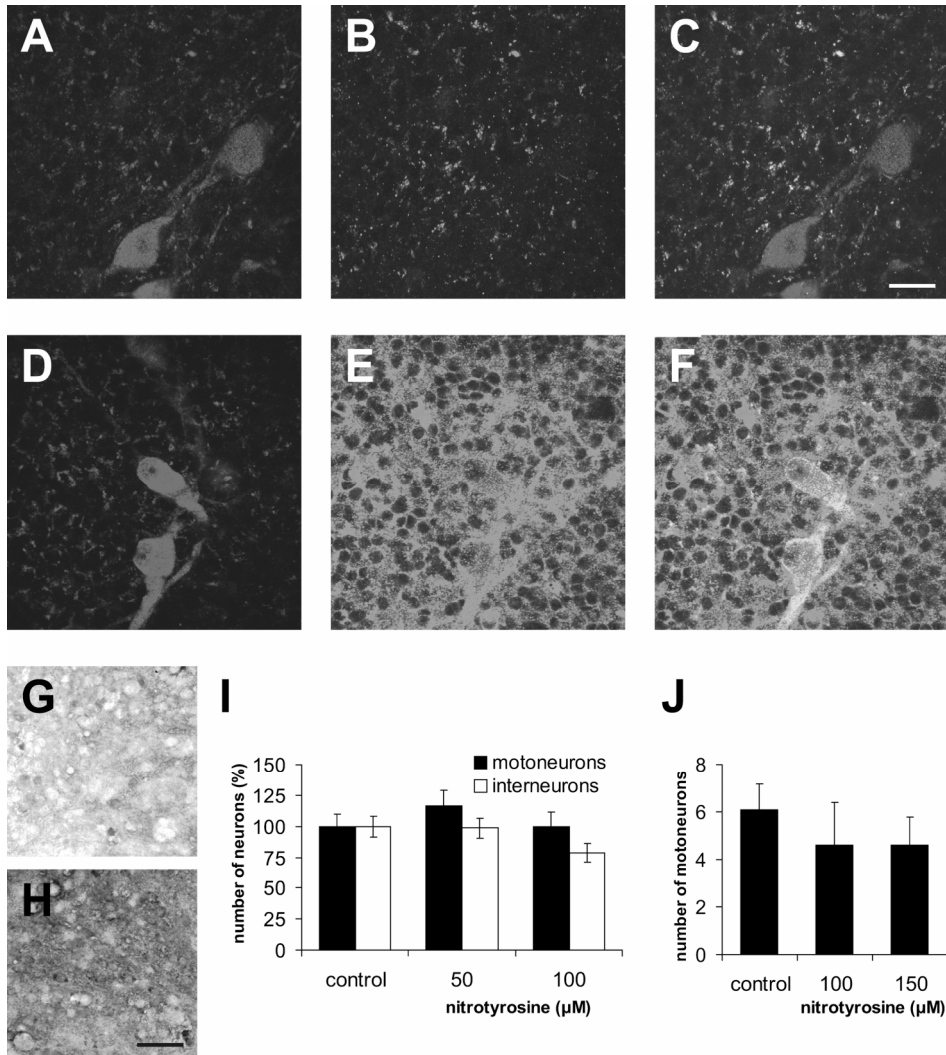
Figure 5:   Chronic exposure to elevated levels of 3-nitrotyrosine does not cause neuronal degeneration in organotypic spinal cord cultures

A-H: Choline acetyltransferase (ChAT, A and D), polyclonal 3-nitrotyrosine (B, E) and monoclonal 3-nitrotyrosine (G, H) labeling of organotypic spinal cord cultures that have been treated for 1 week with 3-nitrotyrosine (50 μM diluted in saline, D-F, H) or saline (A-C, G). In 3-nitrotyrosine-treated slices strong polyclonal 3-nitrotyrosine-immunoreactivity is found in motoneurons (E). Notably, the slices treated with 3-nitrotyrosine also show increased monoclonal 3-nitrotyrosine labeling (H). Scale bars = 50 μm.

I: Counts of motoneurons stained with SMI32-antibody and of SMI32-positive interneurons in organotypic slices after treatment with saline, 50 or 100 μM 3-nitrotyrosine; no significant effects on survival of motoneurons or interneurons was found (I). Values represent means $\pm$ SEM of 20-35 organotypic slices. The number of neurons is expressed as percentage of mean number of neurons in the control group. Mean numbers of motoneurons/slice and interneurons/slice in control group were 6.3 and 170, respectively.

J: Counts of motoneurons stained with ChAT in organotypic slices after treatment with saline, 100 or 150 μM 3-nitrotyrosine; no significant effects on survival of motoneurons was found. Values represent means $\pm$ SEM of 10-15 organotypic slices.

of 3-nitrotyrosine (10 µM) as compared to concentrations needed to inhibit endogenous 3-nitrotyrosine labeling in the brain (i.e. 10 mM), which represents protein-bound 3-nitrotyrosine epitopes. Second, microinjected 3-nitrotyrosine was not labeled by a monoclonal antibody against protein-bound 3-nitrotyrosine epitopes. Endogenous free 3-nitrotyrosine may not be detected by the polyclonal 3-nitrotyrosine antibody because its concentration in the CNS is much lower (nanomolar range [7,11]) than the concentrations of 3-nitrotyrosine shortly after micro-injections, which are likely to be in the low millimolar to high micromolar range (1 or 10 nmol spread over a volume of 6.5 µl, see results).

3-Nitrotyrosine is considered to be a relatively stable a marker for damage left by nitric oxide-derived species, but our data showed that, although a large portion of 3-nitrotyrosine injected in brain tissue entered neurons, most of it disappeared within 60 min after injection. One possibility is that 3-nitrotyrosine is metabolized within neurons. A half-life of 1-2 hours has been reported for free 3-nitrotyrosine in plasma and various tissues without any indication that it is build into proteins, but by what mechanism it is metabolized is not understood [11,26]. Denitrase- (or nitratase-) activities have been found in tissue-homogenates but no specific enzymes have yet been identified [13,19,20], and free 3-nitrotyrosine may not be a substrate for these denitrase activities [18]. An alternative possibility is that injected 3-nitrotyrosine leaves the brain by diffusion.

Mihm et al. [22] have reported degeneration of nigral dopaminergic neurons in mice after a single striatal 3-nitrotyrosine injection. In contrast to these findings we found no evidence for neurodegenerative changes in the striatum or the substantia nigra 2 day after acute injections of 3-nitrotyrosine. More importantly, also chronic intra-striatal administration of 3-nitrotyrosine via osmotic pumps did not result in any evidence of neurodegenerative changes in the nigro-striatal system, although this treatment resulted in prolonged elevation of intraneuronal 3-nitrotyrosine levels as visualized immunocytochemically. Differences in the experimental approaches may explain the differences in results, since Mihm et al. [22] injected higher doses of 3-nitrotyrosine (32 nmol instead of 10 nmol) and a considerable larger injection volume (4 µl instead of 100 nl). Our data do not exclude the possibility that a single injection of a very high concentration of 3-nitrotyrosine causes neuronal degeneration in the nigrostriatal system. However, as suggested by our data, prolonged application of 3-nitrotyrosine in the micromolar range does not damage the nigro-striatal pathway.

A recent study has indicated that also motoneurons are vulnerable to 3-nitrotyrosine, since 50 to 100 µM of 3-nitrotyrosine induced apoptosis in the majority of neurons in isolated embryonic motoneuron culture [23]. This finding is relevant in view of evidence showing increased 3-nitrotyrosine levels in spinal cord of ALS patients and mouse models [2,11]. Increased levels of 3-nitrotyrosine also have been associated with excitotoxic degeneration of motoneurons [6,27]. Our data in organotypic slices, however, indicated no effect of 3-nitrotyrosine on the viability of motoneurons. The difference with the results of Peluffo et al. [23] al least in part can be explained by the use of different culture systems (purified motoneurons versus slice cultures that contain different populations and glia), developmental age of the neurons at the onset of culture (embryonic day 13 versus

postnatal day 7), and/or differences in culture media composition. In fact, the presence of glia or trophic factors attenuated the vulnerability of motoneurons towards 3-nitrotyrosine [23]. Hence, in '*in vivo*-like conditions' as modeled in organotypic slices [9] motoneurons may be resistant to 3-nitrotyrosine at doses up to 100 μM. The absolute levels of 3-nitrotyrosine in control and diseased brain and spinal cord are not precisely known, but may be in the order of 1 or 2 μM or lower, since the tyrosine concentration in the CNS is below 100 μM, and the highest estimate of 3-nitrotyrosine concentration is 2% of total tyrosine. We therefore conclude that increased levels of free 3-nitrotyrosine as reported for amyotrophic lateral sclerosis and other neurodegenerative diseases [11,25] are unlikely to contribute to neuronal degeneration in these disorders.

References

[1]   D. Alonso, J.M. Encinas, L.O. Uttenthal, L. Bosca, J. Serrano, A.P. Fernandez, S. Castro-Blanco, M. Santacana, M.L. Bentura, A. Richart, P. Fernandez-Vizarra, J. Rodrigo, Coexistence of translocated cytochrome c and nitrated protein in neurons of the rat cerebral cortex after oxygen and glucose deprivation, Neuroscience 111 (2002) 47-56.

[2]   M.F. Beal, Oxidatively modified proteins in aging and disease, Free Radic Biol Med 32 (2002) 797-803.

[3]   J.S. Beckman, W.H. Koppenol, Nitric oxide, superoxide, and peroxynitrite: the good, the bad, and ugly, Am J Physiol 271 (1996) C1424-1437.

[4]   C.G. Bisig, S.A. Purro, M.A. Contin, H.S. Barra, C.A. Arce, Incorporation of 3-nitrotyrosine into the C-terminus of alpha-tubulin is reversible and not detrimental to dividing cells, Eur J Biochem 269 (2002) 5037-5045.

[5]   M. Coesmans, P.A. Smitt, D.J. Linden, R. Shigemoto, T. Hirano, Y. Yamakawa, A.M. van Alphen, C. Luo, J.N. van der Geest, J.M. Kros, C.A. Gaillard, M.A. Frens, C.I. de Zeeuw, Mechanisms underlying cerebellar motor deficits due to mGluR1-autoantibodies, Ann Neurol 53 (2003) 325-336.

[6]   M.M. Doroudchi, S. Minotti, D.A. Figlewicz, H.D. Durham, Nitrotyrosination contributes minimally to toxicity of mutant SOD1 associated with ALS, Neuroreport 12 (2001) 1239-1243.

[7]   M.W. Duncan, A review of approaches to the analysis of 3-nitrotyrosine, Amino Acids 25 (2003) 351-361.

[8]   J.P. Eiserich, A.G. Estevez, T.V. Bamberg, Y.Z. Ye, P.H. Chumley, J.S. Beckman, B.A. Freeman, Microtubule dysfunction by posttranslational nitrotyrosination of alpha- tubulin: a nitric oxide-dependent mechanism of cellular injury, Proc Natl Acad Sci U S A 96 (1999) 6365-6370.

[9]   J.L. Elliott, Experimental models of amyotrophic lateral sclerosis, Neurobiol Dis 6 (1999) 310-320.

[10] B.I. Giasson, J.E. Duda, I.V. Murray, Q. Chen, J.M. Souza, H.I. Hurtig, H. Ischiropoulos, J.Q. Trojanowski, V.M. Lee, Oxidative damage linked to neurodegeneration by selective alpha-synuclein nitration in synucleinopathy lesions, Science 290 (2000) 985-989.

[11] S.A. Greenacre, H. Ischiropoulos, Tyrosine nitration: localisation, quantification, consequences for protein function and signal transduction, Free Radic Res 34 (2001) 541-581.

[12] T. Horiguchi, K. Uryu, B.I. Giasson, H. Ischiropoulos, R. LightFoot, C. Bellmann, C. Richter-Landsberg, V.M. Lee, J.Q. Trojanowski, Nitration of tau protein is linked to neurodegeneration in tauopathies, Am J Pathol 163 (2003) 1021-1031.

[13] Y. Irie, M. Saeki, Y. Kamisaki, E. Martin, F. Murad, Histone H1.2 is a substrate for denitrase, an activity that reduces nitrotyrosine immunoreactivity in proteins, Proc Natl Acad Sci U S A 100 (2003) 5634-5639.

[14] H. Ischiropoulos, J.S. Beckman, Oxidative stress and nitration in neurodegeneration: cause, effect, or association?, J Clin Invest 111 (2003) 163-169.

[15] D. Jaarsma, E.D. Haasdijk, J.A. Grashorn, R. Hawkins, W. van Duijn, H.W. Verspaget, J. London, J.C. Holstege, Human Cu/Zn superoxide dismutase (SOD1) overexpression in mice causes mitochondrial vacuolization, axonal degeneration, and premature motoneuron death and accelerates motoneuron disease in mice expressing a familial amyotrophic lateral sclerosis mutant SOD1, Neurobiol Dis 7 (2000) 623-643.

[16] D. Jaarsma, F. Rognoni, W. van Duijn, H.W. Verspaget, E.D. Haasdijk, J.C. Holstege, CuZn superoxide dismutase (SOD1) accumulates in vacuolated mitochondria in transgenic mice expressing amyotrophic lateral sclerosis-linked SOD1 mutations, Acta Neuropathol (Berl) 102 (2001) 293-305.

[17] E.C. Kaal, A.S. Vlug, M.W. Versleijen, M. Kuilman, E.A. Joosten, P.R. Bar, Chronic mitochondrial inhibition induces selective motoneuron death in vitro: a new model for amyotrophic lateral sclerosis, J Neurochem 74 (2000) 1158-1165.

[18] Y. Kamisaki, K. Wada, K. Bian, B. Balabanli, K. Davis, E. Martin, F. Behbod, Y.C. Lee, F. Murad, An activity in rat tissues that modifies nitrotyrosine-containing proteins, Proc Natl Acad Sci U S A 95 (1998) 11584-11589.

[19] T. Koeck, X. Fu, S.L. Hazen, J.W. Crabb, D.J. Stuehr, K.S. Aulak, Rapid and selective oxygen-regulated protein tyrosine denitration and nitration in mitochondria, J Biol Chem 279 (2004) 27257-27262.

[20] W.N. Kuo, R.N. Kanadia, V.P. Shanbhag, R. Toro, Denitration of peroxynitrite-treated proteins by 'protein nitratases' from rat brain and heart, Mol Cell Biochem 201 (1999) 11-16.

[21] A. Maatkamp, A. Vlug, E. Haasdijk, D. Troost, P.J. French, D. Jaarsma, Decrease of Hsp25 protein expression precedes degeneration of motoneurons in ALS-SOD1 mice, Eur J Neurosci 20 (2004) 14-28.

[22] M.J. Mihm, B.L. Schanbacher, B.L. Wallace, L.J. Wallace, N.J. Uretsky, J.A. Bauer, Free 3-nitrotyrosine causes striatal neurodegeneration in vivo, J Neurosci 21 (2001) 1-5.

[23] H. Peluffo, J.J. Shacka, K. Ricart, C.G. Bisig, L. Martinez-Palma, O. Pritsch, A. Kamaid, J.P. Eiserich, J.P. Crow, L. Barbeito, A.G. Estevez, Induction of motor neuron apoptosis by free 3-nitro-l-tyrosine, J Neurochem 89 (2004) 602-612.

[24] J.D. Rothstein, L.A. Bristol, B. Hosler, R.H. Brown, Jr., R.W. Kuncl, Chronic inhibition of superoxide dismutase produces apoptotic death of spinal neurons, Proc Natl Acad Sci U S A 91 (1994) 4155-4159.

[25] F.J. Schopfer, P.R. Baker, B.A. Freeman, NO-dependent protein nitration: a cell signaling event or an oxidative inflammatory response?, Trends Biochem Sci 28 (2003) 646-654.

[26] S. Takizawa, N. Fukuyama, H. Hirabayashi, H. Nakazawa, Y. Shinohara, Dynamics of nitrotyrosine formation and decay in rat brain during focal ischemia-reperfusion, J Cereb Blood Flow Metab 19 (1999) 667-672.

[27] M. Urushitani, S. Shimohama, T. Kihara, H. Sawada, A. Akaike, M. Ibi, R. Inoue, Y. Kitamura, T. Taniguchi, J. Kimura, Mechanism of selective motor neuronal death after exposure of spinal cord to glutamate: involvement of glutamate-induced nitric oxide in motor neuron toxicity and nonmotor neuron protection, Ann Neurol 44 (1998) 796-807.

[28] L. Viera, Y.Z. Ye, A.G. Estevez, J.S. Beckman, Immunohistochemical methods to detect nitrotyrosine, Methods Enzymol 301 (1999) 373-381.

[29] A.S. Vlug, D. Jaarsma, Long term proteasome inhibition does not preferentially afflict motor neurons in organotypical spinal cord cultures, Amyotroph Lateral Scler Other Motor Neuron Disord 5 (2004) 16-21.

[30] M. Zedda, G. Lepore, S. Gadau, P. Manca, V. Farina, Morphological and functional changes induced by the amino acid analogue 3-nitrotyrosine in mouse neuroblastoma and rat glioma cell lines, Neurosci Lett 363 (2004) 190-193.

Chapter 3

LONG TERM PROTEASOME INHIBITION DOES NOT PREFERENTIALLY AFFLICT MOTOR NEURONS IN ORGANOTYPICAL SPINAL CORD CULTURES

Angela S Vlug and Dick Jaarsma

Department of Neuroscience, Erasmus MC, Rotterdam, The Netherlands

3.1   Abstract

Ubiquitinated inclusions are a constant feature of amyotrophic lateral sclerosis (ALS). It has been hypothesized that these inclusions reflect overload or failure of the ubiquitin-proteasome system, and that this failure contributes to the degeneration of motoneurons.

In the present study we have examined the effect of low concentrations of proteasome inhibitors on protein aggregation and viability of neurons in organotypic spinal cord cultures. We found a dose-dependent degeneration of neurons after a one-week exposure to the proteasome inhibitors lactacystin and epoxomicin. Neuronal degeneration was associated with an increase in poly-ubiquitination, consistent with failure of the ubiquitin-proteasome system. Proteasome inhibition caused degeneration of both motoneurons and interneurons, and no difference in survival between motoneurons and interneurons was observed.

Since protein aggregation may particularly play a role in ALS-patients with superoxide dismutase 1 (SOD1) mutations, we have compared the effect of proteasome inhibition between spinal cord cultures from non-transgenic and G93A-SOD1 transgenic mice. There was no difference between the viability of motoneurons from transgenic and non-transgenic mice.

3.2   Introduction

Amyotrophic lateral sclerosis (ALS) is a progressive neurodegenerative disease of motoneurons, resulting in a loss of spinal, bulbar and cortical motoneurons. ALS causes progressive paralysis that leads to death an average of 3 years after diagnosis. Approximately 10% of ALS cases are familial, with the majority of cases deemed to be sporadic (without known genetic linkage). About 20% of familial ALS (fALS) cases are associated with mutations in the Cu/Zn superoxide dismutase (SOD1) gene. More than 90 different mutations have been found in the SOD1-gene that can cause fALS. The mutations are found in different parts of the SOD1 protein, such as the dimer interface or the metal-binding sites. Some mutated proteins have full SOD1 function while other mutations disrupt the normal activity of SOD1 [19]. Despite these obvious different effects of mutations on the function of the protein, all these mutations cause a clinically similar disease. The cause of sporadic ALS (sALS) and the mechanism by which mutated SOD1 (mSOD1) causes ALS, remain still largely unknown. Hypotheses about the effect of SOD1-mutations include decreased copper and zinc binding, enhanced peroxidase activity and enhancement of other oxidative reactions causing oxidative stress. A more recent hypothesis poses that the mutant protein may be sufficiently unstable that it precipitates to form aggregates. The formation of aggregates is a common feature of many neurodegenerative diseases. Although the presence of abnormal intracellular inclusions in ALS was described more than 40 years ago, it is only the last decade, that much attention has been given to the possibility that aggregation of proteins could be a cause of ALS. Misfolded or unfolded proteins can form small oligomers that arise from non-native protein-protein interactions. These oligomers are often poorly soluble and, if they are not degraded, they will form cytosolic aggregates. Inclusion bodies are defined as intracellular foci into which aggregated proteins are sequestered. There are two models for the formation of inclusion bodies. In the first model, single proteins or small oligomers diffuse to the site of the inclusion body forming a 'giant aggregate'. In the second model, multiple aggregates are formed throughout the cell, and fuse into an 'aggregate of aggregates'. A variant of the latter model suggests active retrograde transport of aggregates on microtubules forming an inclusion body, also called an 'aggresome' [10]. It has been shown that protein aggregation can impair the ubiquitin-proteasome system, possibly caused by saturation of molecular chaperones involved in proteasomal function or by overloading of the proteasome by undegradable aggregates. This inhibition could lead to further aggregate formation, creating a positive-feedback system [1].

In ALS it is hypothesized that in Cu/Zn superoxide dismutase (SOD1)-related ALS, protein aggregation is the toxic gain of function of mutated SOD1 (mSOD1). Aggregates containing ubiquitin and SOD1 have been found in fALS patients [17], and mSOD1 transgenic mice [2,7], and it has been demonstrated that mutant SOD1 forms small aggregates in mSOD1 transgenic mice long before formation of large inclusion bodies or motoneuron dysfunction [7]. SOD1 has also been found in Lewy body-like inclusions of sporadic ALS patients [16]. A decrease in abundance of large aggregates after overexpression of HSP70, however, does not affect the survival of mSOD1 (G85R) transgenic mice [12]. This raises the question whether

these aggregates can be the cause of mSOD1 toxicity or are just a harmless by-product of the disease, or if they even protect against damage by mutant SOD1.

Degeneration of neurons in ALS is primarily restricted to motoneurons. This implies that, if aggregates are the cause of motoneuron degeneration, motoneurons are either more prone to aggregate formation or more sensitive to the harmful effects of aggregates. If the former is the case, it might be explained by the fact that motoneurons have a longer half-life and higher concentration than other cell-types, thus increasing the chances for oxidative modifications by reactive oxygen species. Oxidative damaged SOD1 is prone to form aggregates [14].

Protein degradation is mediated predominantly through the ubiquitin-proteasome pathway. Overload or failure of this system to degrade mSOD1 could lead to aggregation of ubiquitinated mSOD1 and other proteins and disruption of cellular homeostasis causing neuronal degeneration. This has been shown experimentally by short-term inhibition of the proteasome that causes accumulation of ubiquitinated proteins and apoptosis [13]. In the present study we used low concentrations of proteasome inhibitors for a relatively long period to study protein aggregation in organotypic spinal cord cultures of normal and G93A-SOD1 transgenic mice. This culture system has also been used to study the effect of chronic mitochondrial inhibition on motoneurons [8]. We hypothesize that formation of aggregates in neurodegenerative diseases is caused by proteasome dysfunction. This implies that motoneurons with mSOD1 should be more sensitive to proteasome inhibition than motoneurons with normal SOD1 because the proteasome system is already stressed by high amounts of abnormal protein. It also implies that, since predominantly only motoneurons are degenerating in ALS, the motoneurons should be more sensitive to proteasome inhibition than spinal interneurons.

3.3   Materials and Methods

3.3.1   Organotypic slice cultures

Experiments were performed in accordance with the "Principles of laboratory animal care"(NIH publication no.86-23, revised 1985) and the guidelines approved by the Erasmus University animal care committee (DEC, protocol nr 115-01-01 and 115-00-09). SOD1^{G93A} mice descendent from the Gurney G1L line were obtained from Jackson Laboratories (strain B6SJL-TgN (SOD1-G93A)1 Gur). In our animal facility, SOD1^{G93A} mice were bred in FVB/N background by mating hemizygous transgenic animals with FVB/N females (Harlan, The Netherlands). Transgenic pups were identified by PCR of tail DNA with primers specific for human SOD1 [6]. Organotypic spinal cord cultures were prepared from the lumbar spinal cord of 7-day-old mouse pups similar to methods described previously [8]. In brief, lumbar spinal cords were dissected and sliced into 350 µm -thick sections. The slices were cultured on membrane inserts (Millicell-CM, Millipore, The Netherlands) with 5 slices per insert. The inserts were placed in 35-mm culture dishes, containing 1 ml of culture medium and kept in a 5% CO_2 incubator at 37°C. The medium consisted
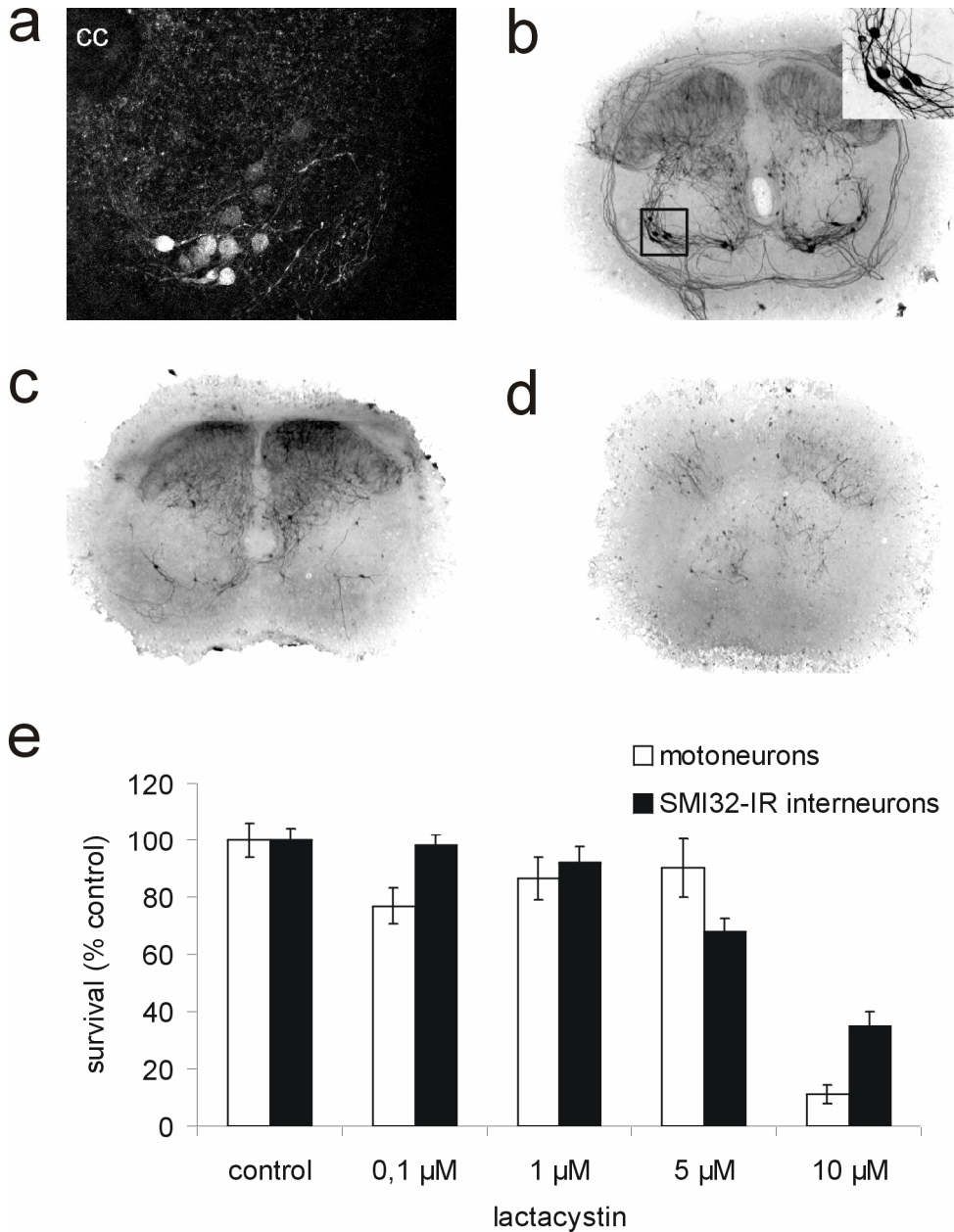
Figure 1: Lactacystin causes a dose-dependent neuronal degeneration. Untreated slices showing ChAT specifically labels motoneurons (a, cc - central canal) while SMI32 labels motoneurons and a sub-population of interneurons (b). (c-d) Slices treated with 1 µM of lactacystin (c) or 10 µM of lactacystin (d) show mild or severe damage respectively, in both the ventral and dorsal horn. (e) Relative amount of motoneurons (white bars) and interneurons (black bars) after treatment with lactacystin. Data represent mean ± SEM based on analysis of more than 10 slices per treatment group.

A

B
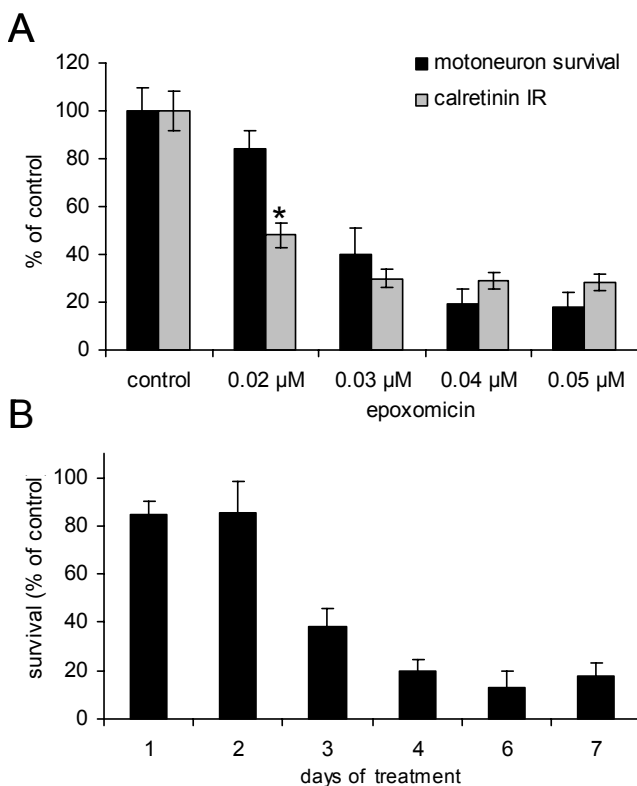
Figure 2: (a) Epoxomicin causes dose-dependent degeneration of motoneurons and dorsal calretinin-immunoreactive neurons in organotypic spinal cord cultures after one week of treatment. In these experiments calretinin-immunoreactive (IR) interneurons were used to examine whether the effect of epoxomicin was cell-type specific. The effect of epoxomicin on survival is much more reliable than the effect of lactacystin. Data are mean ± SEM from 18-24 slices per treatment group. * P<0.01 (b) Relative amount of motoneurons after 1-7 days of epoxomicin treatment. The effect of epoxomicin on survival is visible only after 3 days of treatment, indicating that epoxomicin is not acutely toxic. Data are mean ± SEM from 15-30 slices.

of Hanks' balanced salt solution (25%), horse serum (25%), minimal essential medium (50%), glucose (6.3 mg/ml), L-glutamine (2 mM), penicillin (100 IU/ml) and streptomycin (100 µg/ml). Culture medium was changed twice weekly.

3.3.2 Treatment

After 2 weeks in vitro, the cultures were treated with various doses of clasto-lactacystin ß-lactone (Calbiochem, USA), epoxomicin (Affiniti, UK) or vehicle for 1 week. Lactacystin was dissolved to a stock-concentration of 1 mM. Epoxomicin was dissolved in DMSO to a stock-concentration of 100 µM. A maximum of 10 µl was added to 1 ml of culture medium to obtain the final concentration.

3.3.3 Immunohistochemistry

At various time points after treatment, the cultures were fixed with 4% paraformaldehyde in 0.1 M phosphate buffer, and processed for fluorescent immunohistochemistry. The primary antibodies were diluted in PBS containing 2% normal horse serum and 0.3% Triton X-100: mouse anti-SMI31, mouse anti-SMI32 (Sternberger monoclonals, USA), rabbit anti-ubiquitin (DAKO, Denmark), goat anti-SOD1, rabbit anti-ATF3, goat anti-ChAT (Chemicon, UK). Fluorescently labeled and biotin-conjugated secondary antibodies were obtained from DAKO (Denmark). Immunofluorescent sections were analyzed with a Zeiss LSM 510 confocal microscope. Motoneurons were defined as large ChAT- and/or SMI32-positive cells in the ventral horn. Results are presented as means ± SEM. Ubiquitin- and

calretinin-immunoreactivity were determined using Scion Image Beta 4.0.2 software (Scion Corporation, USA).

3.4   Results

Different types of neurons were present in the spinal cord cultures. Motoneurons were identified using ChAT or SMI32-staining (Figure 1a-b). Double-labelling experiments showed that almost 90% of motor neurons showed both ChAT and SMI32 immunoreactivity, but to remove any existing doubts about SMI32 staining as a means to identify motor neurons we used either ChAT- or SMI32-staining in subsequent experiments. After 2-3 weeks in culture ± 10 motoneurons per slice were present. In the next weeks the number of motoneurons decreased slightly (approximately 7 motoneurons per slice after 8 weeks in culture). culture). After 3 weeks in culture the number of SMI32-immunoreactive interneurons was approximately 250 while the number of calretinin immunoreactive neurons was about 215. In the proteasome inhibitor experiments we started the treatment after two weeks in culture and treated for one week. Initial experiments were carried out using lactacystin, an antibiotic derived from *Streptomyces*, that is currently the most often used proteasome inhibitor. Treatment with 0.1-10 µM lactacystin for one week resulted in a dose-dependent degeneration of motoneurons and interneurons (Figure 1) but only 10 mM had a consistent significant effect. Lactacystin also has inhibitory effects on some non-proteasomal proteases such as cathepsin A [11]. We therefore used epoxomicin in subsequent experiments. Epoxomicin is a more selective, irreversible proteasome inhibitor that does not inhibit non-proteasomal proteases such as trypsin, chymotrypsin and calpain [13]. As with lactacystin, a one-week treatment with epoxomicin (0.01-0.1 µM) resulted in a dose-dependent death of motoneurons (Figure 2a and 5b): 0.02 µM epoxomicin did not affect cell survival, whereas 0.03 µM and 0.04 µM epoxomicin caused 60% and 80% motoneuron death, respectively. A decrease in the number of motoneurons was first visible after 3 days of epoxomicin (0.05 µM) treatment, indicating that epoxomicin had a chronic effect and was not acutely toxic (Figure 2b). The total immunoreactivity for
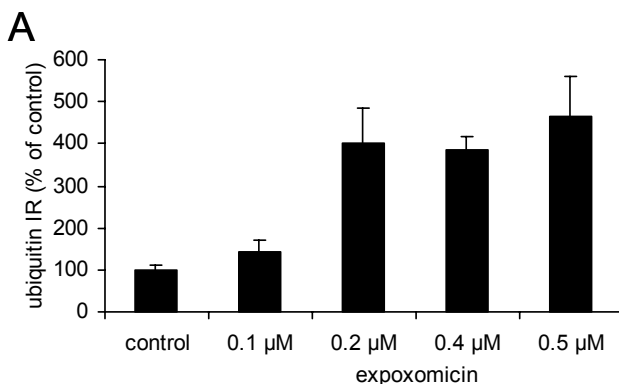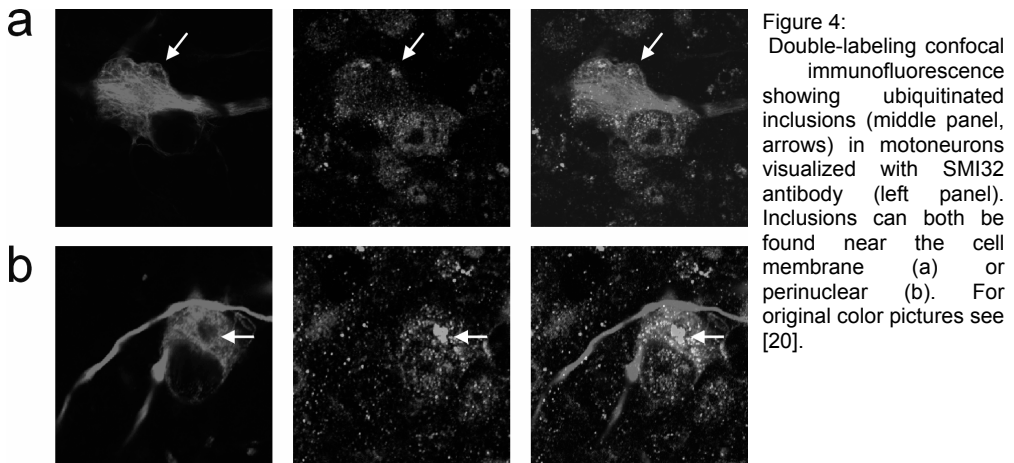

A

Figure 3: Optical density readings for the poly-ubiquitin immunoreactivity of the ventral horn of spinal cord slices. The increase in poly-ubiquitin immunoreactivity indicates that epoxomicin inhibits the proteasome in our culture system. Data are mean ± SEM from 5 slices per treatment group

Figure 4:
Double-labeling confocal immunofluorescence showing ubiquitinated inclusions (middle panel, arrows) in motoneurons visualized with SMI32 antibody (left panel). Inclusions can both be found near the cell membrane (a) or perinuclear (b). For original color pictures see [20].

poly-ubiquitin of the ventral horn of the spinal cord cultures increased significantly with the higher dosages of epoxomicin(Figure 3), showing that epoxomicin causes an elevation of the amount of ubiquitinated proteins in the cells.

Motoneurons that received a sub-lethal dose of epoxomicin (0.02 µM) showed morphological changes that suggested degeneration (irregular cell shape, shortening of neurites). Aggregates were found in the cell body near the membrane or juxta-nuclear (Figure 4). Confocal microscopy using triple staining with antibodies against non-phosphorylated neurofilament (SMI32) and ubiquitin showed aggregates containing ubiquitin but not SOD1 in motoneurons (results not shown).

To determine whether motoneurons were specifically vulnerable for the effects of proteasome inhibition we also looked at other populations of neurons. SMI32-immunoreactive interneurons show no decreased vulnerability to epoxomicin (Figure 1e). Calretinin-immunoreactive interneurons seem to be more vulnerable to 0.02 µM of epoxomicin, but with higher doses of epoxomicin there is no difference in the survival between motoneurons and small interneurons (Figure 2a).

Neurons expressing mutant SOD1 spontaneously develop aggregates and inclusions. We found no spontaneous formation of aggregates in non-treated spinal cord cultures from SOD1^{G93A} mice (results not shown).We subsequently looked at the effect epoxomicin in cultures from G93A-SOD1 mice. We hypothesized that the high amount of mutant SOD1 in cultures from G93A-SOD1 spinal cord could make those cultures more vulnerable to proteasome inhibition. However, we did not find any significant differences in the survival of motoneurons and interneurons (Figure 5a), or in the number of aggregates between normal and G93A-SOD1 spinal cord. There was no apparent difference in the survival of motoneurons between spinal cord slices from non-transgenic littermates and slices from G93A-SOD1 mice after epoxomicin treatment (Figure 5b).
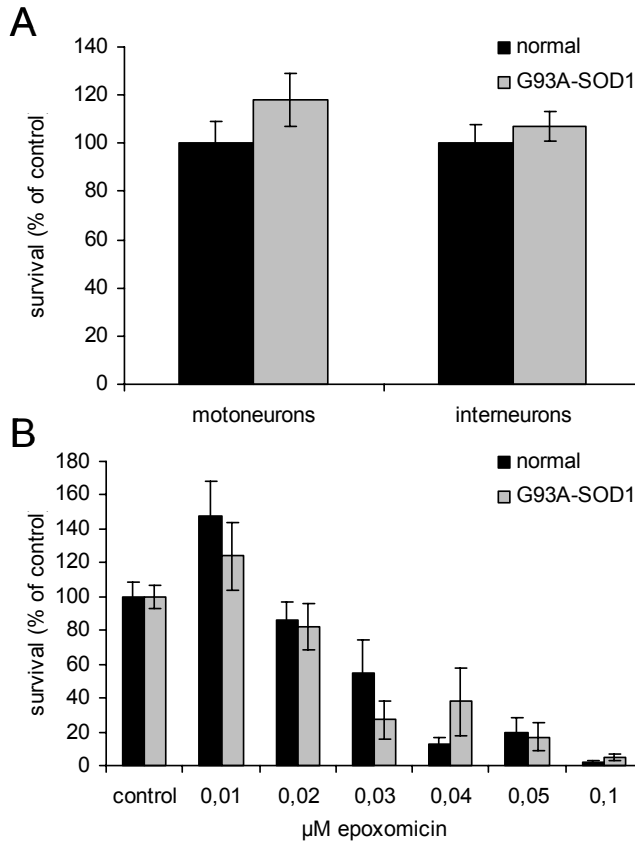
A

B

Figure 5: (a) Slices from G93A-SOD1 mice show the same number of motoneurons and calretinin immunoreactive dorsal interneurons as normal mice. This indicates that there is no decrease in the survival of neurons in G93A-SOD1 transgenic cultures. (b) Motoneurons from G93A-SOD1 mice show the same survival after one week of treatment as control motoneurons. Which means that expression of G93A-SOD1 does not increase the vulnerability of neurons to proteasome inhibition. Data are mean ± SEM from 9-20 slices.

3.5   Discussion

Several lines of evidence indicate that accumulation of misfolded proteins is a central event in ALS and other neurodegenerative diseases. The main question is whether the formation of aggregates causes motoneuron degeneration or is just a harmless by-product of the disease. The current opinion, corroborated by findings in Parkinson's disease research, is that protein aggregates are formed by an overload of the proteasome and possibly also by overloading the chaperone system [3]. In agreement with this we also hypothesized that formation of aggregates in ALS is caused by proteasome dysfunction. If this hypothesis is correct, motoneurons with mutant SOD1 (mSOD1) should be more sensitive to proteasome inhibition than motoneurons with normal SOD1 because the proteasome system is already stressed by high amounts of abnormal protein. In our experiments with organotypic spinal cord cultures, however, we did not find a difference between neurons from normal mice and G93A-SOD1 mice. Although the mice we use are only 7 days old, they already have a high expression of G93A-SOD1, excluding the possibility that a low expression of mSOD1 is the cause of the lack of difference between G93A-SOD1 cultures and control cultures. These data do not favor our hypothesis.

Inhibition of the proteasome causes an increase in posttranslationally modified proteins, probably by the loss or degradation of these proteins. The subsequent elevation of posttranslationally modified proteins produces cellular symptoms of oxidative stress and mitochondrial dysfunction [9]. Proteasome inhibition also causes an increase in levels of cell death factors [4]. Both effects of proteasome inhibition may cause cell death without formation of protein aggregates, explaining why we could find no difference in survival between normal and G93A-SOD1 neurons. The opposite might happen after treating the slices with a low concentration (0.01 µM) of epoxomicin which caused a significant increase in the survival of motoneurons in organotypic slice cultures of non-transgenic mice. Other cases of increased survival of cells after treatment with proteasome inhibitors have been reported, including decreased apoptosis of growth factor-deprived sympathetic neurons [15,22]. In these cases the degradation of survival factors might be inhibited more than the degradation of death factors which cause apoptosis of motoneurons in culture. Both pro-apoptotic and antiapoptotic factors are known to be degraded by the ubiquitin-proteasome system][22], but how low-level proteasome inhibition can have other effects on apoptosis factors than high-level inhibition is not clear. A third possible explanation for cell death after proteasome inhibition is the unfolded protein response (UPR), which is a signal transduction pathway that is activated when misfolded or aggregated proteins accumulate in the endoplasmic reticulum. Although this reaction is meant to enhance protein folding capacity and increase survival, prolonged UPR-activation leads to programmed cell death [5].

We found no selective motoneuron degeneration. In contrast to our results, Kikuchi et al (2002) found that motoneurons are more susceptible to proteasome inhibition than other neurons. Unlike us, however, they used dissociated total spinal cord cultures and a different non-motoneuron population. Our choice of control population was based on earlier publication of different vulnerabilities found between motoneurons and calretinin-immunoreactive interneurons [8]. Other important differences between our experiments and those performed by Kickuchi et al (2002) are the dose and time-frame; they completed short-term high dose experiments while we performed relatively long-term, low dose experiments. Based on our results, we cannot conclude that motoneurons are more susceptible than all other types of neurons in the spinal cord. The selectivity of degeneration in ALS is either not proteasome dependent, or the inhibition of proteasomes in our experiments was too robust and the duration was insufficient to obtain the kind of aggregation that occurs in ALS.

Since mSOD1 is abundant in slice cultures from G93A-SOD1 spinal cord, the lack of SOD1-immunoreactivity in aggregates is probably due to an antibody-binding defect and not to an absence of SOD1 in aggregates. In cultured cells expressing high levels of mSOD1, aggregates containing SOD1 haven been shown after proteasome inhibition [Hyun, 2003 #429]. The absence of SOD1 does not have to mean, however, that this model is not a suitable representation of ALS because little or no SOD1 has been found in ubiquitin-immunoreactive aggregates from sporadic ALS patients [16,21]. Possible factors leading to protein aggregation in sporadic ALS are lipid peroxidation and protein glycation caused by oxidative stress [18,19] and neurotoxic compounds. It is probable that aggregates containing

SOD1 are present in our experimental system, but that these aggregates are too small to be visible using lightmicroscopy. Aggregates containing mSOD1 have been found in vitro after proteasome inhibition but those cells probably had much higher mSOD1-expression.

Our findings that inclusions may be a side-product of ALS, rather than a disease-causing event seem to support the findings of Liu et al. [Liu, 2001 #261] who found that a decrease in the number of large aggregates did not affect the survival of mSOD1 transgenic mice. Since inclusions are also common in other neurodegenerative diseases it might be useful to further look at the toxicity of different types of inclusions in neurons in other neurodegenerative diseases.

References

[1]   N.F. Bence, R.M. Sampat, R.R. Kopito, Impairment of the ubiquitin-proteasome system by protein aggregation, Science 292 (2001) 1552-1555.

[2]   L.I. Bruijn, M.K. Houseweart, S. Kato, K.L. Anderson, S.D. Anderson, E. Ohama, A.G. Reaume, R.W. Scott, D.W. Cleveland, Aggregation and motor neuron toxicity of an ALS-linked SOD1 mutant independent from wild-type SOD1, Science 281 (1998) 1851-1854.

[3]   D.W. Cleveland, J.D. Rothstein, From Charcot to Lou Gehrig: deciphering selective motor neuron death in ALS, Nat Rev Neurosci 2 (2001) 806-819.

[4]   Q. Ding, J.N. Keller, Proteasomes and proteasome inhibition in the central nervous system, Free Radic Biol Med 31 (2001) 574-584.

[5]   M.S. Forman, V.M.-Y. Lee, J.Q. Trojanowski, 'Unfolding' pathways in neurodegenerative disease, Trends Neurosci 26 (2003) 407-410.

[6]   D. Jaarsma, F. Rognoni, W. van Duijn, H.W. Verspaget, E.D. Haasdijk, J.C. Holstege, CuZn superoxide dismutase (SOD1) accumulates in vacuolated mitochondria in transgenic mice expressing amyotrophic lateral sclerosis-linked SOD1 mutations, Acta Neuropathol (Berl) 102 (2001) 293-305.

[7]   J.A. Johnston, M.J. Dalton, M.E. Gurney, R.R. Kopito, Formation of high molecular weight complexes of mutant Cu,Zn-superoxide dismutase in a mouse model for familial amyotrophic lateral sclerosis, Proc Natl Acad Sci U S A 97 (2000) 12571-12576.

[8]   E.C. Kaal, A.S. Vlug, M.W. Versleijen, M. Kuilman, E.A. Joosten, P.R. Bar, Chronic mitochondrial inhibition induces selective motoneuron death in vitro: a new model for amyotrophic lateral sclerosis, J Neurochem 74 (2000) 1158-1165.

[9]   S. Kikuchi, K. Shinpo, M. Takeuchi, S. Tsuji, I. Yabe, M. Niino, K. Tashiro, Effect of geranylgeranylaceton on cellular damage induced by proteasome inhibition in cultured spinal neurons, J Neurosci Res 69 (2002) 373-381.

[10]   R.R. Kopito, Aggresomes, inclusion bodies and protein aggregation, Trends Cell Biol 10 (2000) 524-530.

[11]   L. Kozlowski, T. Stoklosa, S. Omura, C. Wojcik, M.Z. Wojtukiewicz, K. Worowski, H. Ostrowska, Lactacystin inhibits cathepsin A activity in melanoma cell lines, Tumour Biol 22 (2001) 211-215.

[12]   J. Liu, D.W. Cleveland, ALS-linked SOD1 mutants mislocalize HSP70 into aggregates but these do not alter the course of disease, Soc. Neurosci. abstr 2001 San Diego, USA (2001) 580.583.

[13]   L. Meng, R. Mohan, B.H. Kwok, M. Elofsson, N. Sin, C.M. Crews, Epoxomicin, a potent and selective proteasome inhibitor, exhibits in vivo antiinflammatory activity, Proc Natl Acad Sci U S A 96 (1999) 10403-10408.

[14]   R. Rakhit, P. Cunningham, A. Furtos-Matei, S. Dahan, X.F. Qi, J.P. Crow, N.R. Cashman, L.H. Kondejewski, A. Chakrabartty, Oxidation-induced misfolding and aggregation of superoxide dismutase and its implications for amyotrophic lateral sclerosis, J Biol Chem 277 (2002) 47551-47556.

[15]   R. Sadoul, P.A. Fernandez, A.L. Quiquerez, I. Martinou, M. Maki, M. Schroter, J.D. Becherer, M. Irmler, J. Tschopp, J.C. Martinou, Involvement of the proteasome in the programmed cell death of NGF-deprived sympathetic neurons, Embo J 15 (1996) 3845-3852.

[16]   N. Shibata, A. Hirano, M. Kobayashi, S. Sasaki, T. Kato, S. Matsumoto, Z. Shiozawa, T. Komori, A. Ikemoto, T. Umahara, et al., Cu/Zn superoxide dismutase-like immunoreactivity in Lewy body-like inclusions of sporadic amyotrophic lateral sclerosis, Neurosci Lett 179 (1994) 149-152.

[17]   N. Shibata, A. Hirano, M. Kobayashi, T. Siddique, H.X. Deng, W.Y. Hung, T. Kato, K. Asayama, Intense superoxide dismutase-1 immunoreactivity in intracytoplasmic hyaline inclusions of familial amyotrophic lateral sclerosis with posterior column involvement, J Neuropathol Exp Neurol 55 (1996) 481-490.

[18]   N. Shibata, R. Nagai, K. Uchida, S. Horiuchi, S. Yamada, A. Hirano, M. Kawaguchi, T. Yamamoto, S. Sasaki, M. Kobayashi, Morphological evidence for lipid peroxidation and protein glycoxidation in spinal cords from sporadic amyotrophic lateral sclerosis patients, Brain Res 917 (2001) 97-104.

[19]   J.S. Valentine, Do oxidatively modified proteins cause ALS?, Free Radic Biol Med 33 (2002) 1314-1320.

[20]   A.S. Vlug, D. Jaarsma, Long term proteasome inhibition does not preferentially afflict motor neurons in organotypical spinal cord cultures, Amyotroph Lateral Scler Other Motor Neuron Disord 5 (2004) 16-21.

[21]   M. Watanabe, M. Dykes-Hoberg, V.C. Culotta, D.L. Price, P.C. Wong, J.D. Rothstein, Histological evidence of protein aggregation in mutant SOD1 transgenic mice and in amyotrophic lateral sclerosis neural tissues, Neurobiol Dis 8 (2001) 933-941.

[22]   Y. Yang, X. Yu, Regulation of apoptosis: the ubiquitous way, Faseb J 17 (2003) 790-799.

Chapter 4

DECREASE OF HSP25 PROTEIN EXPRESSION PRECEDES DEGENERATION OF MOTONEURONS IN ALS-SOD1 MICE

Angela S. Vlug,[1,*] Arjen J. Maatkamp,[1,*] Elize D. Haasdijk[1], Dirk Troost[2], Pim J. French[1], and Dick Jaarsma[1]

* These authors contributed equally to this paper
1) Department of Neuroscience, Erasmus MC, Rotterdam, The Netherlands
2) Department of (Neuro)Pathology, Academic Medical Center, University of Amsterdam, Amsterdam, The Netherlands

4.1 Abstract

We have investigated the expression of Hsp25, a heat shock protein constitutively expressed in motoneurons, in amyotrophic lateral sclerosis (ALS) mice that express G93A mutant SOD1 (G93A mice). Immunocytochemistry and Western blotting showed that a decrease of Hsp25 protein expression occurred in motoneurons of G93A mice prior to the onset of motoneuron death and muscle weakness. This decrease in Hsp25 expression also preceded the appearance of SOD1 aggregates as identified by cellulose acetate filtration and Western blot analysis. In contrast to Hsp25 protein levels, Hsp25 mRNA as determined by in situ hybridization and RTPCR, remained unchanged. This suggests that the decrease in Hsp25 protein levels occurs post-transcriptionally. In view of the cytoprotective properties of Hsp25 and the temporal relationship between decreased Hsp25 expression and the onset of motoneuron death, it is feasible that reduced Hsp25 concentration contributes to the degeneration of motoneurons in G93A mice. These data are consistent with the idea that mutant SOD1 may reduce the availability of the protein quality control machinery in motoneurons.

4.2   Introduction

Amyotrophic lateral sclerosis (ALS) is a neurodegenerative disease of motoneurons causing progressive paralysis. In a subset of ALS patients the disease is caused by mutations in the cytosolic CuZn superoxide dismutase (SOD1) gene [2], a small homodimeric metalloenzyme that catalyses the conversion of superoxide anion to hydrogen peroxide. More than 100 different SOD1 mutations have been identified that all cause a rather similar disease phenotype [2]. Mutant SOD1s display reduced conformational stability [49], abnormal metal binding [31], toxic oxidative catalytic activities [49], and an increased tendency to aggregate [10,13,23]. Several mechanisms have been put forward by which these properties could lead to the degeneration of motoneurons, which include (1) overload or disruption of the protein quality control machinery [23,36,43,48] and (2) disruption of vital intracellular processes (e.g. intracellular transport) by oligomeric SOD1 species [23,49] or by toxic oxidative reactions [29].

To prevent protein aggregation in the cell, molecular chaperones like heat shock proteins bind to unfolded and misfolded proteins. They regulate (re)folding and appropriate cellular compartmentalization, and target abnormal proteins for proteolysis [42]. Mutant but not wild-type SOD1 has been found to interact with several heat shock proteins, including Hsp70, Hsp40, αB-crystallin and Hsp27 [36,43] and to reduce their availability [36]. It has been suggested that the selective vulnerability of motoneurons towards mutant SOD1 toxicity may depend on their relative inability to up regulate Hsp70 [4]. Indeed, increasing the level of Hsp70 reduced formation of mutant SOD1 aggregates in cultured primary motor neurons and a neuronal cell line, and prolonged survival [6,45]. Insufficiency of chaperones would not only facilitate aggregation and precipitation of mutant protein, but also could affect other functions of chaperones.

Motoneurons constitutively express Hsp27, a member of the small heat shock protein family [38]. Hsp27 has different functional properties that depend on its degree of oligomerization. Multimeric (16-meric to 32-meric) complexes of Hsp27 may act as molecular chaperones by scavenging misfolded and denatured proteins through the formation of large (4000 kDa) complexes containing both Hsp27 and misfolded protein [12,41]. In a phosphorylated state Hsp27 forms small oligomeric (dimeric or tetrameric) complexes that interfere with specific cell death programs [7,32]. In addition, Hsp27 has been implicated in the regulation of actin dynamics and antioxidative enzymes [32]. Importantly, motoneurons are capable of up regulating Hsp27 expression after injurious stimuli such as axotomy, hyperthermia and hypoxia [8,34], and this response may be critical for their survival [5]. In the present study we have examined the expression of the mouse orthologue of Hsp27, Hsp25 in a line of transgenic mice that expresses G93A mutant SOD1 (G93A mice) and that develops an ALS like disease [16]. Hsp25 and Hsp27 are orthologues but show differences in the number of phosphorylation sites and oligomeric configuration [41]. Therefore the murine protein is named Hsp25, whereas the rat and human variants are named Hsp27]. Rather than an up regulation of Hsp25 expression, the G93A mice show a marked decrease in Hsp25 expression that precedes the onset of motoneuron death.

4.3 Materials and methods

4.3.1 Transgenic mice

Mice were handled in accordance with the 'Principles of laboratory animal care' (NIH publication no. 86–23, revised 1985). Low-copy G93A mice descendent from the Gurney G1-line [16] were bred in an FVB background by mating transgenic males with nontransgenic FVB females (Harlan Netherlands), housed at a 12-h dark : 12-h light cycle, fed ad libitum with a standard diet (AM2-14–10, Hope farm, The Netherlands), and inspected twice a week for onset of paresis as previously described [20,21]. Our G93A mice develop weakness in one or more limbs from age 24–30 weeks, and reach endstage disease 2–10 weeks after onset of limb weakness [20,21]. For the immunocytochemical characterization of Hsp25 expression in G93A mice we analysed 14 age groups (6–8, 10, 12, 14, 16, 18, 20, 22, 24, 26, 28, 30, 32 and > 32 weeks) with 2–6 animals per group. In most other experiments three groups of G93A mice were used: (1) early presymptomatic (age 10 weeks); at this age our G93A mice show swelling and mild vacuolization of a subset of mitochondria but no other pathological features [21] (Table 1). (2) Late presymptomatic (age 20 weeks); at this age our G93A mice in addition to mitochondrial abnormalities show several degenerative features in motoneurons (e.g. ubiquitination, induction of the 'injury transcription factor' ATF3 [51]) but no or minimal (< 10%) motoneuron loss (Table 1). (3) Symptomatic (age 30 weeks); this group consisted of G93A mice with moderate to severe muscle weakness in one

Table 1: Time of appearance of selected clinical and pathological changes in G93A mice

	Age (weeks)					
	5–9	10–14	15–19	20–24	25–29	> 30
Clinical changes						
Hind limb weakness	0	0	0	0 or +	+	++
Death	0	0	0	0	0 or +	++
Mutant SOD1 (whole spinal cord)						
NP40-insolluble SOD1	+	+	++	++	++	++
Cellulose-acetate filterable SOD1	0	0	0	+	+	++
High-molecular weight SOD1	0	0	0	+	+	++
Motoneurons (in L4)						
Mitochondrial vacuolization	+	++	++	++	++	++
Polyubiquitination, neuritis	0	0 or +	+	++	++	++
Decreased Hsp25 expression	0	0	+	++	+	+
ATF3-expression	0	0	0 or +	+	+	+
Polyubiquitination, somata	0	0	0	0 or +	+	+
Hsp70 expression	0	0	0	0 or +	+	+
Motoneuron loss	0	0	0	<20%	10-60%	>20%
Other neurons (in L4)						
c-Jun∕ATF3-expression	0	0	0	0 or +	+	++
Argyrophilic degeneration	0	0	0	0 or +	+	++
Astrocytes (in L4)						
Increased GFAP staining	0	0	0 or +	+	++	++
Increased Hsp25 staining	0	0	0	0 or +	++	++
Polyubiquitination	0	0	0	0	+	+

Degree of change: 0, absent or no change; +, infrequent, moderate occurrence or moderate degree; ++, frequent occurrence or severe degree.

or more limbs. Where indicated homozygous transgenic G93A mice were used. These G93A ∕ G93A mice show an earlier disease onset and shorter survival similar to high-copy G93A mice [20]. Non-transgenic littermates and transgenic mice expressing wild-type hSOD1 (hSOD1 mice) derived from the Gurney N29 line and aged 10–100 weeks [20] were used as controls.

4.3.2 Human tissue

Paraffin sections from L3 lumbar spinal cord from four ALS patients (average age 56 years; range 42–68 years), and three controls (average age 57 years; range 45–65 years) were obtained from files of The Netherlands ALS tissue bank. Tissue was obtained and used in a manner compliant with the Declaration of Helsinki. Informed consent was obtained for the use of brain tissue. All autopsies were performed within 8 h after death of patients. The ALS cases were sporadic with either bulbar (n=2) or spinal onset (n=2). Average duration of disease after diagnosis was 33 months (range 20–72 months). Control cases died from myocardial infarct (n=1) or cancer (n=2). One control case showed mild Alzheimer's pathology.

4.3.3 Primary and secondary antibodies

Primary antibodies reported in this study are: mouse anti-actin (Chemicon; Western blot (WB) 1 : 4000); rabbit anti-ATF3 (Santa Cruz; immunohistochemistry (IHC) and immunofluorescence (IF) 1 : 1000); mouse anti αB-crystallin (Santa Cruz; IHC and WB 1 : 1000); rabbit anti-CGRP (Calbiochem; IHC and IF, 1 : 10 000); goat anti-ChAT (Chemicon; IHC and IF 1 : 500); rabbit anti-GFAP (DAKO; IHC 1 : 10 000; IF 1 : 5000); rabbit anti-GluR2∕3 (Chemicon; IHC 1 : 2000); rabbit anti-mouseHsp25 (StressGen; IHC 1 : 10 000, IF and WB 1 : 5000); goat anti-humanHsp27 (Santa Cruz; IHC and WB 1 : 2000, IF 1 : 1000); sheep anti-phospho(ser15)- Hsp27 (Upstate; IHC 1 : 2000); mouse anti-Hsp70 (SantaCruz; IF and WB 1 : 1000); rabbit anti-neurofilament-H (Chemicon; IHC 1 : 5000); mouse anti-neurofilament M (Sigma; IHC 1 : 50 000); mouse anti-neurofilament-L (Sigma; IHC 1 : 1000); rabbit antiperipherin (Chemicon; IHC 1 : 2000); rabbit anti-NMDA-R1 (Chemicon; IHC 1 : 2000); mouse anti-MAP2 (Sigma; IHC 1 : 2000); goat anti-human SOD1 (Calbiochem; IF 1 : 10 000); rabbit anti-murine SOD1 (SOD100, StressGen; WB 1 : 8000); rabbit anti-SOD1 (SOD101, StressGen; WB 1 : 5000); goat anti-c-Ret (R & D systems; IF 1 : 200); and rabbit anti-ubiquitin (Dako; IHC and IF 1 : 2000); mouse anti-ubiquitin (clone FK2, Affiniti; IF 1 : 2000).

For avidin-biotin-peroxidase immunocytochemistry biotinylated secondary antibodies from Vector Laboratories diluted 1 : 200 were used. FITC-, Cy3-, and Cy5-conjugated secondary antibodies raised in donkey (Jackson Immunoresearch, USA) diluted at 1 : 200 were used for confocal immunofluorescence. Horseradish peroxidase (HRP) conjugated secondary antibodies against mouse or rabbit IgG (DAKO) diluted 1 : 5000 were used for Western blot analysis and the filter trap assay.

4.3.4 Immunocytochemistry

For immunocytochemistry and immunofluorescence mice were anaesthetized with pentobarbital and perfused transcardially with 4% paraformaldehyde. The lumbar and cervical spinal cord were carefully dissected out and postfixed overnight in 4% paraformaldehyde. Unless otherwise stated, spinal cord tissue was embedded in

gelatine blocks [20], sectioned at 40 µm with a freezing microtome and sections were processed, free floating, employing a standard avidin-biotin-immunoperoxidase complex method (ABC, Vector Laboratories, USA) with diaminobenzidine (0.05%) as the chromogen, for immunofluorescence [21]. Alternatively, tissue was embedded in paraffin, sectioned at 5 µm, deparaffinized and also processed for peroxidase-immunocytochemistry or immuno-fluorescence. Human paraffin sections were processed in the same way. Both gelatine and paraffin sections were usually pretreated with an antigen retrieval procedure consisting of a 30 min incubation in 40 mm sodium citrate (pH 8.5) at 80 °C [22]. Immunoperoxidase stained sections were analysed and photographed using a Leica DM-RB microscope and a Leica DC300 digital camera. Optical densities were determined with Scion Image for Windows Beta 4.0.2. Sections stained for immunofluorescence were analysed with a Zeiss LSM 510 confocal laser scanning microscope.

4.3.5   mRNA in situ hybridization

In situ hybridization was performed as previously described [9]. Mice were decapitated, the lumbar and cervical enlargements of their spinal cords quickly removed, rapidly frozen on powdered dry-ice and sectioned at 12-µm thick using a cryostat microtome (JUNG CM3000). Sections were thaw-mounted on charged glass slides (SuperFrost Plus), fixed in 4% paraformaldehyde, acetylated and hybridized overnight at 65 °C with digoxigeninlabelled probes, diluted at 20–100 ng ⁄ mL (see Results). Sense and antisense digoxigenin-labelled cRNAs were transcribed from linearized pCMVsport6 plasmids containing full-length Hsp25 cDNA (IMAGE clones 5097030 and 5327224) using a digoxigenin RNA labelling kit (Roche) according to the manufacturer's instruction. The digoxigenin-labelled RNA-RNA complex was detected immunocytochemically using alkaline phosphatase conjugated sheep-anti-digoxigenin (Roche) with 5-bromo-4-chloro-3-indolyl phosphate and nitro-blue tetrazoleum as substrate and chromagen, respectively.

4.3.6   Western blot, gel filtration and filter trap

The spinal cords of G93A mice and their non-transgenic littermates were homogenized in ten volumes of PBS with 1X protease inhibitors cocktail (Sigma, St. Louis, MO), centrifuged at 800 g for 5 min at 4 °C, and protein concentrations of the supernatants (S1) were determined using the BCA method (Pierce, Rockford, IL). Samples containing 2–10 µg protein were electrophoresed on 10% or 13% SDS-page gels and blotted on PVDF membranes (Millipore). For quantitative analysis of Hsp25-immunoreactivity recombinant Hsp25 protein (0.5–20 ng; StressGen) was electrophoresed and blotted together with the tissue samples. The membranes were blocked with 5% non-fat dry milk (BioRad) in PBS with 0.05% Tween20 (PBST), incubated in primary antibody, diluted in PBST with 1% dry milk followed by an incubation in secondary antibody, incubated in chemiluminescence reagent (ECL, Amersham), exposed to film or a Kodak Image station, and analysed with Kodak Image analysis and ImageQuant 2.2 software. To determine the molecular mass of Hsp25 complexes in spinal cord homogenates we used gel filtration with a Precision Column PC3.2 ⁄ 30 prepacked with Superdex 200 in a SMART system (Pharmacia) as previously described [46]. The optimal range for the separation of globular proteins in this column is 10–600 kDa, with an exclusion limit of 1300 kDa. Supernatants (S1, see above) of spinal cord homogenates were

centrifuged at 15 000 g for 5 min at 4 °C, and 100 μL of the supernatant (S2) was injected in the SMART system. Fractions (50 μL) were collected separately with a flow of 50 μL ∕ min and analyzed by Western blot for the presence of Hsp25 and SOD1. The molecular size of the eluted fractions was determined in a separate run using protein markers [46]. For the filter trap assay spinal cord supernatants (S1, see above) were diluted to a final concentration of 2 μg protein ∕ mL in PBS with 0.1% or 1% SDS and filtered under vacuum through a 0.2-μm cellulose acetate membrane (Schleicher & Schuell) using a 96-well dot blot apparatus (Schleicher & Schuell) as described by Wang et al. (2002)[53]. Proteins trapped by the filter were detected on the membranes using the same procedure as for the Western blots.

4.3.7   Preparation of detergent-soluble and detergent-insoluble protein extracts

The spinal cords of G93A mice and their non-transgenic littermates were homogenized in ten volumes of PBS containing 0.5% Nonidet P-40 and 1 protease inhibitors cocktail and centrifuged at 15 000 g for 15 min at 4 °C. After collection of supernatants, pellets were thoroughly washed five times with PBS-0.5% Nonidet P-40 and then resuspended in sample buffer for SDS-page electrophoresis and Western-blotting.

4.3.8   RT-PCR

To examine the level of Hsp25 RNA total RNA was extracted from spinal cord tissue using Trizol, and treated with DNAse. The RNA (5 μg) was converted into cDNA using oligo(dT) primer and reverse transcriptase in a total reaction volume of 20 μL (RT-reaction mixture). PCR was performed with 0.1 μL of the RT-reaction mixture in a reaction volume of 25 μL. Primers used for Hsp25 were:

5'-GAGATCACTGGCAAGCACGAAG-3' (forward) and

5'-TGTTCAGACTTCCCAGCTTCTGG-3' (backward).

Primers for ChAT:

5'–GCGAATCGTTGGTATGACAAGTC-3' (forward),

5'-TTGAAGTTTCTCTGCCGAGGAG-3' (backward) and

Primers for G6PDH:

5'-CTTTGGACCCATCTGGAATCG-3' (forward),

5'-CACTTTGACCTTCTCATCACGGAC-3' (backward).

PCR cycles used were determined to be within the linear range of the reactions. To quantify the PCR products, they were electrophoresed on a 2% agarose gel, stained with ethidium bromide and scanned on a Molecular Dynamics Typhoon instrument. The relative expression level of Hsp25 mRNA was calculated using ChAT and G6PDH as a reference.

4.4   Results

Immunocytochemistry showed that in non-transgenic mice Hsp25 immunoreactivity was present in motoneurons in all cranial nerve motor nuclei and the spinal motor columns (Figs 1–3). Labeling occurred throughout the soma, the dendritic arbors, and the axon, but not in the cell nuclei (Figs 3 and 4). Hsp25 immunoreactivity was present in approximately 60% of the motoneurons identified by choline acetyltransferase (ChAT) staining (Figs 2 and 3). Hsp25- immunonegative motoneurons were small (somal diameter 12– 20 µm). Apart from motoneurons, light or moderate Hsp25 staining occurred in sensory afferents in the dorsal horn, in astrocytes in the superficial part of the spinal white matter, and in endothelial cells. Next we examined the expression of Hsp25 immunoreactivity in the spinal cord of G93A mice, aged 8–40 weeks. Young adult G93A mice (age 8–14 weeks, early presymptomatic) showed the same Hsp25 labeling as controls (Fig. 1a and d, 2a and b). However, as outlined below, older G93A mice developed marked differences.
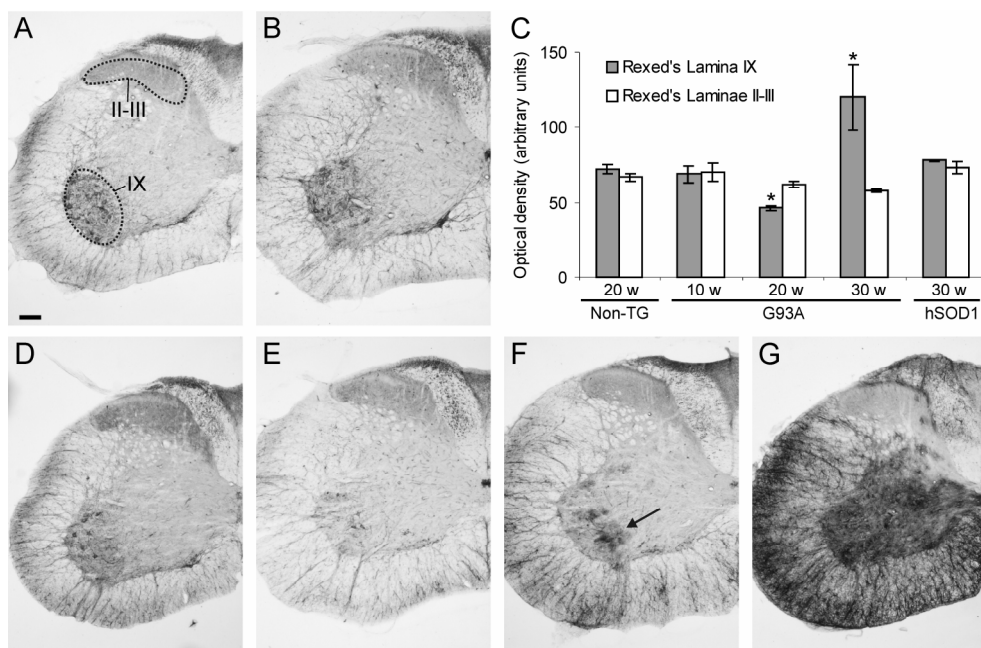
Figure 1:   Late presymptomatic G93A mice show a decrease of Hsp25 expression in their spinal motor columns. Low magnification of C6 spinal cord sections of a non-transgenic mouse of 20 weeks (A), a wild-type hSOD1 transgenic mouse of 30 weeks (B), and G93A mice of 10 weeks (D), 20 weeks (E), 25 weeks (F) and 30 weeks (G) immunostained for Hsp25. Note the decrease of Hsp25 immunoreactivity in the motor column (IX) of G93A mice of 20 weeks (E) as compared to controls (A and B) and G93A mice of 10 weeks. Also note the onset of astroglial Hsp25 expression in G93A mouse of 25 weeks (F) and dramatic astroglial Hsp25 expression in a G93A mouse of 30 weeks that showed severe muscle weakness (G). Calibration bar, 100 µm (A). (C) Optical density readings of Hsp25 immunoreactivity in the motor columns (Rexed's Lamina IX) and dorsal horn (Rexed's Lamina II–III) of C6 spinal cord of non-transgenic, G93A and hSOD1 mice. Bars represent means ± SEM with five mice per group. Values for each mouse represent the mean of five serial C6 sections. *$P < 0.01$ compared with nontransgenic mice, and 10-week-old G93A mice (unpaired two-tailed Student t-test).

4.4.1 Decreased Hsp25 protein expression precedes motoneuron loss in G93A mice

Late presymptomatic G93A mice, i.e. from 15 weeks to symptom onset (24–30 weeks of age), showed a striking decrease of Hsp25 immunoreactivity in their spinal motor columns (Figs 1c and e, 2c and 3b). Densitometry showed that reduced Hsp25 labeling was specific for the motor columns and did not occur in the dorsal horn (Fig. 1c). Reduced Hsp25 labeling was never observed in non-transgenic mice of 10–120 weeks (Fig. 1). Moreover, reduced Hsp25 labeling never occurred in age-matched (10–40 weeks) and old (120 weeks) transgenic mice that expressed wild-type hSOD1 (Fig. 1b). Homozygous G93A mice, which show an earlier disease onset and shorter survival as compared to hemizygous G93A mice [20], showed reduced motoneuronal Hsp25 staining at ten, but not at six weeks.
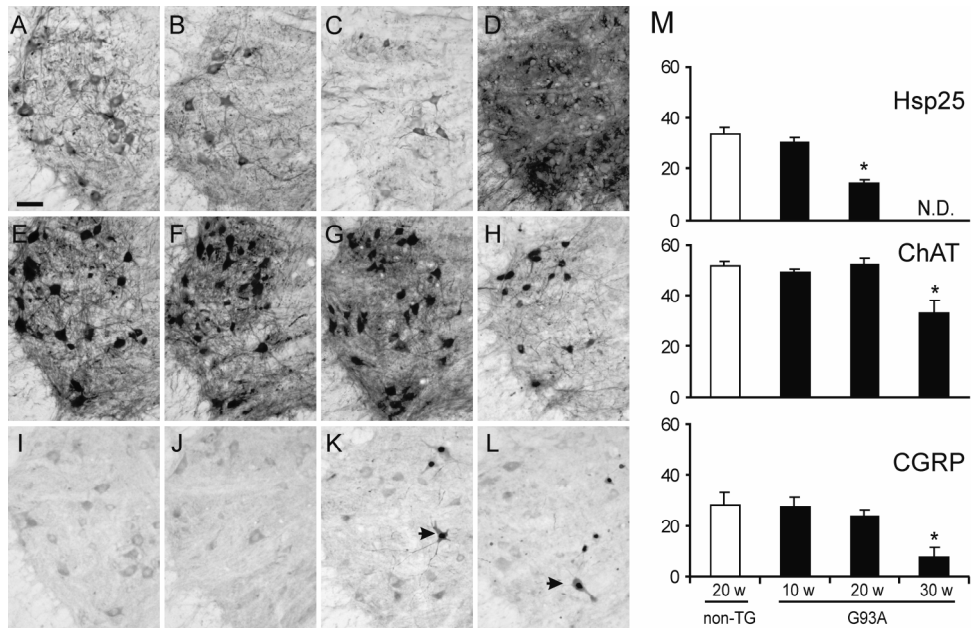
Figure 2: Decreased Hsp25 expression precedes motoneuron loss. (A–L) High magnification of C6 spinal cord sections of a non-transgenic mouse of 20 weeks (A, E and I) and G93A mice of 10 (B, F and J), 20 (C, G and K) and 30 weeks (D, H and L) immunostained for Hsp25 (A–D), ChAT (E–H), and ATF3 (I–M). Note that in presymptomatic (20 weeks) G93A mice Hsp25 staining in motoneurons is decreased (C), whereas the number and morphology of motoneurons identified by ChAT staining has not changed (G). Also note that the reduction of Hsp25 is associated with appearance of the injury marker ATF3 in a subset of motoneurons in late presymptomatic and symptomatic G93A mice (arrows in K and L, respectively). Bar in A, 50µm. (M) Quantification of the number of Hsp25, ChAT and CGRP immunoreactive motoneurons per C6 spinal cord section of non-transgenic and G93A mice. Values represent means ± SEM with 5 mice per group. Values are based on counting of five sections per animal. *P < 0.005 compared with non-transgenic mice, and 10 weeks old G93A mice (unpaired two-tailed Student t test). N.D., not determined.

To examine whether decreased Hsp25 expression in presymptomatic G93A mice was specific for Hsp25 we have immunocytochemically screened the expression of a number of proteins that are expressed by motoneurons and that may show altered expression after injury, i.e. ChAT, calcitonin gene-related peptide (CGRP), AMPA and NMDA receptor subunits, peripherin, and neurofilament subunits [28]. None of these proteins showed altered expression in late presymptomatic G93A mice. Next, we have counted the number of motoneurons in serial sections immunostained for Hsp25, ChAT or CGRP, which like Hsp25 is preferentially localized in large motoneurons [3]. This analysis showed that late presymptomatic G93A mice (20 weeks), which showed a significant loss of Hsp25 labeled motoneurons, did not show a change in the number of ChAT or CGRP immunoreactive motoneurons (Fig. 2m). Motoneuron loss, as determined by ChAT immunocytochemistry occurred at a later time point (Figs 2h and m, and 3c). Therefore our data indicate that motoneurons of G93A mice show decreased Hsp25 immunoreactivity prior to the onset of motoneuron death.

4.4.2 No correlation between Hsp25 and ATF3 expression in G93A mouse spinal cord

The onset of reduced Hsp25 staining was in the same time window as the onset of expression of the stress transcription factor, ATF3, in a number of motoneurons in G93A mice, i.e. from 15 weeks (Fig. 2k and m, Table 1, see also Vlug et al., 2001 [51]). As ATF3 has recently been identified as an activator of Hsp27 expression [35], we have examined Hsp25 expression in ATF3 positive motoneurons by double-labeling immunofluorescence. This analysis revealed no correlation between ATF3 and Hsp25 expression: of 100 ATF3 positive motoneurons analyzed in lumbar sections of late presymptomatic and symptomatic G93A mice 31 showed significant Hsp25 immunostaining, 46 showed light Hsp25 staining (arrow heads in Fig. 3e), and 23 showed no Hsp25 staining. The lack of a correlation between ATF3 and Hsp25 expression also follows from the fact that all Hsp25 expressing motoneurons in control mice and young G93A mice and most Hsp25 positive motoneurons in late presymptomatic and symptomatic G93A mice are negative for ATF3. Notably, a subset of motoneurons that show both a high level of ATF3 and Hsp25 expression showed an abnormal appearance (Fig. 3e; see below).

4.4.3 Symptomatic G93A mice show induction of glial Hsp25 expression

In contrast to the reduction in Hsp25 expression observed in presymptomatic mice, symptomatic G93A mice showed a dramatic increase of Hsp25-immunostaining as compared to controls (Figs 1c and g, and 2d). Double labeling confocal immunofluorescence showed that this increased Hsp25 immunoreactivity co-distributed with the astroglial marker GFAP (glial fibrillary acidic protein, Fig. 4). Reactive astrogliosis, characterized by increased GFAP synthesis and astrocyte proliferation, is a well known phenomenon associated with neuronal degeneration. In our G93A mice a mild increase in GFAP staining occurred in late presymptomatic mice (Fig. 4d), whereas a high level of GFAP staining occurred in symptomatic mice (Fig. 4e and f). The onset of the induction of astroglial Hsp25 expression was highly focal, starting with single or small groups of labeled
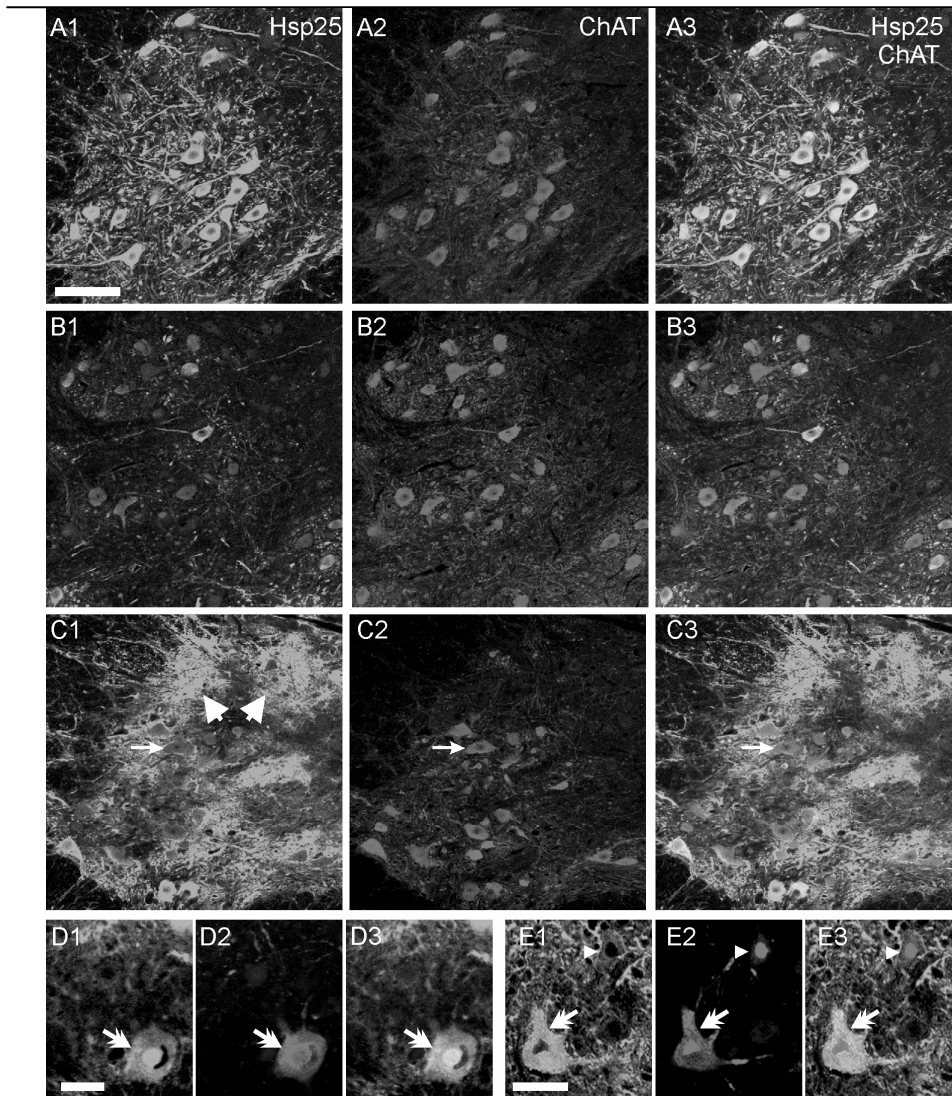
Figure 3:   (A–C) Decreased Hsp25, but not ChAT expression in G93A mouse motoneurons. Double-labelling confocal immunofluorescence of Hsp25 (A1–C1) with ChAT (A2–C2) in lumbar spinal cord sections of a control mouse of 20 weeks (A), and G93A mice of 20 weeks (B) and of 30 weeks (C). Merged images are shown in A3–C3. Hsp25 staining is reduced in motoneurons of presymptomatic G93A mice (B1), as compared to age-matched controls (A1), whereas the amount of ChAT staining is unchanged (A2 and B2). Symptomatic (30 weeks) G93A mice also show reduced Hsp25 staining in motoneurons (arrow in C), and show a dramatic up regulation of glial Hsp25 expression. Note that glial Hsp25 staining shows a patchy appearance (large arrows in C). Optical section, 4.6 µm. Scale bar, 100 µm (A). (D and E) Hsp25 accumulate in ill-appearing ubiquitinated motoneurons. Double-labelling of Hsp25 (D1 and E1) with ubiquitin (D2) and ATF3 (E2) in lumbar spinal cord sections of a 30-week-old G93A mouse. A small number of motoneurons in late presymptomatic and symptomatic G93A mice is intensely immunoreactive for both Hsp25 and ubiquitin (double-headed arrow in D). These neurons usually show an ill appearance characterized by a flattened eccentric ATF3 immunoreactive nucleus, and abnormal cytosolic ATF3 labelling (double-headed arrow in E). Note that ATF3 expressing motoneurons do not necessarily express high levels of Hsp25 (arrow head in E). Optical sections, 4.6 µm. Scale bars, 25 µm (D); 50 µm (E). For color photographs see published manuscript.
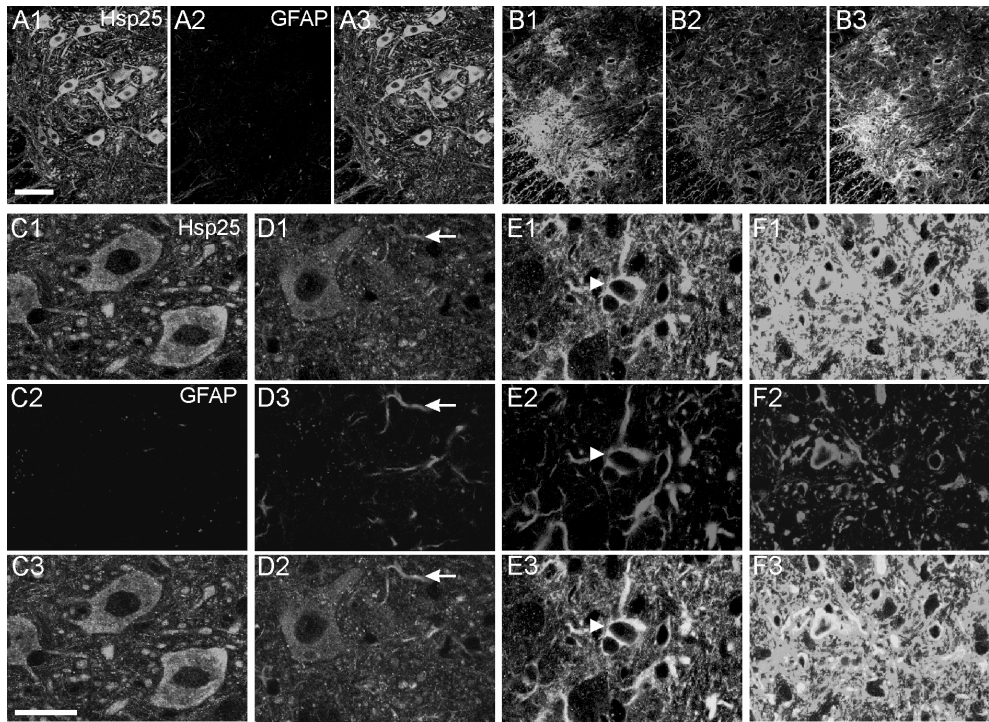
Figure 4:   Symptomatic G93A mice show induction of glial Hsp25 expression. Double-labeling immunofluorescence of Hsp25 (A1–F1) and GFAP (A2–F2) in lumbar spinal cord sections of G93A mice of control (A) and G93A mice of 10 (C), 20 (D), 28 weeks (B and E) and 33 weeks (end stage disease, 33 week, F). Merged images are shown A3–F3. Note the colocalization and age-related increase of Hsp25 and GFAP staining in G93A mouse spinal cord. Also note the 'patchy' distribution of Hsp25 immunoreactivity in B1 (see also Figs 1f and 3c1). Arrow in D indicates an astroglial process with intense GFAP and weak Hsp25 staining. Arrow head in E shows the cell body of an astrocyte stained for both Hsp25 and GFAP. Optical sections, 4.6 µm (A and B) and 1 µm (C–F). Scale bars, 100 µm (A1); 25 µm (C3). For color photographs see published manuscript

astrocytes in the motor columns (arrow in Fig. 1f), subsequently spreading to multiple foci (Fig. 4). In endstage G93A mice a very high level of glial Hsp25 labeling occurs throughout the ventral horn and the intermediate zone of the spinal cord (Figs 1g, 2d and 4f).

4.4.4   Hsp25 accumulate in the juxta-nuclear region of ill-appearing ubiquitinated motoneurons in late presymptomatic and symptomatic G93A mice

A number of studies have indicated a stress-dependent redistribution of Hsp27 to the nucleus in several cellular systems [30,39], and a nuclear distribution of Hsp25 in motoneurons of endstage G93A mice [50]. We have therefore extensively screened cervical and lumbar spinal cord sections of our G93A mice for motoneurons with nuclear Hsp25 expression. However, no nuclear Hsp25 expression was observed. Instead, we identified a small number of motoneurons with a juxtanuclear accumulation of Hsp25 (Fig. 3d). These motoneurons in

addition showed a flattened eccentric nucleus, suggestive of ill health. The frequency of this type of abnormal motoneurons in L4 spinal cord varied from 0.1 to 4%, with the highest number in early symptomatic mice (25–30 weeks of age). No juxta-nuclear Hsp25 expressing motoneurons were identified in G93A mice younger than 18 weeks. Double labelling showed that juxta-nuclear Hsp25 expressing motoneurons also were immunoreactive for ubiquitin (Fig. 3e) and the injury transcription factor ATF3 (Fig. 3e). ATF3 usually shows a nuclear localization, but in juxta-nuclear Hsp25 expressing cells also occurred in the cell body and the dendrites (Fig. 3e).

4.4.5 Decreased Hsp25 protein expression in late presymptomatic G93A mice is not associated with a change in Hsp25 mRNA expression

Quantitative immuno-Western blot confirmed our immunohistochemical data that Hsp25 expression is decreased in late presymptomatic G93A mice and increased in symptomatic G93A mice (Fig. 5a and b). Hsp25 is a relatively abundant protein
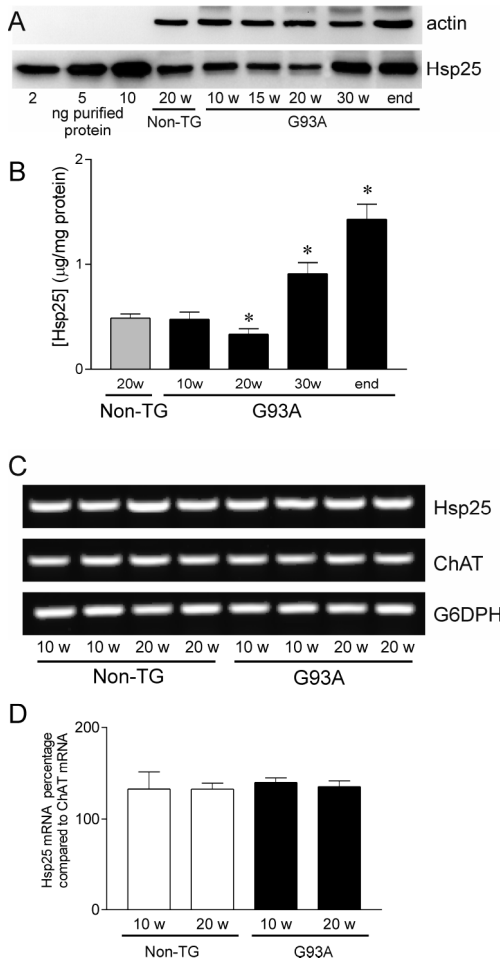

Figure 5: Decreased Hsp25 protein expression is not associated with decreased Hsp25 mRNA expression in late presymptomatic G93A mice. Representative results (A) and quantification (B) of Western blot analysis of Hsp25 in crude total spinal cord homogenate (5 µg) of non-transgenic and G93A mice. Recombinant Hsp25 was electrophoresed and blotted together with tissue samples. Values in B represent means ± SEM from 4 to 6 mice. The same results were obtained with calibration for the actin signal. Note decreased Hsp25 concentration in G93A mice of 20 weeks, and increased Hsp25 concentration in older G93A mice. *P < 0.05 compared to non-transgenic mice and 10 weeks old G93A mice (unpaired two-tailed Student t-test). Representative results (C) and quantification (D) of RT-PCR analysis of the relative Hsp25, ChAT, and G6DPH mRNA concentration in total RNA samples isolated from control and G93A mouse spinal cord. Values in D represent semiquantitative estimates of Hsp25 mRNA expressed as a percentage of the ChAT mRNA signal (means ± SEM from three mice).

in control crude spinal cord homogenate (0.49 ± 0.04 µg ∕ mg, mean ± SEM). Its concentration in crude homogenates from 20-week-old G93A mice was decreased by 32% and 31% as compared to non-transgenic controls and young G93A mice, respectively.

To examine whether decreased Hsp25 expression in presymptomatic G93A mice is associated with changes in Hsp25 mRNA levels we have used semiquantitative RT-PCR and in situ hybridization. Using RT-PCR no change in Hsp25 mRNA expression was observed in spinal cord of 20-week-old G93A mice as compared to controls and 10-week-old G93A mice (Fig. 5c and d). In situ hybridization, in accordance with the immunocytochemical data, showed that in control spinal cord Hsp25 mRNA was predominantly distributed in motoneurons (Fig. 6a and c). No change in Hsp25 mRNA expression occurred in presymptomatic G93A mice (Fig. 6b), whereas symptomatic G93A mice showed astroglial induction of Hsp25 mRNA expression (Fig. 6). To enable semi-quantitative comparison of Hsp25 mRNA expression between 20-week-old G93A mice and controls, sections were incubated with different concentrations of labeled RNA probe. The number of labeled motoneurons depended on the probe concentration (Fig. 6f), which can be explained by the fact that at low probe concentrations (20 ng ∕ mL) only cells expressing intermediate or high Hsp25 mRNA concentrations were stained, whereas at higher probe concentration (40–100 ng ∕ mL) also cells expressing low levels of Hsp25 mRNA were stained. As shown in figure 6f, the number of labeled motoneurons was similar between 20-week-old G93A mice and controls, irrespective of the probe concentration, strongly suggesting similar levels of Hsp25 mRNA.

4.4.6 Decreased Hsp25 expression in late presymptomatic G93A mice is not associated with changes in its oligomeric configuration and solubility

As the oligomeric configuration and solubility of Hsp25 and Hsp27 are controlled by various mechanisms [11,41], and may vary with the conditions of the cell [17,26,30,41], we have examined whether decreased Hsp25 expression in late presymptomatic G93A mice is associated with changes in its oligomerization and solubility. Both in the absence (not shown) and the presence of non-ionic detergent (0.5% Nonidet-P40) most of the Hsp25 is present in the soluble fraction (Fig. 7b, see below). Analysis of the soluble fraction by gel filtration chromatography showed a biphasic elution profile of Hsp25, indicating that approximately 50% of soluble Hsp25 is present in complexes of 50–250 kDa, whereas the other 50% occurs in complexes of approximately 500–800 kDa (Fig. 7a). This elution profile is similar to the elution profile of recombinant Hsp25 in vitro [41]. Spinal cord homogenates from 20-week-old G93A mice show the same elution profile as control mice (Fig. 7a), indicating that decreased Hsp25 expression in presymptomatic G93A mice does not alter its oligomeric distribution. Accordingly, immunocytochemical analysis of phosphorylation of Hsp25, which controls its oligomerisation [41], indicated that Hsp25 with a phosphorylated ser15 residue occurs in all motoneurons expressing Hsp25, and that late presymptomatic G93A mice show a decrease in phospho-Hsp25 (ser15) expression that is proportional to the decrease in total Hsp25 expression.

To determine whether decreased Hsp25 expression in late presympromatic G93A mice is associated with a change in solubility we examined the relative amount of Hsp25 in the Nonidet-P40-soluble and insoluble fractions. As shown in Fig. 7b, young G93A mice showed the same amount of Hsp25 in the Nonidet-P40 insoluble fraction as controls, and late presymptomatic (20 weeks) mice showed a reduction of the insoluble Hsp25 concentration that is roughly proportional to the reduction of soluble and total Hsp25. This indicates that decreased Hsp25 expression in late presympromatic G93A mice is not associated with altered solubility. Also in symptomatic G93A mice, which show astroglial induction of Hsp25 expression, the concentration of insoluble Hsp25 was proportional to that of total Hsp25 (Fig. 7b).

4.4.7 Hsp25-immunoreactivity co-distributes with mutant SOD1 in ubiquitinated dendrites

Because of evidence indicating that Hsp25 may bind to mutant SOD1 in permanently transfected mouse neuroblastoma N2A cell lines [36], we used several methods to examine whether Hsp25 binds to mutant SOD1 in vivo in spinal cord of G93A mice. First, analysis of the fractions of the gel filtration experiments,
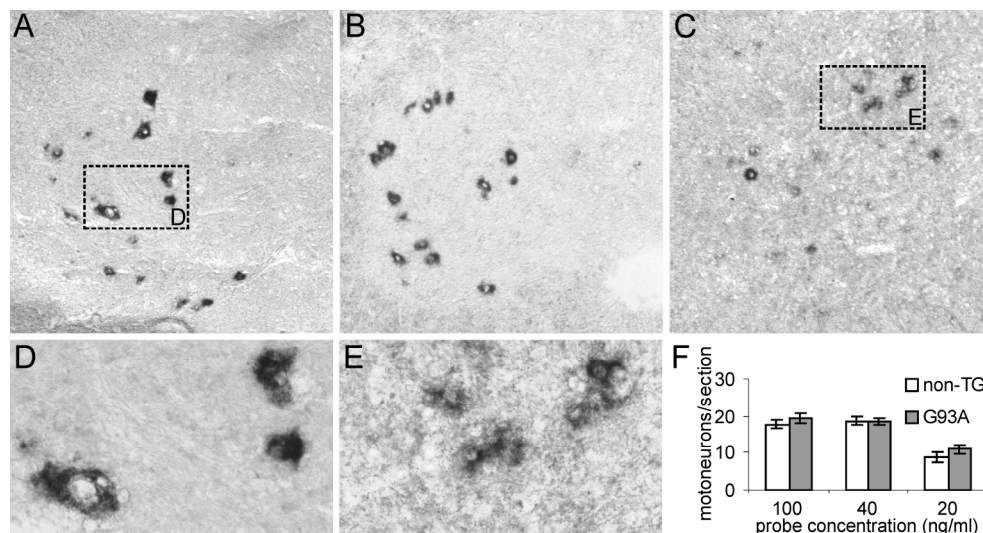

Figure 6: Late presymptomatic G93A mice show the same distribution of Hsp25 mRNA as controls. (A–E) In situ hybridization signal of antisense digoxigeninlabelled Hsp25 cRNA (100 ng ∕ mL) on the ventral horn of C6 spinal cord sections from control (20 weeks, A), and presymptomatic (20 weeks, B) and symptomatic G93A mice (30 weeks, C). Dand E are magnifications of inserts in A and C, showing motoneuronal and glial Hsp25 mRNA labelling, respectively. Note the same Hsp25 mRNA staining in motoneurons of presymptomatic G93A and control mice. No staining was obtained with sense Hsp25 probes (not shown). (F) Number of Hsp25 mRNA labelled motoneurons in C6 spinal cord sections of 20-week-old G93A and control mice after incubation with different probe concentrations (20, 40 or 100 ng ∕ mL). The number of labelled motoneurons was dependent upon the probe concentration, and was the same in 20-week-old G93A and control mice. Bars represent means ± SEM with four mice per group. Values for each mouse represent the mean of eight serial C6 sections. All sections used to obtain this graph were processed into a single in situ hybridization run with sections from a control and G93A mice on the same slides.
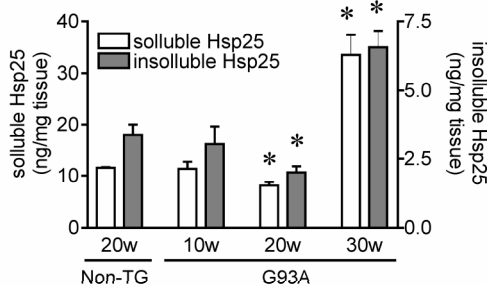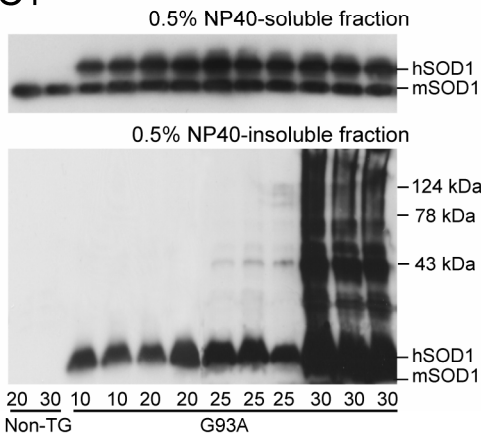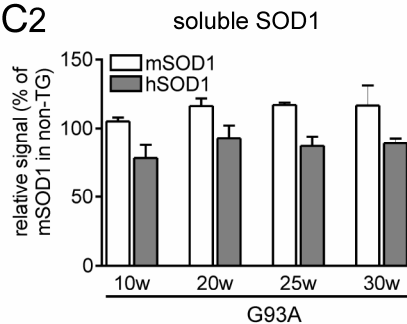
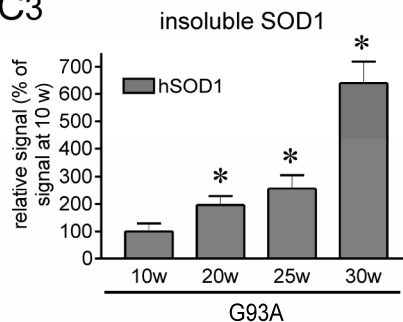A1

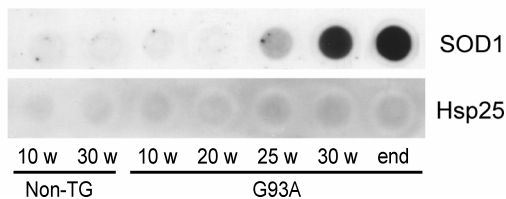Hsp25

non-TG

G93A

SOD1

non-TG

G93A
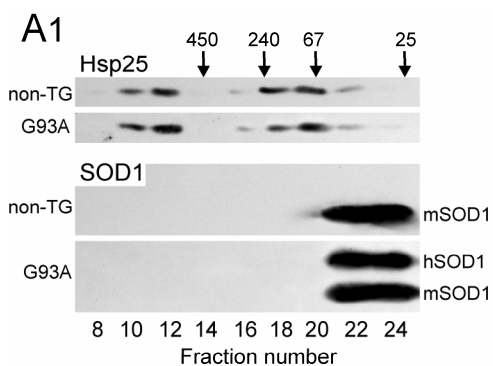
A2
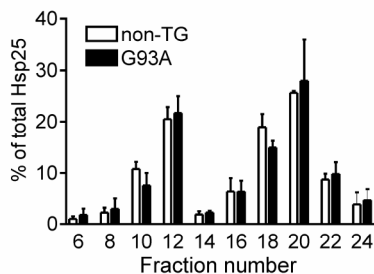
B1
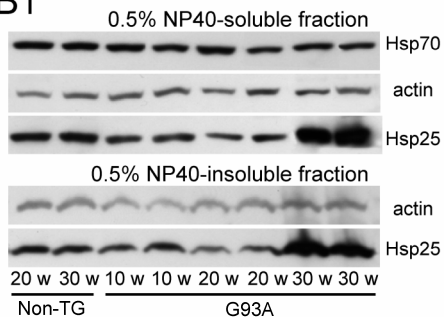
B2

C1

C2

C3

D1

showed that mutant SOD1 eluted in the same fraction as endogenous mouse SOD1, and did not elute with Hsp25 (Fig. 7a).This suggests that, at least in the soluble fraction, Hsp25 does not interact with mutant SOD1. Accordingly, using standard immunoprecipitation procedures [36,43] we did not succeed in co-immunoprecipitating mutant hSOD1 with Hsp25 from cleared spinal cord homogenate (not shown). Furthermore, other immunoprecipitation methods that start with cross-linking of protein complexes in the whole homogenate to prevent premature dissociation of interacting proteins [55] also did not reveal an interaction with Hsp25 and mutant SOD1 (not shown).

To further examine whether Hsp25 was associated with mutant SOD1 we have used a filter trap method that allows the detection of aggregated mutant SOD1 species [53]. Detectable levels of filterable SOD1 complexes occurred in spinal cord of G93A mouse older than 20 weeks, but these mutant SOD1 filtrates were immunonegative for Hsp25 both in 1% and 0.1% SDS (Fig. 7d). The time of appearance of filterable SOD1 correlated with the time of appearance of high molecular weight forms of mutant SOD1 as detected by Western blot (Fig. 7c). Significantly, these abnormal SOD1 species predominantly appeared after the onset of reduced Hsp25 expression (compare Fig. 7b and c).

Our gel filtration and immunoprecipitation experiments do not exclude the possibility that a small fraction of Hsp25 and mutant SOD1 interact in spinal motoneurons. To further study putative interactions between Hsp25 and mutant transgenic SOD1 we have examined colocalization of Hsp25 and mutant SOD1 with double labeling immunofluorescense using SOD1 antibodies that specifically recognize transgenic human mutant SOD1, and do not immunoreact with sections of non-transgenic mice (Fig. 8a2). In G93A mice mutant SOD1 is expressed in all cells throughout the CNS [20,21]. In motoneurons mutant SOD1 like Hsp25 showed a relatively homogeneous distribution throughout the cell body, the

---

Figure 7:   Decreased Hsp25 expression in late presymptomatic G93A mice is not associated with changes in its oligomeric configuration and solubility. (A) Representative results (A1) and quantification (A2) of Western blot analysis of Hsp25 and SOD1 in fractions obtained after gel filtration chromatography of cleared spinal cord homogenate from control (non-TG) and G93A mice. Note that Hsp25 has a biphasic elution profile, and that this elution profile is not changed in G93A mice. Also note that endogenous mouse SOD1 (mSOD1) and transgenic mutant human SOD1 (hSOD1) eluted in the same fractions, and that SOD1 was not present in the same fractions as Hsp25. N.B. SOD1 is detected with SOD-101 antibody (StressGen), which preferentially binds to mSOD1, but since the concentration of transgenic hSOD1 is 4 to 5 fold the concentration of mSOD1 (Jaarsma et al., 2001) gives the same signal for mSOD1 and hSOD1. Values in A2 represent means ± SE from 2 non-TG and 3 G93A mice of the % of total Hsp25 in each fraction. B and C: Representative results (B1, C1) and quantification (B2, C2, C3) of Western blot analysis of Hsp25 (B) and SOD1 (C) expression in 0.5% Nonidet-P40-soluble and insoluble fractions of spinal cord homogenates of nontransgenic and G93A mice of different ages. Recombinant Hsp25 was electrophoresed and blotted together with tissue samples (not shown). Values represent means ± SEM from 3 mice. In B2 and C3, * = P < 0.01 compared to non-transgenic mice or 10 weeks old G93A mice (unpaired two-tailed Student t-test). Note in B2 the differences in scaling of the vertical axes for soluble and insoluble Hsp25, respectively. Also note in C the absence of endogenous mouse SOD1 (mSOD1) and an age related increase of transgenic mutant human SOD1 (hSOD1) in the insoluble fraction. (D) Cellulose-acetate filter assay of spinal cord homogenate in buffer with 1% SDS to trap high molecular weight protein complexes, showing the appearance of SODI-immunoreactive complexes in G93A mice older than 20 weeks. Trapped protein complexes were immunonegative for Hsp25. The same results were obtained with homogenate diluted in 0.1% SDS which is less disruptive for protein-protein interactions.
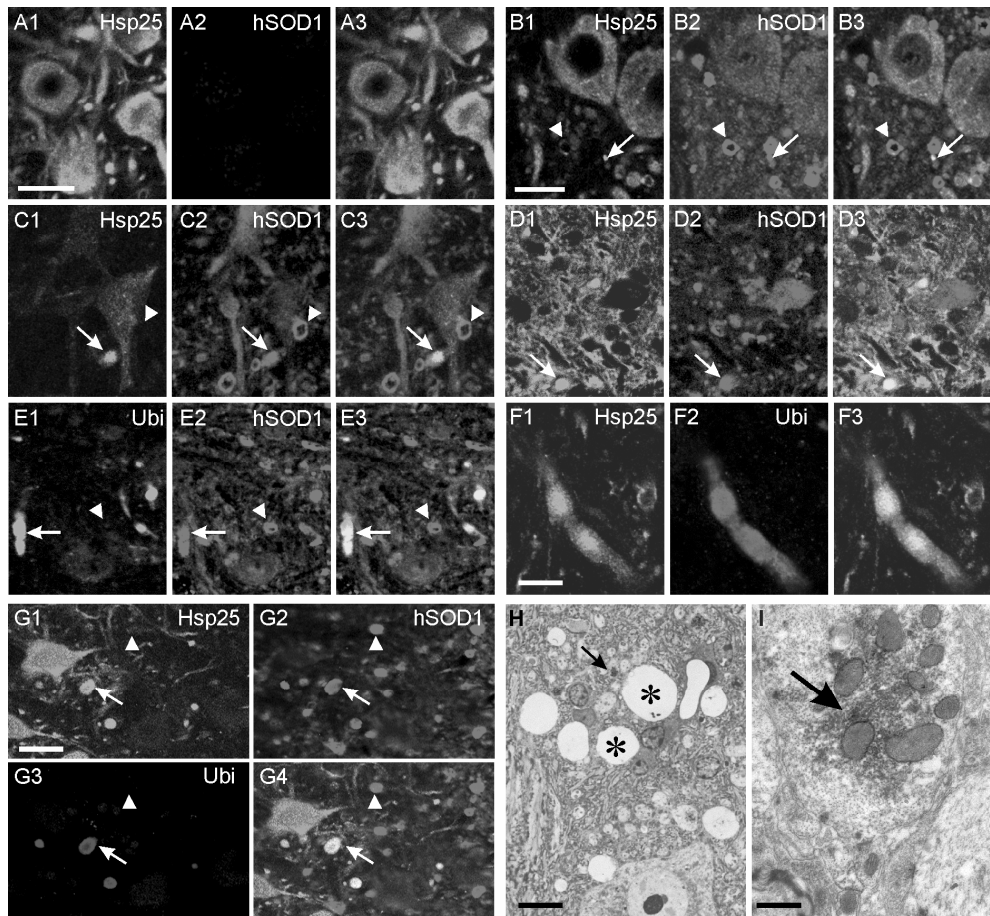
Figure 8: (A–G) Hsp25-immunoreactivity co-distributes with mutant SOD1 in ubiquitinated dendrites. Double-labelling confocal immunofluorescence of Hsp25 (A1–D1, F1 and G1), transgenic human SOD1 (A1–E1 and G1) and ubiquitin (B1, F2 and G3) in lumbar spinal cord sections of a non-transgenic mouse (A), and G93A mice of 15 (B), 20 (C, E, F and G) and 28 weeks (D). Merged images are shown in A3–F3 and G4. Transgenic mutant hSOD1, visualized with an antibody that does not stain endogenous mouse SOD1 (A2), like Hsp25 shows a diffuse distribution throughout the somatodendritic domain of motoneurons (B and C), but, in addition, accumulate in vacuolated mitochondria (arrow heads in B, C, E, and G see also [Jaarsma, 2001 #254]) and in ubiquitinated dendrites (arrow in E). Hsp25 co-distributes with a subset of intensely hSOD1 immunoreactive structures (arrows in B–E) and with ubiquitinated profiles (F). Triple labeling shows co-distribution of Hsp25, hSOD1 and ubiquitin (arrow in G). Optical sections, 4.6 µm (A, C–E and G) and 1 µm (B and F). Scale bars, 25 µm (A1) (also for C–E); 15 µm (B1); 10 µm (F1); and, 25 µm (G1). (H and I) Light- (H) and electron photomicrograph (I) of consecutive semi-thin (0.5 µm, H) and ultra-thin (50 nm, I) sections of a lumbar section of an 18-week-old G93A mouse immunoperoxidase stained for ubiquitin. The electron photomicrograph in I shows the labeled dendritic profile indicated by the arrow in H. Note that ubiquitin immunoreactivity is associated with amorphous and filamentous material in the core of dendritic profiles. Scale bars, 10 µm (I); 0.5 µm (B). For color photographs see published manuscript.

dendrites and the axon, but, unlike Hsp25, also occurred in the nucleus (Fig. 8b). As previously reported [20,21] with ageing motoneurons of G93A mice showed the accumulation of mutant SOD1 into two pathological structures, i.e. (1) in the

intermembrane space of swollen and vacuolated mitochondria, which represent an early (from 4 weeks) pathological feature of G93A mice; and (2) in cytosolic aggregates, which appear at a later time point (from 12 to 15 weeks) in the proximal dendrites of motoneurons, and occur at a relatively low frequency as compared to vacuolated mitochondria [21]. Intramitochondrial SOD1 'accumulates', which can be detected light-microscopically as intensely SOD1-immunoreactive dot or ring-like structures (arrow heads in Fig. 8b and c; see also Jaarsma et al., 2001 [21]) were not immunoreactive for Hsp25 (Fig. 8b and c). Cytosolic SOD1 aggregates can be distinguished from intramitochondrial SOD1 accumulates because of their immunoreactivity for ubiquitin (Fig. 8e, h and i). Double labeling for Hsp25-hSOD1 (Fig. 8b–d) and Hsp25-ubiquitin (Fig. 8f) and triple labeling (Fig. 8g) showed that these dendritic ubiquitinated SOD1 aggregates were strongly immunoreactive for Hsp25. In late presymptomatic and symptomatic G93A mice, i.e. several weeks after the appearance of dendritic ubiquitinated SOD1 aggregates, ubiquitin immunoreactivity also occurred in cell bodies of motoneurons and in glia [19,44]. Ubiquitinated motoneurons (see above; Fig. 3d) and astrocytes (not shown) usually were immunoreactive for Hsp25, whereas ubiquitinated structures in oligodendrocytes were not stained for Hsp25 (not shown).

4.4.8   Human control and ALS motoneurons express Hsp27

Although Western blot analysis has revealed the constitutive presence of Hsp27 in human spinal cord, immunohistochemical studies have failed to detect Hsp27 in human motoneurons [38]. Therefore we have re-examined the distribution of Hsp27 immunoreactivity in human spinal cord, and studied the distribution of Hsp27 in ALS tissue. As shown in figure 9 intense Hsp27 immunostaining was present throughout the cell body, dendritic arbours, and the axon of human motoneurons (Fig. 9). Hsp27 did not occur in neurons in the dorsal horn and the intermediate zone. Comparison of Hsp27 staining with haematoxylin and eosin staining indicated that approximately 80–90% of the neurons in the motor column were stained for Hsp27. Also motoneurons in ALS spinal cord were stained for Hsp27, but the overall staining in the motor columns was reduced as compared to controls (Fig. 9b and d). Also the number of Hsp27 immunoreactive motoneurons was reduced (Fig. 9). However, the relative amount of Hsp27 stained vs. unlabelled motoneurons was not changed (Fig. 9). Unlike the G93A mice, ALS spinal cord did not show an increase in astroglial Hsp27 expression (Fig. 9)
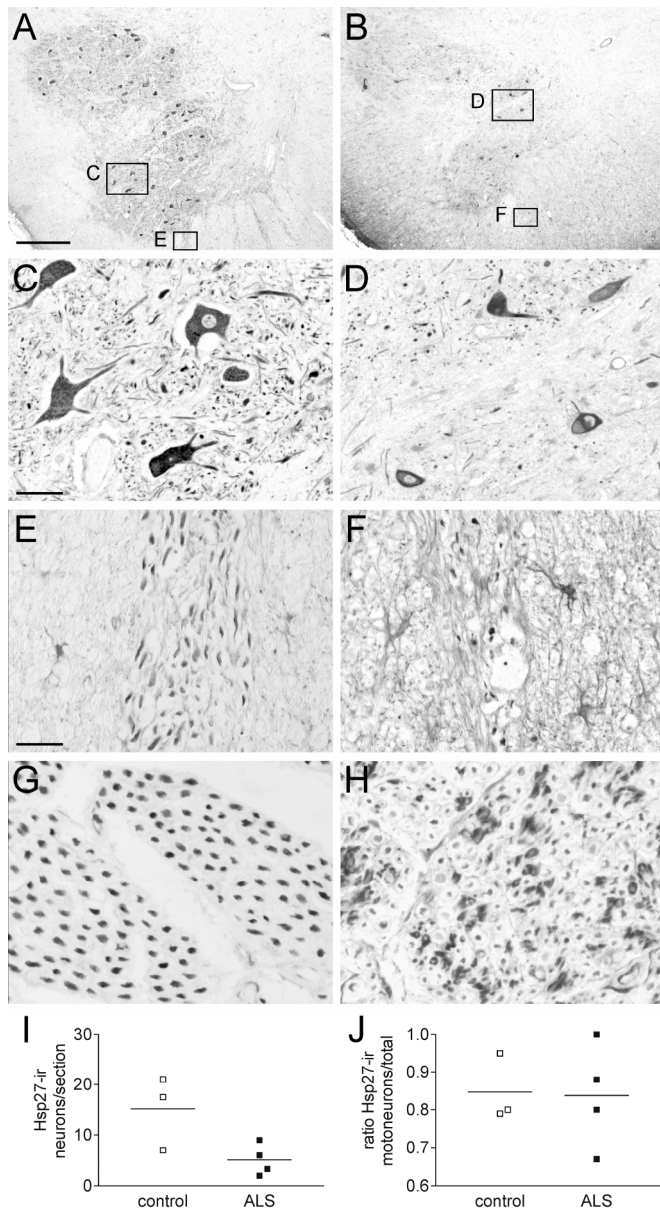
Figure 9:   Hsp27 is expressed in control and ALS human motoneurons. Low (A and B) and high (B–H) magnification of a control (A, C, E and G) and ALS (B, D, Fand H) human L3 spinal cord section (A–F) and ventral roots (G and H) stained for Hsp25. Note in D, Hsp27 immunoreactivity in surviving motoneurons and reduced Hsp27 immunoreactivity throughout the neuropil of that human ALS spinal cord. Some Hsp27 positive astrocytes are seen in white matter of ALS spinal cord (F). Calibration bars, 500 μm (A); 50 μm (C); 25 μm (E) (also for F–H). (I and J) Absolute (I) and relative (J) number of Hsp27-immunoreactive neurons in the motor column (Rexed's lamina IX). In ALS patients the number of Hsp27 labelled neurons is decreased, but the relative amount, as compared to the total number of motoneurons, is not changed.

4.5   Discussion

Hsp27 and its murine orthologue Hsp25 are multifunctional proteins that are constitutively expressed by motoneurons, and show increased expression in motoneurons after injury [8,33]. In this study we find a decreased expression of Hsp25 protein in motoneurons of a transgenic mouse model for ALS that express G93A mutant SOD1. Decreased Hsp25 expression occurred several weeks prior to the onset of motoneuron death (Table 1). Hsp25 so far is the only motoneuronal protein investigated in our laboratory that shows a decreased expression in this time window. Although the function of Hsp25 in motoneurons is not known, it has several properties that may protect motoneurons against toxic properties of mutant SOD1, including its ability to scavenge misfolded proteins [12,41] and its ability to inhibit certain programmed cell death pathways [5,7]. In view of these properties and the temporal relationship between decreased Hsp25 expression and the onset of motoneuron death, it is feasible that reduced Hsp25 concentration contributes to the degeneration of motoneurons in G93A mice. For instance, reducing the Hsp25 concentration may facilitate the accumulation and aggregation of mutant SOD1. Accordingly, we found that the accumulation of high molecular weight SOD1 species in the G93A mice occurs after the onset of reduced Hsp25 expression (Table 1). Reducing Hsp25 also may cause the dysinhibition of the mitochondrial cytochrome c- dependent cell death pathway. There is evidence for the activation of this pathway in G93A mice [15], but it may not be executed in motoneurons unless the Hsp25 concentration is decreased.

What causes decreased motoneuronal Hsp25 protein expression in G93A mice? Our data point to a post-translational mechanism, as decreased Hsp25 expression was not associated with a change in Hsp25 mRNA levels. Interestingly, a reduction of Hsp27 protein, but not mRNA expression also has been observed in cells expressing mutant ataxin-3 [54], which indicates that a posttranscriptional reduction of Hsp27 protein levels can be induced by the presence of mutant protein.

Hsp27 and Hsp25 have the ability to bind to misfolded and denatured proteins resulting in large (4000 kDa) precipitable complexes [12,41,52]. Accordingly, in permanently mutant SOD1 transfected mouse neuroblastoma N2A cell lines Hsp25 binds to mutant SOD1, which causes a redistribution to a non-ionic detergent-insoluble fraction and decreased expression of Hsp25 [36]. On the basis of these data we hypothesized that mutant SOD1 causes a similar redistribution of Hsp25 in motoneurons of G93A mice and that this redistribution underlies reduced Hsp25 expression. However, we found no evidence for altered oligomerization and solubility of Hsp25 in G93A mice, i.e. the fraction of insoluble Hsp25 was the same in either control, young and late presymptomatic G93A mice, in spite of the accumulation of insoluble mutant SOD1 in the G93A mice. Gel filtration indicated that Hsp25 did not bind to mutant SOD1 in the soluble fraction, but we can not exclude the possibility of such an interaction in the insoluble fraction, which contains approximately one-third of total Hsp25. Hence, our data leave open the possibility that a fraction of Hsp25 binds to mutant SOD1 and redistributes to the insoluble fraction without changing the ratio between soluble and insoluble Hsp25. For instance, an interaction between Hsp25 and mutant SOD1 may occur in cytosolic SOD1 aggregates, which appear in the proximal dendrites of

motoneurons in late presymptomatic G93A mice and are immunoreactive for Hsp25.

The concentration of Hsp25 in control and young G93A mouse spinal cord is approximately 0.5 µg ∕ mg protein, but, as Hsp25 is expressed in only a subset of structures in the spinal cord, the actual concentration in motoneurons is likely to be higher. Hsp25 levels therefore may be of the same order of magnitude as the concentration of mutant SOD1, which is 5–10 µg ∕ mg protein [21]. Together our data indicate that Hsp25 and mutant SOD1 are expressed in the same cellular compartment in motoneurons at approximately equal and abundant levels, but show little or no interaction. This can be explained by the fact G93A mutant SOD1 is relatively stable and shares many properties with wild-type SOD1, and only after secondary phenomena like (auto)oxidation, disulphide reduction, or heat shock [47,49], or in a metal-free configuration immediately after its synthesis [14], may be sufficiently abnormal to bind to Hsp25. A recent study with ALS patients and transgenic mice expressing mutant SOD1 with the G127insTGGG mutation, in fact showed that only minute quantities of mutant SOD1 (below 0.5% of control SOD1 levels) accumulate in the spinal cord of these patients and mice, indicating that a small amount of abnormal SOD1 protein is sufficient to cause the disease [24].

Recently, two studies on the distribution of Hsp25 in SOD1-ALS mice have been reported, but unlike our study no changes in motoneuronal Hsp25 expression were observed [4,50]. This discrepancy might be explained by the fact that the time between the onset of decreased motoneuronal Hsp25 expression and astroglial Hsp25 induction is short. In accordance with the previous studies, however, we found a large increase of Hsp25 immunoreactivity in astrocytes of symptomatic G93A mice. Astroglial Hsp27 induction has been reported for different pathological conditions, including ischemia [25], excitotoxicity [27,37], and Alzheimer's disease [40] and therefore seems to be a common characteristic of very different types of brain pathology [18]. It is surprising in this context that astroglial Hsp27 induction did not occur in postmortem human ALS spinal cord, despite a large increase in GFAP expression.

Increasing the expression of Hsp27 has been shown to protect neonatal motoneurons from dying after axotomy [5] and other neurons against excitotoxic injury [1]. It remains to be determined whether viral or transgenic delivery of Hsp27 or Hsp25 is neuroprotective in G93A mice. Another question is whether reduced Hsp27 expression precedes the degeneration of motoneurons in human ALS patients. Data from the present study indicate that Hsp27 expression is decreased in motor columns in sporadic ALS cases, but this may be consequence of the degeneration of motoneurons.

References

[1]   M.T. Akbar, A.M. Lundberg, K. Liu, S. Vidyadaran, K.E. Wells, H. Dolatshad, S. Wynn, D.J. Wells, D.S. Latchman, J. de Belleroche, The neuroprotective effects of heat shock protein 27 overexpression in transgenic animals against kainate-induced seizures and hippocampal cell death, J Biol Chem 278 (2003) 19956-19965.

[2]   P.M. Andersen, K.B. Sims, W.W. Xin, R. Kiely, G. O'Neill, J. Ravits, E. Pioro, Y. Harati, R.D. Brower, J.S. Levine, H.U. Heinicke, W. Seltzer, M. Boss, R.H. Brown, Jr., Sixteen novel mutations in the Cu/Zn superoxide dismutase gene in amyotrophic lateral sclerosis: a decade of discoveries, defects and disputes, Amyotroph Lateral Scler Other Motor Neuron Disord 4 (2003) 62-73.

[3]   U. Arvidsson, F. Piehl, H. Johnson, B. Ulfhake, S. Cullheim, T. Hokfelt, The peptidergic motoneurone, Neuroreport 4 (1993) 849-856.

[4]   Z. Batulan, G.A. Shinder, S. Minotti, B.P. He, M.M. Doroudchi, J. Nalbantoglu, M.J. Strong, H.D. Durham, High threshold for induction of the stress response in motor neurons is associated with failure to activate HSF1, J Neurosci 23 (2003) 5789-5798.

[5]   S. Benn, D. Perrelet, A. Kato, J. Scholz, I. Decosterd, R. Mannion, J. Bakowska, C. Woolf, Hsp27 upregulation and phosphorylation is required for injured sensory and motor neuron survival, Neuron 36 (2002) 45.

[6]   W. Bruening, J. Roy, B. Giasson, D.A. Figlewicz, W.E. Mushynski, H.D. Durham, Up-regulation of protein chaperones preserves viability of cells expressing toxic Cu/Zn-superoxide dismutase mutants associated with amyotrophic lateral sclerosis, J Neurochem 72 (1999) 693-699.

[7]   J.M. Bruey, C. Ducasse, P. Bonniaud, L. Ravagnan, S.A. Susin, C. Diaz-Latoud, S. Gurbuxani, A.P. Arrigo, G. Kroemer, E. Solary, C. Garrido, Hsp27 negatively regulates cell death by interacting with cytochrome c, Nat Cell Biol 2 (2000) 645-652.

[8]   M. Costigan, R.J. Mannion, G. Kendall, S.E. Lewis, J.A. Campagna, R.E. Coggeshall, J. Meridith-Middleton, S. Tate, C.J. Woolf, Heat shock protein 27: developmental regulation and expression after peripheral nerve injury, J Neurosci 18 (1998) 5891-5900.

[9]   C.I. De Zeeuw, E. Chorev, A. Devor, Y. Manor, R.S. Van Der Giessen, M.T. De Jeu, C.C. Hoogenraad, J. Bijman, T.J. Ruigrok, P. French, D. Jaarsma, W.M. Kistler, C. Meier, E. Petrasch-Parwez, R. Dermietzel, G. Sohl, M. Gueldenagel, K. Willecke, Y. Yarom, Deformation of network connectivity in the inferior olive of connexin 36-deficient mice is compensated by morphological and electrophysiological changes at the single neuron level, J Neurosci 23 (2003) 4700-4711.

[10]   H.D. Durham, J. Roy, L. Dong, D.A. Figlewicz, Aggregation of mutant Cu/Zn superoxide dismutase proteins in a culture model of ALS, J Neuropathol Exp Neurol 56 (1997) 523-530.

[11]   P. Eaton, W. Fuller, M.J. Shattock, S-thiolation of HSP27 regulates its multimeric aggregate size independently of phosphorylation, J Biol Chem 277 (2002) 21189-21196.

[12]   M. Ehrnsperger, H. Lilie, M. Gaestel, J. Buchner, The dynamics of Hsp25 quaternary structure. Structure and function of different oligomeric species, J Biol Chem 274 (1999) 14867-14874.

[13]   J.S. Elam, A.B. Taylor, R. Strange, S. Antonyuk, P.A. Doucette, J.A. Rodriguez, S.S. Hasnain, L.J. Hayward, J.S. Valentine, T.O. Yeates, P.J. Hart, Amyloid-like filaments and water-filled nanotubes formed by SOD1 mutant proteins linked to familial ALS, Nat Struct Biol 10 (2003) 461-467.

[14]   L.S. Field, Y. Furukawa, T.V. O'Halloran, V.C. Culotta, Factors controlling the uptake of yeast copper/zinc superoxide dismutase into mitochondria, J Biol Chem 278 (2003) 28052-28059.

[15]   C. Guegan, M. Vila, G. Rosoklija, A.P. Hays, S. Przedborski, Recruitment of the mitochondrial-dependent apoptotic pathway in amyotrophic lateral sclerosis, J Neurosci 21 (2001) 6569-6576.

[16]   M.E. Gurney, H. Pu, A.Y. Chiu, M.C. Dal Canto, C.Y. Polchow, D.D. Alexander, J. Caliendo, A. Hentati, Y.W. Kwon, H.X. Deng, et al., Motor neuron degeneration in mice that express a human Cu,Zn superoxide dismutase mutation, Science 264 (1994) 1772-1775.

[17]   H. Ito, K. Kamei, I. Iwamoto, Y. Inaguma, R. Garcia-Mata, E. Sztul, K. Kato, Inhibition of proteasomes induces accumulation, phosphorylation, and recruitment of HSP27 and alphaB-crystallin to aggresomes, J Biochem (Tokyo) 131 (2002) 593-603.

[18]   T. Iwaki, A. Iwaki, J. Tateishi, Y. Sakaki, J.E. Goldman, Alpha B-crystallin and 27-kd heat shock protein are regulated by stress conditions in the central nervous system and accumulate in Rosenthal fibers, Am J Pathol 143 (1993) 487-495.

[19]   D. Jaarsma, E.D. Haasdijk, Mutant SOD1 protein accumulates in vacuolated mitochondria, in cytosolic filamentous aggregates, and in periaxonal glia in ALS-SOD1 mouse spinal cord, Soc. Neurosci. abstr 27 (2001) 984.982.

[20]   D. Jaarsma, E.D. Haasdijk, J.A. Grashorn, R. Hawkins, W. van Duijn, H.W. Verspaget, J. London, J.C. Holstege, Human Cu/Zn superoxide dismutase (SOD1) overexpression in mice causes

mitochondrial vacuolization, axonal degeneration, and premature motoneuron death and accelerates motoneuron disease in mice expressing a familial amyotrophic lateral sclerosis mutant SOD1, Neurobiol Dis 7 (2000) 623-643.

[21]   D. Jaarsma, F. Rognoni, W. van Duijn, H.W. Verspaget, E.D. Haasdijk, J.C. Holstege, CuZn superoxide dismutase (SOD1) accumulates in vacuolated mitochondria in transgenic mice expressing amyotrophic lateral sclerosis-linked SOD1 mutations, Acta Neuropathol (Berl) 102 (2001) 293-305.

[22]   Y. Jiao, Z. Sun, T. Lee, F.R. Fusco, T.D. Kimble, C.A. Meade, S. Cuthbertson, A. Reiner, A simple and sensitive antigen retrieval method for free-floating and slide-mounted tissue sections, J Neurosci Methods 93 (1999) 149-162.

[23]   J.A. Johnston, M.J. Dalton, M.E. Gurney, R.R. Kopito, Formation of high molecular weight complexes of mutant Cu,Zn-superoxide dismutase in a mouse model for familial amyotrophic lateral sclerosis, Proc Natl Acad Sci U S A 97 (2000) 12571-12576.

[24]   P.A. Jonsson, K. Ernhill, P.M. Andersen, D. Bergemalm, T. Brannstrom, O. Gredal, P. Nilsson, S.L. Marklund, Minute quantities of misfolded mutant superoxide dismutase-1 cause amyotrophic lateral sclerosis, Brain 127 (2004) 73-88.

[25]   H. Kato, K. Kogure, X.H. Liu, T. Araki, K. Kato, Y. Itoyama, Immunohistochemical localization of the low molecular weight stress protein HSP27 following focal cerebral ischemia in the rat, Brain Res 679 (1995) 1-7.

[26]   K. Kato, H. Ito, K. Kamei, I. Iwamoto, Y. Inaguma, Innervation-dependent phosphorylation and accumulation of alphaB-crystallin and Hsp27 as insoluble complexes in disused muscle, Faseb J 16 (2002) 1432-1434.

[27]   K. Kato, R. Katoh-Semba, I.K. Takeuchi, H. Ito, K. Kamei, Responses of heat shock proteins hsp27, alphaB-crystallin, and hsp70 in rat brain after kainic acid-induced seizure activity, J Neurochem 73 (1999) 229-236.

[28]   J.H. Kennis, J.C. Holstege, A differential and time-dependent decrease in AMPA-type glutamate receptor subunits in spinal motoneurons after sciatic nerve injury, Exp Neurol 147 (1997) 18-27.

[29]   S.I. Liochev, I. Fridovich, Mutant Cu,Zn superoxide dismutases and familial amyotrophic lateral sclerosis: evaluation of oxidative hypotheses, Free Radic Biol Med 34 (2003) 1383-1389.

[30]   S.A. Loktionova, O.P. Ilyinskaya, V.L. Gabai, A.E. Kabakov, Distinct effects of heat shock and ATP depletion on distribution and isoform patterns of human Hsp27 in endothelial cells, FEBS Lett 392 (1996) 100-104.

[31]   T.J. Lyons, E.B. Gralla, J.S. Valentine, Biological chemistry of copper-zinc superoxide dismutase and its link to amyotrophic lateral sclerosis, Met Ions Biol Syst 36 (1999) 125-177.

[32]   P. Mehlen, K. Schulze-Osthoff, A.P. Arrigo, Small stress proteins as novel regulators of apoptosis. Heat shock protein 27 blocks Fas/APO-1- and staurosporine-induced cell death, J Biol Chem 271 (1996) 16510-16514.

[33]   A.K. Murashov, S. Talebian, D.J. Wolgemuth, Role of heat shock protein Hsp25 in the response of the orofacial nuclei motor system to physiological stress, Brain Res Mol Brain Res 63 (1998) 14-24.

[34]   A.K. Murashov, I. Ul Haq, C. Hill, E. Park, M. Smith, X. Wang, D.J. Goldberg, D.J. Wolgemuth, Crosstalk between p38, Hsp25 and Akt in spinal motor neurons after sciatic nerve injury, Brain Res Mol Brain Res 93 (2001) 199-208.

[35]   S. Nakagomi, Y. Suzuki, K. Namikawa, S. Kiryu-Seo, H. Kiyama, Expression of the activating transcription factor 3 prevents c-Jun N-terminal kinase-induced neuronal death by promoting heat shock protein 27 expression and Akt activation, J Neurosci 23 (2003) 5187-5196.

[36]   A. Okado-Matsumoto, I. Fridovich, Amyotrophic lateral sclerosis: a proposed mechanism, Proc Natl Acad Sci U S A 99 (2002) 9010-9014.

[37]   J.C. Plumier, J.N. Armstrong, J. Landry, J.M. Babity, H.A. Robertson, R.W. Currie, Expression of the 27,000 mol. wt heat shock protein following kainic acid-induced status epilepticus in the rat, Neuroscience 75 (1996) 849-856.

[38]   J.C. Plumier, D.A. Hopkins, H.A. Robertson, R.W. Currie, Constitutive expression of the 27-kDa heat shock protein (Hsp27) in sensory and motor neurons of the rat nervous system, J Comp Neurol 384 (1997) 409-428.

[39]   X. Preville, H. Schultz, U. Knauf, M. Gaestel, A.P. Arrigo, Analysis of the role of Hsp25 phosphorylation reveals the importance of the oligomerization state of this small heat shock protein in its protective function against TNFalpha- and hydrogen peroxide-induced cell death, J Cell Biochem 69 (1998) 436-452.

[40]   K. Renkawek, G.J. Bosman, W.W. de Jong, Expression of small heat-shock protein hsp 27 in reactive gliosis in Alzheimer disease and other types of dementia, Acta Neuropathol (Berl) 87 (1994) 511-519.

[41]   T. Rogalla, M. Ehrnsperger, X. Preville, A. Kotlyarov, G. Lutsch, C. Ducasse, C. Paul, M. Wieske, A.P. Arrigo, J. Buchner, M. Gaestel, Regulation of Hsp27 oligomerization, chaperone function, and protective activity against oxidative stress/tumor necrosis factor alpha by phosphorylation, J Biol Chem 274 (1999) 18947-18956.

[42]   M.Y. Sherman, A.L. Goldberg, Cellular defenses against unfolded proteins: a cell biologist thinks about neurodegenerative diseases, Neuron 29 (2001) 15-32.

[43]   G.A. Shinder, M.C. Lacourse, S. Minotti, H.D. Durham, Mutant Cu/Zn-superoxide dismutase proteins have altered solubility and interact with heat shock/stress proteins in models of amyotrophic lateral sclerosis, J Biol Chem 276 (2001) 12791-12796.

[44]   A. Stieber, J.O. Gonatas, N.K. Gonatas, Aggregates of mutant protein appear progressively in dendrites, in periaxonal processes of oligodendrocytes, and in neuronal and astrocytic perikarya of mice expressing the SOD1(G93A) mutation of familial amyotrophic lateral sclerosis, J Neurol Sci 177 (2000) 114-123.

[45]   H. Takeuchi, Y. Kobayashi, T. Yoshihara, J. Niwa, M. Doyu, K. Ohtsuka, G. Sobue, Hsp70 and Hsp40 improve neurite outgrowth and suppress intracytoplasmic aggregate formation in cultured neuronal cells expressing mutant SOD1, Brain Res 949 (2002) 11-22.

[46]   F. Tamanini, L. Van Unen, C. Bakker, N. Sacchi, H. Galjaard, B.A. Oostra, A.T. Hoogeveen, Oligomerization properties of fragile-X mental-retardation protein (FMRP) and the fragile-X-related proteins FXR1P and FXR2P, Biochem J 343 Pt 3 (1999) 517-523.

[47]   A. Tiwari, L.J. Hayward, Familial amyotrophic lateral sclerosis mutants of copper/zinc superoxide dismutase are susceptible to disulfide reduction, J Biol Chem 278 (2003) 5984-5992.

[48]   M. Urushitani, J. Kurisu, K. Tsukita, R. Takahashi, Proteasomal inhibition by misfolded mutant superoxide dismutase 1 induces selective motor neuron death in familial amyotrophic lateral sclerosis, J Neurochem 83 (2002) 1030-1042.

[49]   J.S. Valentine, P.J. Hart, Misfolded CuZnSOD and amyotrophic lateral sclerosis, Proc Natl Acad Sci U S A 100 (2003) 3617-3622.

[50]   V. Vleminckx, P. Van Damme, K. Goffin, H. Delye, L. Van Den Bosch, W. Robberecht, Upregulation of HSP27 in a transgenic model of ALS, J Neuropathol Exp Neurol 61 (2002) 968-974.

[51]   A.S. Vlug, E.D. Haasdijk, P.J. French, J. Voogd, J.C. Holstege, D. Jaarsma, Activation of c-Jun and ATF3 in degenerating neurons in amyotrophic lateral sclerosis (ALS)-SOD1 transgenic mice., Soc. Neurosci. abstr 27 (2001) 984.981.

[52]   S. Walter, J. Buchner, Molecular chaperones--cellular machines for protein folding, Angew Chem Int Ed Engl 41 (2002) 1098-1113.

[53]   J. Wang, G. Xu, D.R. Borchelt, High molecular weight complexes of mutant superoxide dismutase 1: age-dependent and tissue-specific accumulation, Neurobiol Dis 9 (2002) 139-148.

[54]   F.C. Wen, Y.H. Li, H.F. Tsai, C.H. Lin, C. Li, C.S. Liu, C.K. Lii, N. Nukina, M. Hsieh, Down-regulation of heat shock protein 27 in neuronal cells and non-neuronal cells expressing mutant ataxin-3, FEBS Lett 546 (2003) 307-314.

[55]   M. Wyszynski, E. Kim, A.W. Dunah, M. Passafaro, J.G. Valtschanoff, C. Serra-Pages, M. Streuli, R.J. Weinberg, M. Sheng, Interaction between GRIP and liprin-alpha/SYD2 is required for AMPA receptor targeting, Neuron 34 (2002) 39-52.

Chapter 5

EXPRESSION OF PHOSPHORYLATED C-JUN AND ATF3 CORRELATES WITH SOMATO-DENDRITIC UBIQUITINATION AND GOLGI FRAGMENTATION AND PRECEDES DEATH OF SPINAL MOTONEURONS IN AMYOTROPHIC LATERAL SCLEROSIS-SOD1 TRANSGENIC MICE

Angela S Vlug, Elize D Haasdijk, Pim J French, and Dick Jaarsma

Department of Neuroscience, Erasmus MC, Rotterdam, The Netherlands

5.1   Abstract

We have examined the expression of N-terminal phosphorylated c-Jun and the 'stress transcription factor' ATF3 in amyotrophic lateral sclerosis (ALS) mice that express G93A-mutant SOD1 (SOD1-G93A mice). Immunocytochemistry and *in situ* hybridization showed that a subset of motoneurons express both ATF3 and phosphorylated c-Jun starting from a relatively early phase of disease before the onset of active caspase 3 expression and motoneuron loss. The onset of phosphorylated c-Jun and ATF3 expression correlated with the onset of dendritic ubiquitination. The highest number of ATF3 and phosphorylated c-Jun expressing motoneurons occurred at symptom onset. At symptom onset phosphorylated c-Jun and ATF3 activation also occurred in spinal interneurons. Confocal-double labeling immunofluorescence showed that phosphorylated c-Jun and ATF3 expression in motoneurons correlated with Golgi fragmentation. A subset of ATF3 and phosphorylated c-Jun immunoreactive motoneurons showed an ill appearance characterized by number of distinctive abnormalities, including an eccentric flattened nucleus, perinuclear accumulation of the Golgi apparatus and the ER, perikaryal accumulation of ubiquitin immunoreactivity and intense Hsp70 immunoreactivity. These abnormal cells were not immunoreactive for active caspase 3. A partially overlapping population of phosphorylated c-Jun and ATF3 immunoreactive motoneurons showed the expression of CHOP, a potential target gene of ATF3. We conclude that motoneurons in SOD1-ALS mice prior to their death show a prolonged phase in which they are compromised and express the injury transcription factors ATF3 and phosphorylated c-Jun. This compromised state is being characterized by an increasing amount of ubiquitinated material that first fills the neurites and subsequently the cell body.

5.2   Introduction

Amyotrophic lateral sclerosis (ALS) is a neurodegenerative disease of motoneurons causing progressive paralysis. In a subset of ALS patients the disease is caused by mutations in the cytosolic Cu/Zn superoxide dismutase (SOD1) gene [1], coding for a small homodimeric metalloenzyme that catalyses the conversion of superoxide anion to hydrogen peroxide. More than 100 different SOD1 mutations have been identified that all cause a relatively similar disease phenotype [1]. Mutant SOD1s display reduced conformational stability, susceptibility to disulfide reduction, abnormal metal binding, toxic oxidative catalytic activities, and an increased tendency to oligomerise and aggregate [33,41,58,60]. Recent studies with spinal cord tissue from ALS patients and transgenic mice expressing SOD1 with the G127insTGGG mutations have shown that minute quantities of mutant SOD1 (below 0.5% of control SOD1 levels) are sufficient to cause ALS [34], and that the toxicity of mutant SOD1 may be represented by a disulfide-reduced hydrophobic fraction [54]. When exposed to the cellular environment these abnormal SOD1 species may interact with a wide range of cellular targets to elicit cellular toxicity [53].

Transgenic mice expressing ALS-related mutant SOD1s develop an ALS-like motoneuron disease and have provided a powerful tool to examine the cellular mechanism by which mutant SOD1 causes the selective degeneration of motoneurons [9]. Biochemical and pathological studies in these mice have revealed several abnormalities in motoneurons prior to their death, including mitochondrial abnormalities [14,31,37,40,65], slowing of axonal transport [6,16,64,66], appearance of ubiquitinated structures [8,34,56,63], Golgi fragmentation [45], loss of neuromuscular synapses [17,18], and activation of programmed cell death pathways [21]. The association of mutant SOD1 with motoneuronal mitochondria is an early and progressive phenomenon in SOD1-ALS mice [31,40] that also has been identified in post-mortem spinal cord tissue from SOD1-ALS patients [40], suggesting that mitochondria may be an early and direct target of mutant SOD1. However, it is not understood how, if indeed, these mitochondrial abnormalities are linked to the functional deterioration and death of motoneurons and to the other abnormalities identified in SOD1-ALS mice. This lack of knowledge is partially due to a poor understanding of the dynamics of the disease process. Next to that, the morphological and molecular correlates of motoneuron degeneration in SOD1-ALS mice are still poorly documented [21].

Neurons including motoneurons respond to injurious stimuli such as axotomy, excessive excitation and survival factor withdrawal by increased expression and phosphorylation of the AP-1 transcription factor c-Jun [26] and by expression of ATF3, a member of the ATF/CREB family of transcription factors [23,59]. These factors play an important role in the control of survival and repair programs, but under specific conditions also may trigger cell death [5,23,25,27,46,52]. Since phosphorylated c-Jun and ATF3 are selectively associated with injured neurons, they might serve as early markers of degenerating motoneurons. Therefore, in this study we have studied their expression in a line of SOD1-ALS mice expressing G93A-mutant SOD1. Our data indicate that ATF3 and phosphorylated c-Jun are expressed in motoneurons in these mice from a relatively early stage of disease,

and that their expression in motoneurons closely correlates with Golgi fragmentation and dendritic ubiquitination. We conclude that ATF3 and phospho-c-Jun mark motoneurons throughout an ill phase that precedes their rapid death and disappearance in SOD1-ALS mice.

5.3   Materials & Methods

5.3.1   Transgenic mice

Experiments were performed in accordance with the "Principles of laboratory animal care" (NIH publication No. 86-23) and the guidelines approved by the Erasmus University animal care committee (DEC; protocol No. 115-97-01 and 115-99-03). G93A-SOD1 mice descendent from the Gurney G1^{del}-line that carry about 8 transgene copy numbers per haploid genome [22] were maintained in a FVB/N background. Our G93A-SOD1 mice develop weakness in one or more limbs starting at age 24-30 weeks, and reach end stage disease 2–10 weeks after onset of limb weakness [29,31]. Pathologically the mice develop swelling and vacuolization of a subset of mitochondria from early age long before the onset of motoneuron loss and gliosis, which starts from 20 weeks of age [42]. For the immunocytochemical characterization of ATF3 and phospho-c-jun expression in G93A-SOD1 mice we analyzed 7 groups: 1) 10 weeks (at this age the mice show swelling and mild vacuolization of a subset of mitochondria but no other pathological features [31]); 2) 15 weeks); 3) 20 weeks (at this age the mice, in addition to mitochondrial abnormalities, show several degenerative features in motoneurons (e.g. ubiquitination, Golgi fragmentation), but no or minimal (<10 %) motoneuron loss [42]); 4) 25 weeks; 5) symptom onset (29-32 weeks: mild muscle weakness in one or more of the hind limbs); 6) 2 weeks post-symptom onset (29-32 weeks: moderate to severe muscle weakness in one or more of the hind limbs); 7) 5 weeks post-symptom onset (32 weeks: severe muscle weakness of the hind limbs). Non-transgenic littermates and transgenic mice expressing wild-type hSOD1 (hSOD1 mice) derived from the Gurney N29 line and aged 10-100 weeks [29] were used as controls.

5.3.2   Antibodies

Primary antibodies (supplier, applications {IHC, immunohistochemistry; IF, immunofluorescence} and dilutions) reported in this study are: rabbit anti-ATF3 (Santa Cruz; IHC and IF 1:1.000); rabbit anti-calreticulin (Affinity BioReagents, IHC and IF 1:5.000), rabbit anti-cleaved caspase 3 (Asp175, Cell Signalling, IHC 1:1.000); rabbit anti-CGRP (Calbiochem, IHC and IF, 1:10.000); goat anti-ChAT (Chemicon, IHC and IF 1:500); rabbit anti-CHOP (SantaCruz, IHC and IF 1:2.000); rabbit anti-c-fos (Ab5; Oncogene IHC, IF 1:20.000); rat anti-CR3 receptor (clone 5C6; Serotec, IHC 1:500); rabbit anti-GFAP (DAKO, IHC 1:10.000, IF 1:5.000); mouse anti-GM130 (Golgi matrix protein of 130 KDa associated with the cis-compartment; Transduction Laboratories, IF 1:1.000); rabbit anti-Hsp25 (Stessgen, IF 1:2.000); mouse anti-Hsp70 (SantaCruz, IHC and IF 1:500); rabbit anti-c-Jun (ab1; Oncogene, IHC 1:10.000 and IF 1:2.000); rabbit anti-phospho-c-Jun (Ser73; Upstate Biotechnology, IHC 1:2.000, IF 1:500); rabbit anti-phospho-c-Jun (Ser63; Cell Signalling, IHC 1:2.000, IF 1:500); mouse anti-phospho-c-Jun (Ser63; Santa

Cruz, IHC 1:2.000, IF 1:500); rabbit anti-Krox24 (Santa Cruz, IHC 1:5.000); goat anti-c-Ret (R&D systems, IF 1:200); goat anti-human SOD1 (Calbiochem, IF 1:10.000); rabbit anti-SOD1 (1:5.000); rabbit anti-STAT3 (Santa Cruz, IHC 1:2000); rabbit anti-phospho-STAT3 (Tyr705; Cell Signalling, IHC 1:2.000); rabbit anti-ubiquitin (Dako, IHC and IF 1:2.000); mouse anti-ubiquitin (clone FK2; Affiniti, IF 1:2.000).

Secondary antibodies: For avidin-biotin-peroxidase immunocytochemistry biotinylated secondary antibodies from Vector Laboratories diluted 1:200 were used. FITC-, Cy3-, and Cy5-conjugated secondary antibodies raised in donkey (Jackson Immunoresearch, USA) diluted at 1:200 were used for confocal immunofluorescence. Cy3-conjugated donkey anti-rabbit Fab fragments (Jackson Immunoresearch, USA) were used in double-labeling experiments with two rabbit primary antibodies.

5.3.3   Immunocytochemical and histochemical analyses

For immunocytochemistry and immunofluorescence mice were anaesthetized with pentobarbital and perfused transcardially with 4% paraformaldehyde with or without glutaraldehyde (0.1 or 0.5%). The lumbar and cervical spinal cord were carefully dissected out and post-fixed overnight in 4% paraformaldehyde. Unless otherwise stated, spinal cord tissue was embedded in gelatin blocks [29], sectioned at 40 μm with a freezing microtome and sections were processed, free floating, employing a standard avidin-biotin-immunoperoxidase complex method (ABC, Vector Laboratories, USA) with diaminobenzidine (0.05%) as the chromogen, or single, double- and triple-labelling immunofluorescence [29,31]. In addition, a selected number of frozen sections were processed for a silver staining procedure that selectively labels dying neurons and their processes [29].

Some spinal cord specimens were sectioned with a vibratome (50-60 μm thick). These sections were used for pre-embedding immunoperoxidase electron microscopy as described [31], or for light-microscopic double-labeling experiments, in which sections were sequentially processed for 2 different primary antibodies using the ABC method for both. To label the first antibody $CoCl_2$ was included in the diaminobenzidine solution to yield a dark-blue precipitate. The second antibody was visualized with diaminobenzidine alone. Following the immunostaining procedure these sections were dehydrated, embedded in Durcupan, sectioned at 1 μm and counterstained with methylene blue.

For double-labeling immunofluorescence with two rabbit antibodies Cy3-conjugated donkey anti-rabbit Fab fragments were used to label and sterically cover the first antibody as described by the manufacturer (Jackson Immunoresearch, USA). Then the sections were incubated with the second primary antibody which consecutively was labeled with FITC-donkey ant-rabbit IgG. Single-labeling experiments were always performed in parallel to these double-labeling experiments to evaluate the specificity of the staining.

Immunoperoxidase-stained sections were analyzed and photographed using a Leica DM-RB microscope and a Leica DC300 digital camera. Quantitative analyses were performed with 20 consecutive L4 lumbar spinal cord sections/mouse that were serially immunoperoxidase-labeled for ATF3, ChAT, CGRP and cleaved caspase 3, respectively (e.g. sections 1, 6, 11, and 16 were labeled for ATF3,
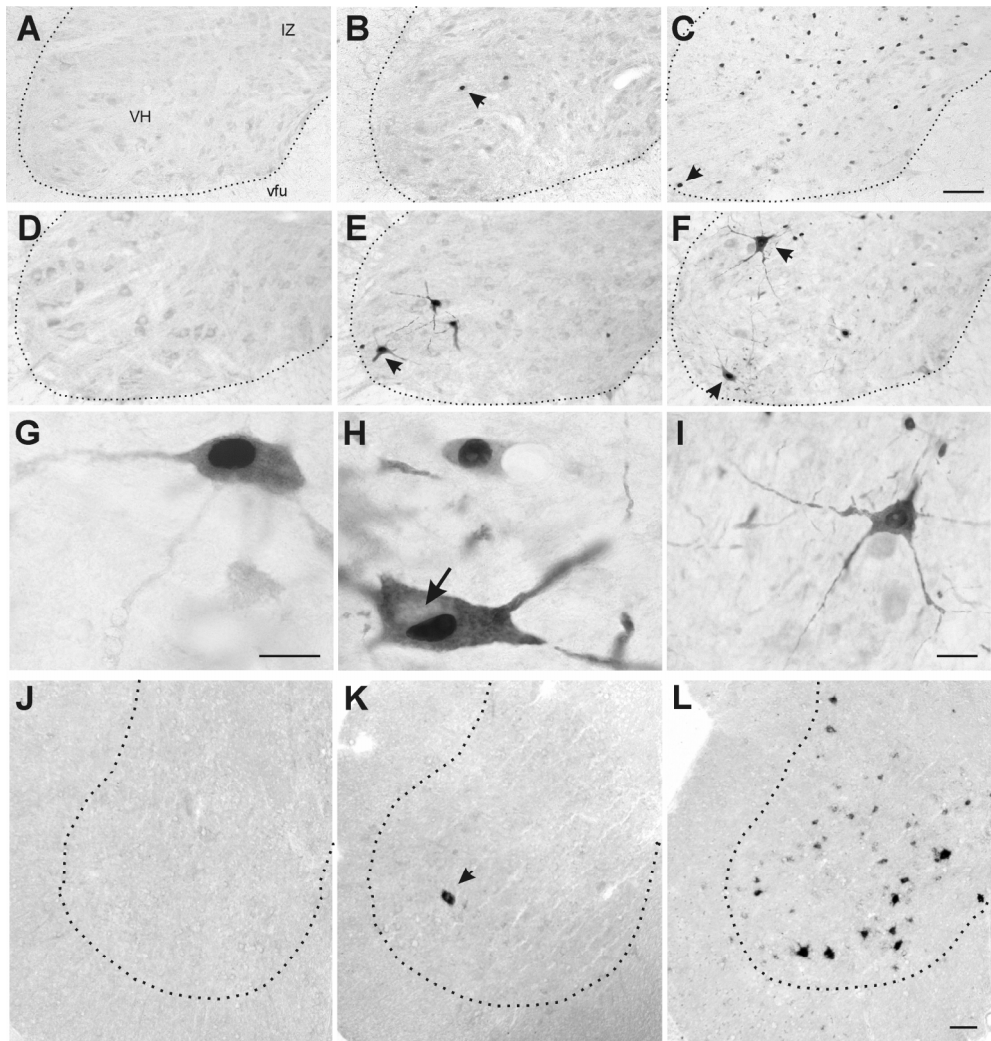
Figure 1: Phospho-c-Jun and ATF3 expression are induced first in motoneurons and subsequently in interneurons in spinal cord of G93A-SOD1 mice

(A-C) Distribution of phospho-c-Jun-immunoreactivity in the ventral horn (vh) and intermediate zone (iz) of the L4-spinal cord of G93A-SOD1 mice of 10 weeks (A), 20 weeks (B) and 30 weeks (C) of age. Note phospho-c-Jun labelled motoneurons in the 20 and 30 weeks old G93A-SOD1 mice (arrows in B and C), and phospho-c-Jun labelled interneurons in the 30 weeks old G93A-SOD1 mouse. (D-L) Distribution of ATF3 immunoreactivity (D-I) and *mRNA* (J-L) in L4-spinal cord of G93A-SOD1 mice of 10 weeks (D, J), 20 weeks (E, G, H, K) and 30 weeks (F, I, L) of age. Note in high-magnification images of ATF3 immunoreactive motoneurons (G-I) that ATF3-immunoreactivity although primarily localised in the nuclei also occurs in the somato-dendritic cytoplasm. Also note the ATF3-immunoreactive motoneuron with an flattened eccentric nucleus (arrow in H). Calibration bars: C and L, 100 µm; G (also for H), 10 µm; and H, 20 µm.

(B) Neurolucida plots of representative consecutive L4 spinal cord sections of G93A-SOD1 mice of different ages showing motoneurons (filled circles) and non-motoneurons (open circles) stained for phosphorylated(ser73)-c-Jun and ATF3, resepectively.

sections 2, 7, 12, 17 for ChAT etc.). The remaining sections were stained for phospho-c-Jun and ubiquitin, respectively. A selected number of sections stained for phospho-c-Jun, ATF3, cleaved caspase 3 and ubiquitin were plotted using an Olympus microscope fitted with a LucividTM miniature monitor and NeurolucidaTM software (MicroBrightField, Colchester, VT, USA). Statistical analysis was done with Graphpad Prism software (San Diego, USA).

Sections stained for immunofluorescence were analyzed with a Zeiss LSM 510 confocal laser scanning microscope. For quantitative analysis of co-localization of ATF3 with other markers (active caspase 3, CGRP, c-Jun, phospho-c-Jun, Gadd153, GM130, Hsp70, ubiquitin) in motoneurons 50 ATF3-labeled motoneurons were randomly selected in L4 sections of 20, 25 and 30 weeks old G93A-SOD1 mice using 20x or 63x objectives. All motoneurons in a field of 150 x 150 µm surrounding the labeled cell were scored for single or double labeling. In the same way 25-50 phospho-c-Jun, Gadd153, Hsp70 or ubiquitin immunoreactive motoneurons were randomly selected and analyzed for co-localization with ATF3.

Ultra thin sections for electron microscopy were and analyzed in a Phillips CM100 electron microscope operated at 80 kV [31].

5.3.4   mRNA in situ hybridisation

In situ hybridization was performed on 12 µm thick cryostat sections using standard methods with digoxigenin-labeled cRNA probes [42]. Sense and anti-sense digoxigenin-labelled cRNAs were transcribed from liberalized plasmids containing full-length ATF3 cDNA (NCBI acc.no. BF166234), c-Jun cDNA (NCBI acc.no. BE283254).

5.4 Results

5.4.1   Phospho-c-Jun and ATF3 expression is induced first in motoneurons and subsequently in interneurons

Non-transgenic mice show constitutive expression of c-Jun in a subset of motoneurons [26,30]. However, motoneurons in non-transgenic mice were not immunoreactive for N-terminal (ser73) phosphorylated c-Jun (phospho-c-Jun) [29]. Also motoneurons of young adult G93A-SOD1 mice (age 10 weeks) were not immunoreactive for phospho-c-Jun (Figs 1a and 2b). In contrast G93A-SOD1 mice older than 15 weeks showed an increasing number of intensely phospho-c-Jun immunoreactive motoneurons (Figs 1b, and c and 2). From 20 weeks-of-age phospho-c-Jun also occurred in neurons in the intermediate zone (Rexed's laminae V-VIII and X) of the spinal cord (Figs 1c and 2b). The number of phospho-c-Jun labeled interneurons varied between G93A-SOD1 mice of the same age, and positively correlated with the duration of symptoms (Fig. 2). G93A-SOD1 mice with severe paresis or at end-stage disease showed phospho-c-Jun immunoreactive neurons throughout all laminae of the spinal cord including the dorsal horn (Fig. 2). Immunocytochemistry and *in situ* hybridization showed that ATF3 is not expressed in control spinal cord, but has the same spatio-temporal distribution as phospho-c-Jun in the spinal cord of G93A-SOD1 mice (Figs 1 and 2). Other inducible transcription factors, i.e. c-fos and krox24, did not show altered expression in
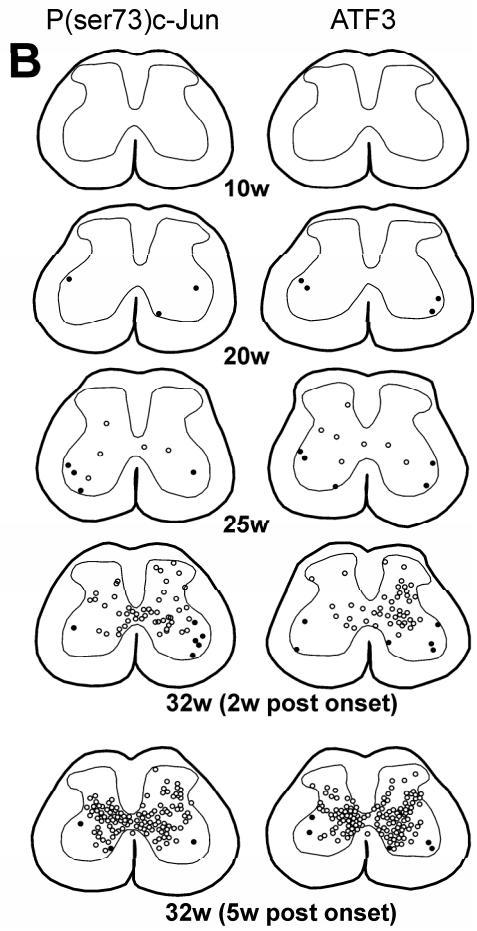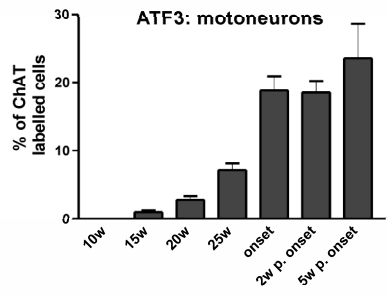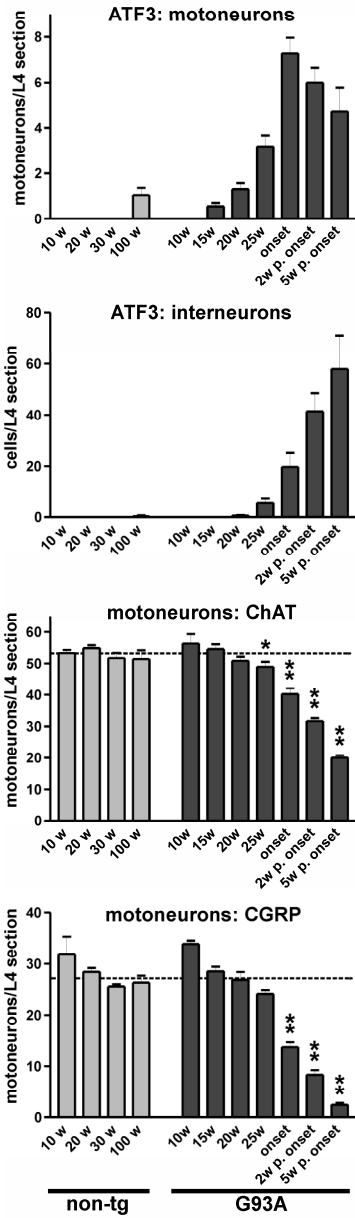
Figure 2: Phospho-c-Jun and ATF3 expression precedes motoneuron loss in G93A-SOD1 mice.
(A) Bar graphs showing the number of ChAT, CGRP and ATF3-labeled motoneurons and ATF3-labeled interneurons in L4-spinal cord sections of non-transgenic and G93A-SOD1 mice of different age (see materials and methods. Dashed line in ChAT and CGRP graphs represent the mean number of ChAT and CGRP-labeled motoneurons, respectively, of 20 and 30 weeks old control mice.c

G93A-SOD1 mice (not shown). Double-labeling confocal immunofluorescence confirmed that ATF3 and phospho-c-Jun were expressed in the same population of motoneurons (Fig. 5e), i.e. 48 of 50 randomly selected ATF3 labeled motoneurons were positive for phospho-c-Jun, and, vice versa, 50 of 50 randomly selected phospho-c-Jun immunoreactive motoneurons were also immunoreactive for ATF3 (see material and methods). Accordingly, all ATF3 motoneurons also were immunoreactive for c-Jun. ATF3 also co-localized with phospho-c-Jun and c-Jun in interneurons of G93A-SOD1 mice (not shown). In contrast with phospho-c-Jun which was exclusively localized in the nucleus, ATF3 immunoreactivity was also found in the cytoplasm of a subset of neurons in G93A-SOD1 mice (Fig 1e and f). As discussed in paragraph 5.4.3, extra-nuclear ATF3 co-localized with ubiquitin immunoreactivity.

ATF3 and phospho-c-Jun labeling did not occur in non-neuronal cells in the spinal cord of control, presymptomatic and early symptomatic G93A-SOD1 mice. However, in a late phase of disease clusters of small cells that showed moderate ATF3 and phospho-c-Jun labeling occurred in areas with severe neuronal pathology (not shown).

5.4.2   Phospho-c-Jun and ATF3 expression precede the activation of caspase 3 and motoneuron death

To determine the relationship between ATF3 and phospho-c-Jun expression on the one hand and motoneuron degeneration on the other hand, we have counted motoneurons in serial sections immunostained for choline acetyltransferase (ChAT) or CGRP, respectively. No or very little loss of ChAT-labeled motoneurons occurred at 20 weeks of age, no to moderate (0-20%) loss at 25 weeks of age, and moderate to severe loss (10-60%) at 29-32 weeks of age, depending on the severity of the symptoms as determined by a hind limb extension test (Fig. 2a) [42]. The same dynamics of motoneuron loss was observed with CGRP (Fig. 2a), a peptide that is preferentially localized in large motoneurons [3]. In accordance with previous studies showing that large motoneurons are selectively afflicted in G93A-SOD1 mice [43], we found that a relatively large percentage (50-95%) of CGRP-immunoreactive motoneurons were lost in symptomatic G93A-SOD1 mice. However, no or little loss of CGRP-labeled motoneurons was observed up to 25 weeks of age (Figs 2a and 6a-c). Since ATF3 and phospho-c-Jun could be identified in motoneurons in G93A-SOD1 mice from 15 weeks of age, it can be concluded that ATF3 and phospho-c-Jun expression precede the onset of motoneuron loss.

To further analyze the relation between ATF3 and phospho-c-Jun expression and motoneuron death we have compared their expression with the expression of caspase 3, an executioner caspase in neurons that has been identified in the spinal cord at the onset of motoneuron death in various lines of SOD1-ALS mice[51]. Immunocytochemistry with an antibody specific for active caspase 3 showed that active caspase 3 was not present in lumbar L4 sections of our G93A-SOD1 mice at 10 and 15 weeks of age, but was present in a minority (2 of 8) of mice at 20 weeks, a majority (6 of 8) of mice at 25 weeks, and all mice (18 of 18) sacrificed at29-32 weeks. In line with previous studies [51] active-caspase 3-
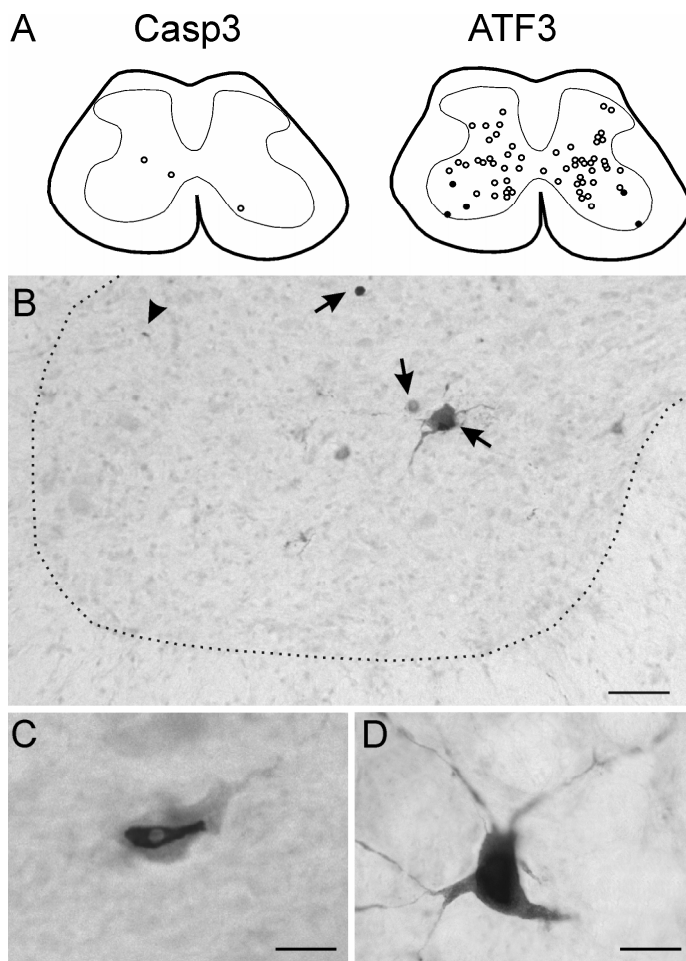
Figure 3: Active caspase 3 shows a different spatio-temporal distribution as ATF3 in G93A-SOD1 mice. (A) Neurolucida plots of representative consecutive L4 spinal cord sections from a symptomatic 30 weeks old G93A-SOD1 mouse showing motoneurons (filled circles) and non-motoneurons (open circles) stained for active caspase 3 (Casp3) and ATF3, respectively. Note the relatively low number of active caspase 3-stained neurons. (B-D) Low (B) and high-magnification (C and D) photomicrographs of active caspase 3 staining in the spinal cord of G93ASOD1 mice. Note in (B) that staining is more abundant in the intermediate zone as compared to the motor column (i.e. left part of the grey matter). In the motorcolumns labeling is usually associated with unidentifiable structures (arrow head). Labeled motoneurons as shown in (C) are very infrequent. Labeled neurons usually were interneurons (arrows in B; D). Calibration bars: B, 50 µm; C, 15 µm; and D, 10 µm.

immunoreactivity was most frequently associated with irregular structures, 1-5 µm in diameter, in the ventral horn and intermediate zone (Fig. 3b). These structures putatively reflect debris of dead cells. The frequency of these structures, which was about 3 per transverse lumbar section in symptomatic G93A-SOD1 mice, did not correlate with the severity of symptoms. Less frequently, active caspase 3 was found in cells that could be identified either as neurons (less than 0.5 per L4 section, Fig. 3a-c) or astrocytes (not shown). In these cells active caspase 3-labeling was concentrated in the nucleus (Fig. 3a-c). Active-caspase 3-labeled neurons were predominantly found in the intermediate zone (Fig. 3a and b) and the dorsal horn (Fig. 3d), and very infrequently (4 cells in over 100 L4 sections examined) in motor columns (Rexed's lamina IX, Fig. 3c). This very low number of active-caspase 3-immunoreactive motoneurons is consistent with our data obtained with a silver degeneration method that stains dying neurons and their processes, which revealed a very low number of argyrophilic motoneurons in our G93A-SOD1 mice (not shown). In sum, compared to ATF3 and phospho-c-Jun,

active caspase 3 is expressed at a later time point and in a considerably lower number of neurons (Fig. 3a).

Analysis of ATF3 and active caspase 3 co-expression by double-labeling confocal immunofluorescence, showed that all ATF3-immunoreactive motoneurons (50 of 50), including motoneurons with an abnormal appearance (see 5.4.4), were immunonegative for active caspase 3. Further analysis of ATF3 and phospho-c-Jun immunoreactivity in semi-thin (1 μm) plastic sections double-stained for ATF3 or phospho-c-Jun and the complement 3 receptor (CR3, a marker of microglia [29]), showed that although ATF3 and phospho-c-Jun expressing motoneurons often were surrounded by microglial processes these cells did not show classical apoptotic changes such as cell shrinkage and chromatin condensation (Fig. 5a). On the other hand in the same material we have identified cells with apoptotic morphology and surrounded by microglial processes that were negative for ATF3 and phosphorylated c-Jun (Fig. 5a). In sum, our data indicate that ATF3 and phosphorylated c-Jun are not associated with cells undergoing apoptosis.

5.4.3 Phospho-c-Jun and ATF3 expression in motoneurons correlates with ubiquitination and Golgi fragmentation

The earliest neuropathological feature in our G93A-SOD1 mice is mitochondrial swelling and vacuolization. These mitochondrial abnormalities appear as early as 4 weeks postnatal [31], and hence precede the appearance of phospho-c-Jun and ATF3 immunoreactive motoneurons by several weeks. The second abnormality in time is the appearance of ubiquitinated neurites, i.e. neuronal processes that are stained by antibodies raised against polyubiquitinated epitopes. Ubiquitinated neurites were present in 1 of 5 G93A-SOD1 mice of 10 weeks old, and in all mice of 15 weeks and older (Fig. 4c and e). Double-labeling confocal immunofluorescence with ChAT and immuno-electron microscopy showed that this ubiquitin immunoreactivity is localized in dendrites (and occasionally the axon) of motoneurons and co-distributes with mutant SOD1 [31,42]. In some instances ubiquitin-immunoreactivity could be 'traced back' to the cell body of motoneurons (e.g. Fig. 5d). Ultrastructurally, dendritic ubiquitination was characterized by a disorganized ensemble of filamentous and amorphous material and, in many occasions, small vesicles (Fig. 5f). These ubiquitinated ensembles were surrounded by normal appearing mitochondria and cytoplasm (Fig. 5f), and were never found in proximity of swollen and vacuolated mitochondria in the same dendrite. The frequency of ubiquitinated neurites increased with aging. In addition with aging ubiquitin immunoreactivity also accumulated in other structures, i.e. in the somata of motoneurons (from 20 weeks of age), in spinal interneurons (from 25 weeks), and in glia (from 20-25 weeks).

The time of appearance and relative density of ubiquitinated structures grossly correlated with the time of appearance and density of phospho-c-Jun and ATF3 positive neurons (Fig. 4a and b). Since in most instances it was not possible to identify the cell bodies of ubiquitinated neurites, analysis of the relation between dendritic ubiquitination and ATF3 or phospho-c-Jun expression was not possible. Indirect evidence from systematic analysis of serial L4 lumbar sections of 10-, 15- and 20-week-old G93A-SOD1 mice suggested that the appearance of ubiquitinated neurites preceded the appearance of ATF3 and phospho-c-Jun immunoreactivity,
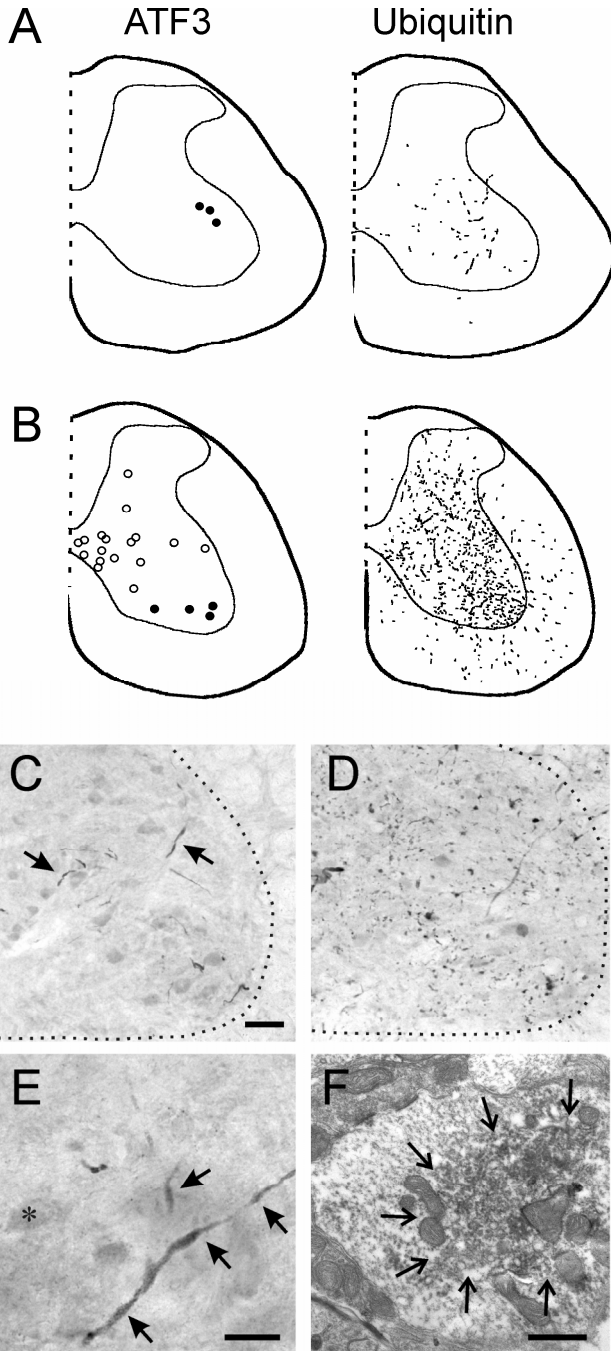
Figure 4: The onset of phospho-c-Jun and ATF3 expression correlate with dendritic ubiquitination.

(A, B) Neurolucida plots of representative consecutive L4 spinal cord sections from a 20 weeks (A) and 30 weeks (B) old G93A-SOD1 mouse showing motoneurons (filled circles) and non-motoneurons (open circles) stained for phosphorylated(Ser73)-c-Jun and ubiquitin-immunoreactive structures, respectively. Note that both the amount of phospho-c-Jun and ubiquitin labeling increased with aging progressive increaserelatively low number of active caspase 3 stained neurons.

(C-F) Low (C, D) and high-magnification (E) light-microscopic photomicrographs, and electron photomicrograph (F) of ubiquitin-immunoperoxidase labeling in the L4 spinal cord 15 weeks (C), 20 weeks (E and F) and a 30 weeks (D) old G93A-SOD1 mouse. In 15 and 20 weeks old G93A-SOD1 mice ubiquitin labeling is selectively associated with neurites in the motor columns (arrows in C and E). Ultrastructurally, this neuritic labeling is associated with core of motoneuron dendrites (area indicated by arrows in F). Note that cytoplasm en mitochondria surrounding the ubiquitinated area have a normal appearance (see also Fig. 8h and i of Chapter 4). In 30 weeks old G93A ubiquitinated structures are associated with both neuronal and glial profiles (not shown) and fill the entire ventral and intermediate gray matter (B and D). Calibration bars: C (also for D), 50 µm; E, 25 µm; and F, 500 nm.

because 1) dendritic ubiquitin immunoreactivity occurred in one 10-week-old G93A-SOD1 mouse in the absence of ATF3 and/or phosphorylated c-Jun labeled motoneurons; and 2) the number and distribution of ubiquitinated dendrites per L4 section in 15-week-old G93A-SOD1 mice suggested that multiple motoneurons per L4 section had ubiquitinated dendrites (Fig. 4a and c), whereas the mean frequency of ATF3 immunoreactive motoneurons was 0.55 or 1.3 per L4 section at 15 and 20 weeks, respectively. Further analysis using double-labeling confocal immunofluorescence of ubiquitin and ATF3 showed that 1) all motoneurons showing focal (Fig. f1) or diffuse (Fig. f2) perikaryal ubiquitin immunoreactivity (20 of 20) also stained for ATF3 (Fig. f1 and f2); 2) the majority of ATF3-immunoreactive motoneurons (37 of 50) did not show perikaryal ubiquitin immunoreactivity in the cell body; and 3) ATF3 immunoreactivity co-distributed with ubiquitin in motoneurons with perikaryal ubiquitin immunoreactivity (Fig. f1 and f2) and in a subset of ubiquitinated neurites (Fig. f2). These confocal data indicate that ATF3 expression precedes perikaryal ubiquitination.

Fragmentation of the Golgi apparatus, i.e. the transformation of the Golgi apparatus from a network of linear profiles to dispersed smaller elements (e.g. see Fig. 5d and 5g1), has been identified as a constant feature in a subset of motoneurons of ALS patients [55] and SOD1-ALS mice [45,56]. To study the relationship between Golgi fragmentation and ATF3 or phospho-c-Jun expression we have used two markers to stain the Golgi apparatus, i.e. the *cis*-Golgi matrix protein GM130 [47]; and CGRP, a peptide selectively expressed in large motoneurons (see above) and that is localized in the *trans*-Golgi, multivesicular bodies, and secretory granules [10]. Motoneurons with fragmented Golgi were identified in our G93A-SOD1 mice from 15 weeks. Double labeling confocal immunofluorescence showed that GM130 and CGRP in motoneurons with fragmented Golgi maintain their adjoining slightly overlapping localization consistent with their distribution in the *cis*- and *trans*-Golgi, respectively (Fig. 5g1). In some motoneurons we noted the redistribution of the fragmented Golgi to a subregion of the cell, usually in close proximity of the nucleus (Fig. 5g1-g4, see below). In addition, we noted that motoneurons with fragmented Golgi labeled for CGRP showed the accumulation of CGRP in the dendrites (Figs 5g4 and 6a-f) and sometimes the soma (Figs. 5g1 and 6c). This dendritic CGRP did not co-distribute with GM130 indicating that it reflects a non-Golgi fraction of CGRP (not shown). Interestingly, at least a portion of dendritic CGRP-immunoreactivity co-distributed with ubiquitin (Fig. 5g4).

Double labeling of ATF3 with GM130 indicated that nearly all ATF3 labeled motoneurons (49 of 50) showed a fragmented Golgi (Fig. 5c and 5g2) and that all of the ATF3-negative motoneurons identified in the same fields (84 of 84) displayed a normal Golgi. Accordingly, all ATF3 motoneurons that were also positive for CGRP (17 of 17) showed an abnormal Golgi, and inversely all CGRP immunoreactive motoneurons with an abnormal Golgi (20 of 20) were immunoreactive for ATF3 (Fig. 5g3). Analysis of phospho-c-Jun and GM130 labeled sections also showed a close relationship between phospho-c-Jun and Golgi fragmentation. Although not systematically studied, Golgi fragmentation also was frequently observed in phospho-c-Jun of ATF3-labeled intermediate zone
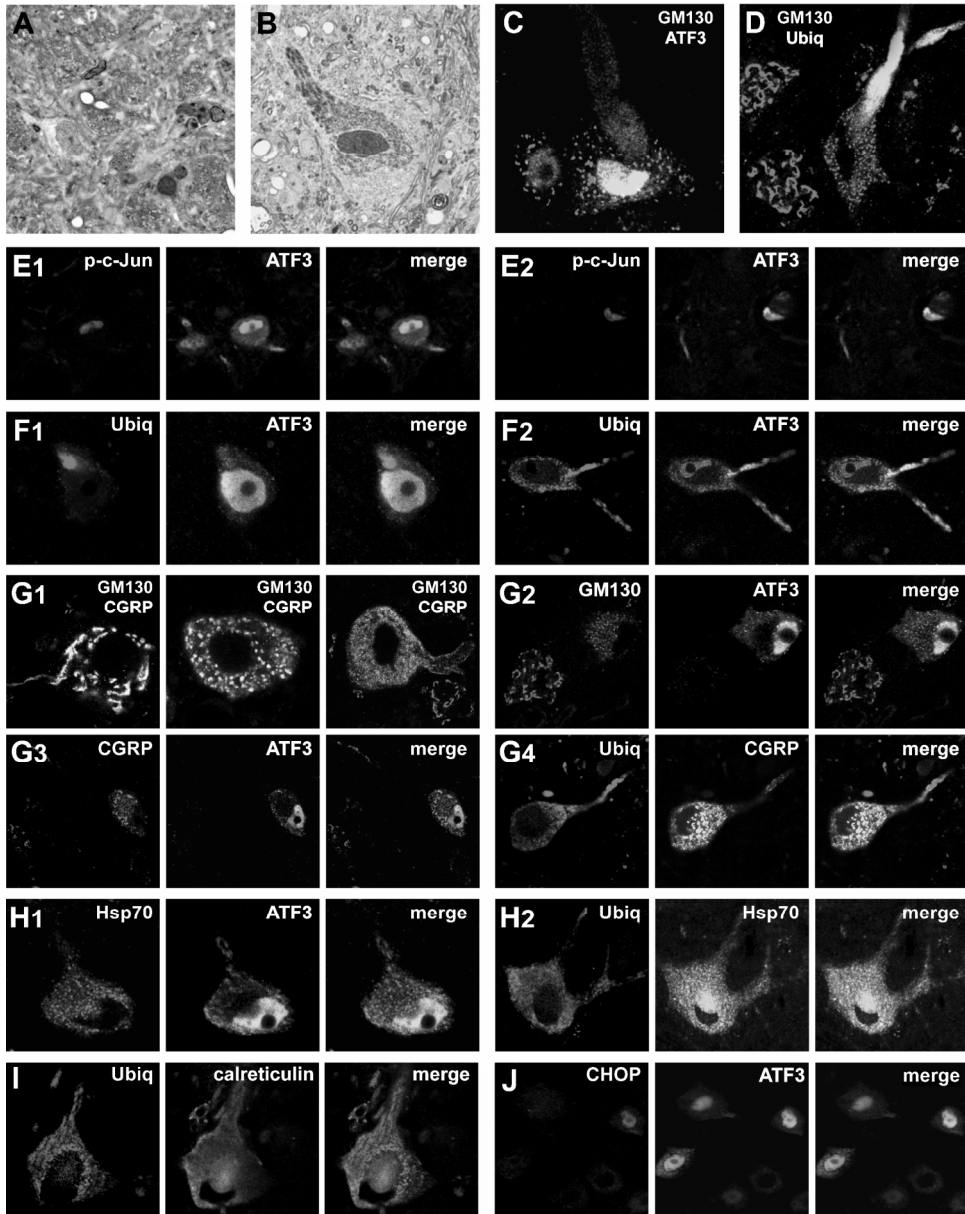
Figure 5: Phospho-c-Jun and ATF3 expression correlates with Golgi fragmentation and ubiquitination.

(A) High magnification of semi-thin (0.5 µm thick) section showing a motoneuron with phospho-c-Jun (dark-brown) labeled nucleus surrounded by CR3-labeled microglial processes (light-brown). Note that the phospho-c-Jun labeled nucleus has a healthy appearance. Also note that the cell with the pyknotic nucleus (arrow) is not phospho-c-Jun labeled. (B) Semi-thin ATF3 stained section showing a motoneuron with intense nuclear and cytosolic ATF3 labeling. Note that part of the cell is ATF3-negative (arrow heads). (C-J) Double-labeling confocal immunofluorescence of ATF3 with phospho-c-Jun (E1 and E2), ubiquitin (F1 and F2), the cis-Golgi protein GM130 (C and G2), CGRP (G3), Hsp70 (H1) and CHOP (J); or of ubiquitin with GM130 (D), CGRP (G4), Hsp70 (H2) and calreticulin (I).

neurons (not shown). In sum our data indicate that ATF3 and phospho-c-Jun expression occur in the same motoneurons that show Golgi fragmentation.

5.4.4   A subset of phospho-c-Jun and ATF3 positive motoneurons show signs of degeneration

As indicated in paragraph 5.4.3 a subset of ATF3 and phospho-c-Jun positive motoneurons showed the accumulation of the fragmented Golgi apparatus in a subregion of the cell. These cells showed an ill appearance in most instances characterized by a flattened eccentric nucleus. The juxta-nuclear area 'left over' by the flattened nucleus was occupied by the Golgi apparatus (Fig. 5f2, 5g2 and 5g4). Further analysis demonstrated that these cells showed moderate to intense ubiquitin and ATF3 labeling throughout most of the perikaryon. Significantly, the region occupied by the Golgi apparatus shows little ubiquitin and ATF3 immunoreactivity (Fig. 5f2, 5g2, 5g3, 5g4 and 5h2). In contrast, calreticulin, an ER protein, also was preferentially distributed in the perinuclear region (Fig. 5i). The ill-appearing cells also were selectively labeled for the heat shock protein Hsp70 (Figs 6h and i). Hsp70, like the Golgi apparatus and ER, was preferentially distributed in the perinuclear region not occupied by ubiquitin (Figs 5h1 and h2). The ill-appearing motoneurons in some cases showed resemblance with active caspase 3 immunoreactive motoneurons (e.g. compare Figs 3c and f2), but double-labeling showed that these cells did not stain for active caspase 3.

In sum, ill-appearing motoneurons in G93A-SOD1 mice showed the accumulation of ubiquitinated structures throughout most of the perikaryon, resulting in the accumulation of organelles in a small usually perinuclear portion of the cell. In spite of these morphological and neurochemical features of ill health, these cells did not (yet) show the activation of the caspase 3.

5.4.5   ATF3 and phospho-c-Jun positive motoneurons do not show signs associated with axonal injury.

Phospho-c-Jun and ATF3 expression are part of a coordinated program induced in motoneurons following axon transection [44,52,59]. To examine to what extend phospho-c-Jun and ATF3 expressing motoneurons are in the process of executing an 'axotomy response' we have examined the expression of a number of proteins known to be upregulated in axotomized motoneurons, including Hsp27, CGRP and phospho-STAT3 [3,13,39]. Previously, we have reported a poor correlation between ATF3 and Hsp27 expression [42]: the onset of ATF3 expression in motoneurons was associated with a global decrease in Hsp27 protein levels, and furthermore ATF3 labeled motoneurons frequently were immunonegative for Hsp27. In the same way we identified a poor correlation between ATF3 and CGRP expression: Thus only a subset of randomly selected ATF3 immunoreactive motoneurons (17 of 25) was immunoreactive for CGRP, and the onset of ATF3 expression was not associated with an increase in CGRP labeling of motoneurons. Finally, we did not identify phospho-STAT3 or nuclear translocation of STAT3 in our G93A-SOD1 mice at any age (not shown). In sum, ATF3/phospho-c-jun immunoreactive motoneurons in G93A-SOD1 mice do not show the gene expression profile of axotomized motoneurons.
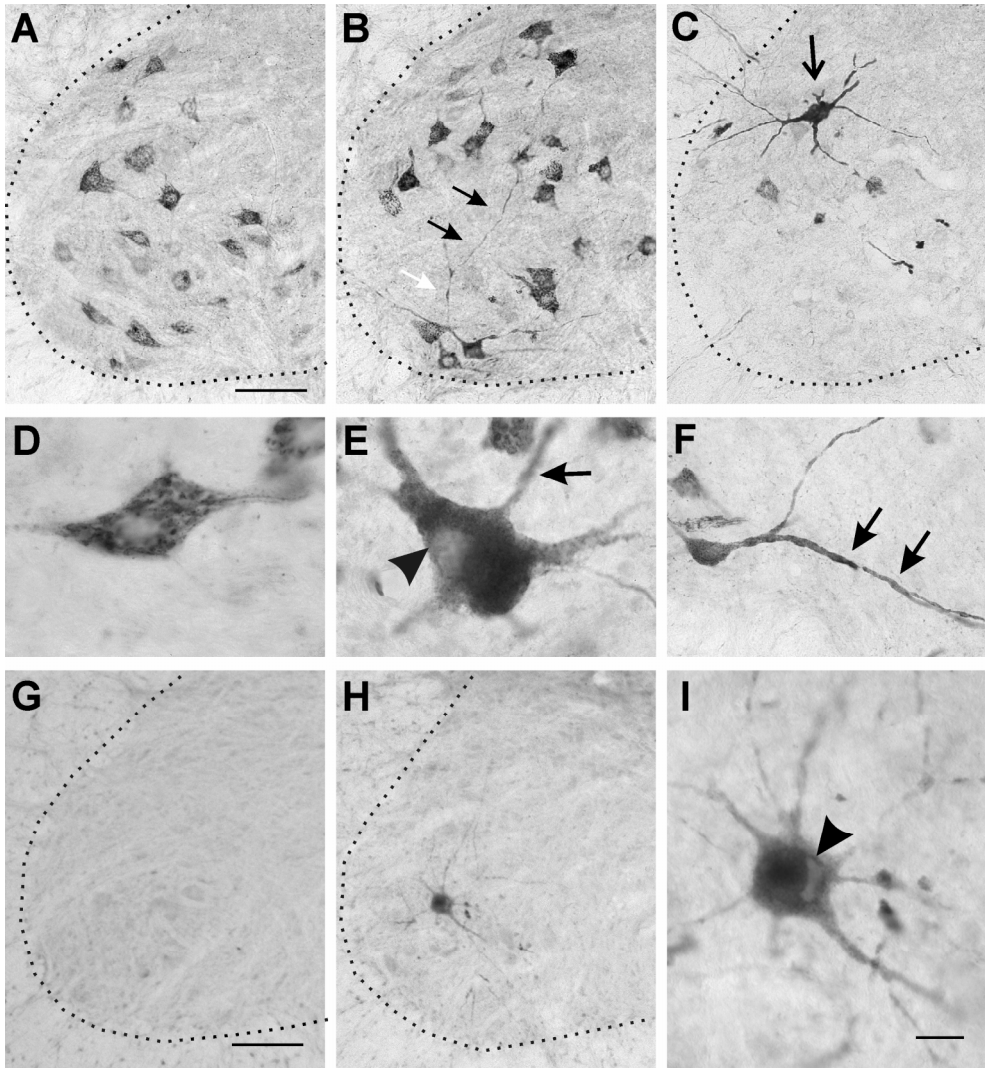
Figure 6: Subsets of motoneurons in G93A-SOD1 mice show dendritic accumulation of CGRP and Hsp70 expression.

(A-F) Low (A-C) and high-magnification (D-F) of CGRP immunoperoxidase labeling in the L4 spinal cord of 20 weeks old non-transgenic (A, D) and G93A-SOD1 mice (B, E, F) and a 30 weeks old G93A-SOD1 mouse (C). In all control and most 20 weeks old G93A-SOD1 motoneurons CGRP was distributed in elongated linear profiles (A, B, D). However, a subset of motoneurons in G93A-SOD1 mice showed a granular labeling pattern, consistent with Golgi fragmentation, and furthermore showed abnormal dendritic CGRP labeling (arrows in B, C, E, F).

(G-I) Low (G-H) and high-magnification (I) of Hsp70-immunoperoreactive motoneurons in the L4 spinal cord of 30 weeks old non-transgenic (G) and G93A-SOD1 mice (H and I). Hsp70-immunoreactivity is associated with a small number of ill-appearing motoneurons. Note the flattened nucleus in the Hsp70 immunoreactive neuron. Calibration bars: A and C, 100 µm; I, 15 µm.

5.4.6   A subset of ATF3 and phospho-c-Jun positive motoneurons is immunoreactive for CHOP/Gadd153

The C/EBP homologous protein CHOP, also named Gadd153, is a stress transcription factor [50] whose expression depends on the presence of ATF3 after specific stress stimuli [23,32]. Double-labeling immunofluorescence showed that a subset of ATF3 labeled motoneurons (15 of 50) also was immunoreactive for CHOP (Fig. 5j). Vice versa, random selection of CHOP-labeled cells showed that nearly all (24 of 25) CHOP-labeled motoneurons were positive for ATF3. The majority of ATF3/CHOP double-labeled motoneurons (11 of 15) showed an ill appearance (Fig. 5j). However, a number of ill-appearing motoneurons were not immunoreactive for CHOP.

5.5   Discussion

The availability of transgenic SOD1-ALS mice that develop an ALS-like motoneuron disease enables the detailed characterization of the morphological and molecular correlates of motoneuron degeneration in ALS. Several studies have uncovered the recruitment of programmed cell death pathways in these mice [21,28,35], but the precise morphological and molecular correlates preceding the death of motoneurons are still incompletely understood. In this study we have used phosphorylated c-Jun and ATF3 to label motoneurons in an early phase of their degeneration in a line of SOD1-ALS mice carrying the G93A mutations. We found that 1) ATF3 and phospho-c-Jun are expressed in a subset of motoneurons starting from several weeks prior to the onset of their death. 2) The number of phospho-c-Jun/ATF3-labeled motoneurons increased with aging and was highest at symptom onset. 3) The morphology of phospho-c-Jun/ATF3 labeled motoneurons varied from normal appearing cells to cells with an ill morphology, but none of the phospho-c-Jun/ATF3 labeled motoneurons showed the expression of active caspase 3, a major neuronal executioner caspase. 4) All phospho-c-Jun/ATF3-labeled motoneurons showed a fragmented Golgi apparatus. 5) The onset of phospho-c-Jun and ATF3 expression in motoneurons did not correlate with the onset of mitochondrial swelling and vacuolization which is the earliest pathological feature in G93A-SOD1 mice, but correlated with the appearance of ubiquitin immunoreactivity in dendrites and perikarya of motoneurons. 6) Phospho-c-Jun and ATF3 are also expressed in spinal interneurons, but in a later phase of disease compared to motoneurons.

Do ATF3 and phospho-c-Jun have an effect on the viability of motoneurons? ATF3 and phospho-c-Jun are well known for their activation after injurious stimuli, and both have been linked to either survival or death. The effect of their activation is variable and depends on the promotor and cellular contexts [23,24,26]. C-Jun is a component of the heterodimeric AP-1 transcription factor and has been identified as an important factor in inducing neuronal degeneration after trophic factor deprivation [25,52]. However, its role in adult neurons is ambiguous [7,27]. The ATF3 homodimer acts as a transcriptional repressor, but the ATF3 heterodimer

with c-Jun (or JunD) functions as a transcriptional activator of specific promoters containing CRE sites. Other bZip proteins that dimerize with ATF3 include ATF2, JunB, and CHOP (also named Gadd153)[23,24]. Recently, it has been shown that ATF3 rescues PC12 cells and superior ganglion cells from c-Jun-activated cell death by promoting Hsp27 expression, and that Hsp27 is a target gene of c-Jun/ATF3 heterodimers [46]. However, there is a poor correlation between phospho-c-Jun/ATF3 and Hsp27 expression in motoneurons of G93A-SOD1 mice [42]. ATF3 under specific conditions may contribute to the induction of the expression of CHOP [32], a stress transcription factor that has been predominantly linked to ER stress and that may promote cell death [50]. We have found that a subset of phospho-c-Jun and ATF3 immunoreactive motoneurons also expresses CHOP, and that the CHOP-positive cells predominantly showed a rather ill appearance. These data raise the possibility that the effect of ATF3 and phospho-c-Jun in motoneurons changes throughout the degeneration process of an individual motoneuron as a consequence of changes in the cellular context throughout this process. In other words the effect may shift from a beneficial role in relatively healthy motoneurons to a cell death promoting role in ill cells. Systematic analysis of the expression of interacting transcription factors and potential target genes is needed to support this possibility. In addition, crossing G93A-SOD1 mice in mice deficient in specific transcription factors may help to clarify the role of phospho-c-Jun and ATF3.

What induces phosphorylated c-Jun and ATF3 expression in motoneurons in G93A-SOD1 mice? The transcriptional activity of c-Jun is controlled by the c-Jun-N-terminal kinase (JNK) pathways, a subgroup of mitogen activated protein kinases (MAPKs) that integrate various intra- and extracellular signals [15,27]. Once activated, c-Jun may positively autoregulate its expression. The c-Jun/JNK-pathway also may trigger ATF3 expression since many of the insults that activate the c-Jun/JNK pathways also induce ATF3, and the ATF3 promotor contains potential AP1 binding sites for c-Jun [24]. Our data indicate that the motoneurons that express phospho-c-Jun and ATF3 represent the same population of cells that show Golgi fragmentation i.e. the transformation of the Golgi apparatus from a network of linear profiles to dispersed smaller elements forming ministacks. This indicates that ATF3 and phospho-c-Jun expression are linked to Golgi fragmentation. Golgi fragmentation has been previously identified in a subset of motoneurons and Betz cells of patients with ALS and other motoneuron disorders [55] and in motoneurons in SOD1-ALS mice [45], but also occurs in some neurons in other neurodegenerative diseases [19]. The mechanism underlying Golgi fragmentation is not yet understood. It differs from Golgi fragmentation as observed after blocking the secretory pathway by brefeldin, but shows similarity with Golgi fragmentation induced by microtubule destabilization [45]. One hypothesis is that Golgi fragmentation is caused by abnormalities in trafficking between Golgi and other membrane compartments [45,56], possibly because of the presence of aggregated protein complexes that may impair dynein trafficking [20,33]. Abnormal trafficking also may explain our observation that motoneurons with fragmented Golgi show an abnormal dendritic accumulation of CGRP.

Our data also indicate that induction of phospho-c-Jun and ATF3 (and Golgi fragmentation) is shortly preceded by the appearance of ubiquitin immunoreactivity

in the proximal dendrites. This is consistent with previous studies showing a correlation between fragmented Golgi apparatus and deposits of ubiquitinated protein in motoneurons of ALS patients [55] and SOD1-ALS mice [56]. These data indicate that Golgi fragmentation and ATF3 and phospho-c-Jun expression are downstream of the accumulation of ubiquitin immunoreactivity. Ubiquitin is a small polypeptide that is enzymatically conjugated to misfolded and denatured proteins to target them for degradation by the proteasome proteolytic complex (see chapter 1, box1). The accumulation of ubiquitin immunoreactivity in neurons has been linked to the presence of aggregates of misfolded protein that can not be effectively degraded by the proteasome [38]. Accordingly, the ubiquitinated structures in SOD1-ALS mice were strongly immunoreactive for mutant SOD1 indicating that they represent ensembles of aggregated SOD1 [8,42,56]. However, ubiquitination may not exclusively represent SOD1 aggregates, because a study in chimeric SOD1-ALS mice that expressed mutant SOD1 in a subset of their motoneurons, showed that accumulation of ubiquitin immunoreactivity also occurred in motoneurons that did not express mutant SOD1 [12]. Hence, ubiquitination may represent a feature associated with degeneration of motoneurons, putatively representing a mix of denatured proteins derived from the collapsing cytoplasm. This may explain our ultrastructural data showing that dendritic ubiquitination is associated with heterogeneous ensembles of filamentous, amorphous and vesicular material, rather than with a single type of aggregate. Our data also show that the accumulation of ubiquitinated material is a progressive process that gradually fills the entire cell and eventually 'pushes away' the Golgi and the ER into a small, usually juxtanuclear portion of the cell. This accumulation of ubiquitinated material in the end also seems to lead to impaired proteasome function, because the motoneurons that were entirely filled with ubiquitin also expressed Hsp70, which in motoneurons has been found to be selectively upregulated after proteasome inhibition and not after other injurious stimuli [4]. Significantly, recently it has been shown that the level of phospho-c-Jun depends on ubiquitination and degradation by the proteasome [48]. Also, ATF3 has been shown to be strongly up regulated after proteasome inhibition [67], raising the possibility that ATF3 and phospho-c-Jun expression result from impaired proteasome function. However, this scenario is not consistent with our observation that Hsp70 is only expressed in a subset of ATF3 and phospho-c-Jun positive motoneurons, indicating that impaired proteasome function occurs after the onset of ATF3 and phospho-c-Jun expression.

How do motoneurons in G93A-SOD1 mice die? Our data are consistent with previous reports suggesting that the motoneurons ultimately die through the activation of programmed cell death pathways [21,28,35]. However, the activation of caspase 3 (a dominant final executioner caspase in neurons) within a single motoneuron is delayed until they reach a very ill appearance. These ill motoneurons are large in size, have an eccentric flattened nucleus, and have a perikaryon filled with ubiquitinated material, with the exception of a small juxtanuclear area containing the Golgi and the ER. This morphology differs from the morphology of motoneurons in acute *in vivo* models of apoptotic and non-apoptotic motoneuron death [36,49,57]. It seems unlikely that these ill

motoneurons are still functional. Whether the ill motoneurons are irreversibly damaged or still can be rescued is an open question.

In conclusion, the present study provides a description of a series of changes in motoneuron death preceding their death and disappearance in a line of SOD1-ALS mice. The data provide a framework to further examine the mechanisms underlying the degeneration of motoneurons in ALS. Importantly, we show that ATF3 and phospho-c-Jun are effective markers to identify motoneurons in an early phase of their degeneration. Questions raised by our data include: 1) How are early mitochondrial abnormalities in motoneurons of SOD1-ALS mice [14,31,37,40,65] related to the further degeneration of motoneurons? Significantly, our data show that mitochondria surrounding ubiquitinated areas in dendrites are normal, whereas swollen and vacuolated mitochondria occur more distally and in the axon. One possibility is that ubiquitination follows from collapse of distal dendrites due to mitochondrial pathology. 2) What mechanism causes dendritic and somatic ubiquitination? 3) How are the neurodegenerative changes in the somato-dendritic domain, as depicted in the present study, related to the functional deterioration and degeneration of the axon? A number of studies have suggested that the axon is the primary target of mutant SOD1 since transport abnormalities and degeneration of the axon and its terminals are early phenomena in SOD1-ALS mice [6,16-18,64,66]. Preliminary analysis of muscle denervation in our G93A-SOD1 mice showed no signs of denervation at 15 weeks of age, and mild denervation at 20 weeks of age, indicating that denervation coincides with or occurs after the onset of ubiquitination and ATF3/phospho-c-jun expression. Significantly, the 'axon first'-hypothesis of mutant SOD1-mediated motoneuron degeneration has been challenged by the recent demonstration that expression of Wlds, which is an axon-protective protein which attenuates the course of disease in axon-first motoneuron diseases [2], does not influence motoneuron loss in SOD1-ALS mice [61]. 4) How are changes in c-Jun and ATF3 signaling related to other signaling events identified in motoneurons and surrounding glia in SOD1-ALS mice [9]? 5) To what extend is the sequence of events identified in our study reproduced in human ALS motoneurons? In accord with our data c-Jun activation has been identified in post-mortem ALS spinal cord specimen [62]. However, unfortunately, so far we have been unsuccessful in obtaining reliable phospho-c-Jun and ATF3 staining in human tissue.

References

[1]	P.M. Andersen, K.B. Sims, W.W. Xin, R. Kiely, G. O'Neill, J. Ravits, E. Pioro, Y. Harati, R.D. Brower, J.S. Levine, H.U. Heinicke, W. Seltzer, M. Boss, R.H. Brown, Jr., Sixteen novel mutations in the Cu/Zn superoxide dismutase gene in amyotrophic lateral sclerosis: a decade of discoveries, defects and disputes, Amyotroph Lateral Scler Other Motor Neuron Disord 4 (2003) 62-73.
[2]	T. Araki, Y. Sasaki, J. Milbrandt, Increased nuclear NAD biosynthesis and SIRT1 activation prevent axonal degeneration, Science 305 (2004) 1010-1013.
[3]	U. Arvidsson, F. Piehl, H. Johnson, B. Ulfhake, S. Cullheim, T. Hokfelt, The peptidergic motoneurone, Neuroreport 4 (1993) 849-856.
[4]	Z. Batulan, G.A. Shinder, S. Minotti, B.P. He, M.M. Doroudchi, J. Nalbantoglu, M.J. Strong, H.D. Durham, High threshold for induction of the stress response in motor neurons is associated with failure to activate HSF1, J Neurosci 23 (2003) 5789-5798.
[5]	A. Behrens, M. Sibilia, E.F. Wagner, Amino-terminal phosphorylation of c-Jun regulates stress-induced apoptosis and cellular proliferation, Nat Genet 21 (1999) 326-329.
[6]	D.R. Borchelt, P.C. Wong, M.W. Becher, C.A. Pardo, M.K. Lee, Z.S. Xu, G. Thinakaran, N.A. Jenkins, N.G. Copeland, S.S. Sisodia, D.W. Cleveland, D.L. Price, P.N. Hoffman, Axonal transport of mutant superoxide dismutase 1 and focal axonal abnormalities in the proximal axons of transgenic mice, Neurobiol Dis 5 (1998) 27-35.
[7]	S. Brecht, R. Kirchhof, A. Chromik, M. Willesen, T. Nicolaus, G. Raivich, J. Wessig, V. Waetzig, M. Goetz, M. Claussen, D. Pearse, C.Y. Kuan, E. Vaudano, A. Behrens, E. Wagner, R.A. Flavell, R.J. Davis, T. Herdegen, Specific pathophysiological functions of JNK isoforms in the brain, Eur J Neurosci 21 (2005) 363-377.
[8]	L.I. Bruijn, M.K. Houseweart, S. Kato, K.L. Anderson, S.D. Anderson, E. Ohama, A.G. Reaume, R.W. Scott, D.W. Cleveland, Aggregation and Motor Neuron Toxicity of an ALS-Linked SOD1 Mutant Independent from Wild-Type SOD1, Science 281 (1998) 1851-1854.
[9]	L.I. Bruijn, T.M. Miller, D.W. Cleveland, Unraveling the mechanisms involved in motor neuron degeneration in ALS, Annu Rev Neurosci 27 (2004) 723-749.
[10]	J. Caldero, A. Casanovas, A. Sorribas, J.E. Esquerda, Calcitonin gene-related peptide in rat spinal cord motoneurons: subcellular distribution and changes induced by axotomy, Neuroscience 48 (1992) 449-461.
[11]	A. Ciechanover, P. Brundin, The ubiquitin proteasome system in neurodegenerative diseases: sometimes the chicken, sometimes the egg, Neuron 40 (2003) 427-446.
[12]	A.M. Clement, M.D. Nguyen, E.A. Roberts, M.L. Garcia, S. Boillee, M. Rule, A.P. McMahon, W. Doucette, D. Siwek, R.J. Ferrante, R.H. Brown, Jr., J.P. Julien, L.S. Goldstein, D.W. Cleveland, Wild-type nonneuronal cells extend survival of SOD1 mutant motor neurons in ALS mice, Science 302 (2003) 113-117.
[13]	M. Costigan, R.J. Mannion, G. Kendall, S.E. Lewis, J.A. Campagna, R.E. Coggeshall, J. Meridith-Middleton, S. Tate, C.J. Woolf, Heat shock protein 27: developmental regulation and expression after peripheral nerve injury, J Neurosci 18 (1998) 5891-5900.
[14]	M.C. Dal Canto, M.E. Gurney, Neuropathological changes in two lines of mice carrying a transgene for mutant human Cu,Zn SOD, and in mice overexpressing wild type human SOD: a model of familial amyotrophic lateral sclerosis (FALS), Brain Res 676 (1995) 25-40.
[15]	R.J. Davis, Signal transduction by the JNK group of MAP kinases, Cell 103 (2000) 239-252.
[16]	L. Dupuis, M. de Tapia, F. Rene, B. Lutz-Bucher, J.W. Gordon, L. Mercken, L. Pradier, J.P. Loeffler, Differential screening of mutated SOD1 transgenic mice reveals early up-regulation of a fast axonal transport component in spinal cord motor neurons, Neurobiol Dis 7 (2000) 274-285.
[17]	L.R. Fischer, D.G. Culver, P. Tennant, A.A. Davis, M. Wang, A. Castellano-Sanchez, J. Khan, M.A. Polak, J.D. Glass, Amyotrophic lateral sclerosis is a distal axonopathy: evidence in mice and man, Exp Neurol 185 (2004) 232-240.
[18]	D. Frey, C. Schneider, L. Xu, J. Borg, W. Spooren, P. Caroni, Early and selective loss of neuromuscular synapse subtypes with low sprouting competence in motoneuron diseases, J Neurosci 20 (2000) 2534-2542.
[19]	N.K. Gonatas, J.O. Gonatas, A. Stieber, The involvement of the Golgi apparatus in the pathogenesis of amyotrophic lateral sclerosis, Alzheimer's disease, and ricin intoxication, Histochem Cell Biol 109 (1998) 591-600.
[20]	N. Gosavi, H.J. Lee, J.S. Lee, S. Patel, S.J. Lee, Golgi fragmentation occurs in the cells with prefibrillar alpha-synuclein aggregates and precedes the formation of fibrillar inclusion, J Biol Chem 277 (2002) 48984-48992.

[21]   C. Guegan, S. Przedborski, Programmed cell death in amyotrophic lateral sclerosis, J Clin Invest 111 (2003) 153-161.
[22]   M.E. Gurney, The use of transgenic mouse models of amyotrophic lateral sclerosis in preclinical drug studies, J Neurol Sci 152 (1997) S67-S73.
[23]   T. Hai, M.G. Hartman, The molecular biology and nomenclature of the activating transcription factor/cAMP responsive element binding family of transcription factors: activating transcription factor proteins and homeostasis, Gene 273 (2001) 1-11.
[24]   T. Hai, C.D. Wolfgang, D.K. Marsee, A.E. Allen, U. Sivaprasad, ATF3 and stress responses, Gene Expr 7 (1999) 321-335.
[25]   J. Ham, A. Eilers, J. Whitfield, S.J. Neame, B. Shah, c-Jun and the transcriptional control of neuronal apoptosis, Biochem Pharmacol 60 (2000) 1015-1021.
[26]   T. Herdegen, J.D. Leah, Inducible and constitutive transcription factors in the mammalian nervous system: control of gene expression by Jun, Fos and Krox, and CREB/ATF proteins, Brain Res Brain Res Rev 28 (1998) 370-490.
[27]   T. Herdegen, V. Waetzig, AP-1 proteins in the adult brain: facts and fiction about effectors of neuroprotection and neurodegeneration, Oncogene 20 (2001) 2424-2437.
[28]   H. Inoue, K. Tsukita, T. Iwasato, Y. Suzuki, M. Tomioka, M. Tateno, M. Nagao, A. Kawata, T.C. Saido, M. Miura, H. Misawa, S. Itohara, R. Takahashi, The crucial role of caspase-9 in the disease progression of a transgenic ALS mouse model, Embo J 22 (2003) 6665-6674.
[29]   D. Jaarsma, E. Haasdijk, J.A.C. Grashorn, W. Van Duijn, H. Verspaget, J. London, J.C. Holstege, Cu/Zn superoxide dismutase (SOD1) overexpression in mice causes mitochondrial degeneration, axonal degeneration and premature motoneuron death, and accelerates the development of motoneuron disease in mice expressing fALS-mutant SOD1., Neurobiol. Dis. 7 (2000) 623-643.
[30]   D. Jaarsma, J.C. Holstege, D. Troost, M. Davis, J. Kennis, E.D. Haasdijk, V.J. de Jong, Induction of c-Jun immunoreactivity in spinal cord and brainstem neurons in a transgenic mouse model for amyotrophic lateral sclerosis, Neurosci Lett 219 (1996) 179-182.
[31]   D. Jaarsma, F. Rognoni, W. Van Duijn, H. Verspaget, E.D. Haasdijk, J.C. Holstege, CuZn superoxide dismutase (SOD1) accumulate in vacuolated mitochondria in transgenic mice expressing amyotrophic lateral sclerosis (ALS)-linked SOD1 mutations, Acta Neuropathol. 102 (2001) 293-305.
[32]   H.Y. Jiang, S.A. Wek, B.C. McGrath, D. Lu, T. Hai, H.P. Harding, X. Wang, D. Ron, D.R. Cavener, R.C. Wek, Activating transcription factor 3 is integral to the eukaryotic initiation factor 2 kinase stress response, Mol Cell Biol 24 (2004) 1365-1377.
[33]   J.A. Johnston, M.J. Dalton, M.E. Gurney, R.R. Kopito, Formation of high molecular weight complexes of mutant Cu, Zn- superoxide dismutase in a mouse model for familial amyotrophic lateral sclerosis, Proc Natl Acad Sci U S A 97 (2000) 12571-12576.
[34]   P.A. Jonsson, K. Ernhill, P.M. Andersen, D. Bergemalm, T. Brannstrom, O. Gredal, P. Nilsson, S.L. Marklund, Minute quantities of misfolded mutant superoxide dismutase-1 cause amyotrophic lateral sclerosis, Brain 127 (2004) 73-88.
[35]   S.J. Kang, I. Sanchez, N. Jing, J. Yuan, Dissociation between neurodegeneration and caspase-11-mediated activation of caspase-1 and caspase-3 in a mouse model of amyotrophic lateral sclerosis, J Neurosci 23 (2003) 5455-5460.
[36]   V.E. Koliatsos, W.L. Price, C.A. Pardo, D.L. Price, Ventral root avulsion: an experimental model of death of adult motor neurons [published erratum appears in J Comp Neurol 1994 Jun 1;344(1):160], J Comp Neurol 342 (1994) 35-44.
[37]   J. Kong, Z. Xu, Massive mitochondrial degeneration in motor neurons triggers the onset of amyotrophic lateral sclerosis in mice expressing a mutant SOD1, J Neurosci 18 (1998) 3241-3250.
[38]   R.R. Kopito, Aggresomes, inclusion bodies and protein aggregation, Trends Cell Biol 10 (2000) 524-530.
[39]   N. Lee, K.L. Neitzel, B.K. Devlin, A.J. MacLennan, STAT3 phosphorylation in injured axons before sensory and motor neuron nuclei: potential role for STAT3 as a retrograde signaling transcription factor, J Comp Neurol 474 (2004) 535-545.
[40]   J. Liu, C. Lillo, P.A. Jonsson, C. Vande Velde, C.M. Ward, T.M. Miller, J.R. Subramaniam, J.D. Rothstein, S. Marklund, P.M. Andersen, T. Brannstrom, O. Gredal, P.C. Wong, D.S. Williams, D.W. Cleveland, Toxicity of familial ALS-linked SOD1 mutants from selective recruitment to spinal mitochondria, Neuron 43 (2004) 5-17.
[41]   T.J. Lyons, E.B. Gralla, J.S. Valentine, Biological chemistry of copper-zinc superoxide dismutase and its link to amyotrophic lateral sclerosis, Met Ions Biol Syst 36 (1999) 125-177.

[42]   A. Maatkamp, A. Vlug, E. Haasdijk, D. Troost, P.J. French, D. Jaarsma, Decrease of Hsp25 protein expression precedes degeneration of motoneurons in ALS-SOD1 mice, Eur J Neurosci 20 (2004) 14-28.

[43]   M.H. Mohajeri, D.A. Figlewicz, M.C. Bohn, Selective Loss of alpha Motoneurons Innervating the Medial Gastrocnemius Muscle in a Mouse Model of Amyotrophic Lateral Sclerosis, Exp Neurol 150 (1998) 329-336.

[44]   L.B. Moran, M.B. Graeber, The facial nerve axotomy model, Brain Res Brain Res Rev 44 (2004) 154-178.

[45]   Z. Mourelatos, N.K. Gonatas, A. Stieber, M.E. Gurney, M.C. Dal Canto, The Golgi apparatus of spinal cord motor neurons in transgenic mice expressing mutant Cu,Zn superoxide dismutase becomes fragmented in early, preclinical stages of the disease, Proc Natl Acad Sci U S A 93 (1996) 5472-5477.

[46]   S. Nakagomi, Y. Suzuki, K. Namikawa, S. Kiryu-Seo, H. Kiyama, Expression of the activating transcription factor 3 prevents c-Jun N-terminal kinase-induced neuronal death by promoting heat shock protein 27 expression and Akt activation, J Neurosci 23 (2003) 5187-5196.

[47]   N. Nakamura, C. Rabouille, R. Watson, T. Nilsson, N. Hui, P. Slusarewicz, T.E. Kreis, G. Warren, Characterization of a cis-Golgi matrix protein, GM130, J Cell Biol 131 (1995) 1715-1726.

[48]   A.S. Nateri, L. Riera-Sans, C. Da Costa, A. Behrens, The ubiquitin ligase SCFFbw7 antagonizes apoptotic JNK signaling, Science 303 (2004) 1374-1378.

[49]   R.W. Oppenheim, R.A. Flavell, S. Vinsant, D. Prevette, C.Y. Kuan, P. Rakic, Programmed cell death of developing mammalian neurons after genetic deletion of caspases, J Neurosci 21 (2001) 4752-4760.

[50]   S. Oyadomari, M. Mori, Roles of CHOP/GADD153 in endoplasmic reticulum stress, Cell Death Differ 11 (2004) 381-389.

[51]   P. Pasinelli, M.K. Houseweart, R.H. Brown, Jr., D.W. Cleveland, Caspase-1 and -3 are sequentially activated in motor neuron death in Cu,Zn superoxide dismutase-mediated familial amyotrophic lateral sclerosis, Proc Natl Acad Sci U S A 97 (2000) 13901-13906.

[52]   G. Raivich, M. Bohatschek, C. Da Costa, O. Iwata, M. Galiano, M. Hristova, A.S. Nateri, M. Makwana, L. Riera-Sans, D.P. Wolfer, H.P. Lipp, A. Aguzzi, E.F. Wagner, A. Behrens, The AP-1 transcription factor c-Jun is required for efficient axonal regeneration, Neuron 43 (2004) 57-67.

[53]   M.Y. Sherman, A.L. Goldberg, Cellular defenses against unfolded proteins: a cell biologist thinks about neurodegenerative diseases, Neuron 29 (2001) 15-32.

[54]   H.G. Stewart, P.M. Andersen, P.A. Jonsson, S.L. Marklund, Disproportionate sub-fractions of hydrophobic, disulfide-reduced SOD1 in the central nervous system of murine transgenic models of amyotrophic lateral sclerosis., Soc. Neuroscience Abstr. 34 (2004) 134.137.

[55]   A. Stieber, Y. Chen, S. Wei, Z. Mourelatos, J. Gonatas, K. Okamoto, N.K. Gonatas, The fragmented neuronal Golgi apparatus in amyotrophic lateral sclerosis includes the trans-Golgi-network: functional implications, Acta Neuropathol (Berl) 95 (1998) 245-253.

[56]   A. Stieber, J.O. Gonatas, N.K. Gonatas, Aggregation of ubiquitin and a mutant ALS-linked SOD1 protein correlate with disease progression and fragmentation of the Golgi apparatus, J Neurol Sci 173 (2000) 53-62.

[57]   O. Tarabal, J. Caldero, J. Llado, R.W. Oppenheim, J.E. Esquerda, Long-lasting aberrant tubulovesicular membrane inclusions accumulate in developing motoneurons after a sublethal excitotoxic insult: a possible model for neuronal pathology in neurodegenerative disease, J Neurosci 21 (2001) 8072-8081.

[58]   A. Tiwari, L.J. Hayward, Familial amyotrophic lateral sclerosis mutants of copper/zinc superoxide dismutase are susceptible to disulfide reduction, J Biol Chem 278 (2003) 5984-5992.

[59]   H. Tsujino, E. Kondo, T. Fukuoka, Y. Dai, A. Tokunaga, K. Miki, K. Yonenobu, T. Ochi, K. Noguchi, Activating transcription factor 3 (ATF3) induction by axotomy in sensory and motoneurons: A novel neuronal marker of nerve injury, Mol Cell Neurosci 15 (2000) 170-182.

[60]   J.S. Valentine, P.J. Hart, Misfolded CuZnSOD and amyotrophic lateral sclerosis, Proc Natl Acad Sci U S A 100 (2003) 3617-3622.

[61]   C.V. Velde, M.L. Garcia, X. Yin, B.D. Trapp, D.W. Cleveland, The Neuroprotective Factor Wlds Does Not Attenuate Mutant SOD1-Mediated Motor Neuron Disease, Neuromolecular Med 5 (2004) 193-204.

[62]   L. Virgo, J. de Belleroche, Induction of the immediate early gene c-jun in human spinal cord in amyotrophic lateral sclerosis with concomitant loss of NMDA receptor NR-1 and glycine transporter mRNA, Brain Res 676 (1995) 196-204.

[63]   J. Wang, G. Xu, D.R. Borchelt, High molecular weight complexes of mutant superoxide dismutase 1: age-dependent and tissue-specific accumulation, Neurobiol Dis 9 (2002) 139-148.

[64]   T.L. Williamson, D.W. Cleveland, Slowing of axonal transport is a very early event in the toxicity of ALS-linked SOD1 mutants to motor neurons, Nat Neurosci 2 (1999) 50-56.
[65]   P.C. Wong, C.A. Pardo, D.R. Borchelt, M.K. Lee, N.G. Copeland, N.A. Jenkins, S.S. Sisodia, D.W. Cleveland, D.L. Price, An adverse property of a familial ALS-linked SOD1 mutation causes motor neuron disease characterized by vacuolar degeneration of mitochondria, Neuron 14 (1995) 1105-1116.
[66]   B. Zhang, P. Tu, F. Abtahian, J.Q. Trojanowski, V.M. Lee, Neurofilaments and orthograde transport are reduced in ventral root axons of transgenic mice that express human SOD1 with a G93A mutation, J Cell Biol 139 (1997) 1307-1315.
[67]   J. Zimmermann, D. Erdmann, I. Lalande, R. Grossenbacher, M. Noorani, P. Furst, Proteasome inhibitor induced gene expression profiles reveal overexpression of transcriptional regulators ATF3, GADD153 and MAD1, Oncogene 19 (2000) 2913-2920.

Chapter 6

GENERAL DISCUSSION

6.1 Discussion

The overall aim of the studies in this thesis was to obtain greater understanding about the pathogenesis of ALS focusing on the role of oxidative and misfolded protein stress. A dominant approach has been the detailed analysis of what happens in the spinal cord of SOD1-ALS mice prior and during the development of muscle weakness. This approach, which might be termed molecular neuropathology, is an invaluable complement of interventional approaches enabling the proper interpretation of these data. As discussed in this chapter the main conclusions from the studies of this thesis are the following:

- Nitro-oxidative damage of protein bound or free tyrosine residues does not contribute to the pathogenesis of SOD1-linked ALS (chapter 2).

- Motoneurons in SOD1-ALS mice may experience a deficient proteasome function in a late phase of their degeneration (chapter 5). The selective vulnerability of motoneurons towards mutant SOD1 can not be explained by an increased sensitivity to proteasome inhibition (chapter 3).

- Mutant SOD1 decreases the availability of a major heat shock protein in motoneurons of SOD1-ALS mice (chapter 4).

- Degeneration of motoneurons of SOD1-ALS mice is characterized by an ordered sequence of events that starts with activation of the injury transcription factors ATF3 and c-Jun (chapter 5).
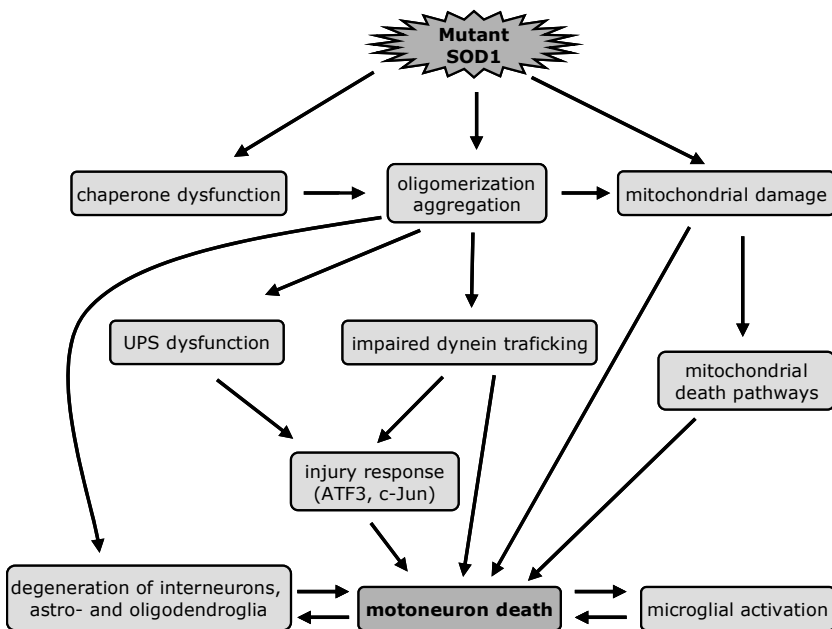

Figure 1: Summary of potential events contributing to motoneuron degeneration caused by mutant SOD1. (UPS, ubiquitin-proteasome system)

- Execution of programmed cell death by caspase 3 is a very late event that only operates in very sick ghost-like motoneurons (chapter 5).

- The mechanism by which mutant SOD1 triggers the functional deterioration and degeneration of motoneurons remains to be determined. Potential contributing events are summarized in Fig. 1.

6.1 The role of oxidative stress in ALS: what is the evidence?

The accumulation of oxidative stress mediated damage has been implicated in multiple age-related disorders. Accordingly, it has long been suspected that oxidative stress contributes to the lesions of ALS. However, precise knowledge about which toxic reactive oxygen (ROS) or nitrogen (RNS) species are involved, their source, their target molecules, and why they selectively afflict motoneurons has been lacking [19,33,54 ,85] (chapter 1). The source of ROS and RNS has been attributed to leakage from the electron-transport chain of mitochondria, and more recently to activated microglia, that can generate large numbers of superoxide ions on their external membranes, from which they are released into the surrounding area. Other, less abundant sources of free radicals are cytosolic enzymes like xanthine oxidase and nitric oxide synthase [19,33,54 ,85].

The identification of SOD1 mutations has stimulated oxidative stress hypotheses of ALS, since it enabled to formulate specific routes of ROS and RNS production. Multiple gained catalytic copper-mediated toxic activities yielding highly toxic ROS and RNS species have been reported for mutant SOD1, which, since SOD1 is an abundant protein, may have an significant impact on the cell [18,34,54,91]. These gained catalytic properties result from improper shielding of the catalytic copper because of conformational changes and altered zinc binding. To explain the selective vulnerability of motoneurons, the 'gain of toxic oxidative function' hypotheses have zoomed in on specific target molecules such as the glial glutamate transporter, cytoskeletal proteins, and mitochondrial membranes [18,34,54,91]. However the idea of a toxic oxidative action of mutant SOD1 as a primary disease mechanism has been controversial for several reasons. First, any specific gained catalytic activity is difficult to reconcile with the great structural and functional diversity of SOD1 mutants (see chapter 1). Second, studies in SOD1-ALS mice have shown that mutant SOD1 toxicity is not influenced by copper loading (see chapter 1). Third, antioxidant drugs like vitamin E, vitamin C, N-acetylcysteine, and selegeline so far have been found to be not or marginally effective in influencing the disease course in SOD1-ALS mice (Table 1) [13,56]. Similarly, anti-oxidant drugs also seem to be ineffective in sporadic and familial ALS patients [27,85]. However, this lack of effect has been attributed to the inability of the tested antioxidants to cope with local overloads of free radicals [19,33,54 ,85] and does not conclusively disqualify oxidative stress hypotheses. In addition to a direct toxic oxidative role of mutant SOD1, several alternative schemes involving oxidative stress mediated toxic activities in ALS pathogenesis have been put forward. For instance, oxidative stress may operate as a secondary phenomenon following microglia activation or after mitochondrial degeneration [19,33,54 ,85].

Evidence supporting a role of oxidative stress in ALS also came from various pathological studies, showing increased levels of molecular markers of free-radical attack in ALS spinal cord [19,33,54,85]. Increased expression in ALS tissue has been reported for 3-nitrotyrosine, a marker for damage left by nitric oxide-derived species, advanced glycation end products (AGEs) and a receptor for AGE, as well as for 4-hydroxy-2-nonenal-histidine and crotonaldehyde- lysine, two markers of lipid peroxidation, and pentosidine, a marker of protein glycooxidation [19,30,33,42,54 ,85].

6.1.1 Immunocytochemical detection of 3-nitrotyrosine in ALS: free or protein-bound?

Since cumulative damage left by nitric oxide-derived reactive species, in particular peroxynitrite (ONOO⁻), was strongly suspected to play a role in both mutant SOD1-linked and sporadic ALS, we have examined the distribution of 3-nitrotyrosine-immunoreactivity in the spinal cord of our G93A mice. 3-Nitrotyrosine is formed by a reaction between nitric oxide-derived reactive species and tyrosine, and has been widely used in neuropathological studies as a marker for damage left by nitric oxide-derived species [6,42]. More importantly, nitration of protein has been identified as a potential cause of aggregate formation. For instance, intracellular filamentous pathology in Parkinson's disease and Alzheimer's disease neurons contains nitrated α-synuclein and tau, respectively [40,50]. Recent studies have suggested that nitration of proteins may play a role in the formation of protein aggregates in the presence of mutant SOD1, and that SOD1 is a target for nitration itself [51]. Hence, the original aim of our analyses was to determine whether 3-nitrotyrosine immunoreactivity was associated with early subcellular abnormalities in our G93A-SOD1 mice that contain high levels of mutant SOD1, i.e. the swollen mitochondria and ubiquitinated dendrites [57]. The following results emerged from these investigations:

 1) The staining pattern obtained with two commonly used and commercially available 3-nitrotyrosine antibodies strongly depends on the type of fixation, and which antibody is used. These differences could, be explained, at least in part by their differential immunoreactivity with free (non-protein-bound) 3-nitrotyrosine in aldehyde fixed tissue. Both antibodies have been raised against nitrated-keyhole limpet hemocyanin (KLH) and have been shown to selectively bind to 3-nitrotyrosine in peptides and proteins [102]. Their specificity for 3-nitrotyrosine epitopes in tissue sections was firmly established, since the antibodies did not produce staining in sections in which 3-nitrotyrosine epitopes were chemically disrupted (see chapter 2). However, as explained in chapter 2 we noted that one of the antibodies (Ab06-284) immunoreacted with free 3-nitrotyrosine microinjected into the brain. This labeling strongly depended on aldehyde fixation suggesting that the antibody recognized 3-nitrotyrosine that is chemically cross-linked to proteins. The concentration of 3-nitrotyrosine recognized by the antibody is in the mid-nanomolar range, which is in the order of magnitude of the concentration of free 3-nitrotyrosine in murine CNS [42]. Since, the other antibody (Mab1A6) did not immunoreact with microinjected 3-nitrotyrosine, this antibody may be specific for protein-bound 3-nitrotyrosine epitopes. The differential affinity of Mab1A6 and

Ab06-284 for aldehyde-fixed free 3-nitrotyrosine may, at least in part, explain the multiple disagreements in the literature on the distribution of 3-nitrotyrosine-immunoreactivity in normal and diseased brain [42].

2) 3-Nitrotyrosine immunostaining patterns in control and G93A mouse spinal cord were different for Mab1A6 and Ab06-284: a diffuse increase in 3-nitrotyrosine immunoreactivity was observed with Ab06-284, whereas no changes as compared to control were observed with Mab1A6 (Fig. 2). Surprisingly, increased Ab06-284 labeling was only observed in pre-symptomatic G93A mice, and no consistent changes were observed in symptomatic mice (Fig. 2). Since Ab06-284 labels free 3-nitrotyrosine and Mab1A6 does not, a possible explanation for these results is that increased staining observed with Ab06-284 represents an increase in free 3-nitrotyrosine in presympromatic G93A mice. This would be consistent with neurochemical studies reporting increased free 3-nitrotyrosine in two lines of SOD1-ALS mice [11,37], but no change in protein-bound 3-nitrotyrosine levels have been consistently reported [11]. However, the data disagree with other
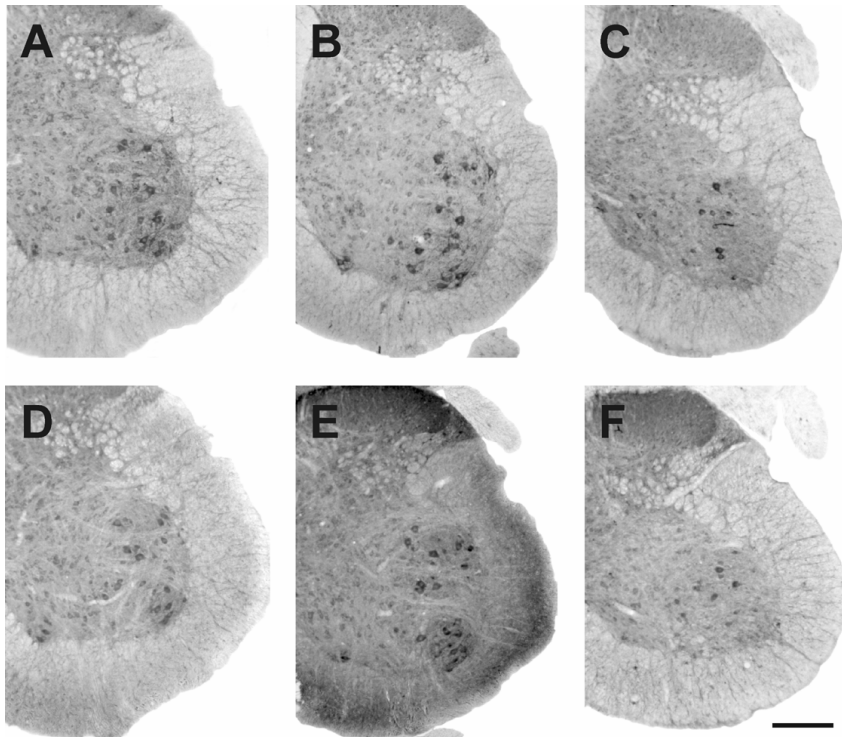
Figure 2: The pattern of 3-nitrotyrosine immunostaining in spinal cord of G93A-SOD1 mouse depends on which 3-nitrotyrosine antibody is used.

Photomicrographs of representative L4-spinal cord sections showing 3-nitrotyrosine labeled with Mab1A6 (A-C) or with Ab06-284 (D-F) in presymptomatic (18 weeks old; B, E) and symptomatic (32 weeks old; C, F) G93A-SOD1 mice and 34 weeks old non-transgenic mouse (A, D). Note, a diffuse elevation in 3-nitrotyrosine-immunostaining in the spinal cord of 18 week-old G93A-SOD1 mice stained with Ab06-284 (E) but not with Mab1A6 (B, H).No change in 3-nitrotyrosine labeling occurred in the spinal cord of symptomatic G93A-SOD1 mice. Scale bar in F = 200 µm.

studies using the same antibodies reporting increased 3-nitrotyrosine immunoreactivity in the spinal cord of symptomatic SOD1-ALS mice [14,37,60,92]. Remarkably, the latter studies disagreed on the cellular distribution of increased 3-nitrotyrosine labeling, in that increased labeling was found in glia [14], in neurons [60], or in both [37,92] independent of which of the two antibodies was used. The source of this variability is not clear, but it is unlikely that it results from non-specific staining since the specificity of 3-nitrotyrosine immunostaining can be reliably determined (see above). In conclusion, data on the distribution of 3-nitrotyrosine in spinal cord SOD1-ALS mice are remarkably variable. Our data indicate that G93A-SOD1 mice may experience a diffuse increase in free 3-nitrotyrosine concentration.

3) The light-microscopic data indicated that 3-nitrotyrosine immunoreactivity was not associated with abnormal mitochondria and ubiquitinated dendrites. The same results emerged from post-embedding immunogold immunocytochemistry. This method showed that 3-nitrotyrosine immunoreactivity in normal brain has a ubiquitous distribution, although the highest level of labeling consistently occurred in mitochondria (Fig. 3A, B). Swollen and vacuolated mitochondria showed a low level of 3-nitrotyrosine immunoreactivity (Fig. 3C) despite high levels of mutant
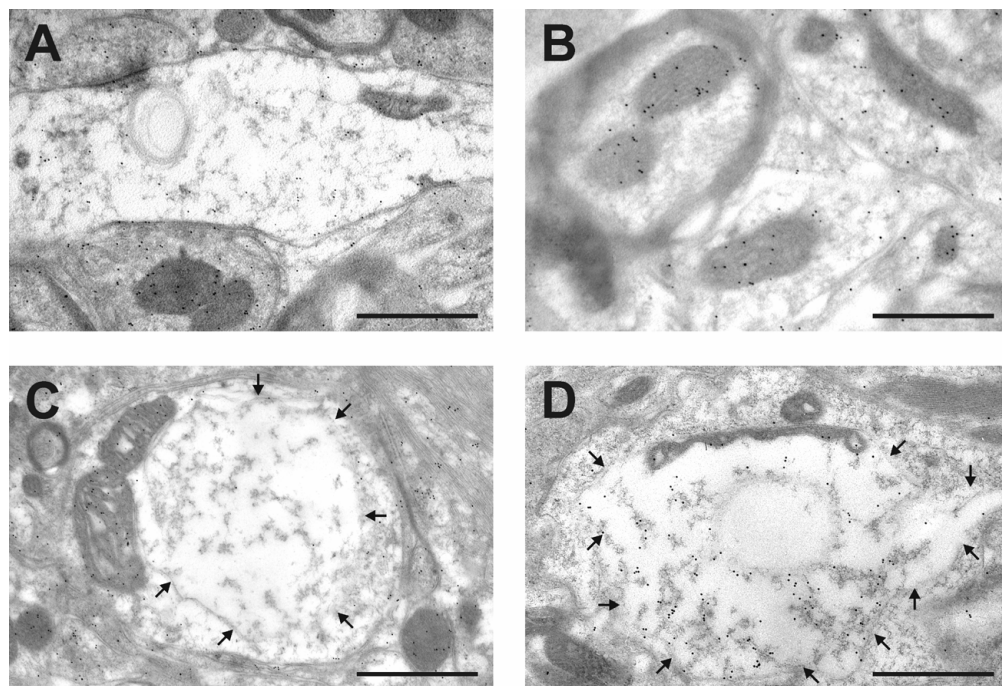
Fig.3. Vacuolated mitochondria in the spinal cord of G93A mice do not show increased 3-nitrotyrosine immunoreactivity.

Post-embedding immunogold immunoelectron microscopy of 3-nitrotyrosine labeling in the spinal cord ventral horn of 20 weeks old control (A, B) and G93A mice (C). In control spinal cord 3-nitrotyrosine labeling occurs in all structures but a higher labeling density can be seen in the mitochondria (A, B). 3-nitrotyrosine has the same subcellular distribution in G93A mouse spinal cord. Vacuolated mitochondria which are characterized by a high level of SOD1 immunoreactivity (D) do not show increased 3-nitrotyrosine labeling (C). Scale bars, 500 nm.

SOD1 ((Fig. 3D). In the same way ubiquitinated dendrites showed a low level of 3-nitrotyrosine immunoreactivity (not shown). This indicates that protein nitration is not a critical factor in the formation of these pathological structures. Accordingly, no increased 3-nitrotyrosine labeling did occur in ubiquitinated inclusions in another line of SOD1-ALS mice that carry the G85R mutation, and in Lewy body-like inclusions in familial ALS patients [63].

6.1.2   Is free 3-Nitrotyrosine neurotoxic?

Nitration of protein-linked tyrosine residues can disturb the function of proteins, because 3-nitrotyrosine is bulkier and more hydrophilic than tyrosine [42,94], and in addition may facilitate the aggregation of proteins [40,50]. It has been proposed that also free 3-nitrotyrosine may affect the function of some proteins. For instance, it can be post-translationaly incorporated in α-tubulin and hence affect microtubule dynamics [31]. Recent data have suggested that free 3-nitrotyrosine may cause neuronal degeneration *in vitro* and *in vivo* [79,88]. Mihm et al. [79] have reported degeneration of nigral dopaminergic neurons 1 week after striatal 3-nitrotyrosine injections. However as discussed in chapter 2 we found no evidence for neurodegenerative changes in the striatum or the substantia nigra using a similar procedure. More importantly, also chronic intra-striatal administration of 3-nitrotyrosine via osmotic pumps did not result in any evidence of neurodegenerative changes in the nigro-striatal system. Peluffo et al. [88] showed that also motoneurons are vulnerable to 3-nitrotyrosine, since 50 to 100 µM of 3-nitrotyrosine induced apoptosis in the majority of neurons in isolated embryonic motoneuron culture [88]. Furthermore, increased levels of 3-nitrotyrosine also have been associated with excitotoxic motoneuronal degeneration [28,100]. However, we identified no effect of 3-nitrotyrosine on the viability of motoneurons in organotypic spinal cord culture (see chapter 2). The mismatch between our data and the results of Peluffo et al. [88] can at least in part be explained by the absence of glia in their culture system, which increases their vulnerability to multiple factors (see chapter 2). As discussed in chapter 2, our data enabled us to conclude that even at very high unphysiological doses (100-150 µM), 3-nitrotyrosine is not neurotoxic, and that mild increases in 3-nitrotyrosine concentration as observed in SOD1-ALS mouse spinal cord are unlikely to contribute to the disease.

6.2   The role of misfolded protein stress and protein aggregation in ALS: what can we learn from the SOD1-ALS mouse model?

The excessive formation and aggregation of misfolded proteins is regarded as dominant pathogenic factor in neurodegenerative diseases including ALS (see chapter 1). In ALS evidence supporting for protein aggregation predominantly came from the neuropathological identification of ubiquitinated inclusions in ALS motoneurons and glia. These inclusions, although diverse in structure are specific for ALS, and therefore have linked to its pathogenesis (chapter 1). The term 'inclusion bodies' has been applied to the intracellular foci into which aggregated proteins are sequestered in such amounts that they are visible by light microscopy, and usually are considered giant aggregates. There has been a recent awareness

that these giant aggregates usually are relatively harm-less to the cell, and may represent a protective response of the cell to sequester toxic stable oligomers of misfolded protein, also termed protoaggregates [4,15,69]. These macroaggregates appear in cells after transfection with mutant aggregate prone proteins or inhibition of the proteasome, and have been termed aggresomes [69]. Aggresomes are defined as inclusions located near the centrosome, predominantly containing aggregated (and usually ubiquitinated) proteins and surrounded by intermediate filaments [69]. The aggresomes serve as a temporary storage of aggregated proteins that are further disposed by an autophagosomal and lysosomal mechanisms [38,108]. The formation of aggresomes depends on dynein-dynactin dependent trafficking [69]. Recently, a histone deacetylase, HDAC6, has been identified as a protein that links polyubiquitinated protein complexes to dynactin [64].

It is now well established that SOD1 mutants under specific conditions represent aggregate prone proteins that form stable oligomeric complexes and aggregates *ex vivo*, in transfected cells, in SOD1-ALS mice and in ALS patients (see chapter 4) [32,58,59,96,101]. In cultured cells mutant SOD1 may accumulate in aggresomes and this process is accelerated after proteasome inhibition [58]. Interestingly, a high throughput analysis aimed at finding drugs that prevented the accumulation of mutant SOD1 into aggregates, yielded two histone deacetylase inhibitors that strongly inhibited HDAC6 function. Closer inspection showed that treatment with these inhibitors prevented aggresome formation and resulted in dispersed mini-aggregates [20]. This indicates that ubiquitinated SOD1 aggregates or protoaggregates may be recognized by HDAC6 and transported to the centrosome in healthy cells.

6.2.1   Aggregates: the role of insufficient proteasome function

Although there is substantial evidence suggesting that mutant SOD1 may afflict motoneurons via oligomerisation or aggregation, it is not known how, if indeed, it does so. It has been shown that protein aggregates can impair the ubiquitin-proteasome system by overloading the proteasome by undegradable aggregates, or because of saturation of molecular chaperones involved in proteasomal function. This inhibition could lead to further aggregate formation, creating a positive-feedback system [7]. Insufficient proteasome function has been identified as an important factor in Parkinson's disease, either because of an overload of misfolded protein trough oxidation or mutation, or because of genetic defects in components of the ubiquitin-proteasome system [16,77]. Accordingly, Lewy body inclusions, a frequent pathological feature in Parkinson's disease brain, have many features in common with aggresomes [78].

Is inhibition of the proteasome a mechanism that contributes to mutant SOD1 toxicity? Studies in cell lines showed that mutant SOD1s mildly decreased proteasome activity [2,51]. We have examined whether the expression of mutant SOD1 increased the vulnerability of motoneurons to prolonged proteasome inhibition. This study indicated that motoneurons expressing mutant SOD1 show the same sensitivity to proteasome inhibition as control motoneurons (chapter 3). These studies also showed that motoneurons were as sensitive to proteasome

inhibition as other spinal neurons. Hence, the selective vulnerability of motoneurons towards mutant SOD1 can not be explained by an increased sensitivity to proteasome inhibition (chapter 3).

A mild dysfunction of the proteasome also was found in the spinal cord of SOD1-ALS mice [61]. However, in this study it could not be determined whether impaired proteasome function Since Hsp70 expression is a signs of impaired proteasome function in motoneurons [5] we studied Hsp70 expression in our G93A mice. This study showed that Hsp70 is only expressed in a small subset of sick-appearing motoneurons, indicating that insufficient proteasome is a late event in the process of motoneuron degeneration (chapter 5).

6.2.2   What happens with chaperones in SOD1-ALS mice?

Molecular chaperones like heat shock proteins are an important part of the protein quality control machinery. They bind to unfolded, misfolded or denatured proteins and either help them refold or direct them to the ubiquitin-proteasome system [95]. It has been proposed that one way by which misfolded protein stress may affect the function of the cell is through overloading the capacity of the chaperone system, which on the one hand would facilitate aggregation of misfolded protein and on the other hand compromise normal function of the chaperones [95]. The inducible heat shock protein Hsp70 is one the main chaperones involved in protecting cells after denaturing conditions [95]. Accordingly, overexpression of Hsp70 has been found to be neuroprotective in various *in vitro* and *in vivo* models of neuronal degeneration [24,104,106], Pathological studies have not reported changes of Hsp70 expression in motoneurons of ALS patients [39]. This may be explained by the fact that motoneurons have a relative inability to induce Hsp70 expression [5], which has been put forward as one of the factors to explain the selective vulnerability of motoneurons towards mutant SOD1. It has been shown that Hsp70 and some other heat shock proteins (i.e. Hsp40, αB-crystallin and Hsp27) bind to mutant SOD1, but not to wild-type SOD1 [96], [83], which results in their reduced availability [83]. Increasing the level of Hsp70 reduced formation of mutant SOD1 aggregates and prolonged survival in cultured primary motor neurons and a neuronal cell line [10,99]. However, *in vivo* overexpression of Hsp70 in SOD1-ALS mice by crossing these mice with Hsp70 transgenic mice did not influence the disease progression and survival [107]. Importantly, crossing the same Hsp70 mice in a mouse model carrying a mutant androgen receptor that develops an early onset motoneuron disease [1], showed that in these mice Hsp70 attenuated motoneuron degeneration. Hence, together the data indicate that although Hsp70 interacts with mutant SOD1 and prevents its aggregation, it does not protect motoneurons against mutant SOD1 in SOD1-ALS mice. This implies that insufficient Hsp70 is not a factor contributing to the pathogenesis in SOD1-ALS mice.

In a recent study, heat shock protein expression has been pharmacologically up regulated in the spinal cord of a line of SOD1-ALS mice (G1H-G93A) with arimoclomol [65]. This treatment which resulted in increased expression of Hsp70 and Hsp90, putatively via activation of Heat shock protein-inducing factor (HSF1), resulted in considerable prolonged life span, even though treatment was started

after disease onset [65]. Direct proof that arimoclomol is beneficial via the activation of heat shock proteins is still lacking, and other modes of actions cannot yet be excluded.

We have performed a detailed analysis of heat shock protein expression in our G93A mice. First, a high throughput gene expression analysis with Affymetrix Gene chips (MG-U74Av2), which enables the mRNA expression profiling of approximately 10.000 murine genes (www.affymetrix.com), did not show any changes in mRNA levels of 150 genes encoding for molecular chaperones in the spinal cord of presymptomatic G93A mice as compared to controls (Fig 4). Also using immuno(cyto)chemical methods no change in Hsp70, Hsp60, Hsp40 and the small heat shock proteins, Hsp27 and α-B-crystallin, were observed in young G93A mice. However, a number of changes in the expression of specific heat shock proteins occurred in mid-late presymptomatic and symptomatic G93A mice (Chapters 4 and 5). In order of time of appearance these changes consisted of 1) a decreased expression of Hsp27 in motoneurons starting from mid-late presymptomatic stages of disease, i.e. several weeks before the onset of motoneuron loss (chapter 4). 2) Induction of Hsp27 expression in astrocytes in late presymptomatic and symptomatic mice (chapter 4). 3) Increased α-B-crystallin in oligodendrocytes in late presymptomatic and symptomatic mice (in preparation), and 4) Induction of Hsp70 expression in of a subset of sick-appearing motoneurons in late presymptomatic and symptomatic mice (chapter 5).
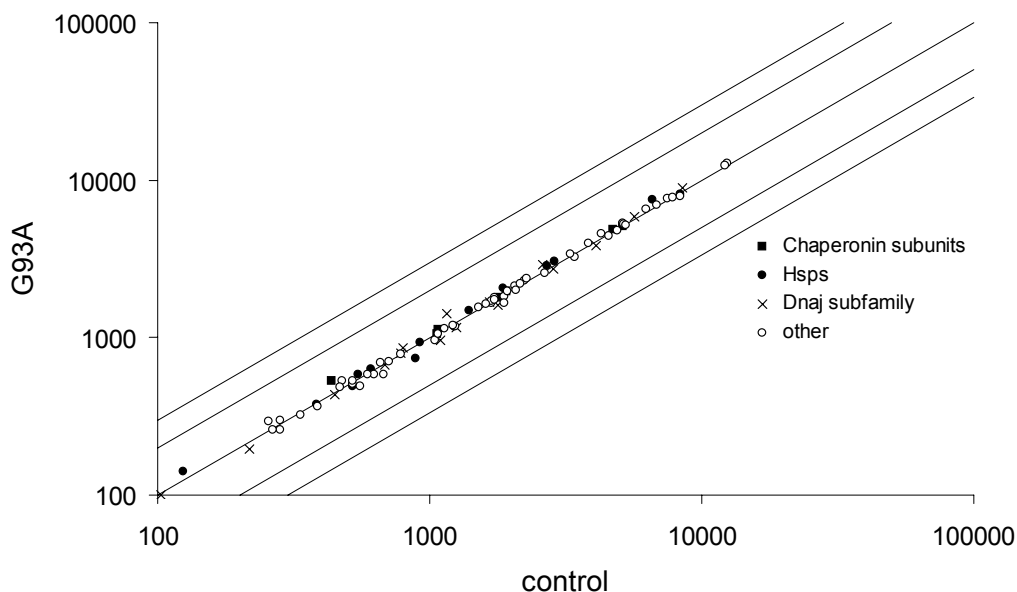

Fig. 4. Affymetrix Genechip analysis shows that the relative mRNA expression of molecular chaperones in the spinal cord of 12-weeks-old G93A mice is not altered as compared to non-transgenic mice

Hsp27 (also called Hsp25 in mice or HspB1) is a multifunctional protein that is constitutively expressed by α-motoneurons. Like Hsp70 it has many neuroprotective properties, including the ability to inhibit misfolded protein aggregation [111]. As discussed in chapter 4, decreased Hsp27 expression prior to the onset of motoneuron death can contribute to the degeneration of motoneurons in several ways, including the facilitation of SOD1 aggregation, facilitation of caspase 3 activation, and troubling of cytoskeletal proteins homeostasis. Importantly, missense mutations in Hsp27 [35] and another small heat shock protein, Hsp22 [53] have been linked to peripheral distal motor and sensory axonopathies. The mutations impair the chaperone function of Hsp27 [35], further supporting the notion that loss of Hsp27 function may be deleterious for motoneurons. Hence, a decreased availability of Hsp27 may be one of the mechanisms that contribute to the toxicity of mutant SOD1. A question that remains to be resolved is what causes decreased motoneuronal Hsp27 protein expression in G93A-SOD1 mice. Our data point to a post-translational mechanism, putatively through an interaction with mutant SOD1, but this hypothesis needs further support (see chapter 4).

Astroglial Hsp27 induction as identified in our symptomatic G93A mice (see chapter 4) has been reported for different pathological conditions, including ischemia, excitotoxicity, and Alzheimer's disease and, therefore, seems to be a common characteristic of very different types of brain pathology [55]. In contrast, increased expression of α-B-crystallin may be more directly linked to mutant SOD1 toxicity since all astro- and oligodendroglial ubiquitinated structures are strongly immunoreactive for α-B-crystallin (in preparation).

The sick Hsp70-immunoreactive cells showed a characteristic set of abnormalities including a strong immunoreactivity for ubiquitin (chapter 5), which together with other data indicate that these cells have an impaired proteasome function (see above). Notably, other cells in G93A mice that contained high levels of ubiquitin, i.e. astrocytes, oligodendrocytes and spinal interneurons, did not show increased Hsp70 expression. This again challenges the idea that the selective vulnerability of motoneurons, is caused by a relative inability to induce Hsp70 expression.

6.2.3   The identity of ubiquitinated structures in SOD1-ALS mice: aggregates, aggresomes or something else?

The advantage of SOD1-ALS mice is that aggregates and ubiquitinated structures can be examined in early phases of disease, and furthermore the temporal relationship between aggregate formation and other signs of neuronal degeneration can be determined. As discussed in chapter 4, the accumulation of oligomeric and aggregated mutant SOD1 species at a level that can be detected by immunochemical methods is a relatively late event, occurring at the onset of the death and disappearance of motoneuron death. In earlier stages of disease accumulation of mutant SOD1 suggestive of aggregates could be detected in mitochondria and dendritic cytosolic ensembles of filamentous and granular material (chapters 4 and 5; [57]). As described by others in a later phase of disease SOD1 aggregates also appear in oligo- and astroglia [12,98]. Together the data indicate that SOD1 aggregation happens independently in different cell types. The

time of appearance suggests that glial SOD1 aggregation occurs secondarily to the degeneration of motoneurons, putatively in association with a stress response induced in these cells by the death of motoneuron.

Mitochondrial SOD1 aggregates were not ubiquitinated (chapter 4) which can be explained by the fact that the ubiquitination machinery does not operate in mitochondria. Accordingly, all neuronal and glial cytosolic SOD1 aggregates were ubiquitinated. In chapter 5 we have focused on the identity of the dendritic cytosolic SOD1 aggregates, since their time of appearance precede the further degeneration of motoneurons (chapter 5). These dendritic cytosolic SOD1 aggregates are not Lewy body-like inclusions or aggresome-like structure, because unlike these structures they are not located at the centrosome. In contrast, they show some resemblance with skeins, i.e. the irregular loosely arranged bundles of filamentous-appearing material which represent a constant feature in ALS motoneurons. The precise identity of ubiquitinated cytosolic remains to be established (chapter 5). A preliminary hypothesis proposes that they represent SOD1 aggregates together with material from collapsing microtubule network.

6.3   How do motoneurons die in ALS?

The mechanisms by which motoneurons die and disappear in ALS has remained an unresolved issue [13,44]. Initially the discussion has been centered on the question whether the death was apoptotic or necrotic. However, this discussion may not be fruitful, since in neurodegenerative disorders a diverse array of degenerative pathways, either apoptotic, necrotic or autophagic may operate sequentially or in parallel to yield degradation and death of neurons that differs from classical apoptosis or necrosis [113]. Hence more important questions are: which death pathways are involved and do they represent targets for therapeutic intervention? Studies in post-mortem human ALS spinal cord and motor cortex have provided evidence favoring a role for apoptotic programmed cell death pathways [93]. An instrumental role for apoptotic programmed cell death pathways also has been suggested for SOD1-ALS mice (see below). The roles of necrotic and autophagolytic programs have not yet been investigated.

6.3.1   The recruitment of programmed cell death pathways in SOD1-ALS mice

The recruitment of molecular pathways in SOD1-ALS mice has been extensively reviewed [44]. Programmed cell death is a complex multi-step process involving many factors that grossly can be grouped into sensors, initiators, modulators and effectors. The two main pathways are the 'death receptor' (extrinsic) and the 'mitochondrial' (intrinsic) pathways that result in the activation of members of the caspase family of proteases, caspases 8 and 9, respectively (Fig. 5) [25,41]. This activation consists of oligomerisation of procaspase 8 and 9, respectively, which results in cleavage and activation of these caspases. This in turn through cleavage cause the activation of downstream caspases that coordinate the proteolytic breakdown of the cell [90,97]. Also the endoplasmatic reticulum (ER) has been
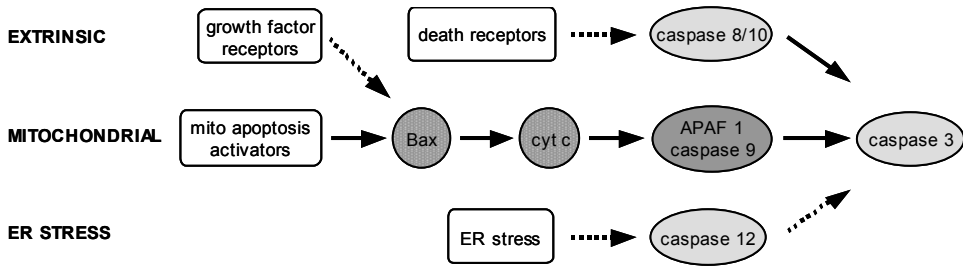
Figure 5: diagram of the main caspase-dependent apoptosis pathways. Both extrinsic pathways are mainly started up by extracellular signals, while the ER-stress pathway is activated specifically when ER-stress occurs. The mitochondrial pathway can be initiated by many kinds of cellular stress causing Bax translocation to mitochondria.

involved in the initiation of programmed cell death operating through the activation of caspase 12 in rodents and putatively caspase 4 in man, who does not produce a functional caspase 12 [49]. The final common pathway of most programmed cell death pathways is the activation of executioner caspases, like caspase 3 (Fig. 5)

Several studies have reported the activation of caspase 3 in the spinal cord of SOD1-ALS mice, strongly supporting a role for programmed cell death in the pathogenesis [44,87]. This was further supported by the finding that the irreversible broad-caspase inhibitor benzyloxycarbonyl-Val-Ala-Asp(O-methyl)-fluoromethylketone attenuates mutant SOD1–mediated cell death and mildly prolongs survival in transgenic G93A-SOD1 mice [71]. Whether the beneficial effect of caspase inhibition operates through delaying the death of motoneurons is not clear. Our data, as reported in chapter 5, indicate that activated caspase 3 predominantly occurs in interneurons, glial cells, and debris of motoneurons, and further suggest that motoneurons show active caspase 3 only in a very late irreversible phase of their degeneration (see chapter 5). Caspase inhibition has been shown to be ineffective in rescuing sick neurons [84]. Hence, inhibition of caspases may predominantly have its beneficial effect via inhibition of interneuron and glia cell death, which indirectly may be beneficial for motoneurons [17].

What mechanism activates caspase 3 in SOD1-ALS mice? Some studies have suggested a role for caspase 1, which is thought to play a role in cytokine maturation rather than programmed cell death [71,87]. However, the role of caspase 1 has been questioned [62]. Most studies point to the activation of a mitochondrial cell death pathway. This pathway is modulated by proteins of the Bcl-2 family that in part may operate by controlling the permeability of the mitochondrial outer membrane, and, hence, control the release of cytochrome c which triggers caspase 9 activation [41]. An early study showed that overexpression of Bcl-2, an anti-apoptotic member of the Bcl-2 family prolongs survival of G93A mice [70]. Subsequently it was found in various lines of SOD1-ALS mice that Bcl-2 levels were decreased and levels of the pro-apoptotic Bcl-2 family members Bax and Bak were increased in the spinal cord [44]. Furthermore caspase 9 activation was shown to occur at about the same time as Bax-translocation to mitochondria and mitochondrial cytochrome c release [45]. Also inhibition of caspase 9 attenuates disease progression in G93A mice [52]. More recently, a direct interaction between mutant SOD1 and Bcl-2 has been

reported, and aggregates containing both mutant SOD1 and Bcl-2 have been found in mitochondria of the spinal cord but not the liver of SOD1-ALS mice suggesting that mutant SOD1 may trap Bcl-2 and hence inhibit its anti-apoptotic property [86]. It is not clear how the latter finding is related to the early accumulation of mutant SOD1 in the mitochondrial intermembrane space and outer membrane [57,72]. Furthermore the specific entrapment of Bcl-2 is difficult to reconcile with the selective vulnerability of motoneurons since both Bcl2 and SOD1 are ubiquitously expressed. Another problem that needs to be resolved is the poor temporal correlation between mitochondrial pathology which occurs in an early phase of disease [57] and active caspase 3 expression. Yet another problem is that swollen and vacuolated mitochondria are morphologically distinct from apoptotic mitochondria, and that mitochondria in sick motoneurons have a normal appearance.

6.3.2   The role of stress transcription factors

In addition to the activation of cell death programs, intracellular damage also may activate survival, repair and regenerations programs. An example of the activation of such a program can be observed in adult motoneurons after axotomy. This event results in a sequence of morphological and genetic rearrangements, such as synaptic stripping, activation of adjacent glial cells, downregulation of glutamate receptors, upregulation of tubulin and many neuropeptides, upregulation of trophic factor signaling, and up-regulation of growth associated proteins [9,48,80]. Several signaling pathways have been implicated in this response. One component is the c-Jun N-terminal kinase (JNK)-stress signaling pathway that activates the AP1 transcription factor c-Jun through phosphorylation (Fig. 6) [48,89]. Importantly, the beneficial effect of c-Jun in axotomized motoneurons strongly depends on the transcriptional context, since under specific conditions activated c-Jun also acts as an activator of neuronal degeneration [103,109]. One factor influencing c-Jun transcriptional activity is its hetero-dimerization partner, which can be other members of the AP-1 family or members of other bZIP motif-containing families like the ATF/CREB, Maf, and C/EBP families. Another stress transcription factor is ATF3, a member of the ATF/CREB family [47]. Like c-Jun, ATF3 is expressed in axotomized motoneurons, and shows both survival and death promoting properties depending on the cellular context [47]. The presence of ATF3 strongly influences the effect of c-Jun. For instance, in trophic factor-deprived neurons it can turn c-Jun from a cell death promoting factor into a factor that promotes neurite outgrowth [81].
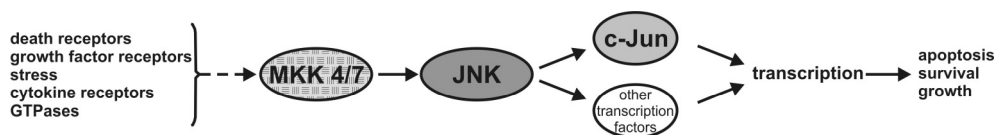

Figure 6: The JNK/c-Jun signaling pathway. The MAP kinase kinases MKK 4 and 7 can activate c-Jun N-terminal kinases (JNK), which can activate multiple transcription factors including c-Jun, ATF2 and p53.

In Chapter 5 we have shown that both phosphorylated c-Jun and ATF3 are expressed in a subset of motoneurons in G93A mice starting from an early phase of disease prior to the onset of motoneuron death. These phosphorylated c-Jun and ATF3 expressing motoneurons showed a variable morphology varying from normal to sick-appearing cells. Importantly, these sick motoneurons were not (yet) immunoreactive for active caspase, and showed a unique morphology that differed from the morphology of dying motoneurons reported in the literature (see chapter 5). We concluded that ATF3 and phosphorylated c-Jun are expressed by motoneurons throughout their degeneration process starting from a relatively early phase until a very sick phase shortly before dying. The activation of c-Jun and ATF3 initially may represent a survival response since there is no activation of programmed cell death pathways in these cells. However, it is possible that the transcriptional context within ATF3/phosphorylated c-Jun expressing motoneurons changes as the cell deteriorates. Accordingly, a subset of (frequently ill-appearing) ATF3/phosphorylated c-Jun expressing motoneurons showed the expression of CHOP (Gadd153), which influences the transcriptional activity of ATF3 [47]. We also concluded that ATF3 and phosphorylated c-Jun are excellent markers to pinpoint motoneurons in an early phase of their degeneration, and may serve as a reference to study the role of other signaling pathways in motoneuron degeneration.

6.4   Is there a future ALS-research in SOD1-ALS mice?

Research on SOD1 mutations has dominated the ALS field in the past decade. Did this research increase our understanding of the pathogenesis of ALS? In case of ALS caused by SOD1 mutations the answer is obviously 'yes'. Although we do not yet fully understand how mutant SOD1 causes the degeneration of motoneurons, a lot has been learned about potential mechanisms (e.g. see this chapter and chapter 1). In terms of therapeutic approaches, data so far have indicated that down-regulating mutant SOD1 expression or preventing its aggregation may be most effective. Although technically challenging, recent studies have shown that this may be achieved using RNAi-approaches [76,112]. In view of the linear relationship between the level of mutant SOD1 expression and the time of onset and severity of disease, even down-regulating mutant SOD1 expression by 10-20% may have a large effect on survival. Thus also drugs that 'slow down' the metabolism of SOD1 in motoneurons may be beneficial. Accordingly, 'unexpected results' obtained in SOD1-ALS mice, such as the dramatic beneficial effect of altering neurofilament expression on survival of SOD1-ALS mice, may be explained by a mechanism affecting the global metabolism of motoneurons and consequently reducing mutant SOD1 expression. Both overexpression of neurofilament H [21], or either deletion or overexpression of neurofilament L in SOD1-ALS mice were found to increase their lifespan [68,110]. These results were counterintuitive since alterations in neurofilament levels cause neurofilament aggregates or reduces axon caliber [73], and hence by themselves are deleterious to motoneurons. However, the results with the neurofilament mice can be easily explained, if motoneurons compromised by altered neurofilament status would

produce 20% less mutant SOD1, which in view of their altered health is conceivable. This illustrates the importance of evaluating the effect of a drug on motoneuron morphology and overall mutant SOD1 expression in every drug trial.

Alternative approaches in SOD1-linked ALS may be directed at preventing protein aggregation, for instance by up regulating heat shock protein expression [65]. Also drugs that interfere with specific neuroprotective signaling pathways may be helpful, but prior of considering such an approach a further molecular dissection of signaling pathways that operate in injured motoneurons is needed. Yet another approach in delaying ALS caused by mutant SOD1 may be the attenuation of inflammatory response. This is suggested by recent findings that prolonged systemic inflammation causes an earlier onset of disease in SOD1-ALS mice [82]. The latter approaches are likely to be also relevant for sporadic ALS, and hence illustrate the importance of SOD1-ALS mice as an ALS research tool. Thus, although the primary disease causing factors may differ, phenomena such as inflammation, protein aggregation, neuron-glia signaling, and perhaps excitotoxicity may play a role (and represent a target for therapeutic approach) in all forms of ALS.

Table 1: A selection of preclinical and clinical drug trials.

Substance	mechanism	Age at start (days)	Onset delay (days)	Death delay (days)	Human effect	ref
riluzole	Anti-excitotoxicity	50	not sign	13	2-3 months [8]	[46]
Topiramate	Anti-excitotoxicity	30	nd	not sign	none [22]	[75]
vitamin E	Anti-oxidant	50	13	not sign	none [26]	[46]
NAC	Anti-oxidant	120 *	not sign	not sign	nd	[56]
		28-35	7	8		[3]
GDNF	Growth factor	63 adenoviral vector	13	17	nd	[105]
		35 wks ** intramuscular injection	not sign	nd		[74]
AR-R 17477	nNOS inhibitor	40	nd	13	nd	[36]
L-NAME	NOS inhibitor	30	nd	not sign	nd	[36]
creatine	Energy supplementation	70	nd	25	none [43]	[66]
celecoxib	Anti-inflammatory	28	16	28	none [23]	[29]
creatine + celecoxib		30	nd	36	nd	[67]
* G1L-G93A mice ** G93A mice with extra low transgenic copy number						

Hundreds of potential drugs now have been tested in SOD1-ALS mice (e.g. see [13]). A selection of tested drugs is shown in table 1. In general results obtained in the SOD1-ALS mice have a relevant predictive value for what will happen in patients as illustrated with drugs like Riluzole and topiramate and anti-oxidants (see table 1). However, the mouse studies also have yielded 'false positives' like, for instance, creatine which had a large beneficial effect in G93A mice [66], but no effect in patients [43]. There are many possible explanations for this type of discrepancies, such as 'a mouse is not a man' or 'creatine may be only beneficial in SOD1-linked ALS cases'. However, another possibility is that false positives, such as creatine, arise from the use of high copy G93A mice that show a number of pathological features that do not occur in other lines of SOD1-ALS mice. Hence, one way of minimizing 'false hopes' is by performing drug trials in multiple lines of SOD1-ALS mice, including low-copy mice which may more realistically model ALS in man.

In sum, the SOD1-ALS mice represent a highly important (and still the only) mouse model for ALS, although as with any model data should be interpreted with care. The neuropathological investigations as presented in this thesis have provided a frame work for future studies with these mice. The future of ALS research will continue to be a multidisciplinary fishing expedition focusing on the following approaches: 1) The identification of new mutations linked to familial forms of ALS. 2) Screening and identification of the mode of action of potential drugs and therapeutic approaches in SOD1-ALS mice. 3) Further characterization of the cell biology of motoneurons. In view of recent data emerging from ALS genetics these studies should focus on trafficking and logistics. 4) Further characterization of motoneurons and surrounding glia in SOD1-ALS mice (and, eventually, novel mouse models of adult onset motoneuron degeneration) to identify novel targets for therapeutic approaches.

References

[1]   H. Adachi, M. Katsuno, M. Minamiyama, C. Sang, G. Pagoulatos, C. Angelidis, M. Kusakabe, A. Yoshiki, Y. Kobayashi, M. Doyu, G. Sobue, Heat shock protein 70 chaperone overexpression ameliorates phenotypes of the spinal and bulbar muscular atrophy transgenic mouse model by reducing nuclear-localized mutant androgen receptor protein, J Neurosci 23 (2003) 2203-2211.

[2]   S. Allen, P.R. Heath, J. Kirby, S.B. Wharton, M.R. Cookson, F.M. Menzies, R.E. Banks, P.J. Shaw, Analysis of the cytosolic proteome in a cell culture model of familial amyotrophic lateral sclerosis reveals alterations to the proteasome, antioxidant defenses, and nitric oxide synthetic pathways, J Biol Chem 278 (2003) 6371-6383.

[3]   O.A. Andreassen, A. Dedeoglu, P. Klivenyi, M.F. Beal, A.I. Bush, N-acetyl-L-cysteine improves survival and preserves motor performance in an animal model of familial amyotrophic lateral sclerosis, Neuroreport 11 (2000) 2491-2493.

[4]   M. Arrasate, S. Mitra, E.S. Schweitzer, M.R. Segal, S. Finkbeiner, Inclusion body formation reduces levels of mutant huntingtin and the risk of neuronal death, Nature 431 (2004) 805-810.

[5]   Z. Batulan, G.A. Shinder, S. Minotti, B.P. He, M.M. Doroudchi, J. Nalbantoglu, M.J. Strong, H.D. Durham, High threshold for induction of the stress response in motor neurons is associated with failure to activate HSF1, J Neurosci 23 (2003) 5789-5798.

[6]   J.S. Beckman, W.H. Koppenol, Nitric oxide, superoxide, and peroxynitrite: the good, the bad, and ugly, Am J Physiol 271 (1996) C1424-1437.

[7]   N.F. Bence, R.M. Sampat, R.R. Kopito, Impairment of the ubiquitin-proteasome system by protein aggregation, Science 292 (2001) 1552-1555.

[8]   G. Bensimon, L. Lacomblez, V. Meininger, A controlled trial of riluzole in amyotrophic lateral sclerosis., N Engl J Med 330 (1994) 585-591.

[9]   I.E. Bonilla, K. Tanabe, S.M. Strittmatter, Small proline-rich repeat protein 1A is expressed by axotomized neurons and promotes axonal outgrowth, J Neurosci 22 (2002) 1303-1315.

[10]   W. Bruening, J. Roy, B. Giasson, D.A. Figlewicz, W.E. Mushynski, H.D. Durham, Up-regulation of protein chaperones preserves viability of cells expressing toxic Cu/Zn-superoxide dismutase mutants associated with amyotrophic lateral sclerosis, J Neurochem 72 (1999) 693-699.

[11]   L.I. Bruijn, M.F. Beal, M.W. Becher, J.B. Schulz, P.C. Wong, D.L. Price, D.W. Cleveland, Elevated free nitrotyrosine levels, but not protein-bound nitrotyrosine or hydroxyl radicals, throughout amyotrophic lateral sclerosis (ALS)- like disease implicate tyrosine nitration as an aberrant in vivo property of one familial ALS-linked superoxide dismutase 1 mutant, Proc Natl Acad Sci U S A 94 (1997) 7606-7611.

[12]   L.I. Bruijn, M.K. Houseweart, S. Kato, K.L. Anderson, S.D. Anderson, E. Ohama, A.G. Reaume, R.W. Scott, D.W. Cleveland, Aggregation and motor neuron toxicity of an ALS-linked SOD1 mutant independent from wild-type SOD1, Science 281 (1998) 1851-1854.

[13]   L.I. Bruijn, T.M. Miller, D.W. Cleveland, Unraveling the Mechanisms Involved in Motor Neuron Degeneration in ALS, Annu Rev Neurosci 27 (2004) 723-749.

[14]   C.I. Cha, Y.H. Chung, C.M. Shin, D.H. Shin, Y.S. Kim, M.E. Gurney, K.W. Lee, Immunocytochemical study on the distribution of nitrotyrosine in the brain of the transgenic mice expressing a human Cu/Zn SOD mutation, Brain Res 853 (2000) 156-161.

[15]   K.K. Chung, V.L. Dawson, T.M. Dawson, The role of the ubiquitin-proteasomal pathway in Parkinson's disease and other neurodegenerative disorders, Trends Neurosci. 24 (2001) S7-S14.

[16]   A. Ciechanover, P. Brundin, The ubiquitin proteasome system in neurodegenerative diseases. Sometimes the chicken, sometimes the egg, Neuron 40 (2003) 427-446.

[17]   A.M. Clement, M.D. Nguyen, E.A. Roberts, M.L. Garcia, S. Boillee, M. Rule, A.P. McMahon, W. Doucette, D. Siwek, R.J. Ferrante, R.H. Brown, Jr., J.P. Julien, L.S. Goldstein, D.W. Cleveland, Wild-type nonneuronal cells extend survival of SOD1 mutant motor neurons in ALS mice, Science 302 (2003) 113-117.

[18]   D.W. Cleveland, J.D. Rothstein, From Charcot to Lou Gehrig: deciphering selective motor neuron death in ALS, Nat Rev Neurosci 2 (2001) 806-819.

[19]   M.R. Cookson, P.J. Shaw, Oxidative stress and motor neurone disease, Brain Pathol 9 (1999) 165-186.

[20]   L.J. Corcoran, T.J. Mitchison, Q. Liu, A novel action of histone deacetylase inhibitors in a protein aggresome disease model, Curr Biol 14 (2004) 488-492.

[21]   S. Couillard-Despres, Q. Zhu, P.C. Wong, D.L. Price, D.W. Cleveland, J.P. Julien, Protective effect of neurofilament heavy gene overexpression in motor neuron disease induced by mutant superoxide dismutase, Proc Natl Acad Sci U S A 95 (1998) 9626-9630.

[22]   M.E. Cudkowicz, J.M. Shefner, D.A. Schoenfeld, R.H. Brown Jr, Jr., H. Johnson, M. Qureshi, M. Jacobs, J.D. Rothstein, S.H. Appel, R.M. Pascuzzi, T.D. Heiman-Patterson, P.D. Donofrio, W.S. David, J.A. Russell, R. Tandan, E.P. Pioro, K.J. Felice, J. Rosenfeld, R.N. Mandler, G.M. Sachs, W.G. Bradley, E.M. Raynor, G.D. Baquis, J.M. Belsh, S. Novella, J. Goldstein, J. Hulihan, A randomized, placebo-controlled trial of topiramate in amyotrophic lateral sclerosis, Neurology 61 (2003) 456-464.

[23]   M.E. Cudkowicz, J.M. Shefner, D.A. Schoenfeld, J. Rothstein, D.B. Drachman, Clinical trial of Celecoxib in subjects with Amyotrophic Lateral Sclerosis, www.alscenter.org/news/briefs/041110.cfm (2004).

[24]   C.J. Cummings, Y. Sun, P. Opal, B. Antalffy, R. Mestril, H.T. Orr, W.H. Dillmann, H.Y. Zoghbi, Over-expression of inducible HSP70 chaperone suppresses neuropathology and improves motor function in SCA1 mice, Hum Mol Genet 10 (2001) 1511-1518.

[25]   N.N. Danial, S.J. Korsmeyer, Cell death: critical control points, Cell 116 (2004) 205-219.

[26]   C. Desnuelle, M. Dib, C. Garrel, A. Favier, A double-blind, placebo-controlled randomized clinical trial of alpha-tocopherol (vitamin E) in the treatment of amyotrophic lateral sclerosis. ALS riluzole-tocopherol Study Group, Amyotroph Lateral Scler Other Motor Neuron Disord 2 (2001) 9-18.

[27]   M. Dib, Amyotrophic lateral sclerosis: progress and prospects for treatment, Drugs 63 (2003) 289-310.

[28]   M.M. Doroudchi, S. Minotti, D.A. Figlewicz, H.D. Durham, Nitrotyrosination contributes minimally to toxicity of mutant SOD1 associated with ALS, Neuroreport 12 (2001) 1239-1243.

[29]   D.B. Drachman, K. Frank, M. Dykes-Hoberg, P. Teismann, G. Almer, S. Przedborski, J.D. Rothstein, Cyclooxygenase 2 inhibition protects motor neurons and prolongs survival in a transgenic mouse model of ALS, Ann Neurol 52 (2002) 771-778.

[30]   M.W. Duncan, A review of approaches to the analysis of 3-nitrotyrosine, Amino Acids 25 (2003) 351-361.

[31]   J.P. Eiserich, A.G. Estevez, T.V. Bamberg, Y.Z. Ye, P.H. Chumley, J.S. Beckman, B.A. Freeman, Microtubule dysfunction by posttranslational nitrotyrosination of alpha- tubulin: a nitric oxide-dependent mechanism of cellular injury, Proc Natl Acad Sci U S A 96 (1999) 6365-6370.

[32]   J.S. Elam, A.B. Taylor, R. Strange, S. Antonyuk, P.A. Doucette, J.A. Rodriguez, S.S. Hasnain, L.J. Hayward, J.S. Valentine, T.O. Yeates, P.J. Hart, Amyloid-like filaments and water-filled nanotubes formed by SOD1 mutant proteins linked to familial ALS, Nat Struct Biol 10 (2003) 461-467.

[33]   J. Emerit, M. Edeas, F. Bricaire, Neurodegenerative diseases and oxidative stress, Biomed Pharmacother 58 (2004) 39-46.

[34]   A.G. Estevez, J.P. Crow, J.B. Sampson, C. Reiter, Y. Zhuang, G.J. Richardson, M.M. Tarpey, L. Barbeito, J.S. Beckman, Induction of nitric oxide-dependent apoptosis in motor neurons by zinc-deficient superoxide dismutase, Science 286 (1999) 2498-2500.

[35]   O.V. Evgrafov, I. Mersiyanova, J. Irobi, L. Van Den Bosch, I. Dierick, C.L. Leung, O. Schagina, N. Verpoorten, K. Van Impe, V. Fedotov, E. Dadali, M. Auer-Grumbach, C. Windpassinger, K. Wagner, Z. Mitrovic, D. Hilton-Jones, K. Talbot, J.J. Martin, N. Vasserman, S. Tverskaya, A. Polyakov, R.K. Liem, J. Gettemans, W. Robberecht, P. De Jonghe, V. Timmerman, Mutant small heat-shock protein 27 causes axonal Charcot-Marie-Tooth disease and distal hereditary motor neuropathy, Nat Genet 36 (2004) 602-606.

[36]   F. Facchinetti, M. Sasaki, F.B. Cutting, P. Zhai, J.E. MacDonald, D. Reif, M.F. Beal, P.L. Huang, T.M. Dawson, M.E. Gurney, V.L. Dawson, Lack of involvement of neuronal nitric oxide synthase in the pathogenesis of a transgenic mouse model of familial amyotrophic lateral sclerosis, Neuroscience 90 (1999) 1483-1492.

[37]   R.J. Ferrante, L.A. Shinobu, J.B. Schulz, R.T. Matthews, C.E. Thomas, N.W. Kowall, M.E. Gurney, M.F. Beal, Increased 3-nitrotyrosine and oxidative damage in mice with a human copper/zinc superoxide dismutase mutation, Ann Neurol 42 (1997) 326-334.

[38]   J. Fortun, W.A. Dunn, Jr., S. Joy, J. Li, L. Notterpek, Emerging role for autophagy in the removal of aggresomes in Schwann cells, J Neurosci 23 (2003) 10672-10680.

[39]   O. Garofalo, P.G. Kennedy, M. Swash, J.E. Martin, P. Luthert, B.H. Anderton, P.N. Leigh, Ubiquitin and heat shock protein expression in amyotrophic lateral sclerosis, Neuropathol Appl Neurobiol 17 (1991) 39-45.

[40]   B.I. Giasson, J.E. Duda, I.V. Murray, Q. Chen, J.M. Souza, H.I. Hurtig, H. Ischiropoulos, J.Q. Trojanowski, V.M. Lee, Oxidative damage linked to neurodegeneration by selective alpha-synuclein nitration in synucleinopathy lesions, Science 290 (2000) 985-989.

[41]   D.R. Green, G. Kroemer, The pathophysiology of mitochondrial cell death, Science 305 (2004) 626-629.

[42]   S.A. Greenacre, H. Ischiropoulos, Tyrosine nitration: localisation, quantification, consequences for protein function and signal transduction, Free Radic Res 34 (2001) 541-581.

[43]   G.J. Groeneveld, J.H. Veldink, I. van der Tweel, S. Kalmijn, C. Beijer, M. de Visser, J.H. Wokke, H. Franssen, L.H. van den Berg, A randomized sequential trial of creatine in amyotrophic lateral sclerosis, Ann Neurol 53 (2003) 437-445.

[44]   C. Guegan, S. Przedborski, Programmed cell death in amyotrophic lateral sclerosis, J Clin Invest 111 (2003) 153-161.

[45]   C. Guegan, M. Vila, G. Rosoklija, A.P. Hays, S. Przedborski, Recruitment of the mitochondrial-dependent apoptotic pathway in amyotrophic lateral sclerosis, J Neurosci 21 (2001) 6569-6576.

[46]   M.E. Gurney, F.B. Cuttings, P. Zhai, A. Doble, C.P. Taylor, P.K. Andrus, E.D. Hall, Benefit of Vitamine E, Riluzole, and gabapentin in a transgenic model of familial amyotrophic lateral sclerosis, Ann. Neurol. 39 (1996) 147-157.

[47]   T. Hai, C.D. Wolfgang, D.K. Marsee, A.E. Allen, U. Sivaprasad, ATF3 and stress responses, Gene Expr 7 (1999) 321-335.

[48]   T. Herdegen, V. Waetzig, The JNK and p38 signal transduction following axotomy, Restor Neurol Neurosci 19 (2001) 29-39.

[49]   J. Hitomi, T. Katayama, Y. Eguchi, T. Kudo, M. Taniguchi, Y. Koyama, T. Manabe, S. Yamagishi, Y. Bando, K. Imaizumi, Y. Tsujimoto, M. Tohyama, Involvement of caspase-4 in endoplasmic reticulum stress-induced apoptosis and Abeta-induced cell death, J Cell Biol 165 (2004) 347-356.

[50]   T. Horiguchi, K. Uryu, B.I. Giasson, H. Ischiropoulos, R. LightFoot, C. Bellmann, C. Richter-Landsberg, V.M. Lee, J.Q. Trojanowski, Nitration of tau protein is linked to neurodegeneration in tauopathies, Am J Pathol 163 (2003) 1021-1031.

[51]   D.H. Hyun, M. Lee, B. Halliwell, P. Jenner, Proteasomal inhibition causes the formation of protein aggregates containing a wide range of proteins, including nitrated proteins, J Neurochem 86 (2003) 363-373.

[52]   H. Inoue, K. Tsukita, T. Iwasato, Y. Suzuki, M. Tomioka, M. Tateno, M. Nagao, A. Kawata, T.C. Saido, M. Miura, H. Misawa, S. Itohara, R. Takahashi, The crucial role of caspase-9 in the disease progression of a transgenic ALS mouse model, Embo J 22 (2003) 6665-6674.

[53]   J. Irobi, K. Van Impe, P. Seeman, A. Jordanova, I. Dierick, N. Verpoorten, A. Michalik, E. De Vriendt, A. Jacobs, V. Van Gerwen, K. Vennekens, R. Mazanec, I. Tournev, D. Hilton-Jones, K. Talbot, I. Kremensky, L. Van Den Bosch, W. Robberecht, J. Van Vandekerckhove, C. Broeckhoven, J. Gettemans, P. De Jonghe, V. Timmerman, Hot-spot residue in small heat-shock protein 22 causes distal motor neuropathy, Nat Genet 36 (2004) 597-601.

[54]   H. Ischiropoulos, J.S. Beckman, Oxidative stress and nitration in neurodegeneration: cause, effect, or association?, J Clin Invest 111 (2003) 163-169.

[55]   T. Iwaki, A. Iwaki, J. Tateishi, Y. Sakaki, J.E. Goldman, Alpha B-crystallin and 27-kd heat shock protein are regulated by stress conditions in the central nervous system and accumulate in Rosenthal fibers, Am J Pathol 143 (1993) 487-495.

[56]   D. Jaarsma, H.J. Guchelaar, E. Haasdijk, J.M. de Jong, J.C. Holstege, The antioxidant N-acetylcysteine does not delay disease onset and death in a transgenic mouse model of amyotrophic lateral sclerosis [letter], Ann Neurol 44 (1998) 293.

[57]   D. Jaarsma, E.D. Haasdijk, Mutant SOD1 protein accumulates in vacuolated mitochondria, in cytosolic filamentous aggregates, and in periaxonal glia in ALS-SOD1 mouse spinal cord, Soc. Neurosci. abstr 27 (2001) 984.982.

[58]   J.A. Johnston, M.J. Dalton, M.E. Gurney, R.R. Kopito, Formation of high molecular weight complexes of mutant Cu,Zn-superoxide dismutase in a mouse model for familial amyotrophic lateral sclerosis, Proc Natl Acad Sci U S A 97 (2000) 12571-12576.

[59]   P.A. Jonsson, K. Ernhill, P.M. Andersen, D. Bergemalm, T. Brannstrom, O. Gredal, P. Nilsson, S.L. Marklund, Minute quantities of misfolded mutant superoxide dismutase-1 cause amyotrophic lateral sclerosis, Brain 127 (2004) 73-88.

[60]   C. Jung, Y. Rong, S. Doctrow, M. Baudry, B. Malfroy, Z. Xu, Synthetic superoxide dismutase/catalase mimetics reduce oxidative stress and prolong survival in a mouse amyotrophic lateral sclerosis model, Neurosci Lett 304 (2001) 157-160.

[61]   E. Kabashi, J.N. Agar, D.M. Taylor, S. Minotti, H.D. Durham, Focal dysfunction of the proteasome: a pathogenic factor in a mouse model of amyotrophic lateral sclerosis, J Neurochem 89 (2004) 1325-1335.

[62]   S.J. Kang, I. Sanchez, N. Jing, J. Yuan, Dissociation between Neurodegeneration and Caspase-11-Mediated Activation of Caspase-1 and Caspase-3 in a Mouse Model of Amyotrophic Lateral Sclerosis, J Neurosci 23 (2003) 5455-5460.

[63]   S. Kato, S. Horiuchi, J. Liu, D.W. Cleveland, N. Shibata, K. Nakashima, R. Nagai, A. Hirano, M. Takikawa, M. Kato, I. Nakano, E. Ohama, Advanced glycation endproduct-modified superoxide dismutase-1 (SOD1)-positive inclusions are common to familial amyotrophic lateral sclerosis patients

with SOD1 gene mutations and transgenic mice expressing human SOD1 with a G85R mutation, Acta Neuropathol (Berl) 100 (2000) 490-505.

[64]   Y. Kawaguchi, J.J. Kovacs, A. McLaurin, J.M. Vance, A. Ito, T.P. Yao, The deacetylase HDAC6 regulates aggresome formation and cell viability in response to misfolded protein stress, Cell 115 (2003) 727-738.

[65]   D. Kieran, B. Kalmar, J.R. Dick, J. Riddoch-Contreras, G. Burnstock, L. Greensmith, Treatment with arimoclomol, a coinducer of heat shock proteins, delays disease progression in ALS mice, Nat Med (2004).

[66]   P. Klivenyi, R.J. Ferrante, R.T. Matthews, M.B. Bogdanov, A.M. Klein, O.A. Andreassen, G. Mueller, M. Wermer, R. Kaddurah-Daouk, M.F. Beal, Neuroprotective effects of creatine in a transgenic animal model of amyotrophic lateral sclerosis, Nat Med 5 (1999) 347-350.

[67]   P. Klivenyi, M. Kiaei, G. Gardian, N.Y. Calingasan, M.F. Beal, Additive neuroprotective effects of creatine and cyclooxygenase 2 inhibitors in a transgenic mouse model of amyotrophic lateral sclerosis, J Neurochem 88 (2004) 576-582.

[68]   J. Kong, Z. Xu, Overexpression of neurofilament subunit NF-L and NF-H extends survival of a mouse model for amyotrophic lateral sclerosis, Neurosci Lett 281 (2000) 72-74.

[69]   R.R. Kopito, Aggresomes, inclusion bodies and protein aggregation, Trends Cell Biol 10 (2000) 524-530.

[70]   V. Kostic, V. Jacksonlewis, F. Debilbao, M. Duboisdauphin, S. Przedborski, Bcl-2: prolonging life in a transgenic mouse model of familial amyotrophic lateral sclerosis, Science 277 (1997) 559-562.

[71]   M. Li, V.O. Ona, C. Guegan, M. Chen, V. Jackson-Lewis, L.J. Andrews, A.J. Olszewski, P.E. Stieg, J.P. Lee, S. Przedborski, R.M. Friedlander, Functional role of caspase-1 and caspase-3 in an ALS transgenic mouse model, Science 288 (2000) 335-339.

[72]   J. Liu, C. Lillo, P.A. Jonsson, C. Vande Velde, C.M. Ward, T.M. Miller, J.R. Subramaniam, J.D. Rothstein, S. Marklund, P.M. Andersen, T. Brannstrom, O. Gredal, P.C. Wong, D.S. Williams, D.W. Cleveland, Toxicity of familial ALS-linked SOD1 mutants from selective recruitment to spinal mitochondria, Neuron 43 (2004) 5-17.

[73]   Q. Liu, F. Xie, S.L. Siedlak, A. Nunomura, K. Honda, P.I. Moreira, X. Zhua, M.A. Smith, G. Perry, Neurofilament proteins in neurodegenerative diseases, Cell Mol Life Sci 61 (2004) 3057-3075.

[74]   Y. Manabe, I. Nagano, M.S. Gazi, T. Murakami, M. Shiote, M. Shoji, H. Kitagawa, Y. Setoguchi, K. Abe, Adenovirus-mediated gene transfer of glial cell line-derived neurotrophic factor prevents motor neuron loss of transgenic model mice for amyotrophic lateral sclerosis, Apoptosis 7 (2002) 329-334.

[75]   N.J. Maragakis, M. Jackson, R. Ganel, J.D. Rothstein, Topiramate protects against motor neuron degeneration in organotypic spinal cord cultures but not in G93A SOD1 transgenic mice, Neurosci Lett 338 (2003) 107-110.

[76]   M.M. Maxwell, P. Pasinelli, A.G. Kazantsev, R.H. Brown, Jr., RNA interference-mediated silencing of mutant superoxide dismutase rescues cyclosporin A-induced death in cultured neuroblastoma cells, Proc Natl Acad Sci U S A 101 (2004) 3178-3183.

[77]   K.S. McNaught, R. Belizaire, O. Isacson, P. Jenner, C.W. Olanow, Altered proteasomal function in sporadic Parkinson's disease, Exp Neurol 179 (2003) 38-46.

[78]   K.S. McNaught, P. Shashidharan, D.P. Perl, P. Jenner, C.W. Olanow, Aggresome-related biogenesis of Lewy bodies, Eur J Neurosci 16 (2002) 2136-2148.

[79]   M.J. Mihm, B.L. Schanbacher, B.L. Wallace, L.J. Wallace, N.J. Uretsky, J.A. Bauer, Free 3-nitrotyrosine causes striatal neurodegeneration in vivo, J Neurosci 21 (2001) 1-5.

[80]   L.B. Moran, M.B. Graeber, The facial nerve axotomy model, Brain Res Brain Res Rev 44 (2004) 154-178.

[81]   S. Nakagomi, Y. Suzuki, K. Namikawa, S. Kiryu-Seo, H. Kiyama, Expression of the activating transcription factor 3 prevents c-Jun N-terminal kinase-induced neuronal death by promoting heat shock protein 27 expression and Akt activation, J Neurosci 23 (2003) 5187-5196.

[82]   M.D. Nguyen, T. D'Aigle, G. Gowing, J.P. Julien, S. Rivest, Exacerbation of motor neuron disease by chronic stimulation of innate immunity in a mouse model of amyotrophic lateral sclerosis, J Neurosci 24 (2004) 1340-1349.

[83]   A. Okado-Matsumoto, I. Fridovich, Amyotrophic lateral sclerosis: a proposed mechanism, Proc Natl Acad Sci U S A 99 (2002) 9010-9014.

[84]   R.W. Oppenheim, R.A. Flavell, S. Vinsant, D. Prevette, C.Y. Kuan, P. Rakic, Programmed cell death of developing mammalian neurons after genetic deletion of caspases, J Neurosci 21 (2001) 4752-4760.

[85]   R. Orrell, J. Lane, M. Ross, Antioxidant treatment for amyotrophic lateral sclerosis / motor neuron disease, Cochrane Database Syst Rev (2004) CD002829.

[86]   P. Pasinelli, M.E. Belford, N. Lennon, B.J. Bacskai, B.T. Hyman, D. Trotti, R.H. Brown, Jr., Amyotrophic lateral sclerosis-associated SOD1 mutant proteins bind and aggregate with Bcl-2 in spinal cord mitochondria, Neuron 43 (2004) 19-30.

[87]   P. Pasinelli, M.K. Houseweart, R.H. Brown, Jr., D.W. Cleveland, Caspase-1 and -3 are sequentially activated in motor neuron death in Cu,Zn superoxide dismutase-mediated familial amyotrophic lateral sclerosis, Proc Natl Acad Sci U S A 97 (2000) 13901-13906.

[88]   H. Peluffo, J.J. Shacka, K. Ricart, C.G. Bisig, L. Martinez-Palma, O. Pritsch, A. Kamaid, J.P. Eiserich, J.P. Crow, L. Barbeito, A.G. Estevez, Induction of motor neuron apoptosis by free 3-nitro-l-tyrosine, J Neurochem 89 (2004) 602-612.

[89]   G. Raivich, M. Bohatschek, C. Da Costa, O. Iwata, M. Galiano, M. Hristova, A.S. Nateri, M. Makwana, L. Riera-Sans, D.P. Wolfer, H.P. Lipp, A. Aguzzi, E.F. Wagner, A. Behrens, The AP-1 transcription factor c-Jun is required for efficient axonal regeneration, Neuron 43 (2004) 57-67.

[90]   S.J. Riedl, Y. Shi, Molecular mechanisms of caspase regulation during apoptosis, Nat Rev Mol Cell Biol 5 (2004) 897-907.

[91]   J.A. Roe, M. Wiedau-Pazos, V.N. Moy, J.J. Goto, E.B. Gralla, J.S. Valentine, In vivo peroxidative activity of FALS-mutant human CuZnSODs expressed in yeast, Free Radic Biol Med 32 (2002) 169-174.

[92]   S. Sasaki, H. Warita, K. Abe, M. Iwata, Inducible nitric oxide synthase (iNOS) and nitrotyrosine immunoreactivity in the spinal cords of transgenic mice with a G93A mutant SOD1 gene, J Neuropathol Exp Neurol 60 (2001) 839-846.

[93]   S. Sathasivam, P.G. Ince, P.J. Shaw, Apoptosis in amyotrophic lateral sclerosis: a review of the evidence, Neuropathol Appl Neurobiol 27 (2001) 257-274.

[94]   F.J. Schopfer, P.R. Baker, B.A. Freeman, NO-dependent protein nitration: a cell signaling event or an oxidative inflammatory response?, Trends Biochem Sci 28 (2003) 646-654.

[95]   M.Y. Sherman, A.L. Goldberg, Cellular defenses against unfolded proteins: a cell biologist thinks about neurodegenerative diseases, Neuron 29 (2001) 15-32.

[96]   G.A. Shinder, M.C. Lacourse, S. Minotti, H.D. Durham, Mutant Cu/Zn-superoxide dismutase proteins have altered solubility and interact with heat shock/stress proteins in models of amyotrophic lateral sclerosis, J Biol Chem 276 (2001) 12791-12796.

[97]   E.N. Shiozaki, Y. Shi, Caspases, IAPs and Smac/DIABLO: mechanisms from structural biology, Trends Biochem Sci 29 (2004) 486-494.

[98]   A. Stieber, J.O. Gonatas, N.K. Gonatas, Aggregates of mutant protein appear progressively in dendrites, in periaxonal processes of oligodendrocytes, and in neuronal and astrocytic perikarya of mice expressing the SOD1(G93A) mutation of familial amyotrophic lateral sclerosis, J Neurol Sci 177 (2000) 114-123.

[99]   H. Takeuchi, Y. Kobayashi, T. Yoshihara, J. Niwa, M. Doyu, K. Ohtsuka, G. Sobue, Hsp70 and Hsp40 improve neurite outgrowth and suppress intracytoplasmic aggregate formation in cultured neuronal cells expressing mutant SOD1, Brain Res 949 (2002) 11.

[100] M. Urushitani, S. Shimohama, T. Kihara, H. Sawada, A. Akaike, M. Ibi, R. Inoue, Y. Kitamura, T. Taniguchi, J. Kimura, Mechanism of selective motor neuronal death after exposure of spinal cord to glutamate: involvement of glutamate-induced nitric oxide in motor neuron toxicity and nonmotor neuron protection, Ann Neurol 44 (1998) 796-807.

[101] J.S. Valentine, P.J. Hart, Misfolded CuZnSOD and amyotrophic lateral sclerosis, Proc Natl Acad Sci U S A 100 (2003) 3617-3622.

[102] L. Viera, Y.Z. Ye, A.G. Estevez, J.S. Beckman, Immunohistochemical methods to detect nitrotyrosine, Methods Enzymol 301 (1999) 373-381.

[103] V. Waetzig, T. Herdegen, Neurodegenerative and physiological actions of c-Jun N-terminal kinases in the mammalian brain, Neurosci Lett 361 (2004) 64-67.

[104] M.J. Wagstaff, J. Smith, Y. Collaco-Moraes, J.S. de Belleroche, R. Voellmy, R.S. Coffin, D.S. Latchman, Delivery of a constitutively active form of the heat shock factor using a virus vector protects neuronal cells from thermal or ischaemic stress but not from apoptosis, Eur J Neurosci 10 (1998) 3343-3350.

[105] L.J. Wang, Y.Y. Lu, S. Muramatsu, K. Ikeguchi, K. Fujimoto, T. Okada, H. Mizukami, T. Matsushita, A. Hanazono, A. Kume, T. Nagatsu, K. Ozawa, I. Nakano, Neuroprotective effects of glial cell line-derived neurotrophic factor mediated by an adeno-associated virus vector in a transgenic animal model of amyotrophic lateral sclerosis, J Neurosci 22 (2002) 6920-6928.

[106] T.T. Wang, A.S. Chiang, J.J. Chu, T.J. Cheng, T.M. Chen, Y.K. Lai, Concomitant alterations in distribution of 70 kDa heat shock proteins, cytoskeleton and organelles in heat shocked 9L cells, Int J Biochem Cell Biol 30 (1998) 745-759.

[107] C.M. Ward, J. Liu, D.J. Young, D.W. Cleveland, Increasing the protein folding chaperone HSP70 does not affect timecourse SOD1-mutant mediated amyotrophic lateral sclerosis, Soc Neurosci Abstr 31 (2001) 107.112.

[108] J.L. Webb, B. Ravikumar, D.C. Rubinsztein, Microtubule disruption inhibits autophagosome-lysosome fusion: implications for studying the roles of aggresomes in polyglutamine diseases, Int J Biochem Cell Biol 36 (2004) 1910-1919.

[109] J. Whitfield, S.J. Neame, L. Paquet, O. Bernard, J. Ham, Dominant-negative c-Jun promotes neuronal survival by reducing BIM expression and inhibiting mitochondrial cytochrome c release, Neuron 29 (2001) 629-643.

[110] T.L. Williamson, L.I. Bruijn, Q. Zhu, K.L. Anderson, S.D. Anderson, J.P. Julien, D.W. Cleveland, Absence of neurofilaments reduces the selective vulnerability of motor neurons and slows disease caused by a familial amyotrophic lateral sclerosis-linked superoxide dismutase 1 mutant, Proc Natl Acad Sci U S A 95 (1998) 9631-9636.

[111] A. Wyttenbach, O. Sauvageot, J. Carmichael, C. Diaz-Latoud, A.P. Arrigo, D.C. Rubinsztein, Heat shock protein 27 prevents cellular polyglutamine toxicity and suppresses the increase of reactive oxygen species caused by huntingtin, Hum Mol Genet 11 (2002) 1137-1151.

[112] X.G. Xia, H. Zhou, S. Zhou, Y. Yu, R. Wu, Z. Xu, An RNAi strategy for treatment of amyotrophic lateral sclerosis caused by mutant Cu,Zn superoxide dismutase, J Neurochem 92 (2005) 362-367.

[113] J. Yuan, M. Lipinski, A. Degterev, Diversity in the mechanisms of neuronal cell death, Neuron 40 (2003) 401-413.

Summary

Neurons are large post-mitotic cells with a high metabolic activity and a highly complex morphology characterized by a dendritic tree that consists of a network of processes, and an axon that can have length of up to 10^4 times the diameter of the cell body. Because of this complexity the maintenance of the functional and structural integrity of neurons throughout life is a complex task that requires sophisticated transport, damage control and repair machineries. Hence, it is not surprising that aging is associated with structural and functional deterioration of the central nervous system and that neurodegenerative diseases (diseases that cause the premature loss of neurons) are among the dominant disorders associated with aging. The knowledge on processes involved in normal aging and neuronal death in neurodegerative diseases is increasing, but far from complete. Intervention in these processes is therefore not yet possible.

Amyotrophic lateral sclerosis (ALS) is a fatal disease in which motoneurons in the spinal cord, brain stem and motor cortex degenerate. This disease has an incidence of 2-3 per 100.000 people, meaning that 300-450 people are diagnosed with the disease each year. The survival of ALS-patients is on average 3 years after diagnosis. The first symptoms are usually fatigue, muscle cramps, and weakness in the muscles of one of the limbs, progressing to paralysis and spreading to other parts of the body, eventually causing total body paralysis. In most patients (about 90%) no apparent genetic cause for their disease has been found, in those cases the disease is called sporadic ALS. In the other 10% a hereditary pattern has been found; familial ALS. In 1993 a mutation was found in the gene for superoxide dismutase 1 (SOD1) which causes ALS in some familial ALS families. By now more than 110 different mutations in the SOD1-gene have been linked to familial ALS and more recently mutations in 5 other genes have been found to cause familial ALS.

The discovery of SOD1-mutations has enabled the production of transgenic mutant-SOD1 expressing mice that develop an ALS-like motoneuron disease. These SOD1-mutant mice develop a disease strongly resembling human ALS. These transgenic mice offer the possibility to study all stages of motoneuron death. In this thesis different aspects of ALS in the transgenic mouse model and in cultured motoneurons are studied and discussed.

In **chapter 2** the possible toxicity of 3-nitrotyrosine is studied. 3-Nitrotyrosine is a modified amino acid that is formed by a reaction between nitric oxide-derived reactive species and tyrosine. Because of a number of studies indicating that 3-nitrotyrosine may be neurotoxic to particular populations of neurons, we have examined the effect of acute and prolonged application of 3-nitrotyrosine in the brain of mice and in murine organotypic spinal cord cultures. Using an antibody that labels 3-nitrotyrosine injected into the brain, we showed that after a single microinjection into the cortex, striatum or hippocampus, 3-nitrotyrosine is predominantly distributed in neurons, but subsequently disappears within 60 min. Neither single microinjections nor prolonged intra-striatal delivery of 3-nitrotyrosine via osmotic minipumps resulted in any evidence for neuronal degeneration. Also prolonged exposure of organotypic spinal cord cultures to high doses of 3-

nitrotyrosine did not influence neuronal viability. From these results we conclude that although increased levels of free 3-nitrotyrosine are reported for various neurodegenerative diseases, free 3-nitrotyrosine is unlikely to contribute to neuronal degeneration.

Defects in protein repair and degradation can lead to protein aggregation and inclusion formation. The proteasome is a complex of enzymes responsible for an important part of the degradation of proteins. In **chapter 3** we studied the effect of mild inhibition of the proteasome on inclusion body-formation in (moto)neurons in organotypic spinal cord cultures. We found a dose-dependent degeneration of neurons after a one-week exposure to proteasome inhibitors. This degeneration was associated with an increase in poly-ubiquitination, consistent with failure of the ubiquitin-proteasome system. No difference in survival between motoneurons and interneurons was observed. Because of our interest in ALS we repeated these experiments with spinal cord cultures from G93A-SOD1 mice, which showed that neurons whit high expression of mutant SOD1 are not more vulnerable to death caused by proteasome inhibition than normal neurons. These results indicate that inclusion formation is not directly caused by a combination of proteasome inhibition and mutant SOD1, but that mutant SOD1 possibly causes formation of inclusion bodies via another mechanism. Whether inclusion bodies are a primary cause of neurodegeneration is discussed in more detail in chapter 6.

We also looked for alterations in the protein repair system. Molecular chaperones are proteins that assist new proteins to fold or that can assist damaged, (partially) unfolded proteins to refold. Heat shock protein 25 (Hsp25) is a molecular chaperone which is constitutively expressed in murine motoneurons. **Chapter 4** describes a decrease in the amount of Hsp25 protein prior to the onset of motoneuron death. This decrease is post-translational since the amount of Hsp25-mRNA is unchanged. In view of the cytoprotective properties of Hsp25 and the temporal relationship between decreased Hsp25 expression and the onset of motoneuron death, it is feasible that reduced Hsp25 concentration contributes to the degeneration of motoneurons in G93A mice. These data are consistent with the idea that mutant SOD1 may reduce the availability of the protein quality control machinery in motoneurons.

If a cell is damaged beyond repair, a process called programmed cell death is started. Apoptosis is a common form of programmed cell death. In **chapter 5** we studied the phosphorylation of c-Jun and ATF3, two factors that play a role in the final phases of survival. Immunocytochemistry and *in situ* hybridization showed that a subset of motoneurons express both ATF3 and phosphorylated c-Jun starting from a relatively early phase of disease before the onset of active caspase 3 expression and motoneuron loss. The onset of phosphorylated c-Jun and ATF3 expression correlated with the onset of dendritic ubiquitination. Confocal-double labeling immunofluorescence showed that phosphorylated c-Jun and ATF3 expression in motoneurons correlated with Golgi fragmentation. A subset of ATF3 and phosphorylated c-Jun immunoreactive motoneurons showed an ill appearance characterized by number of distinctive abnormalities, including an eccentric

flattened nucleus, perinuclear accumulation of the Golgi apparatus and the ER, perikaryal accumulation of ubiquitin immunoreactivity and intense Hsp70 immunoreactivity. These abnormal cells were not immunoreactive for active caspase 3. We conclude that motoneurons in SOD1-ALS mice prior to their death show a prolonged phase in which they are compromised and express the injury transcription factors ATF3 and phosphorylated c-Jun. This compromised state is being characterized by an increasing amount of ubiquitinated material that first fills the neurites and subsequently the cell body.

In **chapter 6** a number of subjects from the previous chapters are discussed more comprehensively. We conclude that mutated SOD1 causes a complex pathology involving protein-repair and –degradation mechanisms, mitochondria and multiple other systems, finally leading to programmed cell death.

Samenvatting

Zenuwcellen worden gekenmerkt door zeer uitgebreide morfologie met enerzijds een dendrietboom met vele uitlopers en anderzijds een axon met een lengte tot 10.000 keer de doorsnede van het cellichaam. Sommige delen van de cel liggen hierdoor zeer ver van het controle centrum van de cel, waardoor het vervangen van onderdelen een complex proces is. Daarnaast worden zenuwcellen in tegenstelling tot de meeste andere cellen in het lichaam niet vervangen gedurende het leven. Om zichzelf in stand te houden zijn zenuwcellen daarom afhankelijk van efficiënte transport-, en reparatiesystemen. Falen van deze systemen gedurende veroudering of door ziekte leidt tot het disfunctioneren en eventueel afsterven van de zenuwcellen. De kennis over veroudering en sterfte van zenuwcellen is zeer onvolledig, en er zijn nog geen effectieve medicijnen die dit proces tegengaan.

Dit proefschrift richt zich op een ouderdomsziekte van de zenuwcellen die de spieren aansturen, de motoneuronen. Deze ziekte, amyotrofische lateral sclerose (ALS), begint meestal tussen de 40 en 60 jaar met vermoeidheid, kramp en/of spierzwakte in één van de ledematen. De spierzwakte wordt steeds ernstiger, uiteindelijk leidend tot volledige verlamming en vervolgens de dood van de patiënt. Per jaar wordt in Nederland de ziekte bij 300-450 personen vastgesteld. De patiënten overlijden gemiddeld 3 jaar na diagnose. Uit genetisch onderzoek blijkt dat de ziekte bij 10% van de patiënten wordt veroorzaakt door een erfelijke afwijking. In 1993 is het eerste ALS-gen ontdekt. Mutaties in dit gen, het superoxide dismutase 1 (SOD1)-gen, veroorzaken ongeveer 20% van de erfelijke ALS. De ontdekking van SOD1-mutaties heeft geleid tot een diermodel waarbij gemuteerd SOD1 als transgen in een muizenlijn is ingebracht. Deze muizen ontwikkelen een ziektebeeld dat nagenoeg identiek is aan menselijke ALS, en vormen daarom een zeer goed proefdiermodel voor de ziekte. In **hoofdstuk 1** wordt een overzicht gegeven van de stand van zaken van het genetisch en experimenteel onderzoek naar de pathogenese van ALS, en worden daarnaast de belangrijkste eigenschappen van de SOD1-ALS muizen besproken.

Een groot voordeel van een muizenmodel is dat men niet alleen systematisch onderzoek kan doen naar mogelijke behandelingen, maar ook zeer vroege stadia van het ziekteproces kan bestuderen; iets wat bij de mens onmogelijk is. Het grootste deel van het onderzoek in dit proefschrift richt zich op het nauwkeurig in kaart brengen van vroege veranderingen die optreden in motoneuronen van SOD1-ALS muizen. Op grond van de resultaten hebben we van een aantal factoren kunnen vaststellen of ze wel, dan wel niet een rol spelen bij het ziekteproces. De resultaten bevestigen het idee dat het degeneratieproces van de motoneuronen samenhangt met opeenhoping en klontering van misvormd SOD1 eiwit. Een dergelijk proces speelt waarschijnlijk ook bij andere ouderdomsziekten van de hersenen, zoals de ziekte van Alzheimer (gekenmerkt door klontering van het tau- en het β-amyloid eiwit), of de ziekte van Parkinson (klontering van synucleine), een centrale rol. Vragen die een dergelijk ziektemechanisme oproepen zijn: 1) Wat veroorzaakt de ophoping en klontering van abnormaal eiwit? 2) Waarom gebeurt dit alleen in een specifiek soort zenuwcellen (zoals bijvoorbeeld de motoneuronen bij ALS)? 3) Hoe veroorzaakt de ophoping en klontering van eiwitten het verval en de dood van zenuwcellen? Het onderzoek in dit proefschrift heeft betrekking op het beantwoorden van deze vragen. Voor geen

van de vragen is er echter nog een eenduidig antwoord. Dit wordt besproken in **hoofdstuk 6**. Hieronder volgt een korte beschrijving van het onderzoek in de hoofdstukken 2 - 5.

Er zijn verschillende oorzaken voor het ontstaan van misvormde eiwitten. In de eerste plaats veroorzaken mutaties vaak ernstige misvorming van het eiwit. Ook niet gemuteerde eiwitten kunnen een foute structuur krijgen, ofwel omdat tijdens het in elkaar vouwen van het eiwit iets mis is gegaan, ofwel door beschadiging van een eiwit door bijvoorbeeld vrije radicalen. Voor veel SOD1 mutaties is aangetoond, dat het eiwit door mutaties in die mate misvormd is dat het 'plakkerig' wordt en kan gaan klonteren. Bij een aantal mutaties heeft het eiwit echter een relatief normale structuur. Een ander mechanisme dat kan bijdragen aan misvormd SOD1 is vrije radicaal schade. De normale functie van SOD1 is het onschadelijk maken van vrije zuurstof radicalen, maar van gemuteerd SOD1 is aangetoond dat het in plaats daarvan bepaalde vrije radicalen genereert, zoals bepaalde schadelijke stikstofoxide verbindingen die onder andere het SOD1 zelf kunnen aantasten. Het onderzoek in **hoofdstuk 2** vloeit voort uit ons onderzoek naar de rol van reactieve stikstofoxide verbindingen in het degeneratie proces bij de SOD1-ALS muis. Stikstofoxide radicalen kunnen o.a. bepaalde aminozuren veranderen. Eén van deze veranderde aminozuren, 3-nitrotyrosine, wordt gebruikt als vingerafdruk voor de aanwezigheid van schade door stikstofoxide radicalen. Bovendien wordt verhoogd 3-nitrotyrosine in verband gebracht de eiwitklontering in zenuwcellen van ALS patiënten. In de SOD1-ALS muis bleek echter geen 3-nitrotyrosine aanwezig te zijn in SOD1-eiwit klonten (deze resultaten worden beschreven aan het begin van **hoofdstuk 6**). Onze (en andere) studies wijzen echter wel op een diffuse verhoging van de concentratie van vrij 3-nitrotyrosine (dus niet gebonden aan een eiwit) in de SOD1-ALS muis. Omdat in studies in de literatuur de suggestie werd gewekt dat ook vrij 3-nitrotyrosine schadelijk kan zijn, hebben we dit in hoofdstuk 2 systematisch onderzocht. Uit onze studies resultaten bleek echter dat 3-nitrotyrosine niet schadelijk was voor zenuwcellen.

De aanwezigheid van gemuteerd plakkerig SOD1, kan op zichzelf het ontstaan van eiwitklonten in de motoneuronen van SOD1-ALS muizen verklaren, maar de vraag blijft dan waarom dit alleen in motoneuronen gebeurd terwijl SOD1 in alle cellen aanwezig is. Een mogelijke verklaring is dat bij motoneuronen de eiwitten en enzymcomplexen die misvormde eiwitten wegvangen en afbreken, relatief minder goed werken. Een belangrijke schakel in het afbreken van misvormde eiwitten is het ubiquitine-proteasoom systeem, waarbij misvormde eiwitten een 'label' krijgen in de vorm van een ketentje van een klein eiwit, ubiquitine, en vervolgens worden afgebroken door een groot eiwitcomplex, het proteasoom. Er zijn aanwijzingen dat mutant SOD1 het proteasoom complex kan overbelasten, en dat remming van het proteasoom leidt tot de vorming van grote microscopisch zichtbare SOD1-eiwit klonten. In **hoofdstuk 3** hebben we gekeken naar het effect van milde remming van het proteasoom op de overleving van motoneuronen in ruggenmergkweken. Uit deze studies bleek dat milde proteasoomremming op de lange duur kan leiden tot het afsterven van motoneuronen. Dit effect werd echter niet beïnvloed door de aanwezigheid van mutant SOD1. Bovendien hadden andere typen zenuwcellen dezelfde gevoeligheid voor proteasoomremming. Deze gegevens pleiten tegen het

idee dat het proteasoom systeem een zwakke schakel is in motoneuronen. Dit wordt ook bevestigd door gegevens uit onze neuropathologische studie beschreven in **hoofdstuk 5**, die erop wijzen dat motoneuronen pas in een zeer late fase van hun degeneratieproces vlak voordat ze sterven, over onvoldoende proteasoomfunctie beschikken.

Een andere schakel in het defensiemechanisme van de cel tegen misvormde eiwitten zijn de 'chaperon eiwitten', die verkeerd-gevouwen of beschadigde eiwitten omringen en zodoende onschadelijk maken. Omdat er aanwijzingen waren dat gemuteerd SOD1 ook bepaalde chaperon eiwitten kon overbelasten, hebben we in **hoofdstuk 4** onderzocht wat er met één van deze chaperons, Hsp25 (bij de mens Hsp27 genoemd), gebeurt in de SOD1-ALS muis. Deze studie toont aan dat de hoeveelheid Hsp25 aanzienlijk is verlaagd in motoneuronen van SOD1-ALS muizen. Dit gebeurt op het moment dat ook andere degeneratieverschijnselen optreden. Het optreden van deze degeneratieverschijnselen kan verklaard worden uit de afname van de hoeveelheid Hsp25, omdat Hsp25 enkele belangrijke beschermende functies heeft in motoneuronen. Hoe de aanwezigheid van gemuteerd SOD1, leidt tot een verlaging van de Hsp25 concentratie is nog niet bekend.

Om inzicht te krijgen in hoe de stapeling en klontering van gemuteerd SOD1, leidt tot het afsterven van de motoneuronen, hebben we in **hoofdstuk 5** het degeneratieproces van motoneuronen in de SOD1-ALS muis nauwkeurig in kaart gebracht. Om 'zieke' motoneuronen te kunnen identificeren hebben we gebruik gemaakt van twee eiwitten, ATF3 en c-Jun, die vaak worden aangemaakt in beschadigde cellen. ATF3 en c-Jun zijn transcriptie factoren, d.w.z. eiwitten die expressie van bepaalde genen kunnen sturen. De belangrijkste conclusies van hoofdstuk 5 zijn (1) dat ATF3 en c-Jun relatief vroeg in het ziekteproces in een deel van de motoneuronen tot expressie komen. Dit hangt samen met het verschijnen van geklonterd SOD1 in de dendrieten van de motoneuronen. (2) De morfologie van ATF3/c-Jun-positieve motoneuronen varieert van gezonde relatief normale cellen tot cellen met een zeer ziek uiterlijk, o.a. gekenmerkt door een platte kern en een cellichaam dat grotendeels is gevuld met geklonterd SOD1 en mogelijk andere abnormale eiwitten. (3) Geprogrammeerde celdood treedt pas op nadat de motoneuronen dit zieke stadium hebben bereikt.

List of publications

Kaal EC, Vlug A, Versleijen MW, Kuilman M, Joosten EA, Bär PR (2000) Chronic mitochondrial inhibition induces selective motoneuron death in vitro: a new model for Amyotrophic Lateral Sclerosis J Neurochem 74 (3) 1158-1165

van Rossum GS, Vlug AS, van den Bosch H, Verkleij AJ, Boonstra J (2001) Cytosolic phospholipase A_2 activity during the ongoing cell cycle J Cell Physiol 188(3) 321-328

Haasdijk ED, Vlug A, Mulder MT, Jaarsma D (2002) Increased apolipoprotein E expression correlates with the onset of neuronal degeneration in the spinal cord of G93A-SOD1 mice Neurosci Lett 335(1) 29-33

Vlug A and Jaarsma D (2004) Long term proteasome inhibition does not preferentially afflict motoneurons in organotypical spinal cord cultures Amyotroph Lateral Scler Other Motor Neuron Disord 5(1) 16-21

Vlug A, Maatkamp AJ, Haasdijk ED, Troost D, French PJ, Jaarsma D (2004) Decrease of HSP25 protein expression precede degeneration of motoneurons in ALS-SOD1 mice Eur J Neurosci 20(1) 14-28

Vlug A, Gerritsen J, van den Burg J, Jaarsma D Increased 3-nitrotyrosine does not cause neuronal degeneration Submitted

Engel DC, Slemmer JE, Vlug AS, Maas AIR, Webber JT Combined effects of mechanical and ischemic injury to cortical cells: secondary ischemia increases damage and decreases effects of neuroprotective agents Submitted

Vlug A, Haasdijk ED, French P, Jaarsma D Expression of phosphorylated c-Jun and ATF3 correlates with somato-dendritic ubiquitination and Golgi fragmentation and precedes death of spinal motoneurons in amyotrophic lateral sclerosis-SOD1 transgenic mice In preparation

Curriculum vitae

Angela Vlug was born in Hilversum on 3 November 1975. She attended the College Stad & Lande in Huizen, from which she graduated in 1994. In that same year she started her biological studies at the faculty of biology from the Utrecht University in Utrecht. As an undergraduate she did research at the laboratory for experimental neurology from the University Medical Centre in Utrecht on the subject of the effect of mitochondrial inhibition on motoneurons in culture. She also did research at the department of cell biology from the faculty of biology at the Utrecht University where she studied the activity of $cPLA_2$ during the cell cycle. After graduating in March 1999, she started working as a PhD-student at what was then named the department of Anatomy from the medical faculty at the Erasmus University, Rotterdam. That department later merged with the department of physiology to become the department of neuroscience, led by Prof. Dr. de Zeeuw. At this department she worked on the research described in this thesis under the supervision of Dr. Jaarsma. After finishing her official time as a PhD student in 2003 she took a position as research scientist with Dr Weber and Prof. Dr. Borst for 1 year, also at the department of neuroscience. After that period ended she accepted a position as post-doctoral researcher at the Institute for medical neurobiology from the Otto von Guericke University in Magdeburg, Germany where she started working in December 2004. Currently she is working there on mechanisms of neuroprotection in a models for stroke.